Design of stimuli-responsive OmpF-conjugates as biovalves for nano-reactors

Inauguraldissertation

zur Erlangung der Würde eines Doktors der Philosophie

vorgelegt der

Philosophisch-Naturwissenschaftlichen Fakultät

der Universität Basel

von

Christoph Edlinger

aus

Österreich

Basel, 2018

Genehmigt von der Philosophisch-Naturwissenschaftlichen Fakultät

auf Antrag von:

Prof. Dr. Wolfgang P. Meier

(Universität Basel)

Fakultätsverantwortlicher/Dissertationsleiter

Und

Prof. Dr. Nico Bruns

(Université Fribourg)

Korreferent

Basel den 27.02.2018   Prof. Dr. Martin Spiess

Dekan

I Summary

Without compartmentalisation, there would be no life, as cells require spatial organization to perform all metabolic processes to sustain it. Compartmentalisation, or physical separation of biological reactions requires defined reaction spaces and active control over all molecules that enters or leaves them. Nature utilises for this purpose cell membranes and a plethora of different membrane proteins, which act as tunnels allowing and controlling molecular flow across the membrane. In a similar manner mimicking nature, by molecular self-assembly, allows us to produce artificial cells as simplified models for better understanding specific parts of cells. Our knowledge allows us today to go a step further, as we can use natural or artificial enzymes and trans-membrane channel proteins to create artificial organelles (nanoreactors) capable of supporting selective reactions and replacement the deficient structures or organelles. That is why the nanoreactors are gaining more and more interest for specific applications in the field of nano-medicine, analytics and advanced functional materials.

To achieve the desired compartmentalization, it was needed to advance from the artificial assemblies, with passive membrane transport, based on permanently open pores. First attempts in this direction are represented by the design of single stimuli triggered transport via structures capable of opening upon acidification or reduction. The second step will be to have reversible triggered transport structures, like cells have. To have reliable artificial replacements of the dysfunctional cell structures is needed.

This thesis, is achieving this necessary step by the development of a biovalve which can open and close on demand in a similar manner that the trans-membrane proteins work. This is a significant advance in the design of new cell-like polymeric compartmentalised structures with sustainable specific function. This new system can be switched on and off by demand, theoretically endlessly, opening new ways in the development of artificial structures to replace the non-functional ones in living cells.

This biovalve was obtained by modifying trans-membrane proteins (Omp F) capable of passive transport of a range of molecules, with selected pH sensitive peptides capable of opening and closing its pore. This new biovalve functionality was tested by reconstituting it in an artificial membrane of a nanoreactor that delimits an inner empty space in which selected enzymes were entrapped. The specific substrate for the entrapped enzyme was added on top of the assembled nanoreactors mixture, outside of the closed polymeric compartments. At physiological pH the biovalve opens, and the substrate molecules diffuse passively in the inner space of the nanoreactor entrapping the enzyme molecules. The enzymatic reaction takes place and the (fluorescent) product formation is monitored. At low pH the biovalve closed blocking the access of the substrate molecules and no fluorescent product can be detected.

The optimal variant proved to be K89R270C-Gala3 modified OmpF, that is open at physiological pH and completely closed at lower pH (only 1.4 units lower). The bio-valve showed its functionality after reconstitution both in liposomes and polymeric nanoreactors, showing the robustness of our new obtained structure. Moreover, the stimuli response overruled the pH dependent activity of the enzyme and the nanoreactor increased the enzyme stability and increased its stability towards pH changes.

II Zusammenfassung

Ohne Kompartmentalisierung, gäbe es kein Leben, da alle Lebensformen eine räumliche Organisation benötigen um ihren Metabolismus zu kontrollieren. Kompartmentalisierung ist die physische Abtrennung von (biologischen) Reaktionen. Es erschafft wohldefinierte Reaktionsräume, welche es erlauben zu kontrollieren, was in sie vordringt und was sie wieder verlässt und wann es dies tut.

In der Natur entwickelten sich zu diesem Zwecke Zellmembranen und eine Vielzahl an Membranproteinen, welche als Tunnel fungieren und damit den Stofffluss durch die Membran kontrolliert.

Molekulare Selbstassemblierung erlaubt künstliche Zellen als vereinfachte Modelle um Zellbestandteile besser verstehen zu können. Nun ist unser Wissen soweit fortgeschritten, dass wir einen Schritt weitergehen können und aus bestehenden Enzymen, Katalysatoren etc. und Membranproteinen künstliche Organellen bzw. Nanoreaktoren herstellen können, welche spezifische Reaktionen erlauben, sogar Defekte in Zellen kompensieren können. Nanoreaktoren werden daher immer interessanter und versprechen ihre Verwendung in der Nanomedizin, Analytik oder in Hightech Funktionsbeschichtungen finden zu können.

Um die erwünschte Funktionalität zu erreichen, reicht es jedoch nicht, aktive Bestandteile in eine schützende Hülle zu verpacken. Selbst die Einführung von Poren, die einen Grössenausschluss ermöglichen, ist nicht immer genug. Zur Kontrolle der Reaktionsräume gehört auch eine zeitliche Steuerung. Fortgeschrittenere Systeme verwenden daher einen molekularen Stöpsel von dem Poreneingang abzulösen und damit ein einziges Mal von *Aus* auf *An* zu schalten. Dies kann durch z.B: einen niederen pH-Wert, reduktive Bedingungen etc. geschehen. Der nächste logische Schritt ist es auch zeitliche Kontrolle über den Stofffluss durch die Membran zu erlangen, ähnlich wie es biologische Zellen tun.

In dieser Doktorarbeit, geht es um eben diesen Schritt, der Entwicklung eines molekularen Ventils, welches nach Bedarf geöffnet und geschlossen werden kann, ähnlich Transmembranproteinen. Dies ist ein entscheidender Fortschritt, in der Erschaffung von zellartigen, polymeren Nanoreaktoren, da es eine langfristige Steuerung verspricht. Theoretisch kann es unendlich oft *An* und *Aus* geschaltet werden, gesteuert über einen spezifischen Parameter. Dies ermöglicht neuartige Nanoreaktoren und die Reparatur von dysfunktionalen Organellen.

Dies wurde bewerkstelligt indem eine permanent offene Pore des Transmembranproteins OmpF (welches weitgehend unselektiv kleine Moleküle bis ca. 600 Da durchlässt) mit verschiedenen Peptiden modifiziert wurde, welche sich je nach pH-Wert ihre Konformation ändern und somit eine molekulare Tür erschaffen. Dieses Modul wurde getestet indem es in eine synthetische Membran eingebaut wurde welche wiederum Enzyme umschliesst und somit einen einfachen Nanoreaktor darstellt. Dazu wurden von Aussen enzym-spezifische Substrate hinzugegeben. Bei einem physiologischen pH-Wert, sind die Poren offen und erlauben dem Enzymsubstrat durch die Membran zu diffundieren. Dadurch kann die Reaktion im Inneren des Nanoreaktors erfolgen und es entsteht ein Fluorophor, dessen Konzentration laufend gemessen werden kann. Bei niedrigem pH-Wert ändert sich die Konformation vom Peptid und die Pore schliesst sich. Dadurch kommt die Reaktion zum Erliegen und kein weiteres Fluorophor entsteht.

Am geeignetsten erwies sich K89R270C-Gala3 OmpF, welches von einer komplett offenen Pore zu einer komplett geschlossenen Pore wechseln kann, bei einer pH-Änderung von nur 1.4 Einheiten. Diese Funktionalität zeigte sich sowohl in Lipid- als auch Polymermembranen, was für die Robustheit des Systems spricht. Darüber hinaus erlaubt dieser Effekt erlaubt es, die pH-Abhängigkeit des Enzymes zu überstimmen und beschützt zudem das Enzym vor seinem Zerfall, wodurch das System mehr pH-Wechsel überlebt und länger lagerbar wird.

III Acknowledgements

I like to thank Prof. Wolfgang P. Meier and Prof. Cornelia G. Palivan, for allowing me to work in their group and Dr. Ozana S. Onaca Fischer for providing the project. I want to thank Prof. Dr. Nico Bruns for being my co-examiner of my thesis. Prof. Dr. Palivan is kindly acknowledged for being the chair.

The PhD thesis would not have been possible without the generous help of Dr. Tomaz Einfalt (since we were working on related projects, we could solve each others problems and provide invaluable help to each other; his most noteworthy contribution was the finding that OmpF is stable or several days after being dialysed for detergent removal and for developing the first reliable procedure for OmpF insertion in polymersomes), Dr. Mariana Spulber (general advice, in particular analytical problem solving and general support and for being a true friend; her main contributions were helping me with SLS/DLS measurements, finding that the type of buffer affected the enzyme kinetics and helping me to reduce autooxidation of the fluorophores), Dr. Stefan Nicolet (teaching me everything about producing OmpF mutants; supplying me with polymerase and ultracompetent cells without having an official collaboration with our group) and Roland Goers (fruitful bio-related discussions, in particular about problem sources related to enzymes and Membranes, such as the effect of detergents on the tertiary mixture in OmpF and how the nature of a detergent affects its removal).

Further, I like to thank Prof. Nico Bruns (general help and advice), Gabriele Percy (TEM), Dr. Michael Devereux (solving IT-problems), the work-shop and our secretaries. Moreover, the group would not have been the same without Dr. Marcus Inglin, Dr. Patric Baumann, Dr. Samuel Lörcher, Dr. Adrian Dinu, Dr. Adrian Najer, Dr. Martin Rother, Sagana Tamboo, Ina Ontaveros and Martina Garni, providing great discussions on and off topic and helping each other out.

There are two more persons deserving special thanks:

Sonja Edlinger, for being my mother and driving over 7h non-stop through the night, to help me, when I fell ill.

Dr. Werner Breitenstein, for correcting my first draft of this PhD thesis without expecting anything in return and helping me to make it easier to understand for you readers.

Lastly, I have to mention SNF, NCCR and the University of Basel for funding me.

IV Table of Contents

V Abbreviations

AB: amphiphilic diblockcopolymer

ABA: amphiphilic triblockcopolymer ($A_6B_{40}A_6$ would have 2x6 hydrophilic and 40 hydrophobic monomers as blocks)

ABCP: amphiphilic blockcopolymer

ABTS: 2,2'-azino-bis(3-ethylbenzothiazoline-6-sulphonic acid)

ALOX: aluminium oxide

ATRP: atom transfer radical polymerisation

a.u.: arbitrary units (typically related to voltage of light detectors)

*t*BuOH: *tert*.-butanol

BCA: bicinchoninic acid (assay for determining protein concentrations)

BSA: bovine serum albumin (a water-soluble protein with a single cysteine group on its surface)

CHAPS: 3-[(3-cholamidopropyl)dimethylammonio]-1-propanesulfonate (CAS: 331717-45-4)

Chol-PEG: pegylated cholesterol (CAS: 69068-97-9)

cmc: critical micelle forming concentration

CPM: counts per molecule

CR: count rate

Da: Dalton [g/mol]

DDM: dodecylmaltoside (CAS: 69227-93-6)

DLS: dynamic light scattering (details see the end of this chapter)

DM decylmaltoside (CAS: 82494-09-5)

DMF: dimethylformamid

DMSO: dimethylsulfoxide

DOL: degree of labelling

DP: degree of polymerisation (number of repeating units)

DSPC: 1,2-distearoyl-*sn*-glycero-3-phosphocholine (saturated lipid)

ELP: elastine like peptide (solubility is temperature dependent)

Encap. eff.: encapsulation efficiency

eq.: equivalents

F_2:	fraction of detected dye within the vesicle
FCS:	fluorescence correlation spectroscopy
GALA3:	MI-CH_2-CO-NH-$(LAEA)_3$-COOH
GPC:	gel permeation chromatography
HPLC:	high pressure liquid chromatography
HRP:	horseradish peroxidase
In:	Initiator for radical reactions
L:	ligand for metal complexes
LB:	Miller Lysogeny Broth (for growing bacteria cultures in solution or plates)
LPO:	lactoperoxidase
M:	molecular mass
MALDI:	matrix assisted laser desorption ionisation
Me_6Tren:	tris[2-(dimethylamino)ethyl]amine; a strong binding ligand
MI:	maleic imide
MP:	membrane protein (a protein with hydrophobic surfaces for integration into cell-membranes)
MS:	mass spectrometry
MTBE:	methyl-*tert*. butyl-ether
MWCO:	molecular weight cutoff (lowest MW where 90% of the molecules remain within dialysis or filter)
N_{dye}:	number of dye molecules
n.d.:	not determined
NIPAAM:	N-isopropylacrylamid
POPC:	natural phosphatidylcholine/ 1-palmitoyl-2-oleoyl-sn-glycero-3-phosphocholine (CAS: 8002-43-5)
NR:	nanoreactor
NR+:	active vesicles with WT-OmpF, or unmodified OmpF inserted
NR-:	active vesicles without OmpF
NRC:	active vesicles with OmpF-C inserted
OG:	octyl-glucopyranoside; a detergent
OG488:	Oregon Green 488 MI (CAS: n.A.)
OPOE:	octyl-polyethyleneoxide; a detergent

OmpF:	outer membrane protein F (prefixes of the type X#Y indicate the position where amino acid X was replaced by Y)
OmpF-C:	OmpF conjugate (OmpF-M with something attached to its thiol groups)
OmpF-M:	OmpF mutant (as opposed OmpF-WT)
OmpF-WT:	natural occurring variant of OmpF
PBS:	phosphate buffered saline
PCR:	polymerase chain reaction (reproduction and mutation of plasmids)
PDI:	polydispersity index (In case of polymers: 1 = no weight distribution; controlled polymerisations PDI=1 – 2; in case of particles it is defined differently and >0.2 refers to small size distribution)
PDMS:	polydimethylsiloxane
pI:	isoelectric point (= pH at which a protein or peptide has a net charge of 0)
PICsome:	poly ion complex polymersomes
pKa:	acid dissociation constant (= logarithmic acid strength)
PMDETA:	pentamethyl-diethylenetriamine; a ligand
PMOXA:	*poly*(methyl-oxazoline)
PNIPAAM:	poly(N-isopropyl acrylamide)
POPS:	1-palmitoyl-2-oleoyl-*sn*-glycero-3-phospho-L-serine (sodium salt); an unsaturated lipid with a negative net charge
Rh:	hydrodynamic radius
SLS:	static light scattering
SM:	sphingomyelin; an unsaturated lipid
τ_2:	diffusion time of the vesicle (τ_1 diffusion time of free dye)
TDOC	sodium taurodeoxycholate hydrate (CAS: 207737-97-1); a cholesterol derivative and detergent
TEM:	transmission electron microscopy
TF:	triplet fraction (of an excited fluorophore)
TFA:	trifluor acetic acid
TG-I:	ThioGlo-1 (CAS: 137350-66-4)
THF:	tetrahydrofuran
TIPS:	tri-isopropyl-silane
TLC:	thin layer chromatography (silica coated plates)
TrisCl:	tris(hydroxymethyl)aminomethane hydro chloride

TrtX   TritonX-100; polyethylene glycol *tert*-octylphenyl ether (CAS: 9002-93-1)

vol%   volume percent

wt%   weight percent

2YT: LB medium with double the amount of yeast extract and tryptone

I Introduction

1.1 Application of nanotechnology

Nanotechnology can be any technology based on nanoscale structures. It is therefore a vast, interdisciplinary field combining chemistry, biology, material sciences and physics ranging from very simple concepts such as nanoscale grains of reagents over nanostructured surfaces to complex nanoreactors (elaborated below). While huge progress was made in this field, such as microchips being downsized to nanotechnology,[1] many concepts are yet too complicated to be realised in particular nanoreactors and nanobots.

Most of the **applied nanotechnology** relies on simple concepts such as surface modifications and nano-composites. The most prominent examples are air-tight plastic;[2] water-repellent[3] and scratch-proof surfaces;[4] but also more complex structures with unique absorption, electric and optical properties.[5]

Another growing subcategory are **bioinspired systems** such as surface-coatings applying the lotus-effect[6] and ultra-strong materials based on the example of the structure of oyster[7] and silk[8]. However, nature had always a knack for intricate structures and finely tuned interactions, which we still struggle to understand and even more so to reproduce in a simplified form. Even the most complex artificial systems are compared to their source of inspiration like a child's drawing compared to the real object.

Nanoreactors and -sensors belong to the particularly challenging research goals. While nanotechnology has been used to create especially fine powder mixtures with faster reactions due to a larger surface[9] e.g. for rocket engines,[10] a nanoreactor would require at least a catalyst and a defined reaction space. In order to qualify as nanotechnology, either the catalyst itself or its supporting structure would need to be on the nanoscale (**Fig. 1**). The latter could be anything that contains the catalyst, protects it from the environment, or alters diffusion to and from the catalyst. In case of metal-clusters and zeolites the size and shape results often in a unique reactivity and selectivity,[11] these structures are mostly catalysts on their own.[12] A more recent approach is to encapsulate the catalyst in nano-compartments creating artificial cells or more precisely **artificial organelles**. This promising branch of nanoreactors is elaborated in the following chapters as it is the foundation of this thesis.
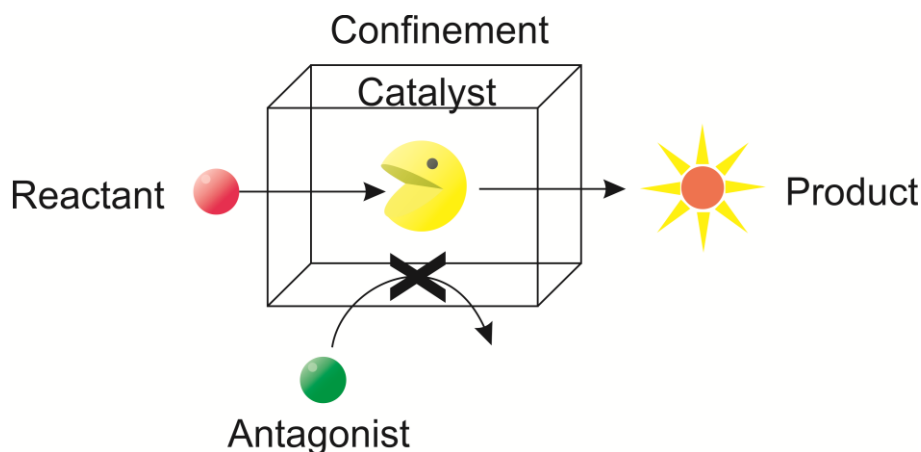
Fig. 1: schematic of a nanoreactor; the nanoreactor is a catalyst in a confined space that allows the reactant to enter and the product to leave but does not allow any antagonist (catalyst poison), undesired reactant or side-product to enter/leave.

1.1.1 Nanoreactors

While chemistry is a very old, yet incredibly fast growing field, many reactions found in nature are still extremely challenging to reproduce (e.g. nitrogen fixation[13] or photocatalytic water oxidation[14] under ambient conditions). Nature's success and probably its very origin is based half on catalysis and half on compartmentalisation.[15] Catalysis tunnels through activation energy barriers, effectively opening new reaction pathways and providing different products. Compartmentalisation on the other hand is the ability of cells and organelles, but also of enzymes themselves to select substrates, bringing them into proximity, so that they can react preventing side reactions and removing the product avoiding thereby back reaction and catalyst poisoning (blocking the active centre with reaction products). Forcing two reagents into proximity similar to the transition state of a reaction can be seen as a form of catalysis increasing the reaction speed and altering the selectivity. Moreover, cells are able to control when reactions take place and to what extent.

While catalysis made huge progress in the last 100 years, the other half (creating well defined reaction spaces) saw far less progress. Nanotechnology is promising to change this by creating **artificial cells** and organelles serving as nanoreactors. Nanoreactors are in the broadest sense nanoscale compartments with a catalytically active entity encapsulated inside. The compartment has to serve a purpose, such as controlling access of the reaction site (changing selectivity and controlling the activity), and/or shielding the catalyst from the environment. However, there is no strict limit to the nanoscale, as multiple units could be combined to a macroscopic structure. Biological cells are

macroscopic and contain typically organelles for special purposes, such as energy production, the Mitochondria contain otherwise hazardous radicals so that they do not harm the cell as a whole.[16]

Nanoreactors were originally regarded as artificial cells, but resemble more closely organelles in their size, their specialisation and lack of controlling and reproducing units. However, many approaches are based on polymeric vesicles (see **1.2 Nanostructures; Fig. 2**) whose membranes relate in their assembly mammalian cell membranes. This type of nanoreactor will be the only one further discussed in the rest of this thesis.

Encapsulating catalysts, in particular enzymes can change the catalytic behaviour and frequently improve their stability.[17] A long shelf-life and high resilience towards the environment makes nanoreactors promising tools for nanosensors (as described in the following chapter).[17b, 17d, 18]

While nanoreactors can be used for drug delivery (in the sense of enzyme replacement therapy, as discussed in **1.1.3 Drug Delivery**), they are not designed to release their cargo, unlike vesicles and micelles made specifically for drug delivery. Although it is fairly straightforward to encapsulate enzymes or catalysts shielding them from the environment (preventing aggregation, degradation through direct contact to harsh environments, catalyst poison, proteases or immune response…), creating precise structures with well-defined reaction spaces is an entirely different story: Controlled encapsulation of different entities in the same cavity, attaching entities on only one side of a membrane or controlling the orientation within the membrane are major challenges.[19] One of the most pressing challenges is **diffusion control:** controlling what enters or leaves the reaction space and when it does.

Polymersome (artificial vesicles/hollow spheres, described in **1.2 Nanostructures**) nanoreactors have to date no practical application, since the technology is still in its infancy, but also due to the fact that their production is currently hard to scale up and the incorporated biomolecules are rather costly to produce. Thus, they are ill-suited for large scale reactions. However, they are very interesting for special purposes. They would allow complex and very selective reactions on small scale or they could be used whenever compartmentalisation is required either to protect the inside (the catalyst or reactive intermediates) or outside (immune response, harmful intermediates…). This would be particularly of interest for samples with very complex matrices (many substances that could interfere) or sensitive environments (human body). They are thus lending themselves to applications such as nanosensors and biomedical uses.

1.1.2 Nanosensors

While nanosensors are in principle a broad topic ranging from AFM-tips over quantumdots,[20] to labelled DNA that identifies targeted DNA via charge transfer.[21] Nano-sensors in context of this thesis refer to nanoreactors that react with certain substrates or indicate their location. They could be used for example as dipsticks or as countermeasures against theft and counterfeit. A key aspect is the long-term stability of these nanoreactors. Encapsulation of enzymes has been proven to significantly increase their lifespan.[17c, 22] Moreover, encapsulating gels could prevent the drying process that would denaturate the involved enzymes.[17a, 17b]

1.1.3 Drug delivery

Drug delivery is the art of directing biologically active molecules such as drugs or enzymes to specific parts of the body. Excretion, digestion, immune response and misplacement of these entities are among the most important complications.[23] The common solution is to bind the active entities (mainly drug molecules or enzymes) together[24] and to shield the active entities if required from the body's defences, in particular enzymes and antibodies. The most common solutions for protecting molecules include: micelles, dendrimers and vesicles.[25] They may moreover solubilise otherwise too hydrophobic drugs and prevent them from distributing indiscriminately over the body. The added size plays an important role too, since smaller molecules (<10nm) diffuse more readily whereas larger molecules cannot pass through the filtering system of the kidneys and are therefore not excreted by them. Particles larger than 100nm are cleared by the reticuloendothelial system (being swallowed by macrophages).[26] Beyond the extended circulation time within the bloodstream, there is another important advantage of nanoparticles in the range of 10-100nm, regarding cancer tissue. Due to the rapid and chaotic growth of tumours, blood vessels are often built with defects. These cracks allow larger particles to diffuse into the tumour and accumulate there, whereas healthy tissue is far less exposed. This effect is called **EPR-effect** (enhanced permeability and retention).[26] It allows releasing the payload of the nanoparticles in the tumour tissue, decreasing the collateral damage of the often very damaging anti-tumour medicine (which hinders cell growth, which affects primarily fast growing cells). The latter does only damage to healthy cells, if it is released in healthy tissue, or is able to diffuse from the tumour to healthy tissue before it is absorbed into cells.

On the other hand, molecules of more than 100nm are targeted by phagues[26] and hence recognized by the human immune system as a foreign body and triggering therefore its defence mechanism. In

particular liposomes (elaborated in the following chapter) suffer absorption of blood-plasma proteins on their surface. Of these proteins, opsonins tag the nanoparticles to be phagocytosed by Kupffer cells.[27] For this reason the surface of the drug carrier may be modified to increase the compatibility with the organism e.g. PEGylation for "stealth"[28]. Also, the surface may be spiked with functional groups that resemble those found in specific tissue such as RGD-cyclic peptides[29] giving it the appearance of a certain cell type or by antibodies binding to specific tissue.[30] In either case the aim is to accumulate the drug carrier in the target tissue. Once the drug is released it tends to diffuse into the cells nearby. Although nanoreactors and polymersomes are fairly new, they are close to be employed as drug delivery vehicles.[31] The advantage of such systems would be that several properties could be united: a certain size for EPR-effect and surface functionalisation causing accumulation of the drug in target tissue combined with release or activation of the drug by a combination of different stimuli such as pH, [32] redox-potential[33] and temperature, [34] but also external forces[35] applied to the body part in question.[36] A further advantage of these carriers would be that they could harbour at least two different drugs that work by different mechanisms thereby overcoming e.g. tumour drug-resistance[37] working as a combination therapy.[38] Finally, it facilitates the combination of drug delivery with sensor applications: so-called **Theragnostics** (derived from therapy and diagnostics).

Comparing polymersomes for drug delivery with nanoreactors, the latter are more suited for **enzyme replacement therapy**, which is a promising concept, but usually suffers from poor uptake of the enzymes and even more so from activity loss in biological environments (blocked e.g. by antibodies, digested by proteases…).[39] A polymersome as a shell could solve both problems at once. Cellular uptake of polymersomes has been achieved and even the delivery of enzymes retaining their activity was reported.[40] As useful as these modular systems are, the disadvantage of these systems in pharmaceutics is that every variation requires a new admission procedure. Yet, polymersomes are close to be employed in drug delivery.[31] and were further investigated for numerous applications including on site production of antibiotics[41] or treatment of reactive oxygen species.[42]

1.2 Nanostructures

Among the potential structures, membranes, micelles, vesicles and dendrimers are the most notable examples. While in context of this thesis only vesicles are truly relevant, most of these structures are related and hence tend to coexist. The exception are dendrimers, which are formed through a multi-step chemical synthesis and result due to the branching of the building blocks in tree or spherical structures (with the density increasing towards the surface).[43] Due to their shape, they offer a great

surface for attaching drug-molecules, catalysts etc. and solubilise them, or shield enzymes, by attaching branches of PEG.

Micelles, membranes and vesicles share the same basic processes in their formation. They are the structures that will be further explored in this chapter. All three are based on the self-assembly of amphiphilic molecules. The driving force behind is the reduction of the exposed hydrophobic surface in aqueous environments. Which structure is ultimately formed depends on various factors.

Amphiles consist of a polar- and an apolar group. Especially in case of lipids, the polar/hydrophilic section is often referred to as head and the apolar/hydrophobic section as tail since it is significantly longer. Isolated amphiphiles are typically not very soluble in water.
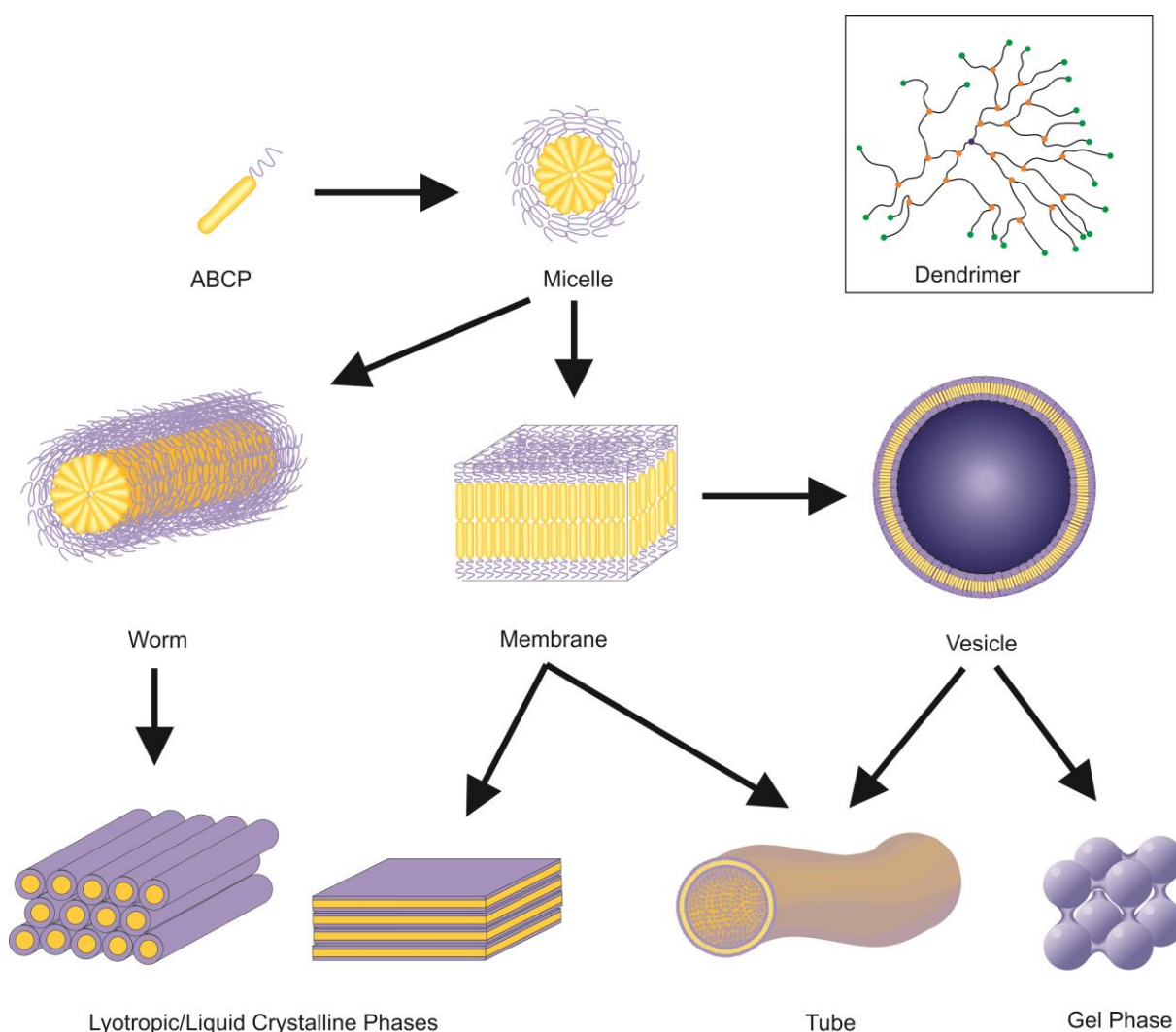
Fig. 2: Overview of the relevant structures; all but the Dendrimer are the result of the self-assembly of ABCPs. The ABCP-concentration increases from top to bottom, with the highest concentration being the lyotropic crystalline phase (dried/precipitated structures) followed by gels of fused vesicles. The diagram does not necessarily represent the precise pathway, nor does it represent all possible self-assemblies.

I Introduction

1.2.1 Micelles and Worms

Both lipids and amphiphilic blockcopolymers (ABCPs) form micelles in the size of 10-100nm (latter rather ABCPs, due to their greater length).[44] Only materials that have a purely hydrophobic surface can be encapsulated in micelles. Apart from encapsulating drugs and proteins, micelles are employed extensively in green chemistry.[45] In these cases water is used as solvent and the reactions benefit through high local concentration due to the lipophilic substrates. Furthermore the catalyst recycling is often simple and straightforward.[45] To mention some examples: Heck-,[46] Suzuki-,[46] metathesis-[47] and ATRP[47] reactions were carried out in micellar reactors. Micelles are also used for the generation of catalytically active metal nanoparticles.[48] Speaking of green chemistry it is often impossible to tell which of these systems are genuine nanoreactors, since the research groups were often only interested in the functionality and not in the structure. Micellar nanoreactors are thus facile to produce but suffer of the restriction to hydrophobic loads and the dependence of the stability on the amphiphile concentration.

Worms have the same cross section as micelles but lack the rotational symmetry. Instead, the slabs of aggregated amphiphiles are stacked on each other. Due to their small diameter, but high mass, they could be interesting for drug delivery regarding cellular uptake and retention time.[49]

Both structures are not suited for the scope of this thesis, but relevant as side products potentially influencing the experiments. Especially micelles tend to coexist with vesicles, as they are formed prior vesicle-formation.

1.2.2 Membranes

Two dimensional assemblies of amphiphiles form monolayers that are usually formed at interfaces, mainly water-air border. They have typically a hydrophobic core and a hydrophilic surface. In case of lipids the individual lipids are assembled in parallel. Often the membrane folds on itself so that the amphiphiles contact tail to tail forming a double membrane (**Fig. 2** and **Fig. 4**). If the assemblies become even more crowed, the layers can be stacked to multiple layers and even precipitate as solids (**Fig. 2**).[50]

Due to the weak intermolecular interactions, macroscopic membranes are very weak, but they can be stabilised on surfaces. Such supported membranes are of particular interest in combination with inserted membrane proteins (**MPs**, further reading, see chapters **1.3.1 self-assembly** and **1.5**

permeability) for filtration[51] and nanosensors as they are able to restrict diffusion from one side to the other and are able to maintain the functionality of nonporous membrane proteins such as transport proteins and sensor-proteins.

At the end of the plane, membranes have edges where the hydrophobic surface would be exposed. However, it can be assumed that the amphiphiles are forming conformations similar as found in micelles and worms to minimise the exposure. Alternatively, they can fuse their ends together and form tubes or vesicles (see the following chapter).

Membranes were found to catalyse reactions without additional catalysts through a hydrophobic effect (similar to micelles). It has been suggested that the reactivity of hydroxyl ions increases within membranes because of their limited possibilities to carry a solvate hull inside the membrane, thus appearing as *naked ions*.[48]

1.2.3 Vesicles and Tubes

If the membrane is sufficiently large, another possible way of reducing the edge exposure emerges, namely the membrane fusing with itself on its edges forming tubes or vesicles. These structures feature in addition to their hydrophobic membrane an aqueous internal compartment. Vesicles are hence hollow spheres surrounded by a membrane without beginning or end.

Vesicles are particularly suited for nanoreactors due to their cell-like nature. Based on liposomes the assembly is identical to mammalian cells (disregarding the numerous membrane proteins). They are thus a good starting point for biomimicry. Depending on the used amphiphiles the resulting vesicles are referred to as **liposomes** (using lipids) or **polymersomes** (using amphiphilic blockcopolymers).

PICsomes[52] are a special case, where the self-assembly does not depend on the hydrophobic effect, but on the combination of two oppositely charged molecules forming poly-ion-complexes compensating the over-all charge. Strictly speaking, they are not composed of ABCPs, but do consist of blockcopolymers whose blocks are immiscible. Due to their nature, they are porous and unable to insert MPs.

Vesicles keep their cargo in the hydrophilic core but also possess the ability of inserting hydrophobic entities within the hydrophobic part of the membrane formed by the amphiphiles trying to hide their hydrophobic parts from the aqueous environment.[31] The first liposomes were described in 1965[53] and the first polymersomes in 1995.[54]

Please note: depending on the context *liposome*, *vesicle*, or *polymersome* will be used. Similarly, *Lipid*, *amphiphile* and *amphiphilic blockcopolymer/ABCP* will be used, with *vesicle* and *amphiphile* referring to cases that apply for both liposomes and polymersomes. Else it will be referred specifically to *lipids* and *ABCPs* respectively.

The typical vesicle size lies between 50nm[55] and 200µm[56] diameter (both lipid or polymer based vesicles). Larger vesicles[1] are formed through electroformation.[57] Vesicles can do the same chemistry as micelles, in that they offer a similar hydrophobic domain, but have the advantage of possessing both a hydrophilic and hydrophobic region. Considering the possibility of functionalizing the outside as well, vesicles offer three distinct and separated regions for reactions (the hydrophilic inside- and outside areas and the hydrophobic membrane itself).

Tubes relate to vesicles as worms relate to micelles as they share the same cross-section but not the rotational symmetry. Thus, amphiphiles aggregate as in the cross section of vesicles but are stacked together forming a tube. While tubes may be too small for nanoreactors, they are none the less interesting for drug delivery.[58]

Vesicles on the other hand are due to their structure the most versatile class for nanoreactors and are ultimately the only structure considered for the experimental part of this thesis. They provide a stable compartment with an almost impenetrable membrane which is moreover suited for embedding membrane proteins.

---

[1] For our *b*-PMOXA-*b*-PDMS-*b*-PMOXA the vesicle size achieved by film rehydration does not exceed ca. 200nm.

1.3 Permeability of vesicle membranes.

The self-assembled structures possess a temperature dependent permeability, since the interactions of the hydrophobic segments are temperature dependent.[59] Similar to the glass transition temperature (**TG**) of solid polymers, which makes polymers soft, there is a certain temperature, when the membrane becomes more fluid.[60] Liposomes tend to be more fluid since they are built of lipids with shorter hydrophobic blocks that are moreover often unsaturated resulting in bent conformations (cis-fatty acids) and overall less densely packed membranes.[61] Similar assumptions can be made for polymersome membranes, however the factors influencing their stability and permeability still require more fundamental studies.[2] However, one of the main research topics for polymersomes is how to introduce permeability or stimuli responsiveness for applications as nano-rectors, sensors or applications in medicine.

1.3.1 Release

While the functionality of **nanoreactors** is typically defined by what was encapsulated, the membrane can be functionalised as well with equal impact on the functionality. This is particularly true for modifications that change the permeability of the membrane. For stimuli responsiveness often the same approaches were tried as those that found use in drug delivery.[62] However, with the additional limitation that the overall architecture need to remain intact rather than reversible disassembly leading to a chaotic rearrangement of the ABCP.

In case of **drug delivery** the majority of the release is triggered by disruption of the structure by polarity changes, which include swelling of the hydrophobic part, reversible dissolution or even decomposition (e.g. by splitting the hydrophilic from the hydrophobic blocks).[62a, 63] They are thus able to release their payload, but due to fundamental changes in the architecture of the macromolecular assemblies, the process is often irreversible in that the cargo remains outside and the size-distribution of the structures changes.[62a, 63-64] The triggers for these changes include pH-changes,[65] temperature-changes,[66] fragmentation by reduction[67] or a combination of salt and pH response.[68]

---

[2] It would be interesting to know how AB in ABA distribute within a polymersome and influence insertion of MPs, the stability of vesicles and how they interact with detergents. Similarly, it would be interesting to know if and how detergents interact differently with polymersomes compared to liposomes; however, unlike the prior question it cannot be easily measured via labelling experiments, since it is not only a question of distribution but could possibly affect the entire equilibrium of structures in solution.

1.3.2 Induced porosity

In polymersomes, an important factor influencing the permeability is the combination of blocks. The different diameter of the polymer blocks may create porosity or force the amphiphile to adapt different shapes. The polymer chain might coil up, angle up to the hydrophilic block, or the amphiphiles form interlocking structures. All of these possibilities reduce the thickness of the membrane. It can therefore be observed that polymersomes have membrane of similar thickness as liposomes, although, the amphiphiles are considerably longer.[69]

So far membranes have been made permeable for substrates by deliberately creating defects disturbing the dense packing of the hydrophobic blocks[70] or generating holes through decomposition of domains.[63a, 71] Also, the packing of the hydrophobic blocks can be temporarily disturbed by creating charges.

A possible solution to the problem of drastic structural changes is **crosslinking** of the ABCPs. Then, even if the hydrophobic block turns completely hydrophilic (through changes in pH, temperature),[63a, 71-72] the vesicular structure remains. The membrane thus transforms into a swelled state, or into a gel-state allowing up to 10nm/25kDa macromolecules to pass through.[63a, 63b, 71] Many crosslinked systems have less dense membranes than other polymersomes, thus they are often permeable to small molecules even without swelling.[63b, 73] This effect has been used for nanoreactors.[74]

A more refined method of controlling the pore size takes advantage of the fact that hydrophobic molecules can be embedded within the membrane, forming channels across the membrane. To date the molecules of choice are membrane proteins.

1.3.3 Membrane proteins

The ideal NR allows only the smaller enzyme substrate and product to diffuse through its membrane, once the correct stimuli is applied, thereby avoiding side-reactions and catalyst deactivation/degradation by excluding substances that are chemically similar to the substrate. Hence, establishing control over diffusion is still by far the most challenging and essential task.

Nature developed for the purpose of diffusion control a great variety of sophisticated membrane proteins with either active or passive transport.[75] They contribute up to 80% of the dry-weight of the membrane and 30% of the cells genome is reserved for them underlining their relevance.[76] A great

variety of different types of Membrane proteins have been developed by nature, some allow passive diffusion of small molecules (e.g. OmpF),[77] others the passive diffusion of specific molecules (AqpZ, Valinomycin).[78] Both types can be referred to as porins. In contrast hereto, many pores allow diffusion only after being triggered by a signal molecule (acetylcholine receptor M2),[78b], or actively translocate the molecules to the other side, via gradient driven diffusion as cotransport/symporter (SGLT)[79] or antiporter (MRP)[80] and specific pumps (ATPase)[81] and transporters of specific large molecules (ABC).[82]

This lends itself to defined permeability of polymersome membranes that does not disrupt the nanoarchitecture through insertion of MP. Once reconstituted in polymersome membranes ,MPs such as AqpZ, LamB, OmpF, Tsx and FhuA[83] and membrane penetrating peptides such as gramicidin[51b, 84] have essential impact on membrane permeability towards small molecular weight molecules and ions.[85]. The choice of membrane protein determines reactivity and selectivity of NRs.[86]. However, most of the investigated MPs are porins without stimuli response and limited selectivity towards the molecules allowed to diffuse through the pore. Mostly the restriction is based on a molecular weight cut-off caused by the pore diameter.

Membrane proteins are adapted for thinner membranes (5nm), but polymer-membranes are far from being static, meaning that they can adjust their shape and thus their thickness. Furthermore, polymerisation produces different chain-lengths. It has been proposed that the shorter chains tend to aggregate around the proteins in order to reduce the strain on the system.[87] Theoretical calculations indicate the importance of the chain flexibility.[87-88] Furthermore, PDMS is known for its flexibility allowing the membrane to adapt.[89] It can nevertheless imply a significant strain on the protein structure. Paradoxically it was found that this increased the activity of the NADH:Ubiquinone Oxidoreductase.[90]

Table 2: List of reported membrane proteins inserted in blockcopolymer membranes

Block copolymer	Polymer type	Membrane protein	Study	Reference
PMOXA-*b*-PDMS-*b*-PMOXA	Triblock ABA	AqpZ	Water-selective permeability	Kumar *et al.* 2007[91]
				Wang *et al.* 2012[92]
				Grzelakowski *et al.* 2015[93]
			mobility of various MPs in polymer membranes	Itel *et al.* 2015[94]
		NtAqp1	CO_2 -selective permeability	Uehlein *et al.* 2012[95]
		bR	Proton transport	Ho *et al.* 2004[96]
		FhuA	Reduction triggered release	Onaca *et al.* 2008[33a]
		GlpF	selective detection of sugars	Zhang *et al.* 2016[97]
		Gramicidin	Monovalent cation-selective permeability	Lomora *et al.* 2015[84b]
		Ionomycin	Divalent cation-selective permeability	Lomora *et al.* 2015[84a]
		KcsA	mobility of various MPs in polymer membranes	Itel *et al.* 2015[94]
		LamB	Virus assisted DNA loading into polymersomes	Graff *et al.* 2002[98]
		MspA	membrane–protein interaction	Morton *et al.* 2015[99]
		NADH-ubiquinone reductase (complex 1)	Complex 1 activity – electron transfer	Graff *et al.* 2010[90]
		OmpF	Size-selective permeability	Nardin *et al.* 2000[100]
				Ranquin *et al.* 2005[101]
				Grzelakowski *et al.* 2009[102]
				Dobrunz *et al.* 2012[103]
				Langowska *et al.* 2013[41]
				Langowska *et al.* 2014[104]
			mobility of various MPs in polymer membranes	Itel *et al.* 2015[94]
			HRP kinetics	Baumann *et al.* 2017[18]
			Stimuli responsive OmpF modifications	Ihle *et al.* 2011[105]
				Einfalt *et al.* 2015[32a]
				Edlinger *et al.* 2017[17d]

Block copolymer	Polymer type	Membrane protein	Study	Reference
PMOXA-*b*-PDMS-*b*-PEO	Triblock ABC	AQP-0	Directed insertion of Aquaporin	Stoenescu *et al.* 2004[19b]
PEtOz-*b*-PDMS-*b*-PEtOz	Triblock ABA	bR and ATPase	ATP production	Choi *et al.* 2005[106]
PIB-*b*-PEO-*b*-PIB	Triblock BAB	FhuA	Size-selective permeability	Muhammad *et al.* 2011[107]
PEO-*b*-PB	Diblock AB	AQP-0	Water-selective permeability	Kumar *et al.* 2012 [108]
		αHL	Ion conductivity	Zhang *et al.* 2013[109]
PMOXA-*b*-PDMS	Diblock AB	MloK1	K$^+$- selective permeability	Kowal *et al.* 2014[110]
PMOXA-*b*-PDMS /DPPC	1)	MloK	Inserting MPs exclusively in Polymer-domains	Kowal *et al.* 2015[111]

1)   = same diblock AB as domains in lipid-membranes

1.3.4 Modified MPs

Most nanoreactors have no stimuli-responsiveness. Up to date only few of the artificial systems for diffusion control (in lipo- and polymersomes) go a step further in the design, as for example channel proteins having an attached responsive molecular cap based on a labile bond, which hinders the diffusion of molecules through the pore until it is cleaved off. Stimuli responsive protein pores were designed to react to external changes in pH (OmpF[32a]) or reduction potential (FhuA[33] and OmpF).[32a] Other groups introduced mutations in order to create charge repulsion in the channel interior (OmpF),[105] or introduced an ELP-loop whose water solubility is temperature dependent (αHL[34]).

Only few of these approaches allow a reversible response; moreover, the stimuli responsiveness cannot be readily altered or transferred to a system based on a different MP. Moreover, charge repulsion alone lacks conformational changes to block other molecules than those bearing the same charge. A more versatile approach is to attach a stimuli responsive group via straight forward click chemistry at the channel entrance or its narrowest point.

So far, this was only reported to have worked for irradiation triggered systems, in particular ion channels (αHL,[35a] nAChR, GrA, IGluR, MscL, ChR2 and Shaker K$^+$ Channel[35b]). However, up to date only the reversibility of the stimuli responsiveness was investigated and none of them was used in the context of NRs, probably since selective ion channels are unsuitable for the transport of enzymatic substrates.

As described, many elaborate designs were conceived, yet a simple, modular and scalable solution is desired to achieve a nanoreactor system with a reversible pore opening and closing. The advantage of a system with a reversible plug is that it is not restricted to a single activation, but can be deactivated again and that, over many cycles, allows long-term usage of nanoreactors/sensors. While the stimuli-response does not stop any reaction within the polymersome directly, it allows the suppression of the in- and out-flow, thereby controlling reaction and release of product.

2 Aim of the thesis

Great attention has been dedicated to the fabrication of nanomaterials with precisely defined architectures and functionality in various domains such as sensors, drug delivery and nanoreactors (NRs).[62b, 112] For these particular applications it is important to create well defined reaction spaces which enable control over timing and selectivity of the reactions by controlling what enters and when it enters the compartment.[83, 112a] In this context the development of a gate that opens and closes on demand would be a major advance. Such a gate needs to be able to allow molecules to diffuse through independently of their chemical nature in its open state (excluding for example diffusion control by charge repulsion).

Like most work in this field, the concepts are bioinspired, attempting to replicate the function of cell membranes and their membrane proteins. Such a nano-device has to consist at least of a tunnel that can be inserted into various membranes of artificial cells/organelles and a stimuli responsive part acting as a gate. Many membrane proteins would serve well as tunnel, however MPs are in their nature restrictive towards the substrates that are allowed to diffuse across the membrane, by setting a molecular weight cutoff with their minimal tunnel diameter and due to their net charge create further, unintended restrictions. Therefore, making elaborate modifications to one specific membrane protein in order to achieve the goal, would merely create a niche-solution. Thus, a modular approach consisting of various stimuli responsive groups that can be linked to various different membrane proteins would be desirable (**Fig. 5**); as it would enable a plethora of different gates tailored according to the individual applications; allowing choosing a class of substrates and a stimulus by combining the right modules.

This novel approach will be exemplified in this thesis on well-established OmpF membrane proteins in combination with various stimuli responsive groups. In order to achieve this, the challenge of finding both a suitable experimental set-up and at the same time finding an adequate analytical method had

to be overcome. Suitable membranes had to be found; various methods of inserting OmpF had to be tried and various dyes and enzymes had to be encapsulated enabling the detection of diffusion (release experiments or enzyme assay see).
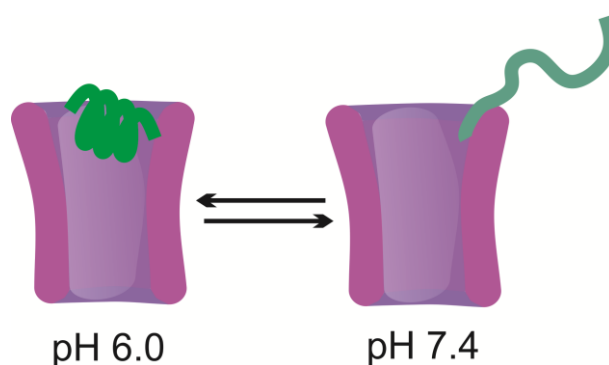
Fig. 5: concept of blocking and opening the pore (magenta) via stimuli responsive group (green)

3 References

[1]   *smallest Transistor*, http://www.bbc.com/news/technology-29066210, accessed: 12.05.2016.
[2]   *Air tight plastic nano composite*,
        http://www.tahan.com/charlie/nanosociety/course201/nanos/AJ.pdf, accessed: 12.05.2016.
[3]   *water repellent surface modifications*, http://ultrahydrophobiccoating.com/, accessed:
        12.05.2016.
[4]   *Scratch proof surface modifications*, http://nanostate.co/, accessed: 12.05.2016.
[5]   a) *Nanooptics*, https://en.wikibooks.org/wiki/Nanotechnology/Nano-optics, accessed:
        12.05.2016;
        b) *Nano Technology Overview*, http://www.understandingnano.com/nanotech-
        applications.html, accessed: 12.05.2016.
[6]   *Lotus Effect*, http://pubs.rsc.org/en/content/articlelanding/2012/sm/c2sm26655e, accessed:
        19.07.2016.
[7]   a) A. Walther, I. Bjurhager, J. M. Malho, J. Ruokolainen, L. Berglund and O. Ikkala,
        Angewandte Chemie-International Edition 2010, 49, 6448-6453;
        b) A. Walther, I. Bjurhager, J. M. Malho, J. Pere, J. Ruokolainen, L. A. Berglund and O. Ikkala,
        Nano Lett 2010, 10, 2742-2748.
[8]   J. G. Fernandez and D. E. Ingber, *Adv Mater* 2012, 24, 480-484.
[9]   a) *Reaction Kinetics and Thermodynamics of Nanothermite Propellants*,
        http://ci.confex.com/ci/2005/techprogram/P1663.HTM, accessed: 12.05.2016;
        b) Thermite for military applications,
        http://web.archive.org/web/2014331085212/http://ammtiac.alionscience.com/pdf/AMPQ6,
        accessed: 12.05.2016
[10]   a) *Al for Rocket engines*, http://what-when-how.com/nanoscience-and-
        nanotechnology/metallic-nanopowders-rocket-propulsion-applications-part-1-
        nanotechnology/, accessed: 12.05.2016;

b) *AFOSR and NASA Launch First-Ever Test Rocket Fueled by Environmentally-Friendly, Safe Aluminum-Ice Propellant*, http://www.wpafb.af.mil/news/story.asp?id=123164277, accessed: 12.05.2016.

[11]   a) S. Cao, F. Tao, Y. Tang, Y. Li and J. Yu, *Chem Soc Rev* 2016, 45, 4747-4765;
b) C. B. Khouw and M. E. Davis, *Shape-Selective Catalysis with Zeolites and Molecular Sieves*. In Selectivity in Catalysis, American Chemical Society: 1993; Vol. 517, 206-221.

[12]   a) G. J. Hutchings, *Nat Chem* 2010, 2, 1005-1006;
b) B. C. Gates, *Chemical Reviews* 1995, 95, 511-522.

[13]   T. Oshikiri, K. Ueno and H. Misawa, *Angew. Chem. Int. Ed.* 2014, 53, 9802-9805.

[14]   R. Brimblecombe, G. F. Swiegers, G. C. Dismukes and L. Spiccia, *Angewandte Chemie-International Edition* 2008, 47, 7335-7338.

[15]   R. J. R. W. Peters, M. Marguet, S. Marais, M. W. Fraaije, J. C. M. van Hest and S. Lecommandoux, *Angewandte Chemie-International Edition* 2014, 53, 146-150.

[16]   a) F. Muller, *J Am Aging Assoc* 2000, 23, 227-253;
b) D. Han, E. Williams and E. Cadenas, *Biochem J* 2001, 353, 411-416.

[17]   a) A. A. Homaei, R. Sariri, F. Vianello and R. Stevanato, *Journal of Chemical Biology* 2013, 6, 185-205;
b) U. Guzik, K. Hupert-Kocurek and D. Wojcieszyńska, *Molecules* 2014, 19, 8995;
c) A. Kuchler, M. Yoshimoto, S. Luginbuhl, F. Mavelli and P. Walde, *Nat Nanotechnol* 2016, 11, 409-420;
d) C. Edlinger, T. Einfalt, M. Spulber, A. Car, W. Meier and C. G. Palivan, *Nano Lett* 2017, 17, 5790-5798.

[18]   P. Baumann, M. Spulber, O. Fischer, A. Car and W. Meier, *Small* 2017, 13, 1603943.

[19]   a) G. Delaittre, I. C. Reynhout, J. J. L. M. Cornelissen and R. J. M. Nolte, *Chemistry – A European Journal* 2009, 15, 12600-12603;
b) R. Stoenescu, A. Graff and W. Meier, *Macromolecular Bioscience* 2004, 4, 930-935.

[20]   M. A. Reed, J. N. Randall, R. J. Aggarwal, R. J. Matyi, T. M. Moore and A. E. Wetsel, *Phys Rev Lett* 1988, 60, 535-537.

[21]   *molecular beacon single stranded DNA detection*, http://www.genelink.com/newsite/products/mbintro.asp, accessed: 12.05.2016.

[22]   D. M. Vriezema, P. M. L. Garcia, N. S. Oltra, N. S. Hatzakis, S. M. Kuiper, R. J. M. Nolte, A. E. Rowan and J. C. M. van Hest, *Angewandte Chemie-International Edition* 2007, 46, 7378-7382.

[23]   K. Park, *Controlled Drug Delivery: Challenges and Strategies*, American Chemical Society, 1997.

[24]   a) R. Haag and F. Kratz, *Angew. Chem. Int. Ed.* 2006, 45, 1198-1215;
b) Y. Wu, D. Y. W. Ng, S. L. Kuan and T. Weil, *Biomaterials Science* 2015, 3, 214-230;
c) H. C. Wang, Y. F. Zhang, C. M. Possanza, S. C. Zimmerman, J. J. Cheng, J. S. Moore, K. Harris and J. S. Katz, *Acs Appl Mater Inter* 2015, 7, 6369-6382.

[25]   J. Du and R. K. O'Reilly, *Soft Matter* 2009, 5, 3544-3561.

[26]   R. A. Petros and J. M. DeSimone, *Nat Rev Drug Discov* 2010, 9, 615-627.

[27]   M. J. Morilla, M. J. Prieto and E. L. Romero, *Mem. Inst. Oswaldo Cruz* 2005, 100, 213-219.

[28]   Y. Cheng and D. A. Tomalia, *Dendrimer-Based Drug Delivery Systems: From Theory to Practice*, Wiley, 2012.

[29]   T. Weide, A. Modlinger and H. Kessler, *Top Curr Chem* 2007, 272, 1-50.

[30]   *What Are Antibody-Drug Conjugates?*, http://adcreview.com/adc-university/adcs-101/antibody-drug-conjugates-adcs/, accessed: 19.07.2016.

[31]   a) J. P. Jain, W. Y. Ayen and N. Kumar, *Curr Pharm Design* 2011, 17, 65-79;
b) J. S. Lee and J. Feijen, *J Control Release* 2012, 161, 473-483;
c) Y. Yu, Z. Pang, W. Lu, Q. Yin, H. Gao and X. Jiang, *Pharm Res* 2012, 29, 83-96;
d) R. P. Brinkhuis, *Polymeric vesicles for drug delivery over the blood-brain barrier and in vivo imaging*, Dissertation, Radboud Universiteit Nijmegen, ISBN 9789090272542, 2012;
e) C. G. Palivan, R. Goers, A. Najer, X. Zhang, A. Car and W. Meier, *Chem Soc Rev* 2016, 10.1039/c5cs00569h.

[32] a) T. Einfalt, R. Goers, I. A. Dinu, A. Najer, M. Spulber, O. Onaca-Fischer and C. G. Palivan, *Nano Lett* 2015, 15, 7596-7603;
b) C. Nardin, J. Widmer, M. Winterhalter and W. Meier, *Eur Phys J E* 2001, 4, 403-410.

[33] a) O. Onaca, P. Sarkar, D. Roccatano, T. Friedrich, B. Hauer, M. Grzelakowski, A. Güven, M. Fioroni and U. Schwaneberg, *Angew. Chem. Int. Ed.* 2008, 47, 7029-7031;
b) A. Guven, M. Fioroni, B. Hauer and U. Schwaneberg, *J. Nanobiotechnol* 2010, 8, 14.

[34] Y. Jung, H. Bayley and L. Movileanu, *J Am Chem Soc* 2006, 128, 15332-15340.

[35] a) S. Loudwig and H. Bayley, *J Am Chem Soc* 2006, 128, 12404-12405;
b) M. R. Banghart, M. Volgraf and D. Trauner, *Biochemistry-Us* 2006, 45, 15129-15141.

[36] S.-H. Hu and X. Gao, *J Am Chem Soc* 2010, 132, 7234-7237.

[37] T. Thambi, J. H. Park and D. S. Lee, *Biomaterials Science* 2016, 4, 55-69.

[38] R. Bakalova, D. Lazarova, B. Nikolova, S. Atanasova, G. Zlateva, Z. Zhelev and I. Aoki, *Biotechnology, Biotechnological Equipment* 2015, 29, 175-180.

[39] B. Thingholm, P. Schattling, Y. Zhang and B. Stadler, *Small* 2016, 12, 1806-1814.

[40] a) B. Thingholm, P. Schattling, Y. Zhang and B. Städler, *Small* 2016, 12, 1806-1814;
b) M. Massignani, C. LoPresti, A. Blanazs, J. Madsen, S. P. Armes, A. L. Lewis and G. Battaglia, *Small* 2009, 5, 2424-2432;
c) S. F. M. van Dongen, W. P. R. Verdurmen, R. J. R. W. Peters, R. J. M. Nolte, R. Brock and J. C. M. van Hest, *Angew. Chem. Int. Ed.* 2010, 49, 7213-7216.

[41] K. Langowska, C. G. Palivan and W. Meier, *Chem Commun* 2013, 49, 128-130.

[42] a) P. Tanner, O. Onaca, V. Balasubramanian, W. Meier and C. G. Palivan, *Chemistry – A European Journal* 2011, 17, 4552-4560;
b) P. Tanner, V. Balasubramanian and C. G. Palivan, *Nano Lett* 2013, 13, 2875-2883.

[43] F. Vögtle, G. Richardt, N. Werner and A. J. Rackstraw, *Dendrimer Chemistry*, Wiley, 2009.

[44] C. G. Palivan, O. Fischer-Onaca, M. Delcea, F. Itel and W. Meier, *Chem Soc Rev* 2012, 41, 2800-2823.

[45] P. Persigehl, R. Jordan and O. Nuyken, *Macromolecules* 2000, 33, 6977-6981.

[46] D. Schönfelder, O. Nuyken and R. Weberskirch, *Journal of Organometallic Chemistry* 2005, 690, 4648-4655.

[47] T. Kotre, M. T. Zarka, J. O. Krause, M. R. Buchmeiser, R. Weberskirch and O. Nuyken, *Macromolecular Symposia* 2004, 217, 203-214.

[48] D. M. Vriezema, M. C. Aragones, J. A. A. W. Elemans, J. J. L. M. Cornelissen, A. E. Rowan and R. J. M. Nolte, *Chemical Reviews* 2005, 105, 1445-1489.

[49] a) B. Discher, Y. Won, D. Ege, J. Lee, F. Bates, D. Discher and D. Hammer, *Science* 1999, 284;
b) Y. Kim, P. Dalhaimer, D. A. Christian and D. E. Discher, *Nanotechnology* 2005, 16, S484-S491.

[50] G. Battaglia and A. J. Ryan, *J Phys Chem B* 2006, 110, 10272-10279.

[51] a) W. Xie, F. He, B. Wang, T.-S. Chung, K. Jeyaseelan, A. Armugam and Y. W. Tong, *J. Mater. Chem. A* 2013, 1, 7592-7600;
b) M. Kumar, M. Grzelakowski, J. Zilles, M. Clark and W. Meier, *Proceedings of the National Academy of Sciences* 2007, 104, 20719-20724.

[52] a) A. Koide, A. Kishimura, K. Osada, W. D. Jang, Y. Yamasaki and K. Kataoka, *J Am Chem Soc* 2006, 128, 5988-5989;
b) A. Kishimura, A. Koide, K. Osada, Y. Yamasaki and K. Kataoka, *Angewandte Chemie-International Edition* 2007, 46, 6085-6088;
c) A. Kishimura, S. Liamsuwan, H. Matsuda, W. F. Dong, K. Osada, Y. Yamasaki and K. Kataoka, *Soft Matter* 2009, 5, 529-532;
d) Y. Anraku, A. Kishimura, M. Oba, Y. Yamasaki and K. Kataoka, *J Am Chem Soc* 2010, 132, 1631-1636.

[53] D. W. Deamer, *The FASEB Journal* 2010, 24, 1308-1310.

[54] a) J. C. M. Vanhest, D. A. P. Delnoye, M. W. P. L. Baars, M. H. P. Vangenderen and E. W. Meijer, *Science* 1995, 268, 1592-1595;
b) L. Zhang and A. Eisenberg, *Science* 1995, 268, 1728-1731.

[55]   E. P. Holowka, V. Z. Sun, D. T. Kamei and T. J. Deming, *Nat Mater* 2007, 6, 52-57.

[56]   a) A. D. Bangham, *Liposome Letters*, Academic Press London 1983;
        b) P. W. P. L. Luisi, *Giant Vesicles*, John Wiley & Sons, Chichester 2000.

[57]   F. M. Menger and M. I. Angelova, *Accounts of Chemical Research* 1998, 31, 789-797.

[58]   a) J. D. Robertson, G. Yealland, M. Avila-Olias, L. Chierico, O. Bandmann, S. A. Renshaw and G. Battaglia, *ACS Nano* 2014, 8, 4650-4661;
        b) J.-P. Douliez, B. Pontoire and C. Gaillard, *ChemPhysChem* 2006, 7, 2071-2073.

[59]   a) M. C. Blok, L. L. M. van Deenen, J. de Gier, J. A. F. Op den Kamp and A. J. Verkleij, *Some Aspects of Lipid-Phase Transition on Membrane Permeability and Lipid-Protein Association*. In Biochemistry of Membrane Transport: FEBS — Symposium No. 42, Springer Berlin Heidelberg: Berlin, Heidelberg, 1977; Vol., 10.1007/978-3-642-66564-6_338-46;
        b) V. A. Parsegian and B. W. Ninham, *Biophys J* 1970, 10, 664-674.

[60]   R. Chandrawati, L. Hosta-Rigau, D. Vanderstraaten, S. A. Lokuliyana, B. Stadler, F. Albericio and F. Caruso, *ACS Nano* 2010, 4, 1351-1361.

[61]   R. B. Gennis, *Biomembranes: molecular structure and function*, Springer-Verlag, 1989.

[62]   a) R. P. Brinkhuis, F. P. J. T. Rutjes and J. C. M. van Hest, *Polym. Chem.* 2011, 2, 1449-1462;
        b) L. Messager, J. Gaitzsch, L. Chierico and G. Battaglia, *Current Opinion in Pharmacology* 2014, 18, 104-111.

[63]   a) I. Dinu, C. Edlinger, E. Konishcheva, C. Palivan and W. Meier, *Polymer Vesicles*. In Encyclopedia of Polymeric Nanomaterials, Springer Berlin Heidelberg: 2014; Vol., 10.1007/978-3-642-36199-9_266-11-11;
        b) J. Gaitzsch, D. Appelhans, L. Wang, G. Battaglia and B. Voit, *Angew. Chem. Int. Ed.* 2012, 51, 4448-4451;
        c) T. Z. Luo, L. R. He, P. Theato and K. L. Kiick, *Macromolecular Bioscience* 2015, 15, 111-123;
        d) F. Liu and A. Eisenberg, *J Am Chem Soc* 2003, 125, 15059-15064.

[64]   E. Cabane, X. Zhang, K. Langowska, C. Palivan and W. Meier, *Biointerphases* 2012, 7, 1-27.

[65]   a) F. Chécot, J. Rodríguez-Hernández, Y. Gnanou and S. Lecommandoux, *Biomolecular Engineering* 2007, 24, 81-85;
        b) J. Du, Y. Tang, A. L. Lewis and S. P. Armes, *J Am Chem Soc* 2005, 127, 17982-17983;
        c) H. Lomas, I. Canton, S. MacNeil, J. Du, S. P. Armes, A. J. Ryan, A. L. Lewis and G. Battaglia, *Adv Mater* 2007, 19, 4238-4243;
        d) I. K. Jeong, G. H. Gao, Y. Li, S. W. Kang and D. S. Lee, *Macromolecular Bioscience* 2013, 13, 946-953;^le) G.-Y. Liu, L.-P. Lv, C.-J. Chen, X.-S. Liu, X.-F. Hu and J. Ji, *Soft Matter* 2011, 7, 6629-6636.

[66]   F. Ahmed, R. I. Pakunlu, G. Srinivas, A. Brannan, F. Bates, M. L. Klein, T. Minko and D. E. Discher, *Mol Pharmaceut* 2006, 3, 340-350.

[67]   T. Thambi, V. G. Deepagan, H. Ko, D. S. Lee and J. H. Park, *J. Mater. Chem.* 2012, 22, 22028-22036.

[68]   a) U. Borchert, U. Lipprandt, M. Bilang, A. Kimpfler, A. Rank, R. Peschka-Süss, R. Schubert, P. Lindner and S. Förster, *Langmuir* 2006, 22, 5843-5847;^lb) M. Sauer, T. Haefele, A. Graff, C. Nardin and W. Meier, *Chem Commun* 2001, 10.1039/b107833j2452-2453.

[69]   a) Z. Hordyjewicz-Baran, L. You, B. Smarsly, R. Sigel and H. Schlaad, *Macromolecules* 2007, 40, 3901-3903;
        b) N. ten Brummelhuis, C. Diehl and H. Schlaad, *Macromolecules* 2008, 41, 9946-9947.

[70]   a) Z. Fu, M. A. Ochsner, H.-P. M. de Hoog, N. Tomczak and M. Nallani, *Chem Commun* 2011, 47, 2862-2864;
        b) M. Nallani, H.-P. M. de Hoog, J. J. L. M. Cornelissen, A. R. A. Palmans, J. C. M. van Hest and R. J. M. Nolte, *Biomacromolecules* 2007, 8, 3723-3728;
        c) D. M. Vriezema, J. Hoogboom, K. Velonia, K. Takazawa, P. C. M. Christianen, J. C. Maan, A. E. Rowan and R. J. M. Nolte, *Angew. Chem. Int. Ed.* 2003, 42, 772-776;
        d) M. Spulber, A. Najer, K. Winkelbach, O. Glaied, M. Waser, U. Pieles, W. Meier and N. Bruns, *J Am Chem Soc* 2013, 135, 9204-9212.

[71]   J. F. Le Meins, O. Sandre and S. Lecommandoux, *Eur. Phys. J. E* 2011, 34, 1-17.

[72] J. Gaitzsch, D. Appelhans, D. Grafe, P. Schwille and B. Voit, *Chem Commun* 2011, 47, 3466-3468.

[73] a) D. Grafe, J. Gaitzsch, D. Appelhans and B. Voit, *Nanoscale* 2014, 6, 10752-10761;
b) J. Gaitzsch, D. Appelhans, A. Janke, M. Strempel, P. Schwille and B. Voit, *Soft Matter* 2014, 10, 75-82.

[74] a) M. V. S. Dinu, M.; Renggli, K.; Wu, D.; Monnier, C. A.; Petri-Fink, A.; Bruns, N., *Macromol Rapid Comm* 2015, 36, 503-506;
b) M. Spulber, P. Baumann, S. S. Saxer, U. Pieles, W. Meier and N. Bruns, *Biomacromolecules* 2014, 15, 1469-1475.

[75] J. A. Alberts B, Lewis J, et al., *Principles of Membrane Transport*, Garland Science, New York, 2002.

[76] a) M. Luckey, *Membrane Structural Biology*, Cambridge University Press, 2014;
b) W. Stillwell, *An introduction to biological membranes from bilayers to rafts*, http://public.eblib.com/choice/publicfullrecord.aspx?p=1178398, accessed.

[77] R. Koebnik, K. P. Locher and P. Van Gelder, *Mol Microbiol* 2000, 37, 239-253.

[78] a) G. Calamita, *Mol Microbiol* 2000, 37, 254-262;
b) L. Rose and A. T. A. Jenkins, *Bioelectrochemistry* 2007, 70, 387-393.

[79] R. G. Wells, T. K. Mohandas and M. A. Hediger, *Genomics* 1993, 17, 787-789.

[80] T. A. Krulwich, G. Sachs and E. Padan, *Nat Rev Micro* 2011, 9, 330-343.

[81] G. Blanco, *Seminars in Nephrology* 25, 292-303.

[82] A. L. Davidson, E. Dassa, C. Orelle and J. Chen, *Microbiology and Molecular Biology Reviews : MMBR* 2008, 72, 317-364.

[83] C. Edlinger, X. Zhang, O. Fischer-Onaca and C. G. Palivan, *Polymer Nanoreactors*. In Encycl. Polym. Sci. Eng., John Wiley & Sons, Inc.: 2013; Vol., 10.1002/0471440264.pst581.

[84] a) M. Lomora, I. A. Dinu, F. Itel, S. Rigo, M. Spulber and C. G. Palivan, *Macromol Rapid Comm* 2015, 36, 1929-1934;
b) M. Lomora, M. Garni, F. Itel, P. Tanner, M. Spulber and C. G. Palivan, *Biomaterials* 2015, 53, 406-414;
c) C. Nardin, J. Widmer, M. Winterhalter and W. Meier, *Eur. Phys. J. E* 2001, 4, 403-410.

[85] a) W. Meier, C. Nardin and M. Winterhalter, *Angewandte Chemie-International Edition* 2000, 39, 4599-4602;
b) M. Nasseau, Y. Boublik, W. Meier, M. Winterhalter and D. Fournier, *Biotechnol Bioeng* 2001, 75, 615-618.

[86] C. G. Palivan, R. Goers, A. Najer, X. Zhang, A. Car and W. Meier, *Chem Soc Rev* 2016, 45, 377-411.

[87] V. Pata and N. Dan, *Biophys J* 2003, 85, 2111-2118.

[88] G. Srinivas, D. E. Discher and M. L. Klein, *Nano Lett* 2005, 5, 2343-2349.

[89] a) F. Itel, *Lateral diffusion processes in biomimetic polymer membranes* PhD thesis, University of Basel, Basel, 2015;
b) K. Kita-Tokarczyk, J. Grumelard, T. Haefele and W. Meier, *Polymer* 2005, 46, 3540-3563.

[90] A. Graff, C. Fraysse-Ailhas, C. G. Palivan, M. Grzelakowski, T. Friedrich, C. Vebert, G. Gescheidt and W. Meier, *Macromol Chem Phys* 2010, 211, 229-238.

[91] M. Kumar, M. Grzelakowski, J. Zilles, M. Clark and W. Meier, *P Natl Acad Sci USA* 2007, 104, 20719-20724.

[92] H. Wang, T.-S. Chung, Y. W. Tong, K. Jeyaseelan, A. Armugam, Z. Chen, M. Hong and W. Meier, *Small* 2012, 8, 1185-1190.

[93] M. Grzelakowski, M. F. Cherenet, Y.-x. Shen and M. Kumar, *J Membrane Sci* 2015, 479, 223-231.

[94] F. Itel, A. Najer, C. G. Palivan and W. Meier, *Nano Lett* 2015, 15, 3871-8.

[95] N. Uehlein, B. Otto, A. Eilingsfeld, F. Itel, W. Meier and R. Kaldenhoff, *Scientific Reports* 2012, 2, 538.

[96] D. Ho, B. Chu, H. Lee and C. D. Montemagno, *Nanotechnology* 2004, 15, 1084-1094.

[97]   X. Zhang, M. Lomora, T. Einfalt, W. Meier, N. Klein, D. Schneider and C. G. Palivan, *Biomaterials* 2016, 89, 79-88.

[98]   A. Graff, M. Sauer, P. Van Gelder and W. Meier, *Proc Natl Acad Sci USA* 2002, 99.

[99]   D. Morton, S. Mortezaei, S. Yemenicioglu, M. J. Isaacman, I. C. Nova, J. H. Gundlach and L. Theogarajan, *Journal of materials chemistry. B, Materials for biology and medicine* 2015, 3, 5080-5086.

[100]   C. Nardin, S. Thoeni, J. Widmer, M. Winterhalter and W. Meier, *Chem Commun* 2000, 1433-1434.

[101]   A. Ranquin, W. Versees, W. Meier, J. Steyaert and P. Van Gelder, *Nano Lett* 2005, 5, 2220-2224.

[102]   M. Grzelakowski, O. Onaca, P. Rigler, M. Kumar and W. Meier, *Small* 2009, 5, 2545-2548.

[103]   D. Dobrunz, A. C. Toma, P. Tanner, T. Pfohl and C. G. Palivan, *Langmuir* 2012, 28, 15889-99.

[104]   K. Langowska, J. Kowal, C. G. Palivan and W. Meier, *J. Mater. Chem. B* 2014, 2, 4684-4693.

[105]   S. Ihle, O. Onaca, P. Rigler, B. Hauer, F. Rodriguez-Ropero, M. Fioroni and U. Schwaneberg, *Soft Matter* 2011, 7, 532-539.

[106]   H. J. Choi and C. D. Montemagno, *Nano Lett* 2005, 5, 2538-2542.

[107]   N. Muhammad, T. Dworeck, M. Fioroni and U. Schwaneberg, *J. Nanobiotechnol* 2011, 9, 8.

[108]   M. Kumar, J. E. O. Habel, Y.-x. Shen, W. P. Meier and T. Walz, *J Am Chem Soc* 2012, 134, 18631-18637.

[109]   X. Y. Zhang, W. Y. Fu, C. G. Palivan and W. Meier, *Scientific Reports* 2013, 3.

[110]   J. L. Kowal, J. K. Kowal, D. L. Wu, H. Stahlberg, C. G. Palivan and W. P. Meier, *Biomaterials* 2014, 35, 7286-7294.

[111]   J. Kowal, D. Wu, V. Mikhalevich, C. G. Palivan and W. Meier, *Langmuir* 2015, 31, 4868-4877.

[112]   a) C. LoPresti, H. Lomas, M. Massignani, T. Smart and G. Battaglia, *J. Mater. Chem.* 2009, 19, 3576-3590;
b) P. Baumann, P. Tanner, O. Onaca and C. G. Palivan, *Polymers* 2011, 3, 173;
c) P. R. LeDuc, M. S. Wong, P. M. Ferreira, R. E. Groff, K. Haslinger, M. P. Koonce, W. Y. Lee, J. C. Love, J. A. McCammon, N. A. Monteiro-Riviere, V. M. Rotello, G. W. Rubloff, R. Westervelt and M. Yoda, *Nat Nano* 2007, 2, 3-7.

II Theoretical background

1 Vesicle formation

1.1 Self-assembly

While at first glance it might seem irrelevant how vesicles are formed, as long as they are obtained through an established procedure, it can be very frustrating when minuscule changes result in drastic changes. The choice of the amphiphile and the conditions during self-assembly, can have vast influence on the resulting structures, their size and stability but also whether or not cargo can be encapsulated or MPs can be inserted. Thus, having a basic understanding of the processes involved can help to avoid or fix problems.

As elaborated later on, the process of self-assembly is very complex and depends on a multitude of different parameters. While most of the mentioned structures (but also gels[1]) have been thoroughly studied, many aspects of the self-assembly processes are still poorly understood due to the lack of confirmed structures of the intermediates and their heterogeneity. It can be assumed that the aggregation processes relate to the following pattern:

1) Due to the hydrophobic nature of the amphiphiles (even more so ABCPs), the solubility can be very low. For the same reasons and the resulting interaction with itself, the solubilisation of individual amphiphiles is slow and results in a gradual increase in concentration. If the bulk of solid amphiphile consists of layers of dried membranes (lyotropic phase), the layers can be rehydrated and membrane-patches can go into solution.[1a, 2]

2) In both cases, the dissolved particles are in a thermodynamically very unfavourable situation. In the prior case amphiphiles minimise their exposure of their hydrophobic segments, by accumulating at the **water-air-interface** (hydrophobic part facing air). In the latter case membrane-patches conceal their hydrophobic edges, by fusing together to larger structures, in particular tubes and vesicles. The latter occurs when the lamellar liquid crystalline phases swell to such an extent that the membranes distance themselves by more than 100-300nm (when the interlamellar distance roughly equals the persistence length).[3]

3) After an amphiphile specific surface concentration is reached, a secondary process becomes energetically, more and more favourable: Due to the hydrophobic effect or more precisely an unfavourable mixing enthalpy and low mixing entropy[4] amphiphilic particles aggregate in water (micro phase separation) with their hydrophobic surfaces resulting in **micelles** hiding their hydrophobic part behind the hydrophilic head-groups; avoiding precipitation. In case of detergents, this phaenomenon is known as **critical micelle forming concentration (cmc)**.

4) At even higher concentrations the exposed surface of the micelles is reduced by fusion to larger micelles.

5) At a certain point, **micelles cannot grow** anymore without becoming hollow at their core. At this point they collapse to small patches of membranes or fuse together forming worms (the latter in case of the amphiphile preferring cone form over cylinders).

6) The size and concentration of membranes continues to grow. Membranes are fusing together to larger membranes, **tubes or vesicles.** [5] These processes reduce not only the number of micelles, but the total number of particles in solution and the total exposed surface.[6] This process most likely has highly unstable intermediates such as bilayer fragments or ill-defined multilayer aggregates.[7] The **growth of vesicles** changes the curvature of the membrane. This change is connected with hydration and change of the density of the amphiphiles.[7] An abrupt change in vesicle size could generate defects in the amphiphile packing or fissures and holes.

7) At even higher concentrations (over 40wt%)[8] vesicles can be packed, partially fuse to complex **gels** or even evolve to lamellar gels.[1a]

Cargo becomes usually **encapsulated** during the vesicles formation, by dissolving the cargo directly in the buffer that is used for film rehydration or detergent removal (see chapter **1.3.3**). Later it can only be added if the vesicles are damaged, e.g. by sonication, freeze-thaw-cycles etc. In that case the damaged vesicles are usually concentrated and rediluted in a buffer containing the cargo (in the hope that the vesicles repair themselves).[9]

As discussed later in this chapter (**1.5**), Membrane proteins (**MPs**) are of great interest for polymersome nanoreactors. These proteins are amphiphiles themselves, with a vast hydrophobic (often cylindrical) surface that interacts with the membrane and one or two hydrophilic surfaces, which protrude out of the membrane. Unlike normal proteins, they need to be stabilised in solution with detergents in order to prevent aggregation, precipitation or denaturation. These detergents not only form a steric hindrance for self-assembly, but also interfere with membranes though insertion into membranes, or stabilisation of ABCPs in solution via their micellar structures.

Membrane proteins can be **inserted** in similar fashion to encapsulation of cargo:[9]

- Adding MPs to the amphiphile **prior** vesicle formation: in that case the MP must survive organic solvents, detergents or drying

- Adding them to the amphiphile **during** vesicle formation: the detergent stabilising the hydrophobic MP is thereby diluted so that the naked MP attracts amphiphiles. The disadvantage is that the MP can form aggregates or precipitate instead.

- Adding them **after** vesicle formation: in that case the vesicle membrane must be damaged via sonication, freeze-thaw cycles or detergent addition; the latter being of particular interest since the membrane protein remains stabilised in solution until the detergent becomes removed via dialysis or adsorbent addition. This method has however the most parameters to optimise. The disadvantage here is that the vesicles might not recover and precipitate instead or form micelles or that the detergent is removed too quickly resulting in the loss of the MP.

- In rare cases, MPs can insert into membranes directly by displacing amphiphiles. This works in particular for very small MPs, that are sufficiently stable in solution. Gramicidine is a well-known example.[10]

Polymersomes are more challenging to insert, due to their thicker membranes and stronger interaction of their hydrophobic segments. In case of liquid-crystalline structures (PS-block,[11] or PICsomes[12]) or polymersomes with crosslinked ABCPs, insertion becomes impossible. On the other hand, ABCPs with flexible, amorphous hydrophobic segments facilitate insertion. It has also been suggested that higher polydispersity[13] closes the gap in hydrophobic mismatch between polymersome membranes and MPs.

Please note that there are several theoretically **possible mechanisms** how membranes and vesicles may grow:

- Single amphiphiles (especially from micelles but also directly out of water) may insert
- Membrane fragments may be incorporated when the vesicle-membrane has a crack at which the fragment can fuse to
- Aggregates can collide forcing fast reorganisation.

The precise mechanism of self-assembly will be dependent on the amphiphile, the concentration of it, the concentration of the various types of aggregates and probably numerous less obvious parameters (shape and amount of the reservoir of undissolved amphiphile; temperature; type of agitation; oxygen content in water…).

Since **polymeric amphiphiles** have usually longer hydrophobic chains than lipids, they are less soluble and feature a lower critical micelle forming concentration (**cmc**). Thus, the amphiphiles are more willing to self-assemble, however they do so slower, due to their significantly greater molecule size.

The question which process is available is relevant for the stability of the structures but also for encapsulation of entities and insertion of membrane proteins. Since the concentration of free amphiphiles is in most scenarios negligible low, the vesicles can change their size either through **fusion or fission**. This explains, why further encapsulation cargo after vesicle formation is unlikely.[6] Obviously, diluting self-assembled structures creates a perturbation of the equilibrium. Polymersomes have proven to be far more resistant in that respect than liposomes.[14]

In case the vesicle formation is a **one-way process**, then there is no equilibrium between the structures, preserving their size, but preventing repair of damaged structures (e.g. vesicles breaking down and aggregating and the remains in solution eventually becoming micelles). This would make weakening the membrane by detergent addition for protein insertion a bad choice.

In case of an **equilibrium,** encapsulated entities may be released and inserted entities could change their orientation, which would result in an unacceptable lack of control for the production of nanoreactors. In particular, in case of polymersomes, these processes are too slow, to cause problems, unless detergents are present and act as catalysts. In this case, even new processes and outcomes are possible.

If vesicles are formed primarily by **insertion of single amphiphiles**, then insertion of membrane proteins becomes near impossible as membrane proteins would be predominantly in (detergent)micelles and small patches of membranes. Thus, membrane proteins are typically inserted during the vesicle-formation, or by damaging vesicles just enough to allow membrane proteins to insert, while the vesicles repair themselves (which in turn probably requires the presence of micelles as reservoirs for amphiphiles). In either case, detergents have to be removed at the end to ensure stability of the vesicles.

1.2 Factors influencing resulting structures

While there is a general trend to shift from micelles over membranes to vesicles with increasing **concentration** of the amphiphile,[4, 15] the **ratio** between its hydrophilic and hydrophobic surface, but also its shape and flexibility determine the possible curvatures of the resulting structures and its chemical nature in general (discussed later) do determine the formed structures.[16] Moreover, the polydispersity (PDI),[4, 17] contamination by the homopolymer,[17b] other impurities and moisture of the ABCP[16] may make two ABCPs behave completely different, although they are identical on paper. In particular, the frequent coexistence of micelles and vesicles has been attributed to the polydispersity

of the ABCPs.[18] On the other hand, shorter ABCPs could accumulate on the inside curvature, especially when bilayers are formed thereby reducing strain.[19]

Micellar structures are prevailing, when the hydrophilic block dominates (over 50%). 40-50% leads to rod-like structures, whereas vesicles are formed at[3] 25-40%.[20] However, there are many other factors determining the self-assembly process, including formation procedure[15b], in case of film rehydration: the thickness of the polymer film to be rehydrated and thus the polymer concentration in ethanol, the vial, its rotation speed and the drying rate.[4, 15b] Similarly, the rehydration speed is important and depending on further factors. Thus ionic strength of the rehydration buffer,[4, 15b, 17b] its pH[15b] and the temperature[4, 15b, 17b] and stirring time.[21] The list should not be regarded as complete.

The **minimal vesicle size** is restricted by the maximal curvature of the membrane. This is determined through the ability of the amphiphile to adapt a conical shape. The shape of the self-assembled structures is hence dependent on the composition of the amphiphile (see **Table 1**). In general, an amphiphile with a strong tendency to a cone over a cylinder results in micelles, whereas a preference for cylinder shape results in membranes. Note: a slight cone shape would facilitate the curvature of a membrane to a sphere, but this would only be true for the outer half of the bilayer, whereas the inner half would have to adapt a conical shape tapering in the opposite direction.

The minimal vesicle size is important since in many cases the size distribution of vesicles features a vast number of small vesicles and few larger ones (which will disappear after purification). Since vesicles size has a great impact on encapsulation efficiency and possibly the curvature of the membrane influences the insertion efficiency of MPs as well, two batches of ABCPs with different minimal vesicles size are not comparable.

Aside from the hydrophilic to hydrophobic block-length ratio, the **packing parameter [P]** is a tool to predict the preferred self-assembled structure (see **Table 1, Equation 1**).[22] It is a unit-less number that puts the volume (V_c) of the hydrophobic block into relation to the ideal area per molecules (A_0) and the critical length (l_c) of the amphiphiles (dependent on the elongation; a U-turn would divide it by two). Vesicles are found when 0.5<[P]>1.[23]

$$P = \frac{V_c}{A_0 \cdot l_c}$$
(1)

---
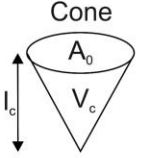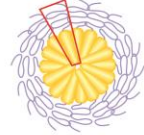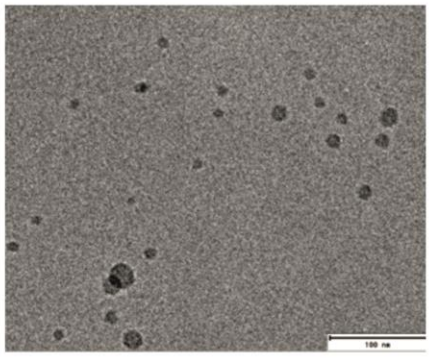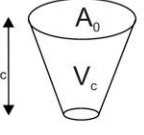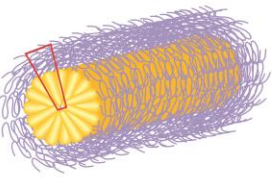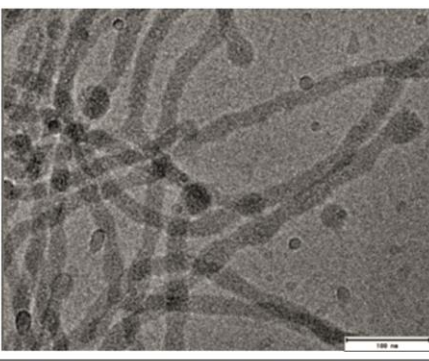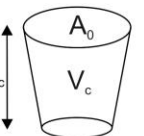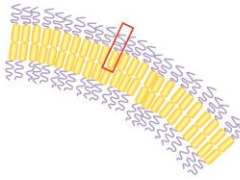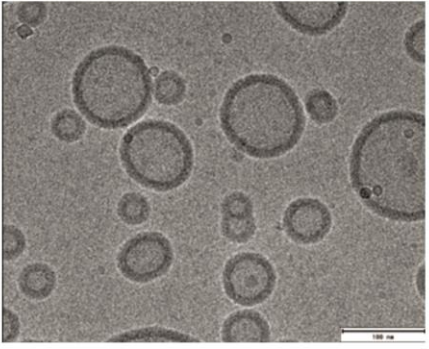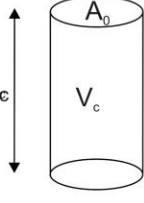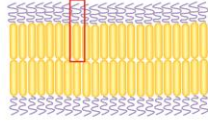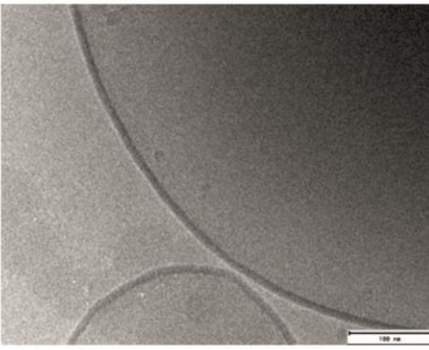
[3] There is no newer publication evaluating the ratios, but in our group, we found significant outliers with e.g. *b*-PMOXA$_{10}$-*b*-PDMS$_{87}$-*b*-PMOXA$_{10}$ with 23% and *b*-PMOXA$_{20}$-*b*-PDMS$_{41}$-*b*-PMOXA$_{20}$ with 97.5%. Both formed vesicles. We further found that very low hydrophilicity resulted in slow film rehydration and very high hydrophilicity resulted in a high micelle population or a slow transition into vesicles. Results not published.

The vesicle size tends to increase when higher polymer concentrations are used. However, the size distribution of the vesicles becomes broader. It is determined through the competing effects surface-area-reduction and entropy loss. The **total surface-area** decreases with increasing vesicle size, considering the diminishing total number of vesicles. In order to enforce a specific vesicle size, the vesicles can be extruded using a membrane with pores of diameter close to the diameter of the smallest vesicles.[5b]

Table 1: Selection of potential structures formed by self-assembly and their dependence on the packing parameter and composition[23]

Critical packing shape	Structures formed	Composition A/B	Critical packing	Examples cryo-TEM
Cone A_0 l_c V_c	Spherical micelles	> 50%	< 1/3	
Truncated Cone A_0 l_c V_c	Cylindrical micelles/worms	50 -40%	1/3 -1/2	
Truncated Cone A_0 l_c V_c	Vesicles	40 -25%	1/2 - 1	
Cylinder A_0 l_c V_c	Giant vesicles/ planar bilayers	< 25%	≈ 1	

1.3 Methods of vesicle-formation

The synthesis of micelles is straightforward: either they are made through direct-dissolution or through film-rehydration. In the latter case the amphiphile is spread through evaporation on a surface and is consecutively redissolved under agitation. For vesicle formation there are three main methods:[24]

Kinetic trapping: a polymer becomes dissolved in an organic solvent and is precipitated in excess of water. The organic solvent has to be miscible with water and should be volatile enough to be removed or has to be able to be removed via dialysis or adsorbent addition.

Thermodynamic trapping: similar to kinetic trapping, with the difference, that water is added to an organic polymer solution. The unfavourable medium is thus added slowly, reducing the solubility slowly, ideally allowing an equilibrium to be formed; hence the distinction in the names of the two trapping methods.

Film-rehydration: first a film of the amphiphile has to be made through dissolution and evaporation. Then the film is slowly dissolved in water or aqueous buffer solution. The agitation is caused through rotating the vial, stirring, shaking, vortexing or even sonication.

The first two methods have the disadvantage, that the removal of the **organic solvent** is often difficult and incomplete. The remains are thus able to interfere with biological systems or cause swelling and fluidation of the membrane. The latter can cause slow vesicle-fusion.[25] Furthermore precipitation- and dilution methods are not suitable for proteins. Lastly, vesicles can also be achieved by dissolving the amphiphiles in water using detergents and then removing the **detergents** again (which could be seen as a variation of thermodynamic trapping). This method is particularly of interest for inserting membrane proteins, which have to be stabilised in detergents.[26] However, the involved detergents can interact unfavourably with the membranes and be almost as difficult to remove as solvents.

The precise method can have a significant impact on the resulting structures and their size. The presence of detergents or organic solvents tends to decrease the vesicle size and increase the micelle population. Therefore, cosolvent methods produce usually smaller vesicles than film rehydration. Similarly, agitation of the solution plays an important role as it affects the concentration gradient at the interface of the solid amphiphile bulk, the extreme would be **electroformation** which is used to create giant vesicles (20-50µm in diameter).[1a]

For this thesis, primarily film rehydration was considered, as OmpF is stable enough to be dried along with ABCPs and withstands ethanol. Detergent removal is a milder alternative and tends to inserts MPs better, but also results in smaller vesicles and more micelles.

2. Properties of vesicle-membranes

2.1 Metastability

As evident it may be that vesicles are formed through self-assembly, it is often overlooked that they can fuse together or disassemble again, for example upon concentration changes, since the self-assembly is an equilibrium process. In case of polymersomes, this may be hindered, due to the strong interaction between the amphiphiles within the membrane, a low solubility of individual amphiphiles and potentially their preference to form membranes over vesicles. The conditions under which the structures disassemble again are of particular importance in medical and pharmaceutical applications, since extreme dilutions[4] are required there.[27] It should be noted further that the concentration of other solutes influences the stability. Phospholipid vesicles may be stabilized through sugars[7], whereas the presence of salt outside of vesicles induces osmotic pressure.

It is noteworthy that, vesicles do not form spontaneously, unlike micelles. They are thermodynamically unstable and thus metastable (similar to many proteins, whose folding is often kinetically determined and do not fold back once denatured[28]).[7] Their preparation is often a non-equilibrium process. The results are therefore not necessarily reproducible.

2.2 Stabilisation of vesicles

In order to increase the stability of vesicles the thickness of the membrane may be increased by using longer amphiphiles;[29] the interactions between the amphiphiles within the membranes could be enhanced by increasing the crystallinity of the assembly.

In **liposomes**, this would mean using longer hardened fatty acids over shorter unsaturated fatty acids. The best approach of creating stronger membranes is by using additives. Their bilayers can be stabilised by introducing structures that connect all parts of the bilayer e.g. cholesterol added to lipids,[30] but also membrane proteins inserted.[31] These additives are less likely to diffuse out of the assembly than the actual amphiphiles. Such transmembrane structures can bind amphiphiles next to them by reducing the likelihood of amphiphiles leaving the vesicle (comparable to dissolving non-volatile compounds thereby reducing the solvents vapour pressure). Cholesterol is also known to increase the fluidity of liposomes.[30a, 32]

---

[4] Considering that an adult has around 5L blood, an injection of e.g. 100μL would translate to 50 000x dilution of the vesicles.

Lastly, fusion of vesicles can be prevented by adding charges to the surface causing charge repulsion among the vesicles. PEGylation can help as well. Both are used for liposomes in drug-delivery.[33] In order to PEGylate the vesicle surface, anchor groups are required (**Fig. 1.2**). In case of liposomes cholesterol is better suited than a lipid for this purpose, similarly in case of polymersomes triblock-copolymers are typically better suited than diblock copolymers (**Fig. 1 3, 4**) due to their size, reducing the likelihood of the anchor becoming detached form the vesicle.

In case of **polymersomes** far more options are available: The length of the hydrophobic block can be changed to a much greater degree and even the very chemical nature of the hydrophobic block can be altered, e.g. by using polystyrene (PS) over poly(dimethylsiloxane) (PDMS). Polystyrene is much stiffer, can be crystalline and its phenyl-sidechains are able to entangle. Moreover, it is possible to introduce interactions between the ABCP other than van der Waals forces such as hydrogen bonds, e.g. by using Kevlar-like segments, or even charge compensation as in PICsomes. However, these PICsomes cannot be used to insert membrane proteins due to their lack of hydrophobic segment. In general, such modifications greatly reduce the ABCPs ability to dissolve in the first place. Even polystyrene based ABCP require a cosolvent to lower the high glass transition temperature to provide sufficient chain mobility.[34] All these modifications directly affect the permeability of the membrane as well and potentially change the self-assembly mechanism up to the point that the structures are no longer in an equilibrium with each other.

2.3 Polymersomes vs Liposomes

Please note: *lipids* refers to *amphiphilic lipids* only (and not lipids for energy storage also known as fat). These lipids usually belong to the category of phospholipids which possess two fatty acids bound to glycerol and one phosphatidylcholine as polar headgroup attached to the third alcohol-group.
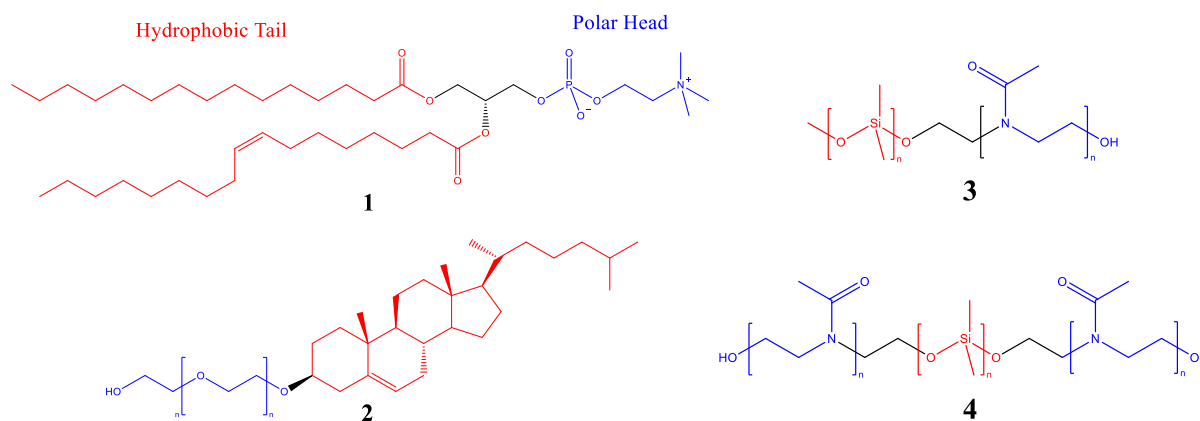
Fig. 1: the lipid POPC (1), Chol-PEG600 (2) and ABCP of the type AB (3) and ABA (4) based on PDMS and PMOXA

Lipids are natural products (**Fig. 1.1**) and are therefore extracted from biological sources, although they can be modified e.g. by hardening, or recombination of fatty acids. Synthesis of well-defined lipids requires protecting groups. The synthesis of fatty acids with precise lengths is even more demanding. Thus, those lipids used for membrane formation are typically a mixture of more or less similar fatty acids pairs. Moreover, they can come with different polar headgroups as well.

Liposomes suffer from leakage attributable to defects in the membrane and from its instability.[35] It should be noted however, that liposomes possess a more fluid membrane which allows faster response to perturbations. They are thus more likely to be damaged but also more likely to recover from damage than polymersomes, as they are able to allow single amphiphiles exchange (ergodicity).[36] This does not mean that polymersomes cannot repair themselves, but it may occure on a timescale larger than observed. Similarly, liposomes are less sensitive to most detergents. One may compare the stability of liposomes and polymersomes with gel and glass: one being softer but able to recover from deformation, whereas the other is unyielding until it shatters.[5]

While liposomes are typically mixtures of various lipids and additives, polymersomes usually consist only of one type of amphiphilic blockcopolymer (**Fig. 1 2,3**), which however varies in length due to its synthesis. The self-assembly of polymersomes is likely the most versatile approach for creating nanocapsules. **Polymersomes** offer several **advantages** over liposomes:

---

[5] This finding will be discussed in detail in later in this thesis. It may also be different for ABCPs other than the PDMS/PMOXA we used.

Polymersome membranes are generally thicker and can be more stable due to stronger interactions between the amphiphiles.[37] Liposome membranes have a thickness of 3-5nm, whereas polymersomes have a thickness of 4-20nm (the thickness correlates to the molecular weight of the amphiphiles, or more precisely the molecular weight of the hydrophobic block by the factor $M^{2/3}$ [38]).[39] The membranes of polymersomes are up to 10x more mechanically stable than those of liposomes and far less permeable, allowing better control over diffusion across the membrane.[40] Polymersomes and PICsomes o are often stable enough to be concentrated through centrifugation.[12b] They are moreover often stable at room temperature for months.[15b] The higher stability and lower permeability of polymersomes is a result of its higher rigidity and membrane thickness. This makes them very interesting for NRs, but the thicker membrane can make it difficult to incorporate membrane proteins that are adapted for much thinner membranes and a somewhat different chemical environment.

Polymersomes are built by well-defined amphiphiles, which contain usually two or three polymer blocks. The control over their precise length varies with the chosen polymerisation method. The choice of the blocks is synthetically straightforward and offers nearly endless possibilities. Various monomers can be used in the polymerisation and their blocklengths and overall length can be adjusted, thus controlling the hydrophilic content (allowing to alter the self-assembly behaviour)[41] and the thickness of the resulting membrane.[39] Lastly, in case of polycondensations and ATRP,[42] the endgroups can and have successfully been selected and used as anchor points for further modification.[43]

Unlike lipids, ABCP can be therefore designed individualised according to the requirements. They can be **functionalized** to bear targeting moieties or linkers for click-chemistry. The latter allows immobilisation of the vesicles, fixation of catalysts/enzymes and other post processing. Moreover, it is possible to fixate vesicle membranes through (radical-) polymerisation of the individual ABCPs. The hydrophilic block retains most of its flexibility, but loses most of its ability to diffuse within the membrane, if the polymerisation occurs at the very end of the ABCP.[44] This increases however the risk of cross-linking vesicles with other vesicles. Membranes can also be stabilized through polymerisation of monomers (by copolymerising monomers similar to those building the blocks of the amphiphile, differing by an additional polymerizable group),[6] which are embedded in the hydrophobic block.[45] Both techniques would stabilize pores and smaller defects from rupturing the membrane. These methods take however the possibility of later introducing membrane proteins, since the ABCP can no longer be displaced.

However, polymersomes have also some **disadvantages**:

---

[6] This double bond requires to be protected or otherwise to be inert to the polymerisation method applied for the amphiphile synthesis.

Lipids developed in order to form vesicles and membranes, whereas ABCPs have to be carefully designed to do the same. Lipids have less problems in becoming rehydrated and form thus self-assembled structures rapidly, whereas ABCPs have a tendency to remain solid due to their poorer solubility.[7] Similarly, many ABCPs do not support the insertion of membrane proteins. For example, poly(styrole) would form to strong interactions between each hydrophobic block and PICsomes are by their nature not hydrophobic, thus they would repel membrane proteins As mentioned above, polymersomes have thicker membranes (up to 7x thicker than the membrane protein, have been used)[39] and the interactions between the amphiphiles can be much stronger than between lipids. Moreover, some ABCPs have hydrophobic blocks that will not be miscible with MPs. It is often already a challenge to find the right lipid mixture. Designing artificial amphiphiles is therefore a major challenge. Even designs that worked before may fail due to minor changes in the synthesis (presumably by deviation in PDI, number of diblocks in triblocks and other contaminations). The PDI or polydispersity-index is a measure for the deviation in chain-length of individual ABCP from the average. The higher its value is, the less homogeneous the ABCP.

Lastly, amphiphilic blockcopolymers differ more from the commonly used detergents than lipids do. This may be the reason why polymersomes discussed in this thesis are more sensitive to detergents. Thus, polymersomes may behave differently from a mechanistic perspective in particular regarding insertion of membrane proteins.

In summary, liposomes are easier to produce and it is easier to insert membrane proteins into liposomes. However, they are less stable and more permeable than polymersomes. Regarding this thesis, liposomes are more preexperiments and polymersomes the final goal.

---

[7] Due to the molecular mass, dissolution can be much slower, but the lower solubility of individual ABCPs and in case of PMOXA the known tendency of forming insoluble crystals can reduce the overall solubility.

2.4 Diblock- and Triblockcopolymers

Polymersomes are typically made of a **diblockcopolymer** (**AB**). The shorter hydrophilic block (A) is typically made of poly(acrylic acid) (PAA), polyethyleneglycol (PEG), poly N-isopropyl methylacrylamid (PNIPAAM), poly N-hydroxypropyl methacrylamide (PHPMA) or polyoxazolidines in particular polymethyloxazolidine (P<M>OXA), whereas the hydrophobic block (B) consist of polystyrene (PS), polybutadiene (PBD) or polydimethylsilicone (PDMS).[46] PEG, PMOXA and PHPMA are considered to be biocompatible and protein repellent and are therefore interesting for medical applications.[47] None of these blockcopolymers would be possible, without modern living polymerisation techniques.

Triblockcopolymers (**ABA**) could form stronger vesicles, since they do not need to form a bilayer, where both sheets can slide laterally. However, it has been suggested that triblockcopolymers may form U-Turns and behave thus like AB-amphiphiles (**Fig. 2**).[48] The synthesis has moreover the problem, that some diblockcopolymers may be formed through capping (side-reactions, that stop a polymerisation), which are then almost impossible to separate. This results in an additional heterogeneity similar to the PDI, which may have adverse effects on the vesicle-formation.

There are some asymmetric triblockcopolymers (**ABC**) that have been used as amphiphiles. When A and C are poorly miscible, the larger block tends to form the outside of the polymersomes.[49]. This was partially conceived to take the asymmetric nature of lipid bilayers into account, which are an important factor for the orientation of inserted membrane proteins. It has been shown with ABC-amphiphiles that this behaviour can be emulated.[50]

The hydrophilic block does not usually contribute to the stabilisation of the structure; it can even destabilise it, in case of charge repulsion. Thus, it should be kept very short (unpublished experiments in our group indicate that in an ABA-blockcopolymer less than 5% of the monomers have to be hydrophilic in order to obtain vesicles).

AB, ABA and ABC can all assemble in different ways each (**Fig. 2**). The hydrophobic block may remain straight and form liquid crystalline phases or entangle in an amorphous phase. Moreover, the hydrophobic blocks may be angled to the hydrophobic block. In case of AB-blockcopolymers a further parameter occurs: the blocks may form a bilayer or be interdigitated. In case of ABA-ABCPs, the ABCPs could go through the membrane, forcing them to remain in a straight conformation, or have both hydrophilic groups coming out at the same side, making them effectively AB-type ABCPs (as marked in green in **Fig. 4**). All these factors determine the stability, density and thickness of the membrane. It can be also assumed that this affects the permeability and readiness of the membrane to incorporate membrane proteins. Which conformation prevails is largely determined by the nature of the ABCPs:

it's stiffness, ability to interact with itself (and the temperature) and the relative thickness of each segment. Lastly, it should be pointed out, that in case of ABC-type ABCPs A and C are rarely miscible, thus forcing them into the membrane conformation with three distinct regions. This can be used for inserting MPs in only one orientation.[51]
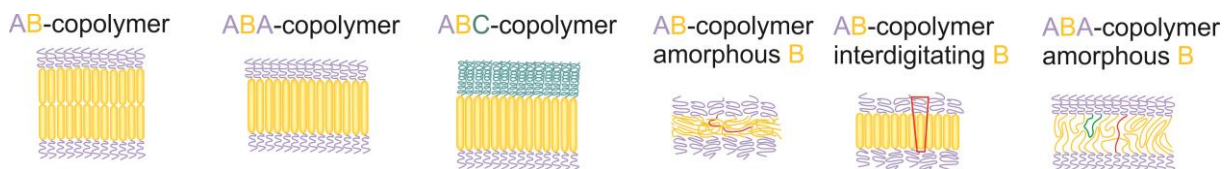
Fig. 2: Possible ways of amphiphilic diblock- and triblock copolymers assemble to form a membrane. The first example is the typical bilayer as found in lipid-membranes [52]

3 Characterisation methods

While analysis of diffusion is the key aspect of the characterisation methods, in this thesis, a variety of other parameters had to be investigated as well, in order to create reproducible data and being able to compare the sample with controls. These parameters can be grouped into structure-analysis and concentration-measurement.

3.1 Structure

In order to create the required nanoreactors, it has to be confirmed that self-assembly results in vesicles and not micelles etc. Therefore, it has to be proven that the structures are spherical and hollow and thus able to encapsulate hydrophilic cargo. For comparable results, the size of the vesicles and their size distribution has to be determined as well. This is particularly important regarding the encapsulation efficiency (elaborated later), but can also affect the stability of the structures, since doubling the vesicle diameter increases its volume 8-fold (since it doubles in all three dimensions, thus results being proportional to 2^3); this further changes the stress of curvature on the membrane and the membrane thickness decreases relative to the vesicle size. This disproportionate increase of diameter to volume holds significance in many other fields e.g. biology and aerodynamics, where it often poses size-limitations.

3.1.1 Light Scattering

Light scattering (LS) is an analytical method based on the fact that nanostructures scatter light. In case of coherent light (typically a laser) it results in partial light cancelling due to interference caused by scattering of two or more bodies. The received light intensity fluctuates due to the movement of the particles. The detected fluctuations in intensity are referred to as correlation function. This fluctuation is dependent on the vesicle size (hydrodynamic radius R_h). With a single exponential fit, the average radius is obtained and distribution as long as the particles differ significantly in size a size distribution can be obtained using a multiple exponential fit.

Measuring the scattering at different angles allows the calculation of the radius of gyration (R_g). The first measurement mode is called dynamic light scattering (due to the autocorrelation required to measure the fluctuations in the scattering intensity) whereas the second is referred to as static light scattering (investigating angular dependence rather than temporary fluctuations of the light scattering).[53] The ratio between the two radii (R_h/R_g) indicates the shape of the scattering particles: 0.5-0.7 solid spheres, 0.7-1 hollow spheres, >1 coils…. This method gives thus information about the size and shape of the structures. Moreover, it can hint whether or not the structure is hollow. With calibration it can also give molecular weights.[54]

3.1.2 Transition Electron Microscopy

Transition Electron Microscopy (TEM) is a straightforward approach of determining size and shape of the nanostructures. Very unlike LS, it provides direct results that require little interpretation. While LS gives average values, TEM shows individual structures (giving thus more information, but making averaging difficult). It is thus very good for spotting mixtures of micelles, vesicles and worms, or aggregates of vesicles, but it does not truly represent the state in solution. The sample preparation (including a drying step) changes the size of the structures and can introduce artefacts such as salt crystals or aggregation. Furthermore, often it can hardly be distinguished between solid spheres and deflated vesicles.[8]

A variation to circumvent the problem of deformation by sample preparation is cryoTEM in which the sample is frozen and only a slice is investigated, allowing the determination of the thickness of

---

[8] Common knowledge in the group, but unpublished

membranes. However, the method is more complicated and salts have to be removed first, which may result in osmotic stress as vesicles are usually made in buffered media.

3.1.3 Fluorescence Correlation Spectroscopy

While Fluorescence Correlation Spectroscopy (FCS) is superficially similar to LS in that diffusion is investigated in order to obtain the hydrodynamic radius, it requires completely different circumstances, as fluorescence is observed. In order to detect a particle, it has to diffuse into the confocal volume illuminated by a laser, become excited and emit fluorescence before leaving said volume. The measurement records an overall fluorescence (count rate: CR) and so-called counts per molecule (CPM) which represents the fluorescence of an individual particle. Again, as in light scattering, the fluctuation of the detected fluorescence correlates to the Brownian motion, and yields the **hydrodynamic radius** of the observed particle.[55] Unlike LS it can give far more information depending on how the fluorophores are employed:

- Encapsulated **cargo labelled**: attaching a fluorophore reduces the diffusion speed of the fluorophore proportional to the size of the particle it is attached to; however, encapsulation of e.g. labelled enzymes reduces the diffusion speed to the speed of the vesicle or micelle containing the cargo. It thus allows determination of the vesicle size without actually attaching a fluorophore to it. Moreover, the CPM allows to calculate the **number of encapsulated** particles, by dividing it though the CPM of free dye. Often a second fraction is observed, which diffuses much faster, consisting of not-encapsulated or released cargo. It can be thus used also for release studies. The CR itself is the sum of all fluorescent particles per time unit and represents the concentration of the sample (of all involved species).

- **Membrane labelling**: the membrane can be labelled by attaching the fluorophore to a small fraction of the amphiphiles, or by addition of a hydrophobic fluorophore which accumulates in the membrane (something very easy and fast to do). It does not give any other information than the size of the vesicle or micelles and their concentration. It is therefore rather applied in fluorescence microscopy, a technique, which most FCS devices are capable of doing as well. It should be noted, that the resolution of fluorescence microscopy is of limited use in case of nanostructures.[56]

- **Membrane proteins labelling**: analogue to labelling the cargo it gives information about the number of labelled groups per vesicle, the vesicle size and the sample concentration. However, labelling of membrane proteins prior to insertion into the membrane might interfere with the

insertion process. Thereafter, the membrane proteins become less accessible, moreover the membrane might accumulate unreacted fluorophore or the labelling might interfere with the functionality of the membrane protein, as the exposed parts are usually also the active parts.

- Fluorescence Cross Correlation Spectroscopy (**FCCS**): by using two different dyes, with different excitation and emission wavelengths, co-encapsulation can be investigated.

While FCS is a very powerful and versatile method, it does come along with a remarkable set of drawbacks:

It is an indirect method that **cannot distinguish** between vesicles and aggregation of micelles of the same size, or whether the fluorophore is encapsulated or embedded in the membrane (unless the dye is polarity sensitive or allows FRET[9]).[57] As every other method it is limited to a certain concentration range, however the high sensitivity requires high dilutions that could render self-assembled structures instable. Likewise, released fluorophores can be easily **outshined** by the vast number of fluorophores encapsulated in vesicles making release studies difficult if not impossible. Another major issue to be addressed is the non-trivial **choice of fluorescent** dye. FCS requires very stable dyes that resist photo bleaching. The fluorophore needs also to be selected according to its colour, size and hydrophobicity. The more the excitation is shifted to red, the larger and more hydrophobic the fluorophore tends to become. Even partial hydrophobicity can cause massive problems, such as dye entering preferably membranes, or even micelles. Additionally, insertion into membranes tends to weaken them significantly eventually resulting in vesicle decomposition.[10] Lastly, it can be complicated to **label** enzymes, due to differences in polarity, multiple labelling or blocking of the active site, but also due to poor accessibility of the anchoring groups. Similarly, stabilising detergents are likely to interfere with labelling.

3.1.4 Summary

For quick estimates whether a sample contains vesicles and of what size, DLS is used. For more reliable data various concentrations and angles are measured. Also, TEM gives complementary data regarding purity and size distribution. FCS is best used to study changes in structure or performing release

---

[9] Förster Resonance Energy Transfer: excited fluorophores are able to lower their energy through internal conversion and transfer it without direct contact to other fluorophores in case that it matches the excitation energy. This allows for in instance to excite cyan fluorescing protein and detect the fluorescence of yellow fluorescent protein that is 5 Å afar of the excited protein.

[10] Common knowledge in the group, but unpublished

experiments and for quantifying the composition of vesicles. It is however ill suited for quick measurements and does not show all particles.

3.2 Quantity

As mentioned above, FCS can be used to determine the concentration of vesicles and the concentration of their cargo; however, it requires labelling of the samples. Therefore, alternatives have to be envisioned.

3.2.1 Scattering

Under the premises that the samples are known to be homogeneous in size, size distribution and prevailing structures, the relative concentration can be determined by comparing their respective ability to scatter light. This facile method requires nothing more than a regular fluorimeter and can be also used to record structural changes over time, since decomposition of vesicles decreases the scattering. This can be used for instance to check thermal stability or tolerable detergent concentrations (if the dead time between addition and structural change is taken into account as well), however the data should be complemented with analysis of the resulting structures.

3.2.2 Encapsulation efficiency

The encapsulation efficiency is a measure for the success of enclosing cargo within vesicles. It is usually defined as the ratio of the encapsulated concentration to the initial concentration. While e.g. enzymes in the size of a few nanometers could theoretically be encapsulated in vesicles of 100nm diameter and more in vast numbers, in reality the encapsulation efficiency is much lower. This is partially due to the solubility limit, charge repulsion between the solute and apparently also other factors. This can be seen as for example otherwise identical vesicles with 100 and 200nm in diameter do not harbour the same concentration of the encapsulated cargo. Experiments in our group proved repeatedly that only 0.1-1% of the initial concentration is found within the vesicles. With smaller vesicles, the concentration can easily decrease by an order of magnitude.

The encapsulation efficiency can be determined by destroying the vesicles and measuring the activity of its released cargo compared it to the initial activity (after having ensured that the activity of the vesicles is negligible). This can be used not just to confirm hollow structures but also as a quick test to determine which fraction has activity after purification (e.g. vesicles vs. micelles)

3.3 Permeability measurement

In order to assess the permeability of the OmpF-conjugate, it needs to be inserted into a membrane. This can have in principle two forms:

- Flat membranes: free floating membranes covering tiny holes or being supported by a grid or resting on a gel. This approach would allow conductivity measurements and sampling directly from either side of the membrane. However, creating a homogeneous membrane, without gaps, or multiple layers is near impossible.
- Formation of vesicles or closed tubes. This experimental set-up allows only release experiments and enzyme kinetics.

In either case, a molecule has to be observed diffusing from one side of the membrane to the other. Flat membranes were only considered second to vesicles, with reproducibility and experimental difficulties in mind. Closed tubes are rare and do not provide significant advantages over vesicles but would introduce new parameters and room for errors. Thus, they were not further considered in this thesis.

3.3.1 Release experiments

The most straightforward approach would be to encapsulate a dye and detect its release. Yet, absorption and fluorescence usually do not change whether the dye is encapsulated or not. Still, there are two main possibilities:

First: the fluorescence can be measured in FCS, which discriminates between different diffusion speeds, or second: a self-quenching concentration of a fluorophore can be used.

FCS gives potentially more interesting information, such as vesicle-size, but the strong laser tends to bleach the fluorophores and dry the sample over time. As mentioned before, it might not be as sensitive as it could be because of the total fluorescence.

Using **self-quenched fluorophores**, the released dye enters a low concentration regime and becomes thus fluorescent. This avoids the problem observed in FCS that the released dye becomes outshined by encapsulated dye.

Release experiments have their limitations: it can be very difficult to encapsulate enough of the fluorophore, it might go into the membranes and thereby destabilise the vesicles or cause them to become leaky, thus the samples have usually to be measured directly after purification. Another important aspect is the selection of the fluorophore, as it could be too large to go through the membrane proteins or be plagued by unfavourable charge interactions. This applies also to FCS.

3.3.2 Enzyme kinetics

Choosing the indirect approach of encapsulating enzymes offers several **advantages**: Since the fluorophore is added in an inactive form outside of the vesicles, the samples can be prepared and stored for a while without having to fear premature release of dye. Several different dyes/enzyme substrates can be tested with the same sample and their concentration can be varied as well. Enzymes are less likely to interfere with the membrane formation than most dyes. Since the dye is added on the outside and has to diffuse through the membrane and be converted on the inside, it allows slower reactions that are not limited by the dye-capacity of the vesicles. The enzyme substrate may be added repeatedly and parameters such as the pH can be changed using the very same sample.

Of course, there are a couple of **disadvantages** as well: The encapsulation efficiency of enzymes is generally low (1%),[11] due to their size and charge. The costly nature of most enzymes aggravates this matter. On the other hand, enzymes can be very sensitive tools so that even traces of unencapsulated enzymes prove detrimental for the experiment. Some enzymes are less suitable, due to hydrophobic patches on their surface, which might result in a preference to membranes or micelles. The prior case further complicates purification.

---

[11] Common knowledge in the group, but unpublished

4 References

[1]   a) G. Battaglia and A. J. Ryan, *J Phys Chem B* 2006, 110, 10272-10279;
        b) T. B. Koynova R, *OA Biochemistry* 2013, 9, 1.
[2]   G. Battaglia and A. J. Ryan, *Nat Mater* 2005, 4, 869-876.
[3]   S. Forster, B. Berton, H. P. Hentze, E. Kramer, M. Antonietti and P. Lindner, *Macromolecules* 2001, 34, 4610-4623.
[4]   K. Kita-Tokarczyk, J. Grumelard, T. Haefele and W. Meier, *Polymer* 2005, 46, 3540-3563.
[5]   a) D. E. Discher and A. Eisenberg, *Science* 2002, 297, 967-973;
        b) Q. Chen, H. Schonherr and G. J. Vancso, *Small* 2009, 5, 1436-1445.
[6]   Q. Chen, H. Schönherr and G. J. Vancso, *Small* 2009, 5, 1436-1445.
[7]   D. D. Lasic, *Biochem J* 1988, 256, 1-11.
[8]   a) R. M. Hill, M. T. He, Z. Lin, H. T. Davis and L. E. Scriven, *Langmuir* 1993, 9, 2789-2798;
        b) J. Braun, *PHASE DIAGRAMS AND APPLICATIONS OF AMPHIPHILIC BLOCK COPOLYMERS IN AQUEOUS SOLUTIONS* PhD thesis, University of Basel, Basel, 2011.
[9]   a) A. M. Seddon, P. Curnow and P. J. Booth, *Biochim. Biophys. Acta, Biomembr.* 2004, 1666, 105-117;
        b) J.-L. Rigaud and D. Lévy, *Reconstitution of Membrane Proteins into Liposomes*. In Methods Enzymol., Academic Press: 2003; Vol. Volume 372, 65-86;
        c) M. le Maire, P. Champeil and J. V. Moller, *Bba-Biomembranes* 2000, 1508, 86-111.
[10]   a) M. Lomora, I. A. Dinu, F. Itel, S. Rigo, M. Spulber and C. G. Palivan, *Macromol Rapid Comm* 2015, 36, 1929-1934;
        b) M. Lomora, M. Garni, F. Itel, P. Tanner, M. Spulber and C. G. Palivan, *Biomaterials* 2015, 53, 406-414;
        c) C. Nardin, J. Widmer, M. Winterhalter and W. Meier, *Eur. Phys. J. E* 2001, 4, 403-410;
        d) M. Kumar, M. Grzelakowski, J. Zilles, M. Clark and W. Meier, *Proceedings of the National Academy of Sciences* 2007, 104, 20719-20724.
[11]   a) R. P. Brinkhuis, F. P. J. T. Rutjes and J. C. M. van Hest, *Polym. Chem.* 2011, 2, 1449-1462;
        b) K. Letchford and H. Burt, *European Journal of Pharmaceutics and Biopharmaceutics* 2007, 65, 259-269.
[12]   a) A. Koide, A. Kishimura, K. Osada, W. D. Jang, Y. Yamasaki and K. Kataoka, *J Am Chem Soc* 2006, 128, 5988-5989;
        b) A. Kishimura, A. Koide, K. Osada, Y. Yamasaki and K. Kataoka, *Angewandte Chemie-International Edition* 2007, 46, 6085-6088;
        c) A. Kishimura, S. Liamsuwan, H. Matsuda, W. F. Dong, K. Osada, Y. Yamasaki and K. Kataoka, *Soft Matter* 2009, 5, 529-532;
        d) Y. Anraku, A. Kishimura, M. Oba, Y. Yamasaki and K. Kataoka, *J Am Chem Soc* 2010, 132, 1631-1636.
[13]   V. Pata and N. Dan, *Biophys J* 2003, 85, 2111-2118.
[14]   I. W. Hamley, *Block Copolymers in Solution: Fundamentals and Applications*, Wiley 2005.
[15]   a) A. N. Goltsov and L. I. Barsukov, *Journal of Biological Physics* 2000, 26, 27-41;
        b) D. Wu, M. Spulber, F. Itel, M. Chami, T. Pfohl, C. G. Palivan and W. Meier, *Macromolecules* 2014, 47, 5060-5069.
[16]   L. Zhang and A. Eisenberg, *J Am Chem Soc* 1996, 118, 3168-3181.
[17]   a) M. Grzelakowski, M. F. Cherenet, Y.-x. Shen and M. Kumar, *J Membrane Sci* 2015, 479, 223-231;
        b) P. L. Soo and A. Eisenberg, *J Polym Sci Pol Phys* 2004, 42, 923-938.
[18]   C. K. Bagdassarian, D. Roux, A. Ben-Shaul and W. M. Gelbart, *The Journal of Chemical Physics* 1991, 94, 3030-3041.
[19]   R. M. Hill, M. He, Z. Lin, H. T. Davis and L. E. Scriven, *Langmuir* 1993, 9, 2789-2798.
[20]   D. E. Discher and F. Ahmed, *Annu Rev Biomed Eng* 2006, 8, 323-341.

[21]   J. D. Robertson, G. Yealland, M. Avila-Olias, L. Chierico, O. Bandmann, S. A. Renshaw and G. Battaglia, *ACS Nano* 2014, 8, 4650-4661.

[22]   D. M. Vriezema, M. Comellas Aragonès, J. A. A. W. Elemans, J. J. L. M. Cornelissen, A. E. Rowan and R. J. M. Nolte, *Chemical Reviews* 2005, 105, 1445-1490.

[23]   J. N. Israelachvili, *Intermolecular and Surface Forces, 3rd Edition* 2011, 10.1016/B978-0-12-375182-9.10020-X535-576.

[24]   K. Kita-Tokarczyk, J. Grumelard, T. Haefele and W. Meier, *Polymer* 2005, 46, 3540-3563.

[25]   D. M. Vriezema, J. Hoogboom, K. Velonia, K. Takazawa, P. C. M. Christianen, J. C. Maan, A. E. Rowan and R. J. M. Nolte, *Angew. Chem. Int. Ed.* 2003, 42, 772-776.

[26]   M. Dezi, A. Di Cicco, P. Bassereau and D. Levy, *P Natl Acad Sci USA* 2013, 110, 7276-7281.

[27]   D. P. D. Lasic, *Medical Application of Liposomes*, Elsevier, Amsterdam 1998.

[28]   T. J. Deming, *Adv Mater* 1997, 9, 299-&.

[29]   H. Y. Chang, Y. J. Sheng and H. K. Tsao, *Soft Matter* 2014, 10, 6373-6381.

[30]   a) L. Redondo-Morata, M. I. Giannotti and F. Sanz, *Langmuir* 2012, 28, 12851-12860;
         b) W. W. Sułkowski, D. Pentak, K. Nowak and A. Sułkowska, *J. Mol. Struct.* 2005, 744-747, 737-747.

[31]   F. S. Jean R. Philippot, *Liposomes as Tools in Basic Research and Industry By Jean R. Philippot*, CRC, 1994.

[32]   M. Ueno, S. Katoh, S. Kobayashi, E. Tomoyama, R. Obata, H. Nakao, S. Ohsawa, N. Koyama and Y. Morita, *Langmuir* 1991, 7, 918-922.

[33]   a) D. C. Drummond, O. Meyer, K. L. Hong, D. B. Kirpotin and D. Papahadjopoulos, *Pharmacol Rev* 1999, 51, 691-743;
         b) V. D. Awasthi, D. Garcia, R. Klipper, B. A. Goins and W. T. Phillips, *J Pharmacol Exp Ther* 2004, 309, 241-248.

[34]   J. S. Lee and J. Feijen, *J Control Release* 2012, 161, 473-483.

[35]   a) M. M. Parmar, K. Edwards and T. D. Madden, *Biochim. Biophys. Acta, Biomembr.* 1999, 1421, 77-90;
         b) M. C. Woodle and D. D. Lasic, *Biochimica et Biophysica Acta (BBA) - Reviews on Biomembranes* 1992, 1113, 171-199.

[36]   Y. Y. Won, H. T. Davis and F. S. Bates, *Macromolecules* 2003, 36, 953-955.

[37]   M. Bieligmeyer, F. Artukovic, S. Nussberger, T. Hirth, T. Schiestel and M. Müller, *Beilstein J. Nanotechnol.* 2016, 7, 881-892.

[38]   H. Bermudez, A. K. Brannan, D. A. Hammer, F. S. Bates and D. E. Discher, *Macromolecules* 2002, 35, 8203-8208.

[39]   F. Itel, *Lateral diffusion processes in biomimetic polymer membranes* PhD thesis, University of Basel, Basel, 2015.

[40]   a) M. Kumar, M. Grzelakowski, J. Zilles, M. Clark and W. Meier, *P Natl Acad Sci USA* 2007, 104, 20719-20724;
         b) P. Baumann, V. Balasubramanian, O. Onaca-Fischer, A. Sienkiewicz and C. G. Palivan, *Nanoscale* 2013, 5, 217-224;
         c) P. Tanner, O. Onaca, V. Balasubramanian, W. Meier and C. G. Palivan, *Chemistry – A European Journal* 2011, 17, 4552-4560;
         d) K. Langowska, C. G. Palivan and W. Meier, *Chem Commun* 2013, 49, 128-130;
         e) M. Lomora, F. Itel, I. A. Dinu and C. G. Palivan, *Phys Chem Chem Phys* 2015, 17, 15538-15546.

[41]   D. E. Discher and F. Ahmed, *Annu Rev Biomed Eng* 2006, 8, 323-341.

[42]   I. Dinu, C. Edlinger, E. Konishcheva, C. Palivan and W. Meier, *Polymer Vesicles*. In Encyclopedia of Polymeric Nanomaterials, Springer Berlin Heidelberg: 2014; Vol., 10.1007/978-3-642-36199-9_266-11-11.

[43]   K. Langowska, J. Kowal, C. G. Palivan and W. Meier, *J. Mater. Chem. B* 2014, 2, 4684-4693.

[44]   a) C. Nardin, S. Thoeni, J. Widmer, M. Winterhalter and W. Meier, *Chem Commun* 2000, 1433-1434;

b) W. Meier, C. Nardin and M. Winterhalter, *Angewandte Chemie-International Edition* 2000, 39, 4599-4602.

[45]   W. Meier, A. Graff, A. Diederich and M. Winterhalter, *Phys Chem Chem Phys* 2000, 2, 4559-4562.

[46]   D. Lensen, D. M. Vriezema and J. C. M. van Hest, *Macromolecular Bioscience* 2008, 8, 991-1005.

[47]   P. Broz, S. Driamov, J. Ziegler, N. Ben-Haim, S. Marsch, W. Meier and P. Hunziker, *Nano Lett* 2006, 6, 2349-2353.

[48]   a) A. Napoli, N. Tirelli, E. Wehrli and J. A. Hubbell, *Langmuir* 2002, 18, 8324-8329;
        b) F. Itel, M. Chami, A. Najer, S. Lörcher, D. Wu, I. A. Dinu and W. Meier, *Macromolecules* 2014, 47, 7588-7596.

[49]   a) G. Battaglia and A. J. Ryan, *J Am Chem Soc* 2005, 127, 8757-8764;
        b) A. Blanazs, S. P. Armes and A. J. Ryan, *Macromol Rapid Comm* 2009, 30, 267-277.

[50]   R. Stoenescu, A. Graff and W. Meier, *Macromolecular Bioscience* 2004, 4, 930-935.

[51]   R. Stoenescu, A. Graff and W. Meier, *Macromolecular Bioscience* 2004, 4, 930-935.

[52]   a) M. Massignani, H. Lomas and G. Battaglia, *Polymersomes: A Synthetic Biological Approach to Encapsulation and Delivery*. In Modern Techniques for Nano- and Microreactors/-reactions, Springer Berlin Heidelberg: Berlin, Heidelberg, 2010; Vol., 10.1007/12_2009_40115-154;
        b) C. LoPresti, H. Lomas, M. Massignani, T. Smart and G. Battaglia, *J. Mater. Chem.* 2009, 19, 3576-3590.

[53]   P. Wyatt, *Light Scattering and the Absolute Characterization of Macromolecules*, 1993.

[54]   J. Hotz and W. Meier, *Langmuir* 1998, 14, 1031-1036.

[55]   A. A. de Thomaz, D. B. Almeida and C. L. Cesar, *Measuring the Hydrodynamic Radius of Quantum Dots by Fluorescence Correlation Spectroscopy*. In Quantum Dots: Applications in Biology, Springer New York: New York, NY, 2014; Vol., 10.1007/978-1-4939-1280-3_685-91.

[56]   R. Heintzmann and G. Ficz, *Briefings in Functional Genomics* 2006, 5, 289-301.

[57]   B. T. Bajar, E. S. Wang, S. Zhang, M. Z. Lin and J. Chu, *Sensors (Basel, Switzerland)* 2016, 16, 1488.

III Preparation of nano-reactors

1 Design of OmpF conjugates as biovalves

1.1 Choice of OmpF Mutants

OmpF was chosen for its known crystal structure and remarkable stability (temperature up to 70°C, solvents, detergents and pH range from 5.5-8.5)[1] and for its pore dimensions allowing molecules of up to 600 Da to pass through.[1] The pore size is thus large enough for most enzyme substrates, smaller dyes, or some smaller pharmaceuticals to pass through, but small enough that a single short peptide, or dye[2] could block the pore. Furthermore, it served as a model pore before, and modifications of specific amino acid residues in the OmpF channel were shown to influence the translocation of small molecular weight molecules.[1b, 2-3]

In order to attach the responsive group to the channel protein, first OmpF was **genetically modified** to introducing cysteine residues at key locations in the OmpF amino acid sequence. The mutation sites D12C (aspartate, the 12th amino acid of the OmpF amino acid sequence replaced by cysteine) K89C (lysine) and R270C (arginine) located inside the pore in the eyelet-region were replaced by cysteines (**Fig. 2**). These locations allow the attachment of molecular groups that can block the molecular flow at the beginning of the pore or point outwards without obstructing the pore, in different conditions (**Fig. 1**).[1a, 3-4]
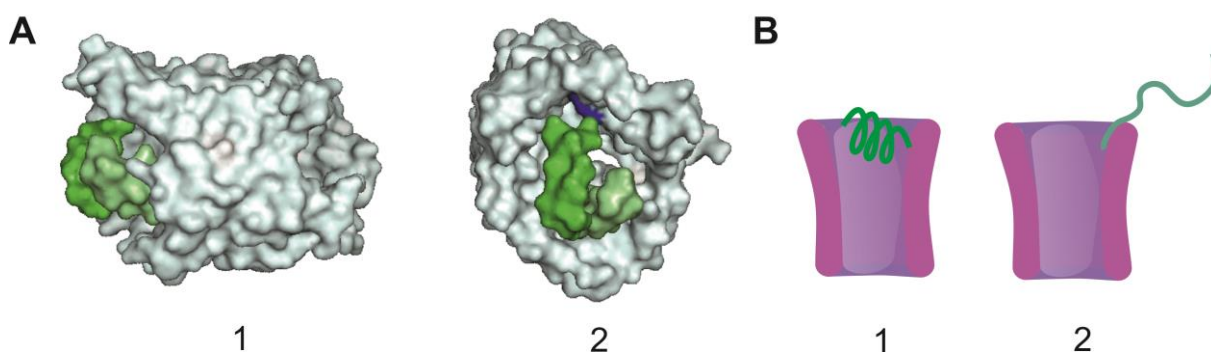
Fig. 1: A. Three-dimensional representation of OmpF-C after binding of the pH responsive peptide Gala3 (green) attached in helical structure (compact state) to cysteine residues (blue) of OmpF-M showing closing of the pore: view from the side (1), and from the top (2). B. Schematic representation of the OmpF-pore in "closed state", with Gala3 blocking the entrance of the pore (1), and in "open state", with the attached Gala3 freely moving in its random-coil state (2). Note that for the sake of simplicity only one peptide is displayed.

The original idea was to use a single mutation as anchor point. Since to this date the accessibility of a single X→C mutation site cannot be 100% guaranteed, three different mutation sites have been chosen: **D12C, K89C** and **R270C**. The double mutants **D12,K89C, D12,R270C** and **K89,R270C** served only as back-up-plan. Since all three mutation sites are in the same region, each anchor-point should work equally, however the degree of labelling might vary, due to possible interactions with charged amino acid sidechains. Using a double mutant would increase the degree of labelling (DOL) and offer better conditions to block the OmpF pore because two peptides will occupy more space inside the pore.
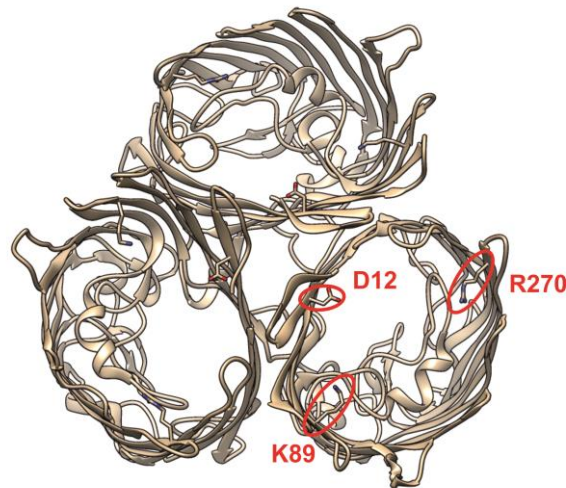
Fig. 2: location of the mutation sites (highlighted only in one of the three channels of the OmpF trimer)

Initial experiments indicated that K89C and R270C work equally well as anchor point. At that time, the determination of the DOL was still not reliable and preliminary experiments indicated only 50% labelling thus the rest of the studies were centred on the double mutants. At the time, all experimental parameters were fixed only R270C- and K89R270C-OmpF were still available. To attach a peptide (or oligomer) to the thiols of the cysteine residues in the OmpF-M, Michael addition (**Fig. 3**) was chosen due to its straightforward approach, fewer side-reactions compared to disulphide bonds formation with the cysteine residues, or to direct alkylation of the cysteine residues with halogenoalkanes.[5] In addition, the chosen glycine maleic imide linker (the connection between OmpF-M and the peptide) is a small molecule (138 Da) and expected to have no impact on substrate translocation through the pore due to its small size.
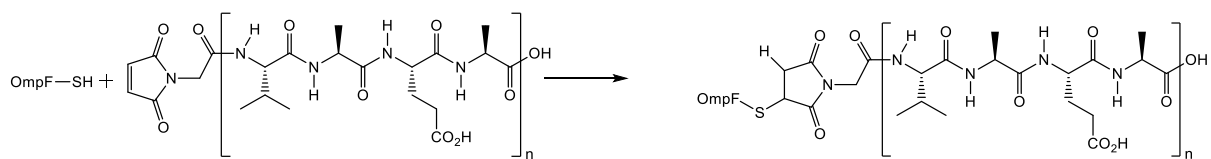
Fig. 3: Michael addition of the Gala3 peptide to the cysteine side chains of the OmpF-M

The **mutation** was performed via polymerase chain reaction of the entire plasmid. The K89C-mutation was introduced first, then the R270C-mutation was introduced by the same procedure. After purification via gel-electrophoresis, the product was isolated and sequenced, confirming the mutation (**Table 1, in Materials and Methods**). The double mutant of the porin, K89C-R270C-OmpF (OmpF-M) was then overexpressed in Omp8 E.coli. Its excess over naturally occurring OmpF-WT made further separation unnecessary. OmpF-M could not be distinguished from OmpF-WT or single mutants K89C-OmpF and R270C-OmpF, indicating a successful expression and good purity, because of the lack of additional bands in the Coomassie stained gel (**Fig. 8, 9, in Materials and Methods**). An OmpF-M concentration of 0.75±0.25mg/mL (extract without further concentration steps) was determined by BCA total protein assay®.

The **presence of thiol groups** and their accessibility was evaluated by binding them with the thiol-reactive fluorophore acrylodan. As expected, OmpF-WT did not reveal any fluorescence intensity upon addition of acrylodan, indicating the lack of nonspecific binding of the fluorophore to the porin. On the contrary, the fluorescence intensity of acrylodan when added to the thiol-bearing mutants (K89C-OmpF, R270C-OmpF and OmpF-M), clearly indicates successful thio-functionalization of the porin. Moreover, the fluorescence intensity of acrylodan when bound to the double mutant K89R270C-OmpF was similar to that resulting from a double concentration of R270C-OmpF bound to acrylodan (**Figure 13 and 15**), indicating that both thiol groups are accessible, and can bind to small molecular weight molecules.

1.2 Designing of the stimuli-responsive group

In order for the OmpF-conjugate to work as a valve, the oligomer or peptide needs to meet multiple requirements:

It must be water soluble in one state and insoluble in another state or remain water-soluble but change its conformation drastically. Regarding **pH-responsive systems**, a noteworthy complication is that it needs to remain water soluble between pH 6.5 and 7.5[6] in order for the Michael addition to work. In addition, it should have a low tendency to aggregate in solution. Similarly, low solubility can become a problem during synthesis or purification. Besides pH responsive groups, temperature (dehydration of PNIPAAM or ELPs in heat), light (cis/trans isomerisation) or reduction sensitive groups could theoretically be used in a reversible manner. Light sensitive groups do not change solubility but switch between a straight and a bent conformation. Due to the size of the pore only small chromatic groups could be used and it relies on a single isomerisation due to size restrictions. However, this has successfully been used, but only for ion channels.[7] For these reasons the focus of research lay on the other potential stimuli, with the exception of reduction sensitive systems. The latter would rely on bending caused by reversible cyclisation by disulphide bond formation, which would interfere with the thiol groups of the OmpF-mutants. Lastly, it should be noted that material properties are all size/mass dependent. Thus, very short peptides may not display any stimuli responsiveness at all. This aspect will be elaborated in later chapters.

The second requirement is **length**. Since the OmpF pore has the size of 7-11 Å[1a], a linear oligomer with a total length of 9 Å should be able to block the pore, however even in the unlikely case that the oligomer remains linear, it could point outwards or lie flat against the pores internal surface. On the other hand, polymers would be hard to attach to the inside of the pore and most probably block it permanently independent of the absence or presence of the stimulus. Regarding these two requirements, a length of 20-50Å was expected to be the most promising.

Lastly, the **synthesis** of the groups needs to remain practical. The synthesis of systems triggered by light, or reduction potential can be expected to exceed 5 reaction steps, which all require different conditions and work ups, without promising a high over all yield, or modularity, which would be important to create libraries, nor does it allow to effectively vary the length of the stimuli responsive group. PAA and PNIPAAM on the other side are easy to synthesise in various lengths, but synthesis of oligomers in the length of 20-30Å, in particular with low polydispersity is without established procedures. All these problems do not exist for peptides, but their synthesis and purification are more complex, yet well established.

1.3 Oligomers as stimuli-responsive groups

It was originally intended to use oligomers synthesised via ATRP as stimuli responsive groups, replicating the stimuli responsive pore of *Chiu et al*,[8] only in a scaled down version so that it fits the OmpF-pore. In their publication, they presented a blockcopolymer which formed vesicles in a very different fashion and featured phase separation providing domains of acrylic acid, which acted as pores on their own (**Fig. 4**).
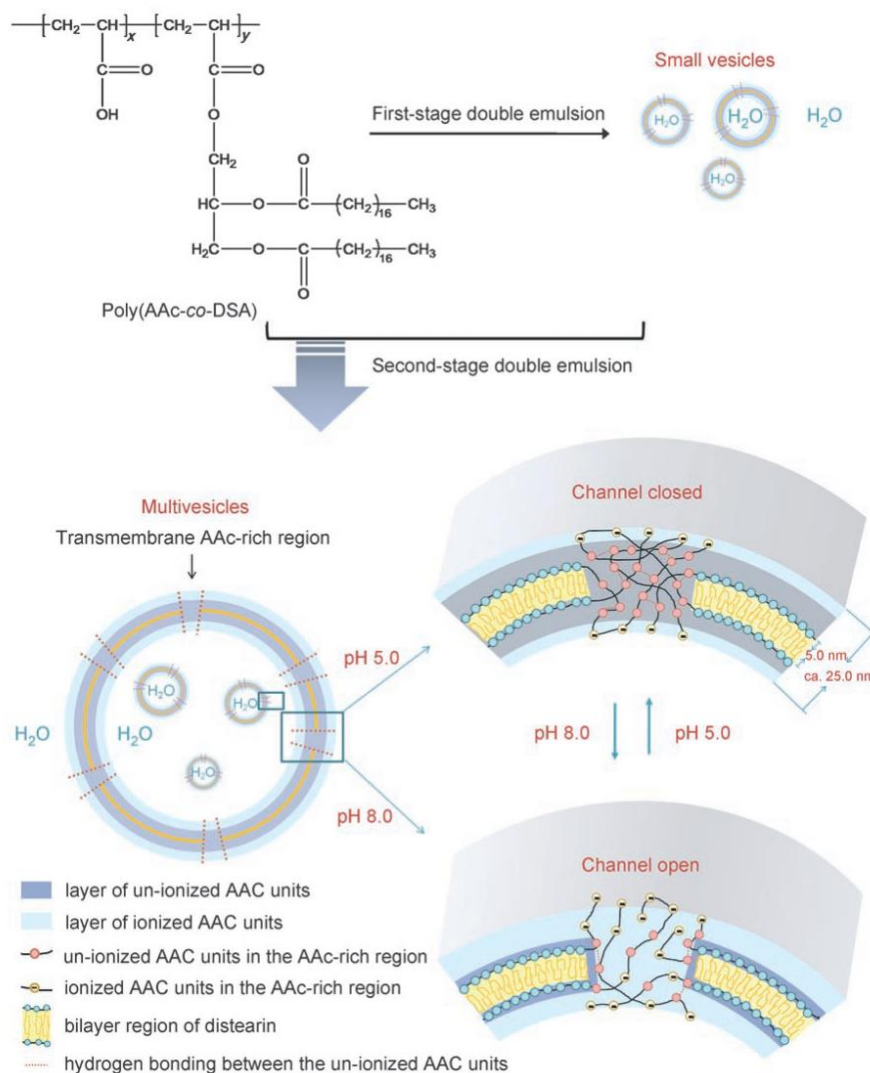
Fig. 4: Illustration from the original publication of Chiu *et al* 2008[8] and the original description: Illustration of multivesicle assemblies equipped with pH-responsive transmembrane channels from two-stage double emulsion of poly(AAc-co-DSA). The AAc-rich regions and the bilayer islets within the vesicle membrane are not drawn to scale.

As an alternative to the pH-responsive *oligo*(acrylic acid), *oligo*(NIPAAM) as temperature sensitive oligomer was considered as well. In both cases ATRP should allow mild reaction conditions, enable good control over the chain-length and allow having an anchoring group on one end only, by using an ATRP-initiator with a protected maleic imide.

While it could be assumed that oligomers are more challenging to attach than shorter molecules to the inside of the OmpF pores (= grafting to), grafting to was still considered superior to grafting from. Performing the ATRP from the anchor points (= grafting from) within the pore would have ensured a high DOL and an even distribution, but the oligomerisation would probably be affected by the constrictions of the pore (transition state, diffusion of the monomers…) which are expected to reduce the reaction speed and probably reduce the expected length of the oligomer. The reaction progress would be difficult to follow and there would be no way of purifying the oligomers. Moreover, in case of *oligo*(acrylic acid) a deprotection step is required as acrylic acid does not polymerise well as such.

The advantage over the stimuli responsive peptides would be its simple design, the relative ease of production and purification. Still, two potential pitfalls could be expected: firstly, no well-defined oligomers of the targeted length were described in literature, as ATRP is meant for polymerisation and not oligomerisation and secondly, downscaling the length of the stimuli responsive polymers to oligomers might change the physical properties.

1.3.1 The ATRP Initiator

The indicator was of the bromo-isobutyryl-type featuring a protected maleic imide for later attachment of the oligomer to thiol groups of the OmpF mutant. It was obtained in three steps in moderate to good yield (90%, 75%, 71% respectively; **Fig. 5**). The yield of the first step was twice as high as in the original publication (90% compared to 42%).[9]

The maleic imide had to be protected for the ATRP as it would react as an alkene terminating the reaction (due to its low electron density) and rendering the anchor useless. The final deprotection is achieved through a retro-Diels-Alder reaction, which requires only heating the compound thus splitting the furan off, reversing the first step. The initiator is very reliable and stable as long as it is pure, however traces of HBr stemming from the 3rd reaction step appears to catalyse the decomposition of the compound. It was once observed that initiator became useless within 3 weeks stored at 4°C whereas in pure form it is stable for years.
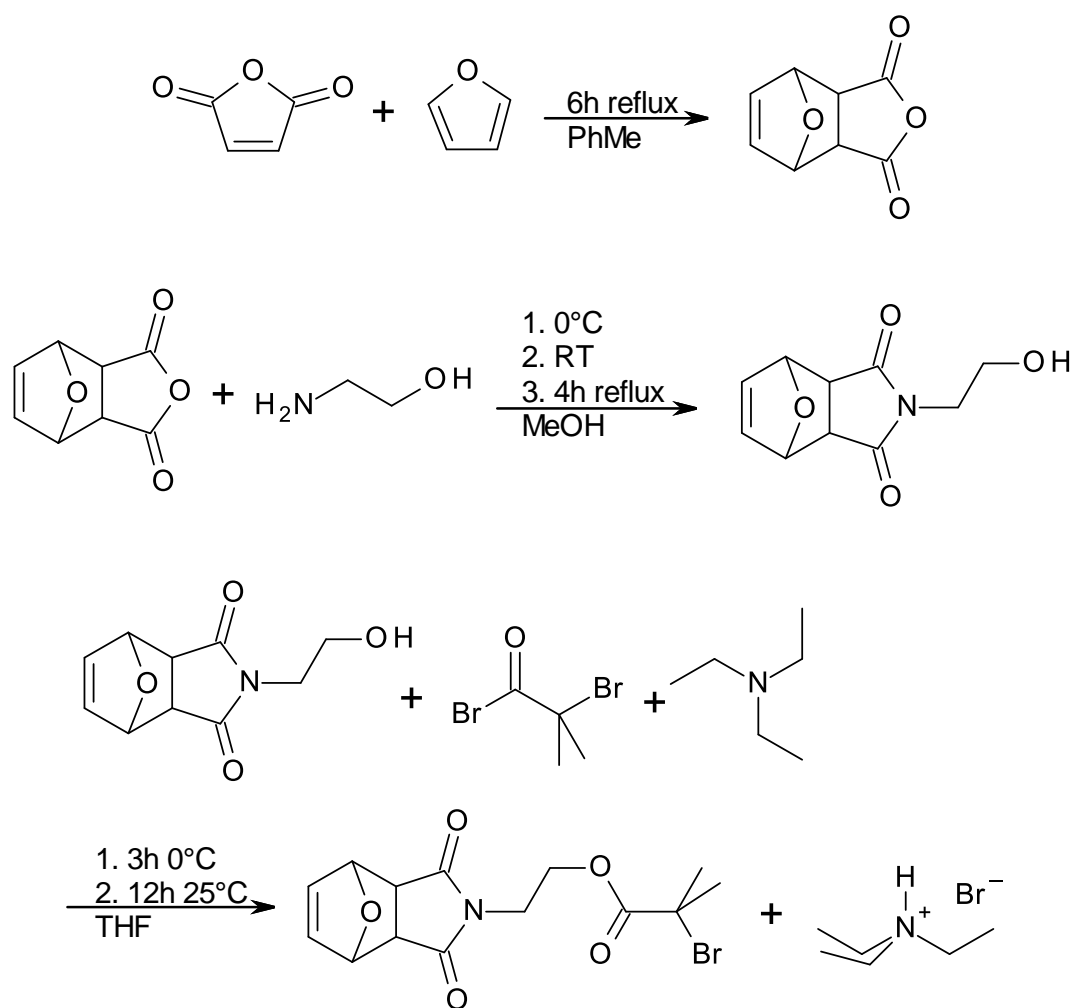
Fig. 5: Synthesis of the initiator.

1.3.2 Oligo(acrylic acid)

Since there was almost no literature available dealing with the synthesis of well-defined oligomers, a series of experiments (see **Table 1 and Fig. 6**) was conducted to find appropriate stoichiometry (monomer:initiator:CuBr:CuBr$_2$:ligand), ligand, solvent, temperature and reaction time. The yield refers to the recovered oligomers featuring the anchor group and does not take into account the subsequent deprotection steps.

Table 1: selection of ATRP experiments involving *oligo*(acrylic acid)

Experiment	[M]:[In]:[CuBr]:[CuBr$_2$]:[L]	Ligand	Solvent	T [°C]	t [h]	Yield [%]	PDI	DP
1	100:1:1:0.1:1	PMDETA	PhMe	75	1	61	1.28	22
2	100:1:1:0.1:1	PMDETA	Anisol	75	15	19	1.18	31
3	75:1:1:0.1:1	PMDETA	DMF	75	15	9	1.33	33
4	20:1:1:0.1:1	PMDETA	PhMe	75	20.5	36	1.51	16
5	20:1:1:0.1:1	PMDETA	Anisol	75	15	75	1.1	6
6	12:1:1:0.1:1	PMDETA	Anisol	75	17	2	1.11	2
7	20:1:1:0.1:1	PMDETA	MTBE	55	21	66	1.36	15
8	15:2:1:0:1	Me$_6$Tren	*t*BuOH	20	3	74.5	1.33	7
9	8:2:1:0:1	Me$_6$Tren	*t*BuOH	20	3	98	1.37	3.5
10	15:1:1:0:1	Me$_6$Tren	*t*BuOH	30	3	84	1.27	6
11	15:1:1:0.1:1	Me$_6$Tren	*t*BuOH	30	3	69	1.79	12
12	16:1:1:1:1	Me$_6$Tren	*t*BuOH	30	4	31	2.03	16
13	15:1:1:1:2	Me$_6$Tren	MTBE	30	3	49	3.22	15
14	15:1:1:1:2	Me$_6$Tren	PhMe	20	4	31.1	1.85	30
15	20:1:1:0.1:1.1	Me$_6$Tren	PhMe	20	3	46.1	2.63/1.3	21.5

Table 1 shows the relation between reacting conditions (monomer M, initiator In and ligand L) and yield, polymerisation index (PDI/size distribution) and degree of polymerisation (PD; number of monomers linked together). Blue: important changes in the experiment; red: undesirable results; green: good results.

The starting point was standard ATRP conditions: Initiator/CuBr/PMDETA 1:1:1, with 0.1 eq. of CuBr$_2$ as retardant (reversibly binding free radicals and thereby avoiding termination side-reactions) all dissolved in toluene and reacted at 75°C (**Table 1**., experiment **1**). Experiments **1-3** (**Table 1**) used the standard conditions but tested various solvents. Experiments **4-7** shifted the focus from kinetic control of the degree of polymerisation to stoichiometric control and tested the solvent effect as well.

The other experiments used a stronger ligand for the ATRP catalyst. Experiment **8** was the recreation of the published experiment.[10] Experiment **9** and **10** tested, the effect of the monomer ratio. Experiments **10-15** tested the effect of the presence of Cu(II) on the ATRP. Experiment **13-15** tested the influence of the solvent again.

Under normal circumstances, the PDI can be kept at a minimum, by stopping the reaction after 40% monomer conversion. Since in this case a very specific polymerisation degree was required, the kinetic

would have to be measured in order to adjust the number of monomers and reaction time. However, the characterisation of the oligomer via NMR was hampered by overlapping signals from aromatic solvents (mainly the CH_3-group). Therefore, the solvent became an important variable in the experiment. Moreover, the choice of solvents changes the kinetics and some solvents were able to interact with the ATRP catalyst (anisole, DMF, *t*BuOH and MTBE) and some solvents were particularly hard to remove (toluene, anisole, DMF).

Typically, the reaction speed increases with the polarity of the solvent. Peculiarly anisole resulted in higher DP and lower yield in kinetic controlled experiments and in lower DP (**2 vs 1**) and higher yield in case of stoichiometric controlled experiments (**5 vs 4**). In both cases it had better PDI than experiments in toluene. Interestingly, MTBE was in between toluene and anisole regarding yield, DP and DPI (experiments **4, 5, 7**). DMF seemed to decrease reaction speed and control (exp. **3 vs 1**; presumably through coordination to copper). Note, that the yields are based on the isolated oligomer in relation to the amount of initiator used and not on the monomer conversion.

The experiments based on kinetic control did not provide the DP desired (6-15), although the standard conditions provided decent yield and PDI. Anisole worked well even though the copper concentration of 0.05N pushed the systems at its limits (partial precipitation). In terms of chain length and conversion MTBE seems to be the best choice for PMDETA catalysed polymerisations (exp. **7 vs 4**). The latter was restricting the reaction temperature to 55°C but allowed fast solvent removal.

Due to the weak ligand to metal binding, a stronger ligand was tried in the hope of creating a more robust system. Me_6Tren (choice based on a paper about NIPAAM oligomerisation[10]) tolerates polar solvents, even alcohols and water. Its copper complex was also catalysing the ATRP significantly faster (ca. 10x at 30°C). Unlike PMDETA it resulted nearly always in full conversion. Sill, experiments **5** and **8** had very similar results. This marks a turning point as Me_6Tren works better for shorter DP, whereas PMDETA works better for higher DP and results in a lower DPI.

Since it was difficult to stop the ATRP in the right moment and since the majority of monomer remained unconverted, it was tested as well, how well limiting the conversion via monomer depletion worked. Limiting the DP with restricting the number of monomers worked surprisingly well. In case of PMDETA anisole and MTBE were the best solvents (experiment **5** and **7**). The downside was that the method works better for higher DPs (experiment **5 vs 6**).

Attempting to decrease the reaction speed of Me$_6$Tren by using apolar solvents and high amounts of CuBr$_2$ failed, resulting in low yields and high PDI-values (experiment **11-15**). Note: experiment **15** apparently lost control during the reaction resulting first in a rather well defined PDI of 1.4 and then broadening to 2.6. In the GPC-graph both peaks were overlapping.

As it turned out, the best option was not to reduce the reaction speed at all. The best solvent was apparently *t*BuOH and the best reaction temperature 30°C (below there was a tendency of the solvent to crystallize or to precipitate the solute). This procedure allowed DP down to 4, although only starting from a DP of 6, the deprotection started to work reliably (longer oligomers were possible as well, but the other method using PMDETA achieved better PDI values). It should be noted that short oligomers behaved very differently. Oligomers with less than ca. 20 repeating units were oils and could therefore not be precipitated. These oils had astonishing vapor-pressure-reducing abilities which impeded the removal of toluene and anisole at the rotavap (even with only 10wt% oligomer). The safest method of removing the solvent, turned out to be the use of flash chromatography.
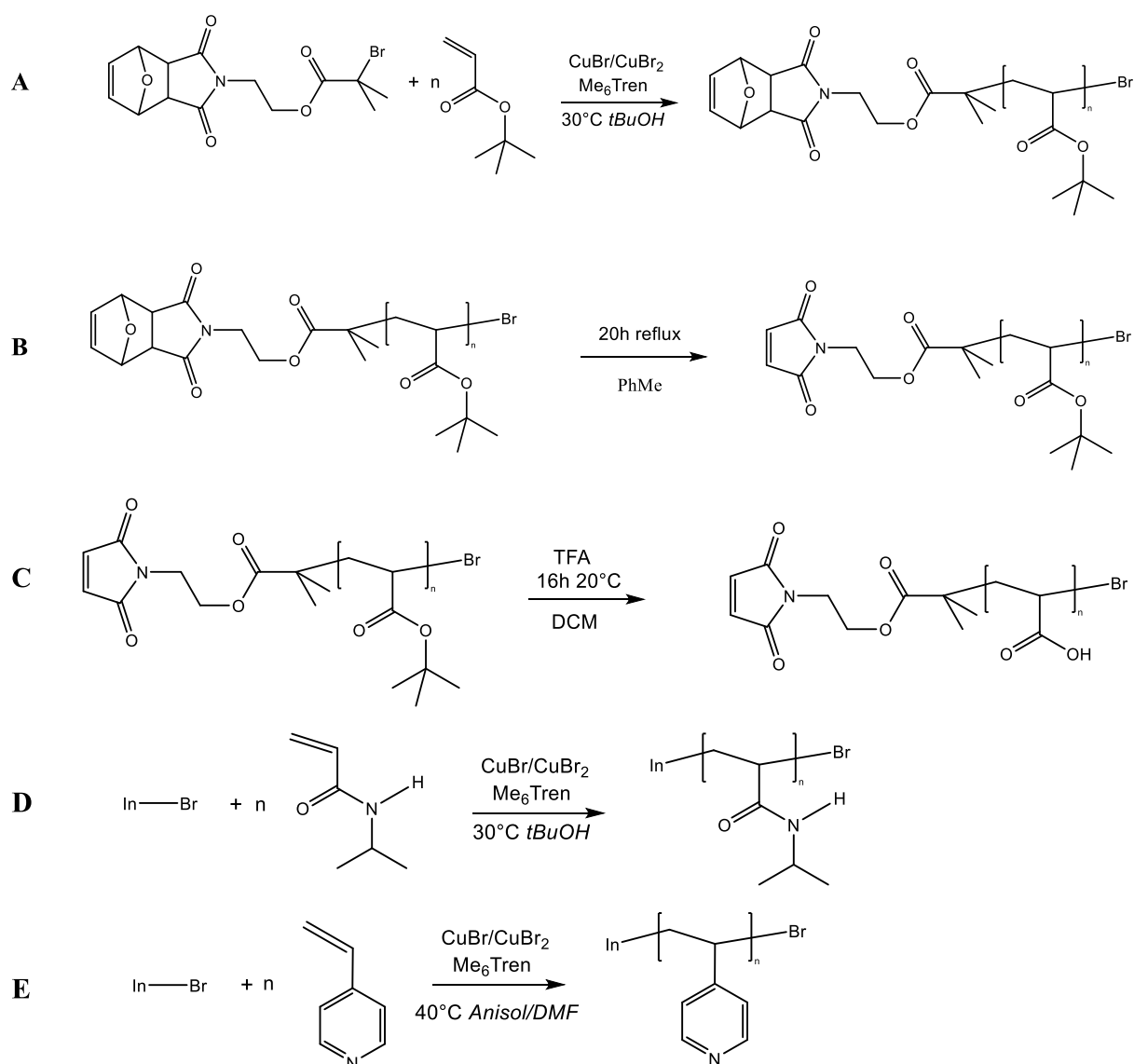
Fig. 6: The synthesis and deprotection of *oligo*(*tert*.-butylacrylate) and the other stimuli responsive oligomers. A: synthesis of *oligo*(acrylic acid); B: its deprotection step 1; retro-Diels-Alder reaction; C: its deprotection step 2; de-tert-butylation; D: synthesis of *oligo*(NIPAAM); E: synthesis of *oligo*(4-vinylpyridine); the latter two must only undergo the first deprotection step.

The **retro Diels-Alder** reaction works well in toluene giving nearly quantitative yield, but the solvent has an unexpectedly low gas-pressure, making evaporation with a rotavapor impossible (requiring high vacuum, or better a Kugelrohr distillation apparatus and high vacuum). Replacing the solvent with isooctane works but it is only poorly dissolving the polymer.

The **de-*t*-Butylation** was successful, except for *oligo*(*tert*.-butylacrylate) with chain lengths below 6. In these cases, a side reaction occurred, which we assume is a polymerisation of the maleic imid, since

the product became insoluble in water. It is in general a tricky step, since the initiator is bound through a primary ester, features a polymerisable alkene and since the product is hydroscopic. The removal of solvent can therefore result in the destruction of the product. Even traces of acid (TFA or HBr) seem to reduce the shelf-life of the product dramatically (stored at 4°C). The product apparently polymerised itself, as it became poorly water soluble, the alkene signal in 1H-NMR disappeared slowly and the detected mass in MALDI experiments (**Fig. 7**) increased multiple times while the signal intensity decreased several orders of magnitude resulting moreover in a distorted mass-spectrum:
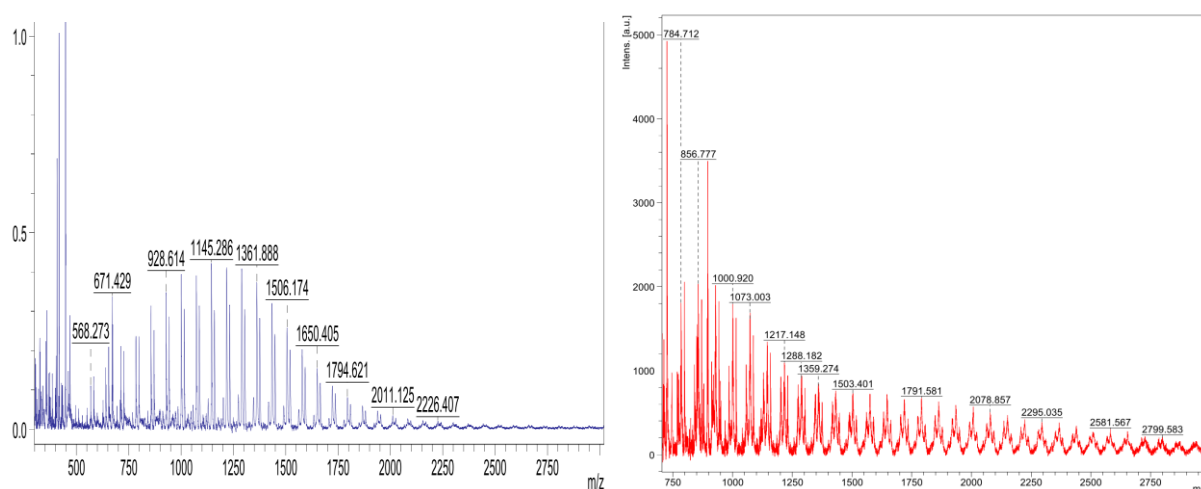
Fig. 7: two examples of *oligo*(acrylic acid); the left one had according to 2D-NMR analysis 7 repeating units whereas MALDI results imply an average PD of 12 (ranging from 4 to 17 repeating units). The right example had according to 1D-NMR a PD of 12 and was apparently already degrading as the MALDI measurement was performed. In both cases no endgroup could be identified.

It can be assumed that the bromine group is detrimental to the shelf-life of the oligomer. It may hydrolyse over time forming HBr, which in turn could catalyse the degradation of the oligomer, or it could split off forming radicals, which in turn polymerise the maleic imide and can cause other side reactions.

It was considered to remove the bromine after the ATRP via reduction, but even the protected maleic imide could react as well. An alternative would be to replace the bromine via an SN1-reaction. Considering that the replacing nucleophile should result in a stable bond and not change the polarity, KCN was the best option. However, due to its highly toxic nature, numerous safety precautions would have had to be enforced and the remaining cyanide would still need to be separated and destroyed. The latter requires oxidants which would harm the oligomer if it was not separated beforehand.

Due to the short living nature of the oligomer, later experiments with OmpF were conducted with peptides. Only after establishing a reliable assay for the functionality of the bioconjugates, the oligomers were revisited.

1.3.3 Oligo(NIPAAM)

PNIPAAM (see **Fig. 6D**) is known to exhibit a lower critical solution temperature above which the hydrated state becomes unstable, thus causing the polymer to precipitate from water. The ATRP was basically identical to the one used for *oligo*(acrylic acid); in fact the procedure used for *oligo*(acrylic acid) was based on a paper applying the ATRP on NIPAAM;[10] the reaction and purification proved to be quite different from those experienced in producing *oligo*(acrylic acid). The reaction speed was somewhat lower and the yield 3-4x lower. On the plus side, the monomer did not require a post-polymerisation deprotection-step. The oligomers could always be precipitated, very unlike *oligo*(acrylic acid), where short oligomers failed to crystalize. The oligomers did not lower the vapour pressure of the solvents, facilitating drying, but the monomer could not be evaporated. Moreover, the oligomers become stuck on silica. Thus, only multiple precipitations or dialysis in *n*-propanol (only solvent found to dissolve oligomer, while not attacking the cellulose acetate membrane) worked. Due to residual monomer, overlapping in the 1H-NMR spectra the DP are rather qualitative by nature.

Table 2: ATRP with NIPAAM

Experiment	[M]:[In]:[CuBr]:[CuBr$_2$]:[L]	Ligand	Solvent	T [°C]	t [h]	Yield [%]	PDI	PD
1	20:2:1:0:1	Me$_6$Tren	*t*BuOH	30°C	3	28	1.19	10
2	12:2:1:0:1	Me$_6$Tren	*t*BuOH	25°C	4	41	1.28	6
3	12:2:1:1:0.1:1	Me$_6$Tren	*t*BuOH	30°C	4	9	1.34	6
4	15:1:1:0.1:1.1	Me$_6$Tren	*t*BuOH	25°C	4.15	23	n.d.	18
5	8:1:1:0.1.1	Me$_6$Tren	*t*BuOH	30°C	3	24	1.23	8

As seen in **Table 2** it was much harder to obtain decent yields with NPAAM compared to acrylic acid esters (**Table 1**). Important changes in the experiment are marked in blue; red marks undesirable results and green good results. Experiments **1** and **2** are to test influence of the monomer ratio, **3-5** tested the influence of Cu(II) and **4** and **5** tested the influence of the monomer ratio again (the PDI of 4 was not determined, as the product was not in the desired length, nor desired yield). As before with

oligo(acrylic acid) it was found that ATRP with Me$_6$Tren worked best without CuBr$_2$ and an initiator/catalyst ratio of 2:1. However, the influence of Cu(II) was vastly diminished.

Due to the experimental difficulties and the consideration that changes in charge would have a stronger effect on stimuli response, *oligo*(NIPAAM) was dropped in favour of *oligo*(acrylic acid) and acidic peptides. Furthermore, heating liposomes deforms and eventually destroys them.

1.3.4 Oligo(vinyl-4-pyridine)

Since the originally used *oligo*(acrylic acid) did not reveal a sufficient change in polarity for unblocking the OmpF pore within the acceptable pH range,[12] a different oligomer was considered. Regarding availability, reactivity and a pK$_a$ value in the middle of the range, 4-vinylpyridine was chosen (see **Fig. 6E**).

The ATRP and purification were plagued by poor solubility, despite the fact that monomer was supposed to be soluble in most organic solvents (toluene, CHCl$_3$, dioxane, THF, DMSO, DMF, MeOH, EtOH, *tert.*-butanol and acetic acid). It was not soluble in anisole despite its similarity to toluene. Thus, the solvent was changed to DMF. Synthesis of oligomers in the desired length worked ([M]:[In]:[CuBr]:[CuBr$_2$]:[Me$_6$Tren] 100:1:10:1:1.1 at 40°C). The degree of polymerisation appears to be around 6 for 3h reaction time and 15 for 6h. The reaction mixture was slightly turbid at the beginning and became more opaque over time. Moreover, the monomer and even more so the oligomer act as ligand and thus interfere with the reaction and copper removal. Furthermore, the product got stuck on ALOX (which was supposed to remove copper catalyst). As it turned out it could be washed out eventually with a large amount of THF, which could also be used for its recrystallization procedure.[13] A better method of removing the copper was precipitating the oligomer in 10mM NaHCO$_3$ pH=8.0 with 1mM EDTA (for removing the copper), although it still dissolves too much product. In general, it appears that with a higher chain length the solubility in ethanol and basic water increases and the solubility in THF decreases (and the amount stuck on ALOX increases).

The choice of reaction conditions and work-up could surely left room for improvement thus the PDI was not determined, although it has to be expected to be broader than *oligo*(acrylic acid) due to the interactions with the catalyst. Hence, it was deemed applicable, but not promising enough to further invest time in it.

---

[12] For the used dyes and enzymes, the acceptable pH range is ca. 5.5-7.5.
[13] The formation of crystals is unlikely, but the crude product can be precipitated in higher purity

1.4 Stimuli-responsive peptides

As an alternative, stimuli-responsive peptides were envisioned. Peptide synthesis offers several advantages over ATRP:

It allows precise control over both the length and composition of the stimuli responsive group. This increases the reproducibility as no longer mixtures are involved. Regarding the rather narrow OmpF pore one amino acid more or less could determine whether the peptide can be attached or if it blocks the pore at all or if it blocks it permanently, irrespective of its protonation state.

Using stimuli responsive group that are not based on ATRP would confirm that the bromine group is the cause of the oligomers low shelf-life. Indeed peptide-based stimuli responsive groups bearing the same maleic imide group proved to be much more stable, although after a year even there the anchoring group became inactive and their solubility decreased.

Peptides allow adjustment of the pH-response via exchanging the pH-responsive groups. Histamine (pKa=7.0), Lysine (pKa=10.5), aspartic acid (pKa=3.9) and glutamic acid (pKA=4.3) lend themselves to be used as such groups. Cysteine would be interesting from its pKa-value (8.3), but it is too nucleophilic and would react with the anchoring group.

Changing to peptides has however also some disadvantages. The synthesis is more complicated and time consuming. More importantly, the purification of peptides is demanding. This is particularly true for short peptides, with repeating amino acid sequences and multiple charges.

A peptide of 12 amino acids would be ca. 48Å in its linear form, or 15Å in shape of an α-helix. A random coil could be anything in between. Thus, peptides with 6-12 amino acids were envisioned as stimuli responsive groups. The following peptides were ordered:

Table 3.: list of investigated peptides

Name	sequence	amino acids	length linear [Å]	length helix [Å]
LAEA3 (Gala3)	LAEALAEALAEA	12	48	15
H6	HHHHHH	6	24	8
HF3	HFHFHF	6	24	8
HL3	HLHLHL	6	24	8
HLG4	HLGHLGHLGHLG	12	48	15
GHLL3	GHLLGHLLGHLL	12	48	15

LAEA saw most extensive investigation since it was reported before to work as a stimuli responsive group.[11] Since it is based on the GALA sequence (WEAALAEALAEALAEHLAEALAEALEALAA), the peptide was referred to Gala3 due to its three repeats of LAEA (see **Fig. 2**).

All other tested peptides (**Table 3**) contained histamine in place of asparagine, due to its pKa of 7 offering the greatest change in protonation between pH 8 and 5 among all considered amino acids (for calculations on protonation as a function of pH see chapter **VI Theoretical calculations**). The main variable in the peptides was the polarity. The more hydrophobic the unprotonated peptide becomes, the stronger the expected stimuli response. However, it reduces the solubility at the pH where the Michael addition takes place. This possibly prevents some of the peptides from being used. Glycine was used in between pH-responsive amino acids, since it increases the flexibility of the peptide and reduces the risk of rigid formations aggregating.

Another factor is the number of pH-responsive groups per peptide. Since the protonation state will not change completely in the physiological relevant pH range a certain number is required to take effect. We chose the lower limit at 3. Taking the synthesis into account, each responsive amino acid had non-responsive, hydrophobic neighbours. Such a peptide would already be at the lower end of the targeted length.

2 Methods for determining the degree of labelling

Since the peptides are of limited solubility, detergents are interfering and the thiol groups inside the OmpF pore might be hard to access. Proving successful labelling is important. However, the peptide bound to the thiol group itself cannot be detected. Thus, only the remaining reagent or thiol groups may be detected, making every attempt of determining the DOL an indirect measurement.

For this purpose, predominantly, addition of fluorophores to remaining thiol groups was investigated. The ideal fluorophore should be cheap, photostable, well soluble in water (for the reaction, but also for its removal) and small enough so that it can reach the thiol groups without having to denaturate the OmpF sample. Moreover, the Stokes-shift should be large and both emission and fluorescence should be accessible for fluorescence correlation spectroscopy (FCS).

2.1 Reagent recovery

The most straightforward approach would be after the Michael addition to separate the product from the excess of the reagent via HPLC and determine both concentrations, however, this concept has several flaws:

- Detection: it would require a preparative HPLC to use a BCA assay for determining the protein concentration. For smaller concentrations, it would rely on the HPLC detectors which in turn would require calibration (specific for the currently analysed reagent). In this case the detection limit might be too high.
- Separation: the reagent might become insoluble and precipitate or stick to the OmpF without being actually bound to it.
- Detergents: OmpF requires detergents for stabilisation in solution. Similarly, the stimuli responsive group may require detergent for its solubilisation. Thus, dilution and inconsistent detergent reduction could significantly affect the accuracy. Furthermore, HPLC is likely to separate the stabilising detergent from the peptides.

2.2 Fluorescence correlation spectroscopy

The most accurate method would be to conjugate the remaining thiol groups with **Bodipy FL** or similar fluorophores and measure the conjugate in FCS, as it would allow to discriminate the conjugate from the free dye due to the difference in diffusion time. However, OmpF requires detergents to remain in solution. These detergents build **micelles** which also enclose the used fluorescent dye as they are all rather hydrophobic. Various ways were tested to drive the free fluorophore out of the micelles:

- Dilution of the sample below the cmc (in the hope that the more hydrophobic OmpF binds enough detergents to stay in solution) worked in principal but was not reliable nor clean enough.
- Addition of biobeads for removing superfluous detergent had a similar result but precipitated OmpF fast.
- Size exclusion chromatography and dialysis did not separate the OmpF from the dye containing micelles as both seem to be of similar size.

2.3 Ellmans Reagent

Ellmans reagent (**Fig. 8**) is one of the most prominent and most frequently used reagent of detecting thiol groups and thus measuring the DOL.
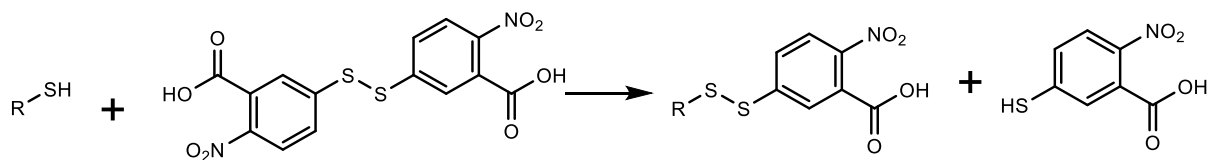
Fig. 8: the reaction of the Ellmans reagent with a thiol group forming the dye on the right.

It is a relatively small molecule that splits of a dye in an active form which can be quantified measuring the absorption. However, the detection limit is too high (ca. 50µM)[12] for the thiol concentrations found in the relevant samples.[14] This is a general problem since absorption measurements are far less sensitive than fluorescence measurements. However, fluorescence measurements are known to be far less reliable regarding the quantification of the samples concentration.

2.4 Thioglo Series

The Thioglo series (**Fig. 9**) is a collection of fluorophores that react with thiols and increase thereby their fluorescence considerably (apparently unfavourable resonance structures that reduce fluorescence are eliminated by the reaction). That way the excess in fluorophore does not need to be removed. In case of **Thioglo-1**[13] the thiol concentration could be reliably measured (linear dependence) in a range of 10 nM to 1 µM. However, it turned out that the unbound fluorophore had still considerable fluorescence.

---

[14] 1% free thiol groups in a 0.5g/L sample of OmpF (37kDa) would correspond to 135nM. Measuring OmpF in vesicles, would require 2-3 orders of magnitude lower concentrations, thus except for FCS, all experiments would require analysing OmpF-solutions directly.

Thioglo-1   Thioglo-3   Thioglo-5
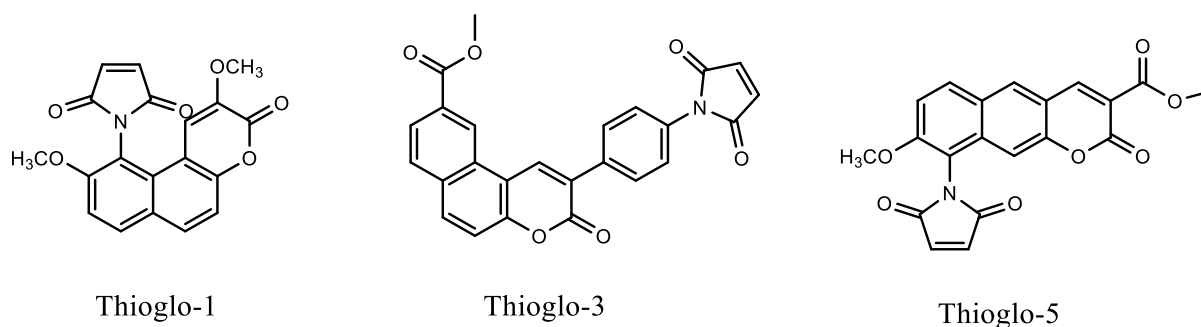
Fig. 9.: The Thioglo-series
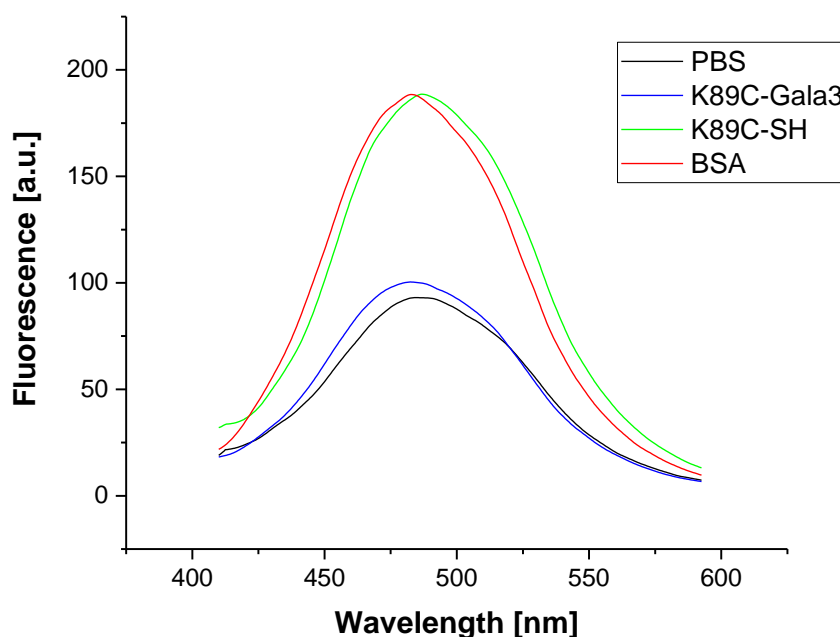
Fig. 10.: labelling K89C-SH and K89C-Gala3 OmpF with Thioglo-1[15] and measuring the fluorescence at 400nm excitation (peak emission 490nm). PBS refers to control containing the same amount of Thioglo and BSA refers to BSA reacting instead of OmpF with Thioglo.

As can be clearly seen in **Fig. 10**, there is a clear difference in fluorescence between reacted and unreacted Thioglo-1 and hence a clear difference between labelled OmpF and unlabelled OmpF. The latter being able to react like BSA with Thioglo-1, despite the thiol groups being not at the outer surface of OmpF.

---

[15] 65µL 10µM Thioglo added to 300nM R-SH and filled up to 500µL with PBS; shaken for 2.5h at 25°C. and then measured as soon as the bubbles disappear (avoiding exposure to light as much as possible).

III Preparation of nano-reactors

Due to the considerable background fluorescence, it was attempted to purify the samples via washing in 10kDa amicon centrifugation tubes or desalination minicolumns in the hope of obtaining a higher sensitivity for quantification of the DOL. However, both methods reduce the fluorescence and hence sensitivity greatly, presumably through precipitation of OmpF. In case of the sample preparation via size exclusion chromatography (minicolumns), the calibration curves became non-linear, but had a significantly lower statistic error (**Fig. 11**). This effect may be explained through more efficient detergent removal.
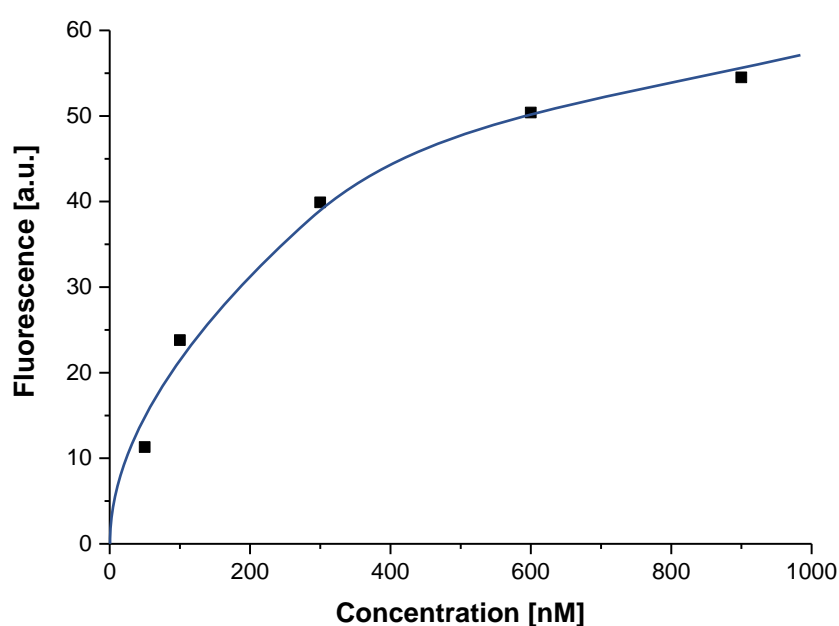
Fig. 11: various concentrations of BSA reacted with Thioglo-1 and then passed through a minicolumn.

Moreover, the size exclusion chromatography produced two fluorescent fractions one with a maximum emission at 440nm and one at 540nm instead of the anticipated 500nm. This is presumably due to a gradient of stabilising detergent (OG, octyl glucopyranoside), rather than due to bound and unbound fluorophore, since in the sample prior size exclusion chromatography did not hint overlapping emission peaks. It is also noteworthy that the emission is maximum at 1% OG and steeply declines at higher detergent concentrations.

The initial thioglo experiments suffered also from a very poor signal to noise ratio (which could be partially explained through photo-bleaching) and the lack of a calibration or standard. Since the apparent difference in fluorescence between unreacted OmpF and labelled OmpF was very small, it was considered that Thioglo-I did not react with all remaining thiol-groups over-night. This left two

options: denaturate OmpF and thereby adding compounds that could quench the fluorescence or try to digest it. OmpF is very resistant to denaturation and even digestion with proteases and Proteinase K proved ineffective and introduced apparently some thiol-containing contaminations which increased the fluorescence rendering the assay useless. Similarly, it was tried to replace unreacted OmpF with BSA for calibration, which also featured exactly one thiol group. However, it also increased the fluorescence beyond expectations. This could be caused either by thiol containing contaminations or more likely indicate that the thiol in OmpF is accessible, but only a fraction reacts reducing the sensitivity of the Thioglo-assay.

Working with Thioglo, the first inconvenience was that the supplier did not disclose the structure of the fluorophore. It could be found and later suppliers did provide it, but the experiments started without knowing whether or not Thioglo would be able to diffuse inside the OmpF pore and have enough room to react with the thiol group. Regarding the structure especially the non-linear arrangement of Thioglo-I could prove detrimental, but experiments indicated that it reacted. Adding to the supplier-related inconveniences was the fact that once the assay was almost established and ready to be used, the supplier announced that the Thioglo-I was discontinued. Since Thioglo-1 was discontinued Thioglo-3 was tested as replacement. It had however the same problems and it appears to be less suited due to its size.

2.5 Acryolodan
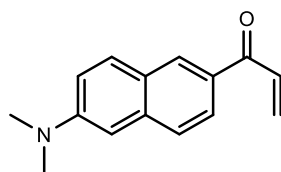
Fig. 12: Molecular structure of Acrylodan.

Acrylodan (**Fig. 12**) works similar to the Thioglo-series but was apparently never used for quantification of thiol groups but rather as a molecular probe which reacts to the polarity of the surrounding (allowing to gain information about proteins, e.g. if the labelled spot is within a membrane or outside, but also indicating structural changes). Its sensitivity towards the polarity of the environment, could be an inherent disadvantage, but since the change in fluorescence is coupled with a shift in emission, its influence on the measurement can be mitigated. Compared to the thioglo-series it is far smaller, cheaper, turned out to be more photostable and had a much greater difference between the emission of the labelled and free fluorophores (ca. 12x stronger fluorescence after the reaction). Thus, even

without further purification it had a higher sensitivity and was hence used for quantitative measurements of the DOL (calculations in chapter **Materials and Methods 3.2.8**).

It was tried to determine the DOL of acrylodan-OmpF directly through measuring the absorption of OmpF and acrylodan at 280 and 372nm respectively. However, the absorption is too weak at the obtained sample quantities.

Its main disadvantage is that the calibration curve deviates more from a line than TG-I at the same range. It also appears to have a higher statistical error than TG-I due to its sensitivity to polarity, which manifests into detection of traces of ethanol from previous washing of the cuvette etc. Thus, variations in detergent concentration or traces of ethanol from washing cuvettes significantly increased fluorescence, but also shifted the emission maxima. Such contaminations were easy to spot and exclude as data-points

Acrylodan was cheaper, better available, smaller and reacted faster and had a far higher thiol-conversion than the thioglo-series. Furthermore, the difference in fluorescence between unreacted and reacted acrylodan was far greater than in the case of Thioglo. All this contributed to a higher difference between unreacted OmpF and modified OmpF. It was also susceptible to bleaching even in the rather dim lab but could be easily avoided using blackened vials.

2.6 Mass spectroscopy

The only method theoretically able to measure the DOL directly (without having to calibrate) and accurately is mass spectroscopy. It would be thus the best method for quantification of the DOL, but membrane proteins are difficult to measure in mass spectroscopy. Membrane proteins have a large hydrophobic surface for binding to membranes, which will obviously interact with itself and detergents making it near impossible to measure the entire protein in gas phase. [14] Thus, the samples need to be fragmented. The entire procedure is tedious as the sample needs to be purified via running an SDS-gel, cutting out the band and milling it, performing in-gel digestion, extracting it, purifying and desalting it via reversed phase chromatography. Unfortunately, the peptide-fragment bearing the attached stimuli responsive group could not be found in the mass spectrum. Thus, this method became an indirect method as well, comparing the peptide fragment bearing unreacted thiol groups with other peptide fragments of the same sample. While the ratio between these peptides could change during the purification procedure, it turned out to be still the most accurate method available to quantify the

DOL (calculation in chapter **Materials and Methods 3.2.9**). However, due to the lengthy sample preparation and since it required the help of an external expert, this method was rarely used.

2.7 Discussion DOL

All the different OmpF mutants and OmpF conjugates were tested via the acrylodan method. First it was established that the single mutants had accessible thiol groups by comparing WT-OmpF with R270C-OmpF (**Fig. 13 left**) and R270C-OmpF with K89C OmpF. Then the double mutants were compared to the single mutants (**Fig. 13 right**). As expected the fluorescence increased only to a significant extent when thiols were present. Both K89C- and R270C-OmpF behaved identical in this respect and the double mutant K89,R270C-OmpF had twice the fluorescence at the same concentration as could be expected from the single mutants (**Fig. 13 right**). However, D12,K89C and D12,R270C-OmpF behaved like a single mutant (**Fig. 14**). Together with the other results it indicates that K89C and R270C thiol groups are available for labelling but not D12C. This might be due by E2 and K46 which flank D12C, or possibly tyrosine Y14 shields it. The fluorescence of these double mutants labelled with acrylodan was therefore at the same level as for the single mutants.
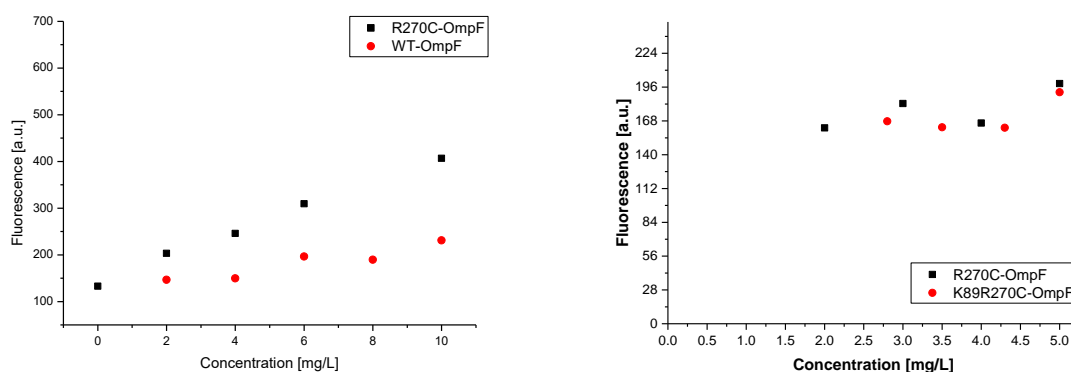
Fig. 13: left: comparing the mixture of acrylodan and WT-OmpF with the mixture of acrylodan and R270C-OmpF (procedure in materials and methods). **Right**: Comparison between the fluorescence of K89R270C-OmpF with R270C-OmpF both labelled with acrylodan. Note: The concentration of K89R270C-OmpF was divided by two to show the overlap. Also, on the left the point for 0 mg/L of OmpF is identical for both samples.
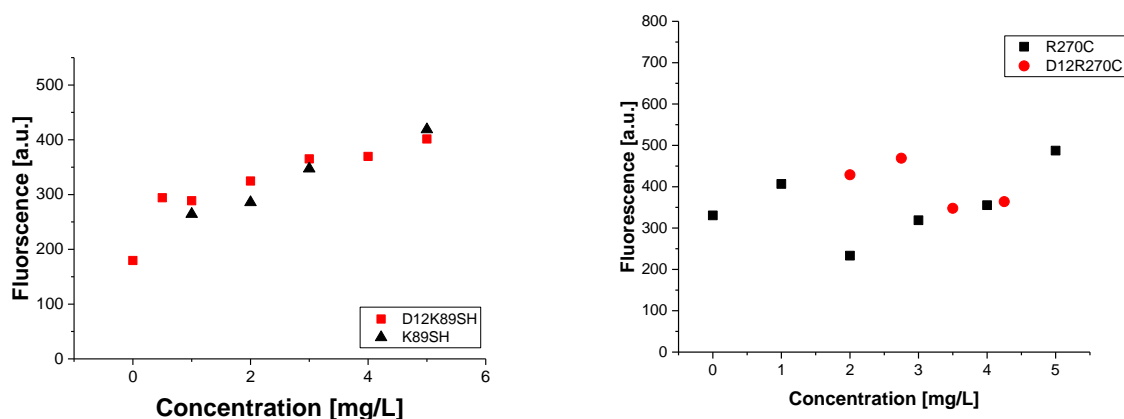
Fig. 14: left: comparison between K89C- and D12K89C-OmpF; **right:** comparison between R270C- and D12R270C-OmpF (concentration calculated as if it was a single mutant). Both prove that D12C was not labelled.

Calibration was performed by binding acrylodan to an aliquot of the same OmpF-M, in order to correct for bleaching, quenching and shifting of the fluorophore emission wavelength. Rather than measuring triplicates of a fixed concentration, the samples and standards concentrations were varied between 2.0 and 5.0 mg/mL. Within the measuring range both sets of measuring points provide two parallel lines. These points can be used for the calculation of the DOL and their results be averaged.

The reason for using a concentration range rather than triplicates, was that the detection window is dependent on the (unknown) concentration of the available thiol groups and hence not directly dependent on the protein concentration itself. Thus, the concentration of acrylodan could not be adjusted to the sample. Hence, it was kept as for labelling 5mg/L OmpF, which corresponds to the highest found thiol concentration.

0mg/L is below the best fit line, since acrylodan undergoes changes in its fluorescence upon reaction with thiol groups and should therefore not be included. The calibration curve changes its slope at 2mg/L and below (**Fig. 15**). At such low concentrations of free thiol-groups the free acrylodan will remain an excess, which could potentially interact with bound acrylodan groups via π- π-interactions or even with other aromatic amino acids.[15] At this point the concentration is too low for the measurement. It can be assumed that the fluorescence of bound acrylodan is lost in the background.

While even without thiol groups the fluorescence increased somewhat with increasing OmpF concentration, it was far lower than for thiol containing mutants. The slight increase in fluorescence may be attributed to non-covalent interactions with aromatic amino acid residues.[15], or may be to a slight increase in the detergent concentration.
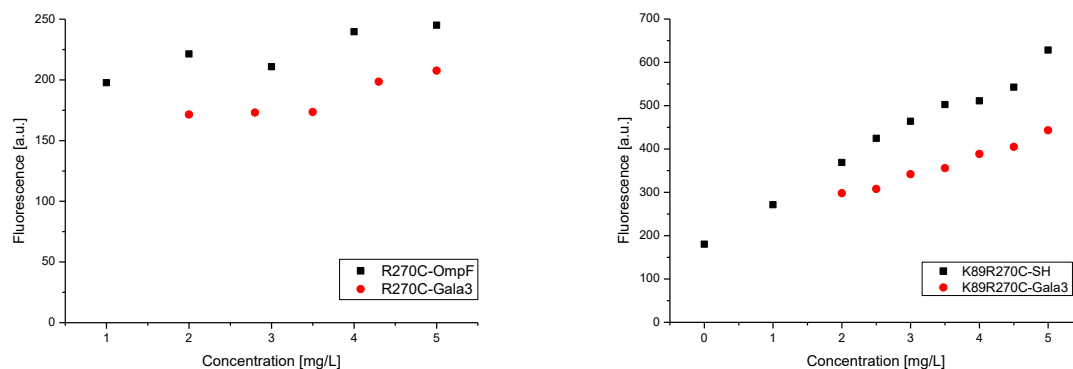
Fig. 15: Acrylodan assay of R270C-Gala3 OmpF (left, red spheres) K89R270C-Gala3 OmpF (right, red spheres) using R270C-OmpF/K89R270C-OmpF respectively as standard (black squares); the DOL was calculated to be 80% for R270C-Gala3 and 68% for K89R270C-Gala3.

In order to increase the measuring speed and excluding ethanol or other washing contaminations well-plates were used. They were however prone to measuring errors due to bubble formation from the detergents in solution. Even considering all these error sources a relatively high statistical error remained. In particular, each experiment had at least one outlier and some measurements had for unknown reasons far higher errors than other measurements indicating the existence of another error source. Interestingly, there must have been also a systematic error. For instance, the acrylodan assay indicated for K89R270C-Gala3 a DOL value of 68% ± 9%, whereas the mass spectrometry (**Table 4**) gave 88% (92% and 96% for each anchor group). A possible explanation is that in the case of the double mutant bearing only one peptide, that this peptide would reduce the fluorescence of the acrylodan binding to the other thiol-group. However, it appears more likely that incorrect assumptions have been made for calibrations. As seen for concentrations below 2mg/L, assuming a linear dependence of fluorescence on concentration is dangerous. Even when taking these limitations into account, subtracting the background fluorescence may be trickier than expected. While applying a least square fit and using the parameters of the trendline does automatically remove the background fluorescence, but only as long as it remains constant. However, if it would e.g. increase with the protein concentration due to non-specific interactions, then an error would remain, which would become worse for the higher the degree of labelling is. Regarding the fact that in many experiments the calibration line was deviating in an S-shape, albeit only slightly, this error source appears very plausible and likely the cause of the deviation between mass-spectrometry and acrylodan-measurements.

III Preparation of nano-reactors

Table 4.: Comparison of acrylodan assay with mass spectroscopy

	DOL Acrylodan	DOL Mass Spectrometry
K89C-Gala3	76%[16]	94%
R270C-Gala3	80%	92%
K89,R270C-Gala3	68%	96%[17]

A DOL value of 68% ± 9% for K89R270C-Gala3 was obtained, indicating a successful binding of Gala3 to the modified OmpF (**Fig. 15; Table 4)**. This value implies that 50% of the pores have one Gala3 attached and 20% have two Gala peptides attached, under the assumption that both the K89C and R270C anchor points are equally reactive (**Eq. 1, Table 5**).

The following calculations were used to calculate from a given DOL (P) how many pores would be labelled twice (N_2) or only once (N_1).

$$P=2(1-p)p+p^2 \qquad (1a)$$

$$N_0=(1-p)(1-p) \qquad (1b)$$

$$N_1=2(1-p) \qquad (1c)$$

$$N_2=p^2 \qquad (1d)$$

P: over all DOL (average of both thiol groups); p: individual DOL; N_n: probability N that n groups have peptides attached

---

[16] since K89C-OmpF was no longer available D12K89C was used instead (D12C was proven inactive see **Fig. 14**)
[17] Mass spectrometry does not measure the overall DOL, thus only K89R270C-Gala3 was measured, and the overall DOL was calculated from the individual DOLs using this equation:

$$P = p_1(1 - p_2) + (1 - p_1)p_2 + p_1 \cdot p_2$$

With P the overall DOL and p_i the DOL for a specific mutation site (sum of the probabilities that exclusively one mutation site is labelled and the probability that both mutation sites are labelled).

Table 5: Anticipated DOL of OmpF-C (P) as a function of the DOL of the individual thiol groups (p)

p	N_0	N_1	N_2	N_{1or2}	P
30%	49%	42%	9%	51%	51%
40%	36%	48%	16%	64%	64%
45%	30.30%	49.50%	20.30%	69.80%	69.80%
50%	25%	50%	25%	75%	75%
60%	16%	48%	36%	84%	84%
70%	9%	42%	49%	91%	91%
80%	4%	32%	64%	96%	96%
90%	1%	18%	81%	99%	99%

Note: the blue row was calculated backwards from the measured DOL of K89,R270C-Gala3 OmpF

Mass spectrometry was used as a complementary method to evaluate DOL of the Ompf-C. For this purpose, OmpF-C and OmpF-M were purified via SDS-gel electrophoresis and digested within the gel, resulting in various peptides. Mass spectrometry is a direct and absolute method for quantification, however, long hydrophobic peptides are particularly difficult to ionize and transfer into the gas phase. Such peptide sequences are typical for membrane proteins such as OmpF.[14] Thus, it was necessary to perform an indirect measurement by comparing the ratio between the intensities of the mass peaks of the cysteine-bearing OmpF fragments (without Gala3) with another peptide without cysteine, and calibrating it with OmpF-M. (**Eq. 2 in chapter Materials and Methods 3.2.9**) This eliminated the dependency on the protein concentration, as the other peptide served as an internal standard. The measurements indicate that 94% ± 5% of the thiol groups within the double mutant OmpF-M bound Gala 3 (92% ± 5% of K89C- and 96% ± 5% of R270C anchor points had the Gala3 peptide attached) (**Table 4**). While both mass spectrometry and acrylodan assays indicate successful thio-functionalization of the OmpF-M, the DOL value determined with acrylodan assay is lower than determined by mass spectrometry. This might be caused by the polarity dependence of acrylodan. If thioglo-1 would have been still available, the measured DOL would have most likely been higher as can be anticipated from **Fig. 15**. However, Thioglo-1 had a lower difference in fluorescence between bound and unbound state, resulting in a higher background fluorescence and lower overall sensitivity.

In addition, the acrylodan assay cannot take into account the case when only one of the thiol groups within the OmpF-M pore is available, the second one being already bound to Gala3, which might influence the polarity of the surroundings of the acrylodan and hinder acrylodan binding to the remaining cysteine.

After a valid method of determining the thiol concentration of OmpF was established and the successful introduction of thiol mutants was confirmed, the labelling with various stimuli responsive groups was tested and the parameters for the Michael addition optimised.

Table 6: overview over the conjugation experiments (selection; all using maleic imid-linker)

Experiment	OmpF mutant	Oligomer/ peptide	Eq. per thiol group	DOL[18]	Remark
1	D12,K89C	Gala3	120	76%	
2	D12,K89C	HLG4	122	27%	
3	D12,K89C	HLG4	100	49%	Same procedure but at pH 6.5
4	D12,K89C	HLG4	100	36%	Same procedure but at 37°C
5	R270C	Gala3	30	37%	
6	R270C	Gala3	60	80%	
7	K89,R270C	Ini	300	83%	Same procedure as for Gala3
8	K89,R270C	(acrylic acid)$_6$	300	50%	
9	K89,R270C	(acrylic acid)$_8$	300	40%	
10	K89,R270C	(acrylic acid)$_{12}$	300	38%	
11	K89,R270C	Gala3	60	68%	
12	K89,R270C	H6	60	0%	
13	K89,R270C	HF3	60	49%	pH 6.5
14	K89,R270C	HF3	60	n.d.[19]	pH 7.4
15	K89,R270C	HL3	60	86%	
16	K89,R270C	HLG4	60	54%	
17	K89,R270C	GHLL3	60	40%	

As shown in **Table 6.** A variety of peptides was successfully attached to three different mutants. In red DOL below 40% are marked and in green DOL above 80% are marked. In the first attempts the stimuli responsive groups were dissolved directly in buffer and added to the OmpF solution (same as in **7-10** but attached to R270C-OmpF). This worked for *oligo*(acrylic acid) due to its high polarity, however most peptides were less soluble in water and had a tendency to precipitate again despite the presence of OG which stabilised OmpF in solution. For this reason, the stimuli responsive peptides were dissolved in DSMO and added dropwise to a vigorously stirred OmpF solution.

For the conjugation experiments the number of equivalents of peptide, the amount of DMSO dissolving the peptide, the reaction time and temperature were varied. Dissolving the peptide in DMSO improved the DOL significantly. The reaction speed might be slowed down through transport phenomena involving micelles. Thus, the concentrations of DMSO and detergent can have a great effect on the

---

[18] DOL according to acrylodan experiments, thus referring to the overall DOL of all available thiol groups.
[19] The DOL was not determined (n.d.) in this case as the solution was opaque and could not properly be purified. It has to be assumed that the DOL was low and that unreacted peptide was dragged along with the stabilising detergent.

reaction rate. Furthermore, very hydrophobic peptides have the tendency to aggregate and precipitate even in presence of micelles (HLG4, H6, HF3, GHLL3). Increasing the number of equivalents or the reaction time resulted in no significant improvement. In general, increasing the number of equivalents beyond 10 per thiol group (or 60 per trimeric double mutant) brought no improvement (compare **5, 6** and **1**). Higher concentrations only promoted precipitation. This trend can be clearly seen from HLG4 over HL3 to HF3 which proved to be the least soluble peptide after H6.

In case of *oligo*(acrylic acid) more equivalents were used since the compound deactivated itself fast resulting in an unknown concentration. Moreover, its solubility was significantly higher (until it deteriorates during storage). Increasing the temperature decreased the DOL and increasing the amount of DMSO up to 10vol% increased the DOL. For basic peptides, a pH of 6.5 improved the DOL significantly (compare **2** and **3**), due to its increased solubility (as intended for the stimuli responsive behaviour). However, lower pH inhibits the Michael addition which work only at a pH range of 6.5-7.5. Above the pH it becomes unselective; below the thiols are not nucleophilic enough and going even lower with the pH the linker can even hydrolyse. While *oligo*(acrylic acid) had superior solubility, it appears that its charge reduced the probability of labelling both pores. The longer the *oligo*(acrylic acid) was the lower the achieved DOL became (compare **7** to **10**).

Table 7.: comparison between DOL measurements with acrylodan and mass spectrometry

Experiment	Sample	DOL via acrylodan assay		DOL via mass spectrometry		
		P	p calculated	p K89C	p R270C	P calculated
8	K89R270C-(acrylic acid)$_6$	50	71	96.2	n.d.	92.5
9	K89R270C-(acrylic acid)$_8$	83	91	52	n.d.	27
10	K89R270C-(acrylic acid)$_{12}$	40	63	84	n.d.	70.6
11	K89R270C-GALA3	68	82	92	96.5	88.8
13	K89R270C-HF3	49	70	40	93	37.2
15	K89R270C-HL3	86	93	91	n.d.	82.8
16	K89R270C-HLG4	54	73	93.1	99.6	92.7
17	K89R270C-GHLL3	40	63	92.7	n.d.	86

Table 7 represents a selection of OmpF conjugates that were measured both with acrylodan and mass spectrometry.: DOL below 40% are marked in red; and those above 80% in green. Acrylodan and mass spectrometry cannot be directly compared since acrylodan gives an over-all-DOL whereas mass spectrometry measures the DOL of an individual mutation site. This already lets the DOL of acrylodan measurements appear significantly smaller. Thus, in order to compare the DOL of both methods, for

the DOL of the acrylodan-measurement a theoretical DOL (**p**) was calculated estimating the DOL of a specific mutation site (assuming K89C and R270C have both the same DOL). For mass spectrometry, the opposite was done (**P**), calculating the overall degree of labelling (if only K89C could be determined then the same DOL was assumed for R270C).

Mass spectrometry worked very well and gave reproducible results (with only two low DOLs found), but the sample preparation did not always work, in particular with old samples. In such cases the peptide fragment with the free thiol group was not visible. This occurred most frequently with the peptide fragment bearing the R270C mutation. Since this issue occurred mostly with OmpF-*oligo*(acrylic acid)-conjugates, it could not be verified if in case of *oligo*(acrylic acid) only one thiol per pore was labelled. If this was the case then K89C must have been more accessible than R270C. Either way it is noteworthy that both methods of DOL measuring had the greatest fluctuations with OmpF-*oligo*(acrylic acid)-conjugates.

The DOL could now be measured and the results were reproducible indicating a low statistic error. However, especially the peptide fragment around R270C was apparently difficult to ionise, resulting often resulting in a missing peak and thus the DOL of this anchor point could not be measured. Whenever the peak could be seen, the measurement appeared to produce dependable data. Similarly, it occurred for both mutation sites that the measured concentration of the internal standard was occasionally too high resulting in negative DOLs. Not even the mass spectrometry expert of the group focussed on mass spectrometry could give an explanation for these two behaviours. Our best guess is that the digestion, washing and purification processes are not fully reproducible thus at times creating longer peptide fragments that remain unionised or smaller peptide fragments that are washed out and lost before ionisation. Interestingly the negative DOLs appeared always at the end of multiple samples. Thus, if multiple bands were cut out of SDS-gel and the digestion and purification done in parallel, the first three samples were never affected but the later ones may have suffered from delays which caused minor but deviations from the established protocol.

3 Vesicles

As mentioned in the introduction, the next step is to insert the OmpF-C into vesicles so that various assays can be used to assess the diffusion through the pores in dependence of the stimuli. However, this step requires several smaller steps:

- Find a lipid-mixture or ABCP, that produces vesicles. Improve the procedure until the vesicles are the only species, have adequate size (75-500nm), are homogeneous.

- Assure that the vesicles withstand the experimental conditions (stable over the observed time, pH, temperature, any potentially interfering molecules…)

- Test whether OmpF can be inserted and optimise the insertion. This step is particularly tricky, since a plethora of parameters have to be considered (see sections on insertion of MPs), which do not only affect the success of the insertion but can also alter the shape and stability of the vesicles. Moreover, it has to be done in parallel with the third major step: developing a reliable assay (detection of diffusion proves correct insertion). To further complicate the task, the assay can also interfere with the vesicle-formation and vesicle-stability…

- Testing the stimuli responsiveness of the OmpF-C containing vesicles.
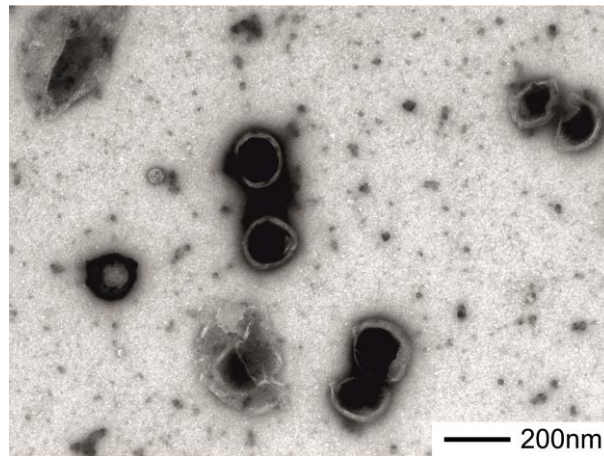
3.1 Liposomes

Liposomes lend themselves as testing platform due to the readiness of membrane-lipids to form vesicles. They are well suited for the insertion of membrane proteins since their membranes are closest to their natural counterpart and are well established as a model for artificial cell membranes. Their drawback is the limited stability of the self-assembled structures. Thus, the experimental question is not just which lipid is suited the most, but rather which mixture, regarding the number of possible additives stabilising the membranes. In particular, the DSPC mixture was made in the intention of creating a liposome platform resembling as closely as possible liposomes in order to safe ABCP in pre-experiments.

3.1.1 Natural phosphatidylcholine

Natural phosphatidylcholine (from egg yolk) proved to have the greatest willingness to form vesicles from all tested amphiphiles. Direct dissolution of POPC bits was sufficient and vesicles formed as soon as the particles dissolved. Compared to other lipids it produced more vesicles, larger vesicles and even without extrusion, more homogeneous vesicles (**Fig. 16**). Both film rehydration and direct dissolution produced very similar vesicles, but for encapsulation experiments film rehydration was used in the hope that better defined starting conditions result in a more reliable encapsulation.

Experiments encapsulating dye and observing it in FCS revealed that most dyes destroyed the vesicles, but if vesicles were formed, then they were relatively stable for hours at room temperature despite the rather hydrophobic nature of the dyes and at a pH as low as 1.0 (no observed change in diffusion time or counts per molecule). However, it is only stable in the fridge for a week. Acidified it lasts about one day in the fridge, probably due to osmotic pressure. The main problem is that the vesicles are not thermally stable, thus incubation with proteinase K at 37°C is not possible (as a means of removing free HRP, elaborated in the chapter **enzyme kinetics**).

Fig. 16: POPC liposomes formed via film rehydration[20]

3.1.2 SM/POPS/cholesterol

This lipid mixture of sphingomyelin, 1-palmitoyl-2-oleoyl-*sn*-glycero-3-phospho-L-serine and cholesterol (an often-used mixture in our lab) was tested in the hope of achieving higher thermal stability by the use of cholesterol which stabilises the lipid-bilayer and by adding POPS thereby introducing a negative charge to the vesicles which should prevent aggregation.

This mixture is particularly suited for detergent removal for two reasons: First the additional charge helps to diminish the negative effect of the presence of detergents on the vesicle formation (detergents tend to cause higher heterogeneity, more micelles, smaller vesicles, less stable vesicles…). Secondly, cholesterol is poorly water soluble, thus no homogeneous mixture can be expected by merely adding all ingredients to water. Detergent removal is also of particular interest for the insertion of membrane proteins into vesicle membranes.

---

[20] 3mg of POPC were dissolved in 1mL ethanol and then dried in a 20mL glass vial. Then 1mL PBS was added and the solution was shaken for 3h.

Compared to POPC (which is very similar to SM but differs in the location of the double bond) the vesicle formation with this mixture is far more laborious as it requires far more components to be weighted and the detergent removal takes considerably longer than film-rehydration. Moreover, samples obtained from this mixture featured a much higher polydispersity (average diameter 1000nm) and required thus extrusion. The mixture had moreover the tendency to block filters so that the extrusion required the pressure of a barrel extruder. This is a further indication for a very heterogeneous mixture. After extrusion (1x1000nm, 2x400nm, 5x200nm filter) the PD was moderate (0.2) and the average diameter 200nm (**Fig. 17**). Please note, that the vesicles in the TEM appear in irregular polyhedral shapes due to the sample preparation involving drying and vacuum causing distortion on softer vesicles. The vesicles had a similar stability towards pH and a considerably improved stability towards temperature. The samples could be dialysed for three days at room temperature without effecting the diameter or polydispersity. However, detergent removal is not suited for the encapsulation of rather hydrophobic cargo, since it would accumulate in micelles rather than vesicles and the chance that the intended cargo becomes inserted into the membrane increases too.
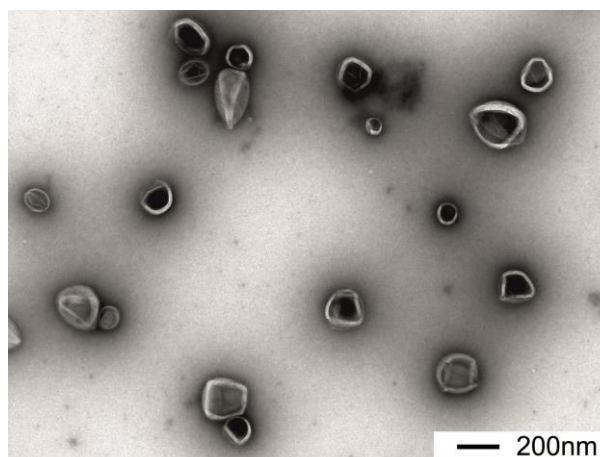
Fig. 17: Liposomes formed via detergent removal (procedure described in materials and methods).

Encapsulating HRP (see chapter **enzyme kinetics**) did not affect the vesicle appearance but inserting OmpF had the tendency to increase the vesicles diameter by 5-10%. While the vesicles were clearly more stable than POPC-liposomes, they were still not stable enough for 1 day at room temperature for measuring light scattering. After the dialysis, the liposomes degenerated to fast at room temperature, aggregating, precipitating and releasing encapsulated HRP. Thus, the samples could not be fully characterised, instead only a fast, dynamic light scattering (DLS) measurement via Zetasizer and transition electron microscopy (TEM)-pictures were used (See **Appendix**).

3.1.3 DSPC/POPS/cholesterol

To address the problem of the low thermal stability POPC/SM was replaced by DSPC (1,2-distearoyl-*sn*-glycero-3-phosphocholine), which does not feature unsaturated carbons and has thus a transition temperature of 55°C.[16] This makes pure DSPC very unwilling to form vesicles at room temperature and within formed membranes DSPC will be very unwilling to change its conformation resulting in a very low membrane fluidity. Thus, it requires elevated temperatures for vesicle-formation and the vesicles should be very stable at room temperature. Two additives were chosen that should increase the fluidity of the self-assembling membranes without sacrificing its stability. POPS introduces charges that should prevent aggregation and help vesicle formation. Moreover, its unsaturated nature creates perturbation increasing the fluidity of the membrane. Cholesterol is known[17] to increase the fluidity of membranes but also stabilises them by interconnecting their bilayer.[17] Right from the beginning it was considered to use PEGylated cholesterol. The PEGylation should serve two purposes. It should create a barrier that prevents aggregation and it should keep hydrophobic entities such as FCS-active dyes and HRP from inserting into the membrane and thereby preventing them from weakening the self-assembled structure. Cholesterol was the ideal anchoring point for PEG since it was already planned as ingredient of the mixture and since it forms much more stable anchors than any lipid due to its length connecting both layers of the liposome.

In the first attempt, the maximal ratio of cholesterol was used, however it turned out that the 100% PEGylation prevented vesicle-formation resulting in only few and odd shaped vesicles (**Fig. 18**). Adding it later to the mixture at the point of film rehydration a relatively high number of vesicles were formed but their formation came to an abrupt end resulting in a great number of small vesicles with holes. Under normal circumstances huge holes in vesicles result in their immediate disassembly, so that they can rarely be seen in TEM, but in this case the membranes were still stable enough so that even after drying and under vacuum the samples the holes could be observed.
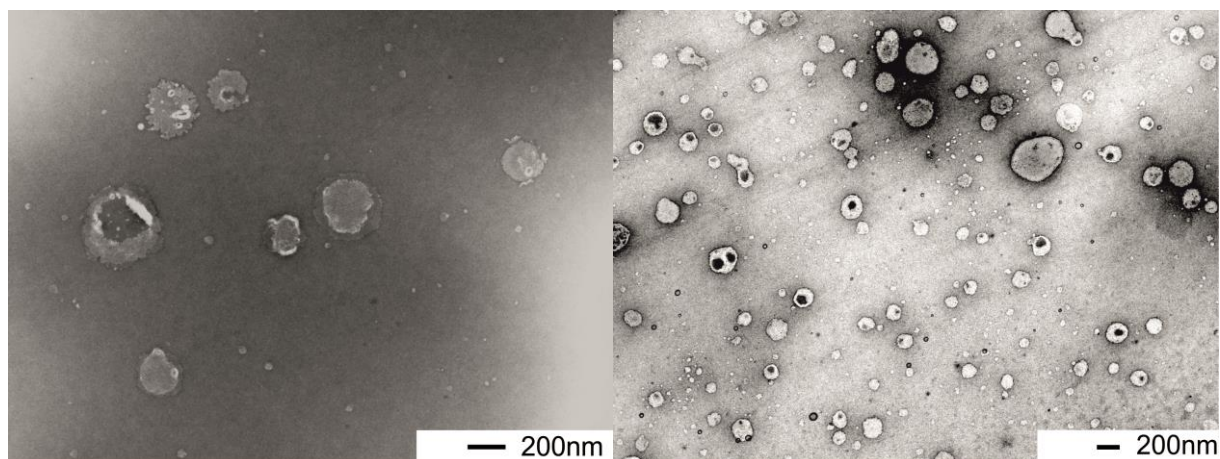
Fig. 18: 100% pegylated cholesterol added to DSPC; left before the drying of the lipid film;[21] right during the rehydration (4h after start, after observing the development of turbidity)

As a consequence of these results, unmodified cholesterol was added to reduce the density of PEG-chains. Compared to other lipid mixtures the formation was slow (17-20h vs 1h) and it required temperatures that would gradually destroy most unsaturated lipid vesicles. It turned out that the addition of cholesterol and POPS facilitated the extrusion, however extrusion was only possible at the same temperature as the vesicle formation (40°C).

These vesicles proved to be the most stable liposomes I am aware of. The vesicles can be treated for 12h at 37°C without any signs of degradation or deterioration and the vesicles could be stored at room temperature for up to three months (**Fig. 19**). The slow degradation is probably the result of slow oxidation.

---

[21] 3mg DSPC and 1 eq. of Chol-PEG600 were dissolved in 1mL ethanol and dried in a 20mL glass vial. Then 1mL of citrate buffer was added and the solution was stirred at 25°C for up to 30h.
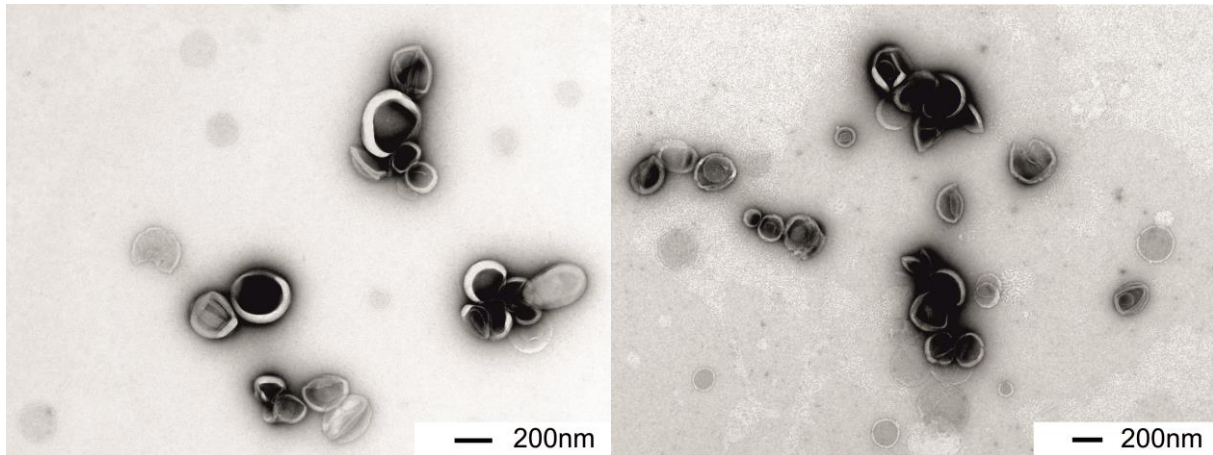
Fig. 19: left DSPC vesicles directly after extrusion (process described in materials and methods); right after 12h at 37°C

It is also noteworthy that most liposomes encapsulating FCS dyes reached encapsulation efficiencies well above 100% implying that the dyes were no longer dissolved but accumulated in the lipid-membrane. The DSPC-mixture did not show this behaviour making it suited for FCS measurements. However, it was found that the encapsulation efficiency could be very low as observed for some polymersomes. It was therefore considered that the PEGylation would be affecting both sides of the membrane thus reducing the inner cavity. Thus, it was tried to add the Chol-PEG only once the first vesicles were formed through film rehydration (**Fig. 20**). That way very similar but larger vesicles were formed and the encapsulation efficiency increased somewhat (Rh 57 to 69nm; encapsulation efficiency 45 to 56%). Still the presence of FCS dyes reduced the size of the vesicles considerably (without Rh ca. 100nm).
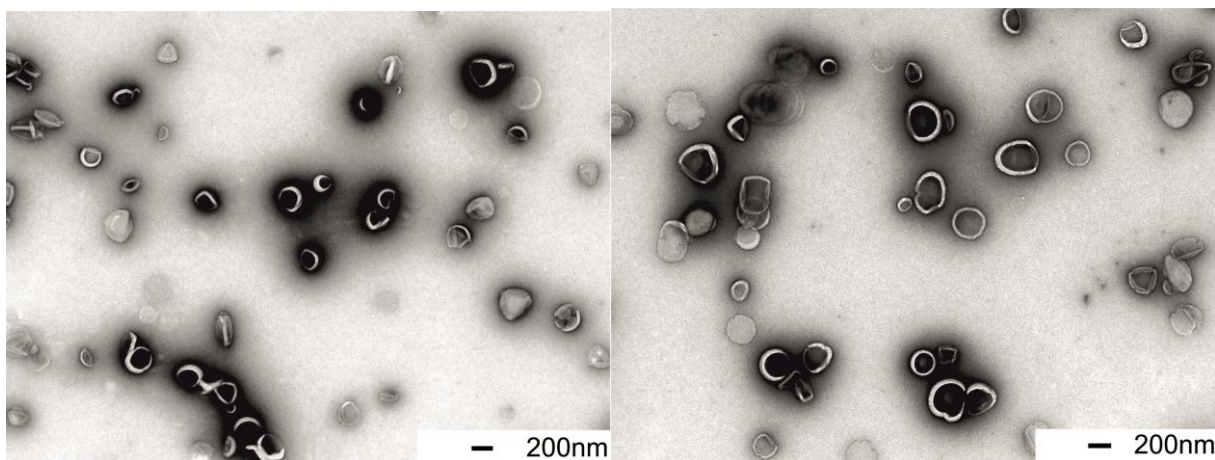
Fig. 20: Liposomes made of DSPC/POPS/cholesterol through film rehydration using citrate buffer containing 100nM sulforhodamin B FCS dye. Left Chol-PEG added before film rehydration; right Chol-PEG added 4h after start of vesicle-formation (beginning of turbidity)

It was also tested, whether sonication could speed up vesicle-formation and what effect it would have on the resulting vesicles (**Fig. 21**). It turned out that the vesicles were somewhat smaller (Rh 50nm), but far more heterogeneous according to light scattering. Furthermore, the encapsulation efficiency of sulforhodamin B or Oregon Green 488 went down considerably (34%, 1% respectively).
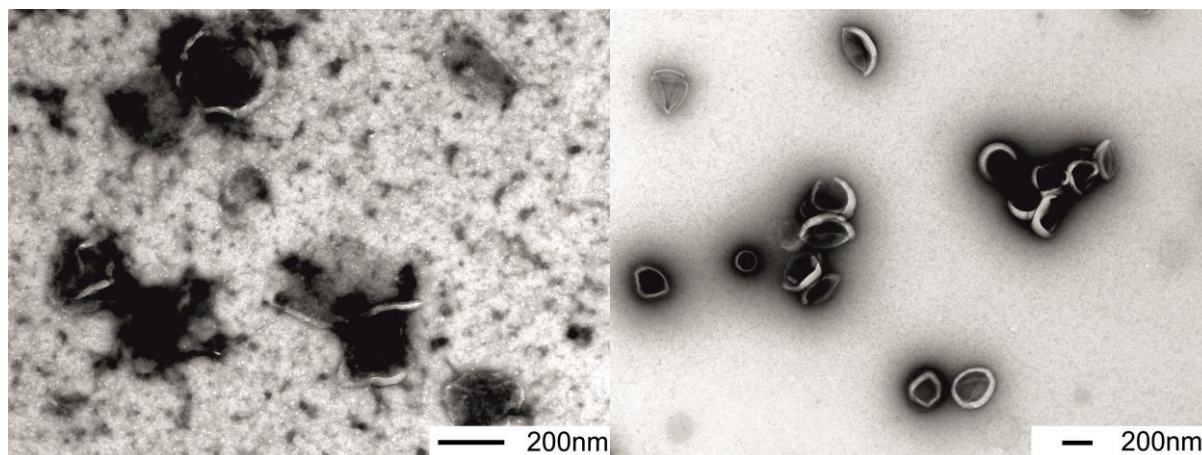
Fig. 21: film rehydration speeds up via 2h sonication; left: encapsulating 100nM sulforhodamine B and right: encapsulating 10nM Oregon Green 488.

It was not further investigated how much of the Chol-PEG actually inserted, nor the stability of the resulting vesicles, since the encapsulation of dye did not improve enough, nor were the FCS experiments as promising as the HRP kinetics, which could work even with very low encapsulation efficiencies (regarding the latter see **Enzyme kinetics** and **Appendix**).

The lipid mixture had also some notable weaknesses. While being ridiculously stable at room temperature, the vesicles were damaged fast and precipitated through dialysis at room temperature indicating a particular vulnerability to osmotic pressure. Keeping the osmotic pressure constant solved this problem. It could be said that these vesicles are particularly hard but have at room temperature no self-healing abilities and have thus a glass like fragility.

It was also tried to form vesicles from this mixture via detergent removal, but the change in polarity causes demixing and precipitation ultimately resulting in very heterogeneous vesicles and many aggregates which were moreover impossible to extrude without a barrel extruder.

The vesicles were moreover considerably more sensitive towards detergents. In that respect, they were in midway between polymersomes and regular liposomes. This was observed when OmpF was added during film rehydration. OmpF in 3% OG could be added to regular liposomes without causing significant changes in the self-assembly process. For the DSPC-mixture it had to be reduced to 0.5%

OG. For polymersomes this residual detergent concentration was still too high resulting in small vesicles and numerous micelles.

The greatest disadvantage was that OmpF was very difficult to insert. This fact can probably be attributed to the PEGylation and higher crystallinity and rigidity of the membrane which were beneficial for dye encapsulation and overall stability.

3.2 Polymersomes

The advantage of polymersomes over liposomes was not only their superior stability but also the fact that hardly any mixtures had to be considered. While AB-ABCPs would form bilayers too, ABAs can form a thick monolayer (see **chapter II**,). Polymersomes do not require additives for further stabilisation and most potential additives would rather weaken the self-assembled structures (in particular due to a mismatch in length). Additives come hence only into play when trying to insert membrane proteins. Therefore, experiments with polymersomes depend first and foremost on the length of the hydrophobic block of the ABCP and the ratio of the hydrophilic block. All the following examples were PMOXA-PDMS-PMOXA based and (disregarding the individual chain-lengths) of the same molecular structure. Since vesicular structures can be found at hydrophilic/hydrophobic ratios of 10-45% the shortest ABCPs was $A_4B_{22}A_4$. Shorter hydrophilic blocks can hardly be made nor would they have a significant influence, yet the ABCPs are considerably longer than the thickest lipid-bilayers. The longest ABCPs were 3x as long (overall length). They tend to be more stable, but the longer the hydrophobic block becomes the harder it gets to dissolve the ABCP and to insert MPs into their membranes.

Note: if not stated otherwise, the vesicles were all prepared via film rehydration as described in materials and methods.

3.2.1 $A_4B_{22}A_4$

The shortest ABCP in this list dissolved rapidly, with little residue in water in comparison to the other ABCPs. For vesicle-formation direct dissolution, film rehydration and the ethanol method (kinetic trapping with ethanol as solvent) were tested. These methods revealed trends that were found with the other ABCPs as well. Direct dissolution worked only poorly despite the relatively good solubility, resulting in a very heterogeneous mixture with only few vesicles (**Fig. 23**). The ethanol method

produced vesicles very fast, but of smaller size. Film rehydration produced the best results (with rather big vesicles with a R_h of 100nm according to light scattering and 120nm according to FCS) and allowed the best encapsulation efficiencies for FCS-dyes.

Unfortunately, only small amounts were still available at the time, thus it was given to a more advanced project, where it was confirmed that it inserts OmpF.
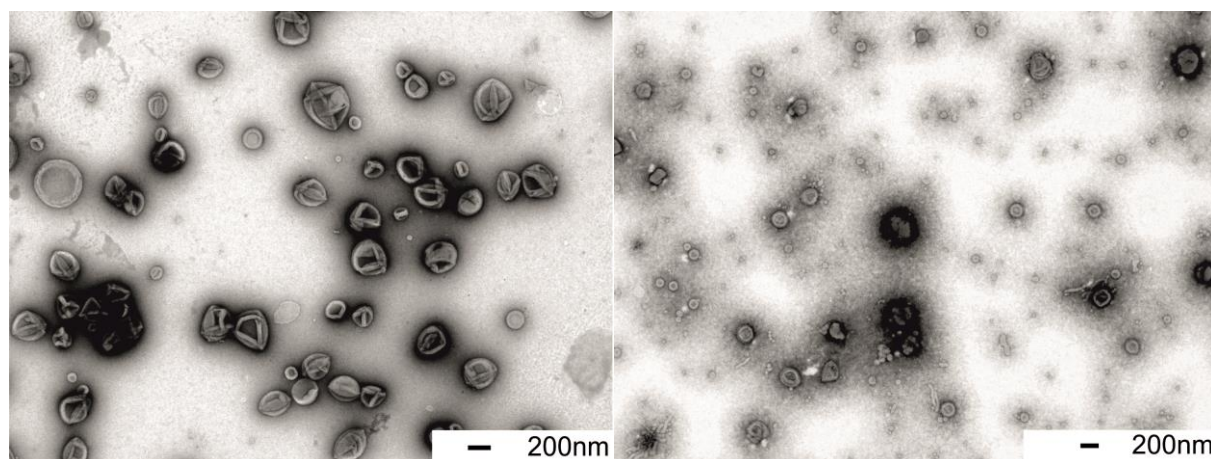
Fig. 23: TEM images of 10x diluted samples. Left: samples produced via film rehydration; right: produced via direct dissolution (adding the same amount of ABCP directly to the stirred buffer).

3.2.2 $A_{14}B_{25}A_{14}$

This is the second old ABCP. It was apparently synthesised in the hope of recreating $A_4B_{22}A_4$, yet the hydrophilic part became significantly longer, thus changing the hydrophilic ratio from 27 to 53% which made it particularly hygroscopic. At such high ratios tubes and even micelles can be expected. It was still tested and peculiarly it dissolved significantly faster and better with the direct dissolution method, rather than using the film rehydration method (**Fig. 24**), very unlike most tested ABCPs. Regarding the exposed surface of solid ABCP this result is paradox and counter-intuitive. Moreover, it was the only ABCP tested that produced more and better vesicles using direct dissolution. These findings were confirmed by those scientists, that worked earlier with it. According to the publications it formed large vesicles, which became smaller and more homogeneous after sonication.[18] However, when I used it, it had started to deteriorate (slightly yellowish, unidentified, broad peaks in the NMR; possibly partial decomposition into diblockcopolymers) and the concentration of tubes and micelles increased over the concentration of vesicles. It was thus no longer suited for further experiments.

Another noteworthy finding is that $A_{14}B_{25}A_{14}$ was reported to insert MPs such as OmpF simply by dropping the solution of the MP onto the ABCP pieces, adding water and stirring it overnight.[19] This could be done with no other ABCP tested since polymersomes are highly sensitive to detergents and MPs tend to precipitate rapidly once their solution is diluted well below the cmc.

The causes of these findings can only be speculated. The relative ease of direct dissolution can be explained however regarding the relatively low molecular weight and the high hydrophilic ratio. These factors could be also responsible for stabilising MPs in solution before they precipitate. The reason film rehydration did not work might be that the films were dried too much and the process increased the crystallinity so that the solubility decreased. Experiments with other ABCP can only confirm that the humidity of the ABCP-films matters. ABCP that are too moist before being dissolved in ethanol formed often more micelles and films that were dried too thoroughly rehydrated only slowly if at all.

Why the vesicle-formation withstood higher detergent concentrations might be explained through the short hydrophobic block. Liposomes are also less sensitive to detergents probably since the mismatch in length and physical-chemical nature of the detergent is less pronounced as in polymersomes. This effects most probably the way detergent interacts with ABCP, micelles and vesicles. For instance, it could be that the detergent inserts in liposomes evenly whereas it produces detergent domains in polymersomes which weaken the membrane.
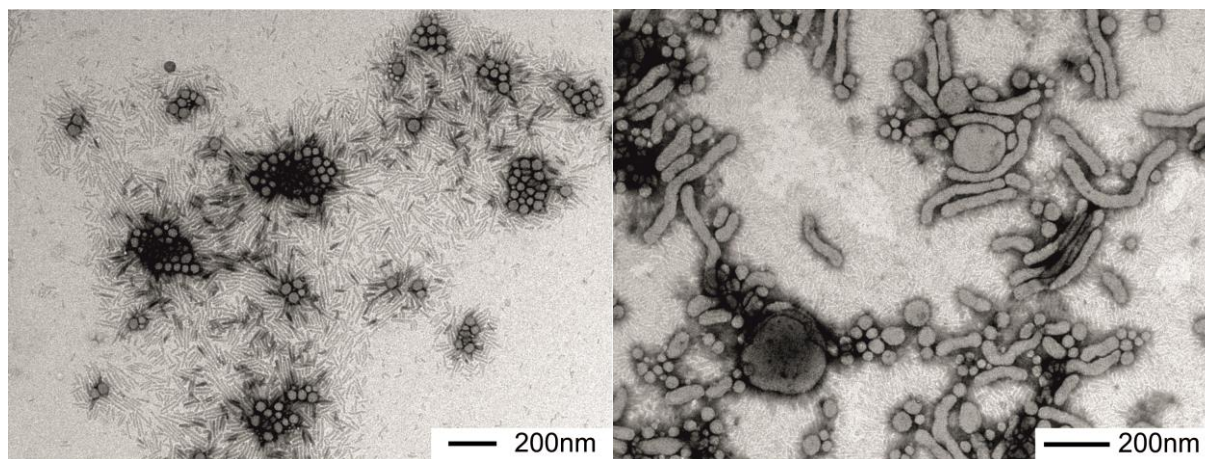
Fig. 24: Resulting structures produced via film rehydration (left) and direct dissolution (right)

3.2.3 $A_6B_{44}A_6$

This and the following ABCP were modelled on $A_4B_{22}A_4$, maintaining the ratios, but without achieving the same length (approximately twice as long). It dissolved rather well using film rehydration and had a great preference towards vesicles.
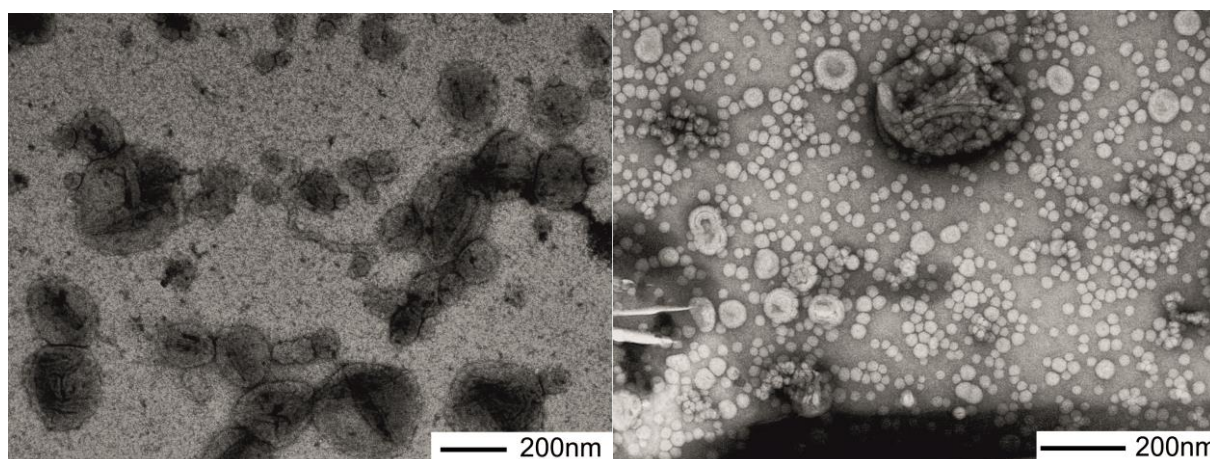
Fig. 25: vesicles encapsulating 0.25g/L HRP produced via film rehydration without (left) and with OmpF (right) stabilised in 3% OG.[22]

The fact that the second sample contains a vast number of micelles and has on average smaller vesicles (but also far more homogeneous in size) is due to 0.15% OG introduced along with the OmpF. It is thus more sensitive to detergents than the ABCPs discussed earlier (**Fig. 25**).

3.2.4 $A_8B_{49}A_8$

It is very similar to $A_6B_{44}A_6$ but forms slightly better vesicles. However, they tended to remain below 120nm in diameter (**Fig. 3 Appendix**). In *cryo*TEM, most appeared to be in the range of 40-60nm (**Fig. 26**). It appears to be even more sensitive to OG than $A_6B_{44}A_6$ (**Fig. 27**). It was thus tested if a gradual removal of detergent could result in functional vesicles, however detergent removal did not form vesicles at all, although it formed some spherical aggregates of micelles that appeared to be hollow (**Fig. 28**).

---

[22] 50μL of 1g/L OmpF was soaked into the film for 30min, then the PBS was added for film-rehydration.
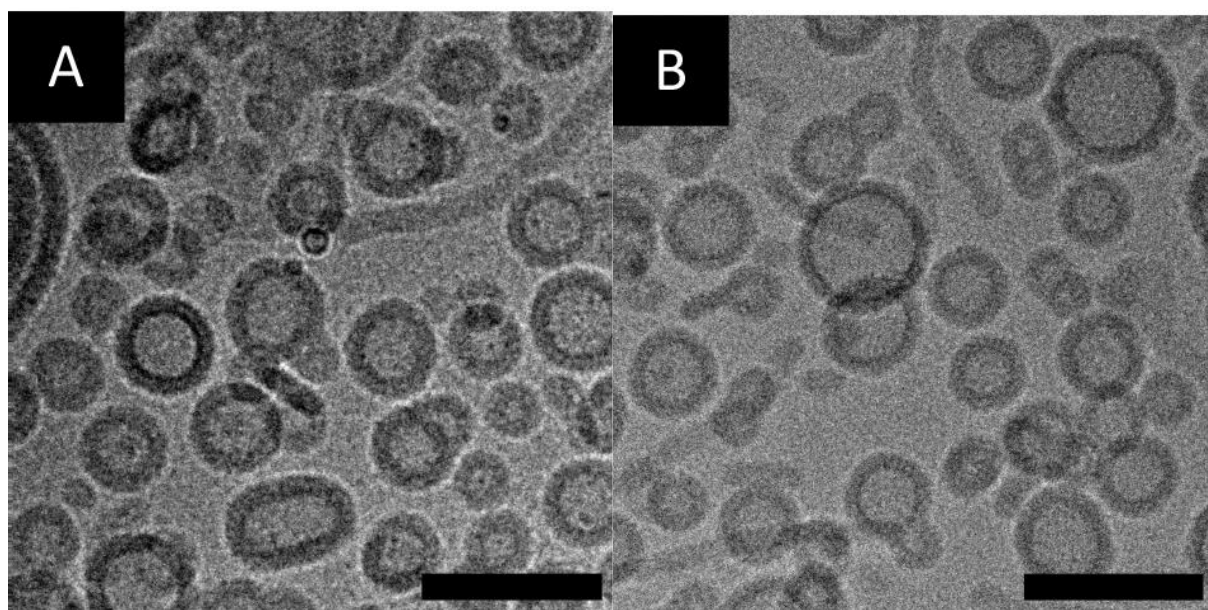
Fig. 26: Cryo-TEM micrograph of A) HRP loaded PMOXA$_6$-PDMS$_{44}$-PMOXA$_6$ polymersomes equipped with OmpF-C, NRC, and B) HRP loaded PMOXA$_6$-PDMS$_{44}$-PMOXA$_6$ polymersomes without OmpF, NR-. Scale bar 100nm.

The polydispersity increased greatly with the OG concentration (0,08 0%; 0.22 0.025%; 0.47 0.15%). Direct dissolution had a similar effect on the polydispersity (0.5). The diameter according to light scattering decreased in presence of 0.025% OG from 190nm to 100nm. Similarly, direct dissolution produced only vesicles with an average diameter of 166nm.
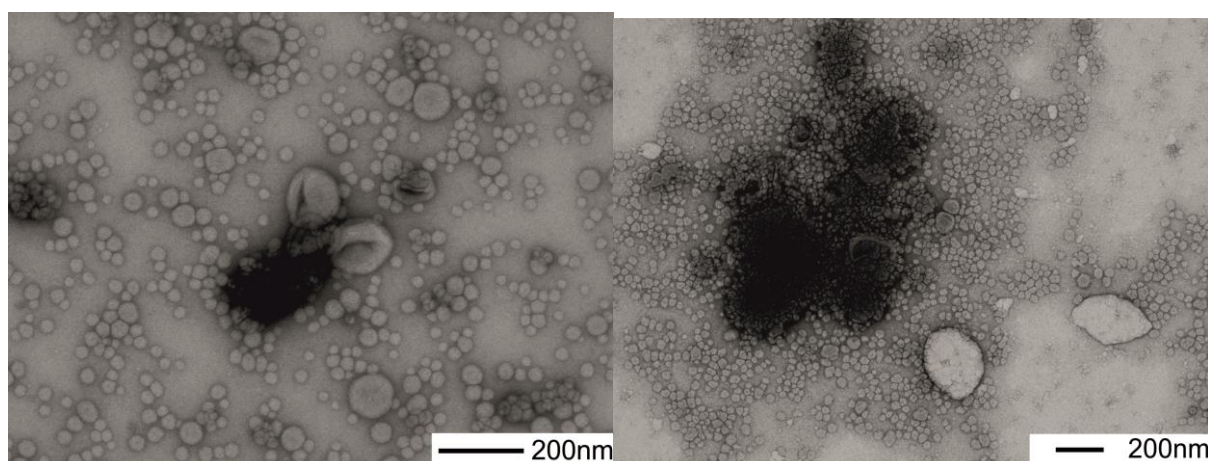
Fig. 27: TEM micrographs revealing the influence of detergent concentrations below the cmc[20] on vesicle formation of PMOXA$_6$-PDMS$_{44}$-PMOXA$_6$ when adding OmpF stabilized in 0.5 (left) and 3% OG (final concentration ca. 0.15 and 0.025% respectively). In both cases the OmpF solution was allowed to soak into the polymer film before film-rehydration.
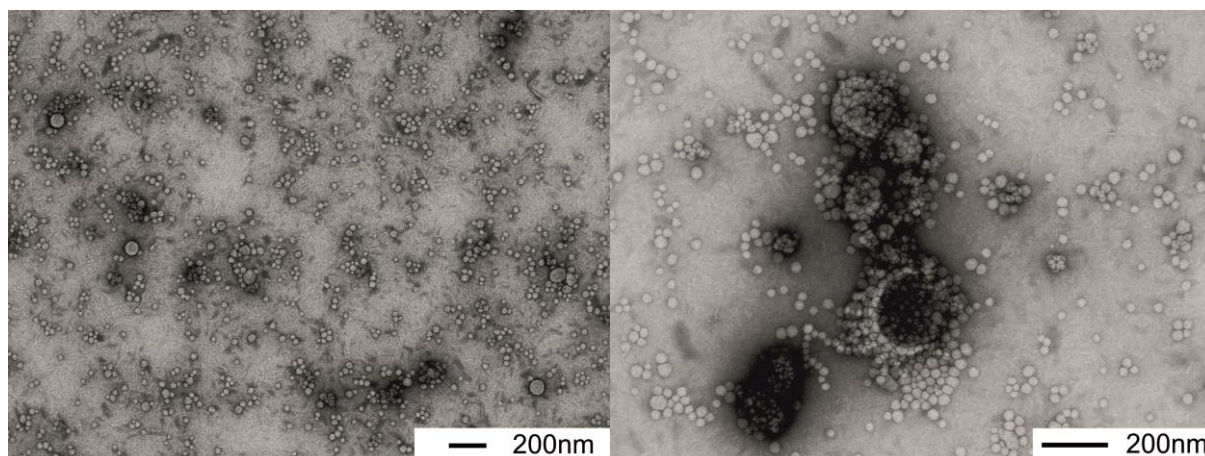
Fig. 28: two TEM images of the same sample of vesicles encapsulating 0.25g/L HRP produced via detergent removal starting from 3% OG using Biobeads and 3-5kDa dialysis tubes.

3.2.5 $A_{20}B_{38}A_{20}$

This was a commercially available ABCP. It is very similar to $A_{14}B_{25}A_{14}$ regarding the hydrophilic ratio. However, it was 47% longer. Due to the similarities, it was expected to be rather water soluble and form vesicles, tubes and micelles. Peculiarly, it dissolved neither well in water, nor ethanol. Also, it did not dissolve in other organic, water miscible solvents. In fact, it was the ABCP that was the hardest to become fully solubilised of all discussed ABCPs.

Changing from film rehydration (**Fig. 29**) over ethanol method to direct dissolution, the opaqueness of the samples increased. This finding is somewhat surprising since in case of the direct dissolution, the majority of the polymer did not dissolve in buffer. Moreover, DLS measurements indicate that film rehydration produced most vesicles, followed by direct dissolution, less than 10% of the aggregates. The ethanol method resulted only in micelles.

Due to the astonishing low solubility, slow rehydration speed and low vesicle population and overall aggregate concentration, it was found to be not suitable for the production of NRs. The low solubility might be explained similar to $A_{14}B_{25}A_{14}$, with the twist that the higher length results in a greater crystallinity (presumably stacked membranes) and hence lower solubility.[21]
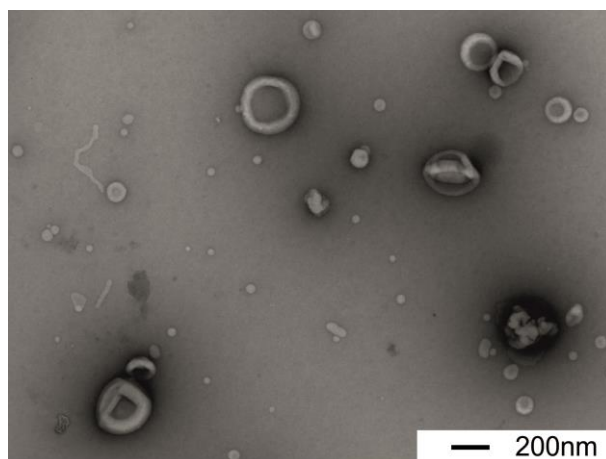
Fig. 29: TEM image of vesicles produced via film rehydration (sample 10x diluted)

3.2.6 $A_7B_{67}A_7$

From a point of hydrophilic ratio, it is similar to $A_4B_{22}A_4$, $A_6B_{44}A_6$ and $A_8B_{49}A_8$, however it is even longer and has a somewhat lower hydrophilic content (17% vs 20-27%). It could be therefore expected to be poorly water soluble and rehydrate more slowly. Similar to $A_{14}B_{25}A_{14}$, it became less soluble with film rehydration. In this case even after several days under vigorous stirring no noticeable opaqueness was reached (TEM indicates micelles and worms, but the film rehydration was not reproducible), whereas detergent removal (3% OG)[23] produced some aggregates. The fact that extrusion did not change the size characteristics in DLS suggests that all structures and aggregates are significantly smaller than the pores of the extrusion membrane (200nm). Adding 1% POPS or TDOC to the ABCPs prior detergent removal reduced the samples ability to scatter light by a factor of 400. The idea of this additive was to add charge in order to facilitate self-assembly, but apparently due to the different chemical nature than liposomes, it had the opposite effect. While POPS did not affect the structural parameters (100nm diameter PDI of 0.3), TDOC reduced the size (36nm) and increased the PDI (1). In summary: $A_7B_{67}A_7$ was found utterly unsuited for further experiments.

---

[23] All dissolved in 1% OG/PBS pH=7.4. OG removed via dialysis over 3 days using 10kDa MWCO tubes and 5x1L PBS.

3.2.7 $A_{17}B_{65}A_{17}$

This ABCP was also difficult to rehydrate from films and took often longer than 1 day. According to TEM it has the tendency to form multilamellar vesicles. Due to the low opaqueness of the samples and the slow rehydration speed detergent removal and addition of charged groups was tested as well (**Fig. 30** along with $A_7B_{67}A_7$).[24] As in the case with most ABCPs, detergent removal resulted in a tendency towards micelles and small vesicles. This experiment was the only instance where DLS and TEM differed significantly. The latter reveals that the number of small particles is much higher and the vesicles are even smaller. Moreover, in case of the film rehydration no reason for 600nm particles could be seen in TEM. However, extrusion through 200nm membranes reduced the particles diameter to 100nm (reducing also the PDI from 0.6 to 0.3). The fact that no vesicles of 200nm were found indicates that the larger structures must have been aggregates, as it is unlikely, that the ABCP would only form stable vesicles with a diameter above 200nm and below 100nm. As in case of $A_7B_{67}A_7$ the charged additives (**Fig. 31**) increased the polydispersity further (film rehydration 0.3; DR. 0.2; 1% POPS 0.3; 1% TDOC 0.6). Moreover, the number of smaller particles increased (film rehydration 0%; DR 19%; 1% POPS 23%; 1% TDOC 39%).
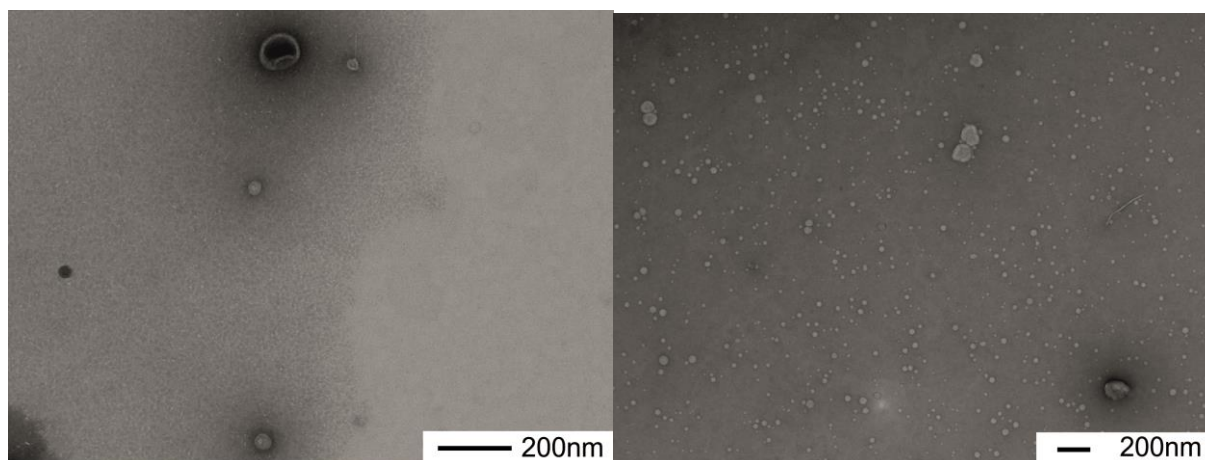
Fig. 30: left: Film rehydration without extrusion, right: detergent removal after extrusion

---

[24] All dissolved in 1% OG/PBS pH=7.4. OG removed via dialysis over 3 days using 10kDa MWCO tubes and 5x1L PBS.

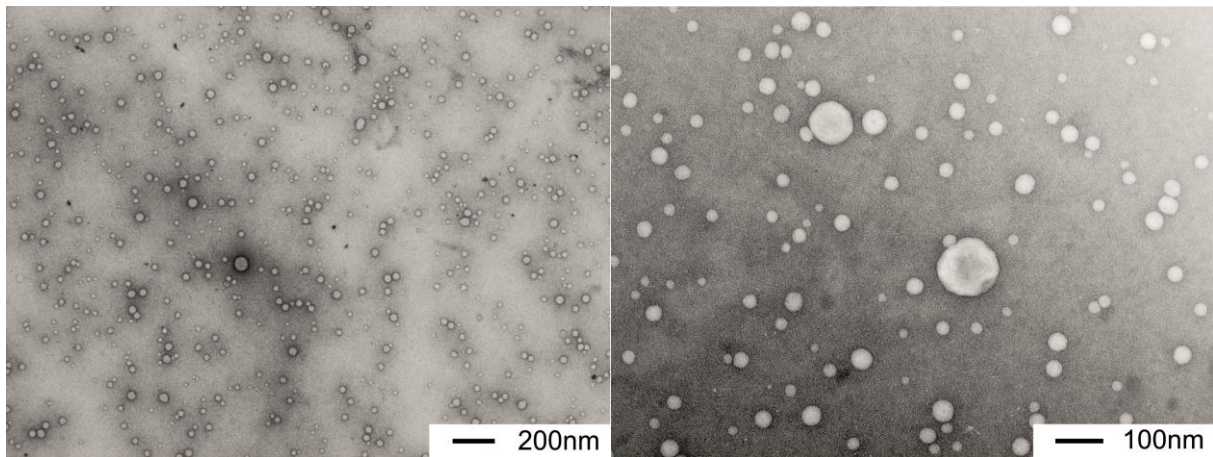**Fig. 31:** detergent removal in presence of 1% POPS and (1% TDOC, right) both extruded through 200nm membranes

3.2.8 $A_{16}B_{72}A_{16}$

While this ABCP is superficially very similar to $A_{17}B_{65}A_{17}$ it proved to be very different in its properties. It rehydrates much more readily than the other ABCP and forms very small vesicles and many micelles, so that it is often hard to distinguish between micelles and vesicles (**Fig. 32**). These factors result in a low encapsulation efficiency of e.g. sulforhodamine B. Furthermore, extrusion appears to reduce the number of vesicles and the encapsulation efficiency further. On the other hand, samples were stable towards concentration steps via filtration through 10kDa amicon at 6000rpm. This is something most liposomes are unable to withstand. However, it was found that dyes like Dylight488 rendered these polymersomes temperature sensitive. In FCS, the diffusion times decreased and the vesicle fraction decreased over time, very similar to sonication of polymersomes.
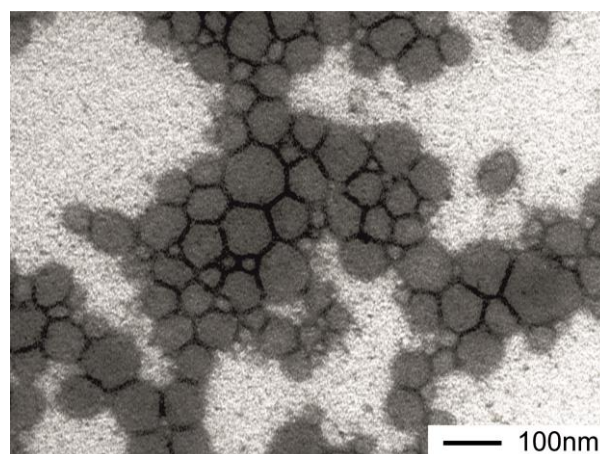
Fig. 32: TEM of vesicles produced via film rehydration.

3.3 Discussion Vesicle-formation

While liposomes are easily formed, they show a lack of stability at elevated temperatures and prolonged storage time. Some even deteriorated at room temperature during the time required for purification or measurement. Polymersomes are far more stable, but also far more challenging to work with. Films of ABCPs often dissolve only slowly due to the large hydrophobic surfaces and the stronger hydrophobic interactions between the ABCPs in the film results in longer rehydration times and often undissolved residues. The latter can also be caused by **Factors** such as the thickness of the **film** (and thus the concentration of ABCP in ethanol,[22] rate of ethanol removal, the shape of the vial and its rotation-speed) and the moisture of the film play thus a much larger role.[23] Too moist films rehydrated too fast resulting in more micelles, whereas completely dry films did not rehydrate at all. Sonicating the films in hope of initiating rehydration of poorly soluble polymer films usually resulted in very heterogenous self-assemblies, since it damages in particular larger vesicles or patches of membranes leaving micelles and worms behind.

Another important set of parameters is the **rehydration** of the film. A film may be redissolved by rotating the vial, shaking the vial or putting a stirring bar inside. The harsher the rehydration procedure is, the faster it takes place potentially resulting in undesired structures,[24] as it was the case with sonication. For the ABCPs used, shaking or stirring proved to be adequate. However, even the size and the shape of the stirring bar appeared to matter. In particular ABCPs with long, hydrophobic B-blocks (PDMS) appear to be sensitive to oxygen stirred into the solution by a too large stirring bar or too high rotation speed. While it had no discernible impact on the polymersomes used in the main experiments, it proves once more how strongly the process and outcome of film-rehydration depends on the lengths of the amphiphiles.

Unfortunately, even if the vesicle-formation process has been optimised and proven reliable, a new **batch** of the same ABCP (as observed with $A_6B_{44}A_6$), or the same being aged ($A_{14}B_{25}A_{14}$) can produce completely different structures or prevent MPs being inserted. One possible explanation is that the PDI of the ABCP may vary with each batch, but also the amount of AB in ABA, or the content of unreacted PDMS.[22a, 25] Similarly, aging could break up ABA in AB+A, or separate the blocks completely or alter them through oxidation. Oxazolines are furthermore known to irreversibly crystallise and become thus insoluble.[21]

To complicate things further, polymersomes behave very differently from liposomes and even polymersomes can be very different from each other. This becomes most evident when attempting to **insert MPs**. A problem related to it, is the fact that polymersomes are more sensitive to detergents and some organic solvents (for reasons discussed at the end of the chapter).[22a, 25] Once a polymersome

is damaged, it appears that the chances of healing itself as liposomes are small, at least on the observed timescale.

Even optimized vesicle-formation procedures failed at times to inconspicuous deviations. This included experimental errors as minute as traces of ethanol from washing the glass wear or detergent-residues from the washing machine. The latter could even be below the critical micelle concentration, thus not visible through foaming. It seems that small contaminations affect both vesicle-formation and vesicle-stability. Another easily overlooked factor is that the time of introduction of these contamination matters as well. For instance, even 0.025% OG caused the prevalence of micelles during vesicle-formation in case of $A_8B_{49}A_8$, whereas already formed polymersomes persevered in presence of the same concentration of OG. Complicating it further, the contamination might not destroy or change the vesicles immediately but reduce their thermal stability, thus a tested detergent concentration appeared to have no impact, but after one-day half of the vesicles become micelles. Ironically, very low concentrations of detergents may help with film-rehydration, since detergents can break up dried films and overcome the hydrophobic barrier and also prevent aggregate formation due to charge repulsion. However, in most cases compounds like **TDOC** or **POPS** which help liposome formation and liposome stability, often proof detrimental to polymersomes, probably due to the mismatching lengths of hydrophobic sections and possibly weakening of polymersomes due to formation of unstable domains. This could be not just a matter of ABA-detergent distribution within a membrane, but also stabilisation of ABA in solution through detergent micelles, but also it could be that detergents induce a separation of AB in ABA. This could explain why some previous publications imply a much higher stability of similar polymersomes towards detergents.

3.4 Insertion methods

MPs are **usually inserted** either by adding it during vesicle-formation[26] (removing or diluting the stabilising detergent so that the MP has to interact with the membrane forming amphiphiles) or by weakening preformed vesicles and adding the MP in the hope that most inserts within the vesicle-membrane before it precipitates out of solution. In the first approach, the vesicle-formation may be hindered or impeded by the involved detergents, whereas in the second approach, the vesicles have to be damaged for the insertion to work. This could be achieved by addition of detergents,[26] sonication,[26a, 26b] or freeze-thawing.[26a, 26b] All of these approaches are very harsh to polymersomes and can result in vesicles turning into micelles rather than repairing themselves.

Fortunately, **OmpF** is a special case among MPs. It is both exceptionally stable towards denaturing conditions (temperature,[1a] pH,[1b] detergents,[1a] urea,[27] solvents[28]…) and moreover able to refold itself without chaperones. It can thus be dried or dissolved in organic solvents such as ethanol enabling other approaches to MP-insertion (just not direct addition as gramicidin etc. since it is too big and would thus need to displace too many amphiphiles within the membrane).

In older publications, [19] describing no longer available ABCPs, had very peculiar methods of vesicle-formation and protein insertion. For instance, $A_{12}B_{55}A_{12}$ was rehydrated by simply adding buffer to the ABCP and stirring it overnight. The involved proteins were added before the rest of the buffer and slowly diluted by the latter.[19] Unfortunately, this could not be reproduced with any available ABCP, as direct dissolution resulted in ill-defined structures (in particular micelles and worms), even in absence of OmpF and detergents. This method might work for liposomes and very few ABCPs. OmpF moreover does not belong to the ion channels that are able to insert themselves into preformed vesicle membranes, as e.g. gramicidine would. If OmpF is added to a vesicle solution it will simply precipitate due to the dilution of the stabilising detergent.

In general, the efficiency and homogeneity of the vesicle formation and OmpF insertion depend on numerous factors (concentration, pH, temperature, presence of ions, surfactants, solvents…).[22, 25] OG was however necessary to prevent aggregation of OmpF (3% OG was used for extraction of OmpF and long-term storage, whereas 0.5% proved to be sufficient for short term storage).

3.4.1 Vesicle-formation through film-rehydration

The first idea to solve said problems was to use film-rehydration and soak the OmpF solution into the film prior rehydration with the buffer. That way OmpF could be stabilised through the ABCPs, increasing the chance of it being incorporated into vesicles. However, the small amount of stabilising detergents, added at this stage, did disturb vesicle-formation, in particular in case of polymersomes (**Fig. 27**).

Experiments encapsulating FCS dyes (elaborated in chapter **release experiments**) did not reveal any significant difference between vesicles without OmpF and those allegedly with OmpF. These results were reproducible for various liposomes and polymersomes. However, it was noted, that in case of liposomes the vesicles had a tendency to be 10-20% smaller than those with OmpF. In terms of membrane permeability, most experiments were a failure. Only in case of experiments encapsulating

HRP in liposomes, occasionally vesicles with OmpF appeared to have a higher activity than those without.

Due to these results, this method was abandoned in favour of more promising approaches, but eventually it was revisited with an important twist: The stabilising detergent of OmpF was removed and the solution was added directly to the ethanolic polymer solution before the film was dried. This method became viable, as it was observed that OmpF does not precipitate immediately, but within hours and due to the fact that OmpF is known[1a] to resist several solvents unlike most other proteins. These would denature irreversibly, thus requiring a less efficient, but milder method.[25a, 29] This variation removed not just the disruptive detergent, but allowed a more homogeneous mixture of OmpF and the ABCPs. It turned out to be the most reliable method for inserting OmpF in a variety of ABCPs.

It was also observed that $A_8B_{49}A_8$ and $A_6B_{44}A_6$ inserted OmpF and $A_6B_{42}A_6$ did not, despite its similar composition. This indicates that there might be other factors influencing the ability to insert membrane proteins, e.g. the content of PDMS without hydrophilic groups, or the content of AB in ABA, or simply the PDI of the ABCP.

3.4.2 Detergent removal

Since detergents are interfering with the process of vesicle-formation, their removal was the next logical step. Since they are initially required for the stability of OmpF in solution, three options are available:

1) Reducing the detergent concentration to the bare minimum (approximately the cmc, 0.5wt% in case of OG), adding the OmpF to the ABCPs and further reducing the detergent concentration during the vesicle-formation

2) Dissolving the ABCPs in a detergent solution and forming the vesicles through detergent removal.

3) Producing the vesicles beforehand and adding the OmpF solution with enough detergent to destabilise the vesicle membranes so that OmpF can insert, but not enough to completely destroy the vesicles. Then the detergent has to be removed to stabilise the vesicles again.

For all three variants two parameters have to be controlled: first the selected detergent, and second the method of the detergent removal. The choice of the detergent can have a huge effect on the interactions with the vesicles and proteins. This in combination with the individual cmc determines the

effective concentrations at which the MP remains stabilised in solution and the concentration at which the vesicles become weakened or destroyed.

In general, there are several methods, how the detergent may be removed: it could be dialysed off, removed through size exclusion chromatography (mainly separating vesicles from micelles) or be removed through addition of adsorbents. While size exclusion chromatography would be the fastest method, the use of adsorbents is far more efficient at removing remaining detergents. It allows the use of detergents that would take forever to be removed through dialysis or size exclusion chromatography due to their low cmc, such as TrtX.[26a, 26b] It has moreover the advantage that the detergent removal rate can be precisely controlled through the number of additions and amount of adsorbent added and by controlling the temperature.

The first two methods would be relatively straightforward. **2)** would have the disadvantage that more detergent is used and has to be removed. **1)** still hindered vesicle-formation resulting in more micelles and smaller vesicles but being considerably more effective than without detergent removal. The method had a poor overall reproducibility. It was moreover observed that an incomplete detergent removal produced vesicles slowly deteriorated into micelles. **2)** was apparently the worst possible choice for ABCPs resulting in micelles only, but it was a very efficient method for insertion of OmpF into liposomes. The notable exception hereto were lipid mixtures with cholesterol, which resulted in demixing during detergent removal (see chapter on DSPC above). Comparing method **1)** and **2)** lipids and ABCPs indicates that they are mechanistically very different.

Method **3)** has the most parameters to optimise since the concentration and choice of detergent are far more important, since it is a delicate balance between weakening of pre-existent membranes just enough to be able to insert MP while at the same time keeping the concentration of detergent low enough that the MP becomes unstable in solution so that it can be inserted. Despite all these complications, it is well established for inserting various MPs into liposomes. It has also successfully been used for polymersomes using 0.5wt% TrtX, sonication and biobeads.[18] However, the known sensitivity of polymersomes towards detergents and the possibility of mechanistical differences reduces further the appeal of this method. Indeed, it was hard to insert MPs into polymersomes and it became apparent that the vesicles do recover much less from damage caused from sonication or detergent addition than liposomes did, resulting in very small particles/micelles and releasing whatever was encapsulated within the vesicles.

An interesting finding was that OmpF could reproducibly be inserted in liposomes formed via detergent removal until a new batch of OmpF was produced (the old batch still worked, thus it has to be assumed

that it was related to the new batch). The new batch could be inserted in polymersomes, applying a different method (adding OmpF once the detergent was removed prior to the addition to the ethanolic polymer-solution). The difference between both batches was that OmpF was extracted in the prior using Octyl-POE and the latter using OG, since OG provided a higher yield. OG is however known to be a harsher detergent, which can denaturate some proteins and destroy vesicles more easily. It can be assumed that the change in the extraction procedure changed the **ternary mixture**, the bacterial lipids that surround OmpF and can be co-extracted.[26c] OG had the advantage that its concentration could be measured with the Möllisch assay, which allowed to reveal how much detergent was accidentally dragged along. It was also easier to remove the detergent.

3.4.3 Detergent titration

In case of MP insertion through detergent addition and removal on preformed vesicles, there is a way of estimating the required detergent concentration. Vesicles can be titrated with detergent and the scattering can be measured over time using a fluorimeter. The scattering is manly dependent on the number of vesicles, but increases slightly probably due to the swelling of vesicles.[26b, 26c] When vesicles become destroyed, the scattering intensity drops rapidly. Once the concentration is known at which vesicles start to disintegrate, it can be tested if MP inserts at said concentration in vesicles (and not in newly formed micelles) and whether enough vesicles survive the process. If the detergent concentration was too high, it is decreased e.g. by half, zeroing in within a few attempts the working concentration at which the vesicles are still stable, but the membrane able to accept MPs, can be found. This pre-experiment has however two minor flaws, that have to be considered. First and foremost, the interaction between vesicles and detergents may take some time. It was noticed for polymersomes, that the determined tolerable concentration after 2h of incubation, destroyed all vesicles overnight. Secondly, changing for example the vesicle concentration (which may happen accidently during the vesicle-formation or purification) changes the required detergent concentration, since the concentration of detergent micelles in solution drops considerably due to insertion of detergent molecules within vesicle membranes.

In the following graphs two ABA with different length (**3** $A_6B_{44}A_6$ and **7** $A_{17}B_{65}A_{17}$)[25] are compared with each other and with liposomes (natural phosphatidylcholine with 10% cholesterol). The vesicles were

---

[25] These experiments are actually not related to the OmpF project, but to the SGLT-project. The insertion of OmpF does not require the detergent addition and removal method, but SGLT is too sensitive to be treated the same. For the OmpF related experiments $A_6B_{44}A_6$ proved to be the best, but since its supplies became low,

stirred in presence of the respective amount of detergent over night at 4°C. The following detergents were considered:

Table 11.: various detergents and their critical micelle forming concentration

Detergent	cmc [mM]	Mw [g/mol]	cmc [wt%]	Description
DDM	0.15	510.62	0.01%	Alkyl-Sugar
TritonX-100	0.24	625	0.02%	Aromatic-PEG
DM	1.6	482.56	0.08%	Alkyl-Sugar
TDOC	2	521.69	0.10%	$Chol\text{-}SO_3^-$
CHAPS	3	614.88	0.18%	$Chol\text{-}SO_3^-$
OPOE	6.6	245.38	0.16%	Alkyl-PEG
OG	20	292.37	0.59%	Alkyl-Sugar

Titrating liposomes with DM produces a negative parabolic correlation (**Fig. 33**). Since for the polymersomes lower detergent concentrations had to be evaluated, all following titration curves are half-logarithmic. Thus, the same graph is displayed twice for better comparison. Even then it can be clearly seen that the scattering increases initially with the detergent concentration.
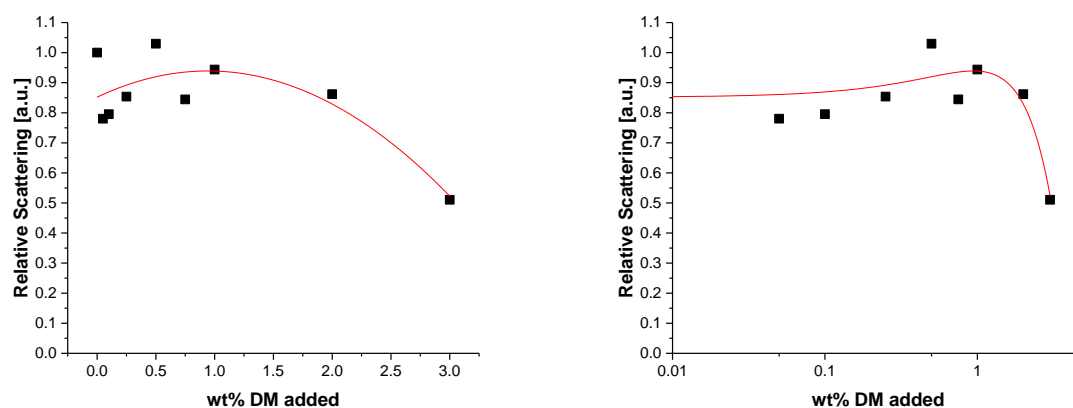
Fig. 33: Titration of POPC/POPS/cholesterol-liposomes with DM. Left: linear scale; right: $\log_{10}$-scale.

---

other ABCPs were investigated for this side project. This cancelled project is mentioned in this thesis, since it gives further insight in the stability and properties of various polymersomes.
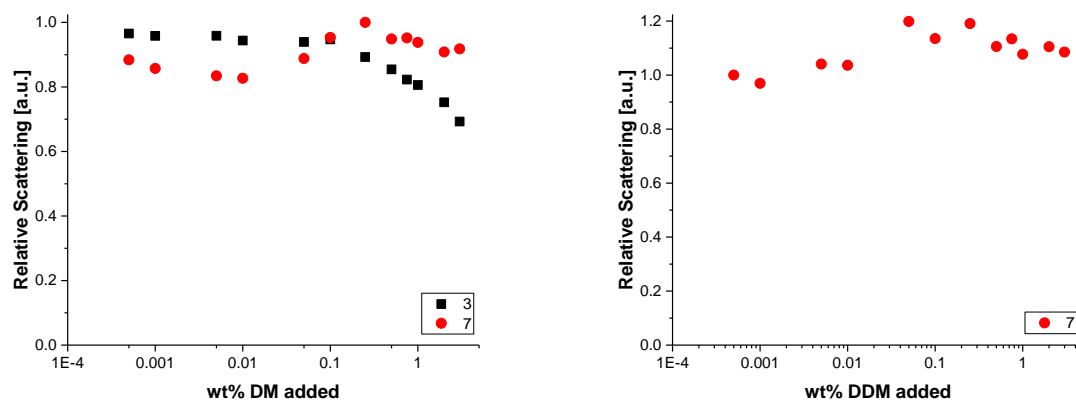
Fig. 34: titration of polymersomes from a short ABCP **3** and a long ABCP **7**. Note that DDM has only two CH$_2$ groups more than DM.
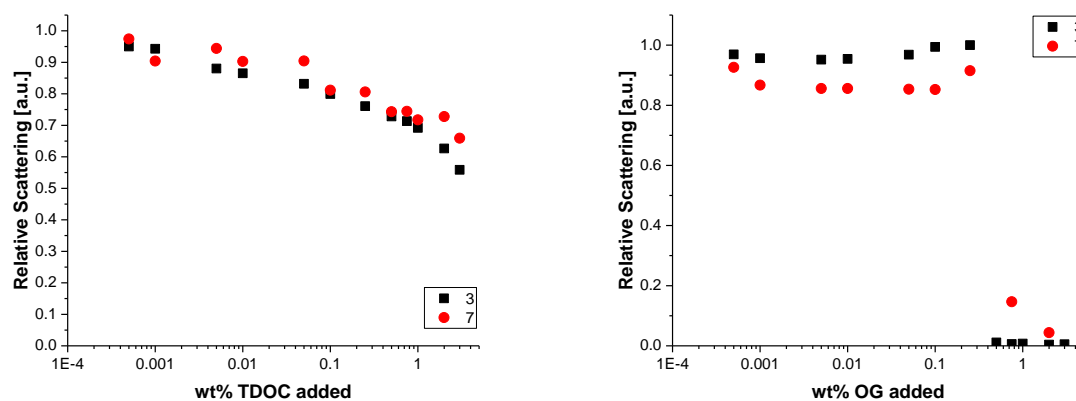
Fig. 34: titration of polymersomes from a short ABCP **3** and a long ABCP **7.** Note: OG is only two CH$_2$ groups shorter than DM.
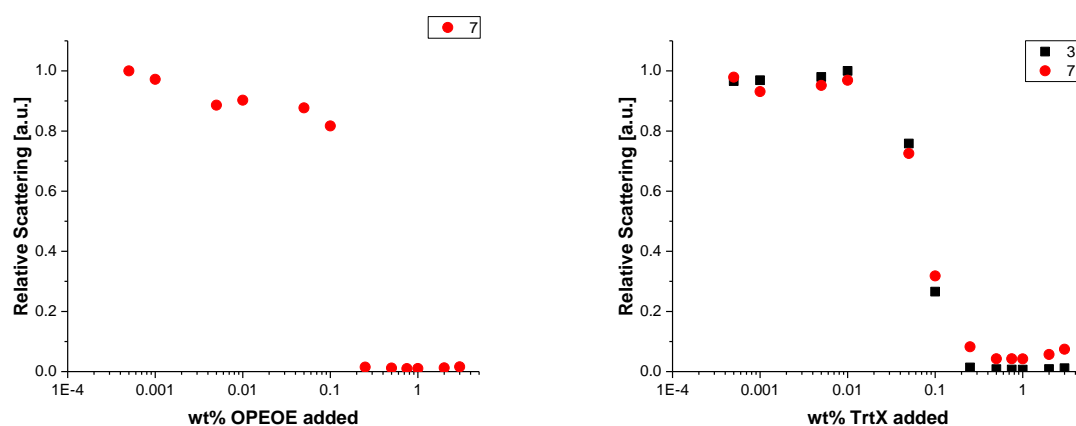
Fig. 35: titration of polymersomes from a short ABCP **3** and a long ABCP **7**. Note: OPOE has only a different head-group than OG.

It becomes immediately clear that polymersomes behave differently than liposomes (**Fig. 33**) in that they are much more sensitive to detergents and that absorption does not initially increase (with the

notable exception of **7** titrated with DM or DDM) but rather decreases slowly. This indicates that the polymersomes do not swell but become unstable as soon as they interact with detergents.

The second obvious result is that the titration curve depends much less on the cmc of the detergent (which only roughly correlates with the transition point) but on the chemical nature (**Fig. 34, 35**). Long chained alkyl-sugars and cholate derivatives show little effect and belong to the detergents that are known[26b, 26c] to mild detergents, that are non denaturating detergents when it comes to protein extraction and which are less harmful to liposomes. Short alkylsugars and short alkyl-PEG detergents are much harsher to the vesicles and result in sharp transitions. This difference is nicely demonstrated in the differences between **OG**, DM and DDM. One can even see a difference although they all differ by only two CH_2 groups. Similarly, longer ABCPs appear to be more sensitive towards detergents as can be seen in the titration with the milder detergents.

It appears that **DM** and **DDM** hardly affect the vesicles in the observed concentration range (0.0005-3wt%). The scattering increases slightly along with the detergent concentration (with DM having a small maximum at 0.25%). The 3rd alkyl-sugar based detergent **OG** appears to be similar but the scattering drops sharp and low between 0.25 and 0.75%.

The cholate based detergent **TDOC** has also only a weak trend but decreases the scattering gradually. It could be that the curve would drop drastically above 3%. Triton X100 has early a transition to low scattering between 0.01 and 0.5%. **OPOE** lies in between the before mentioned **OG** and **TrtX**, having a transition at 0.1 to 0.25%. Thus, all turning points with the possible exception of TDOC are around the cmc. This could be due to the fact that cholesterol based detergents do not form regular micelles.[26a]

These results are noteworthy for two reasons. First, they indicate liposomes and polymersomes are mechanistically different, which manifests in a different stability but also in the fact that procedures regarding the insertion of MPs in liposomes cannot be translated to polymersomes. This is possibly due to the mismatch of the length of the hydrophobic block and the length of the alkylchain (thus only DDM might cause quelling of the vesicles). In the worst case, the pair of selected ABCP and detergent do not allow any insertion, but the detergent catalyses the destruction of the vesicles. Secondly the detergent which is used to stabilise OmpF in solution (OG or OPOE) are more destructive to the vesicles than TrtX which is traditionally used to destroy membranes.
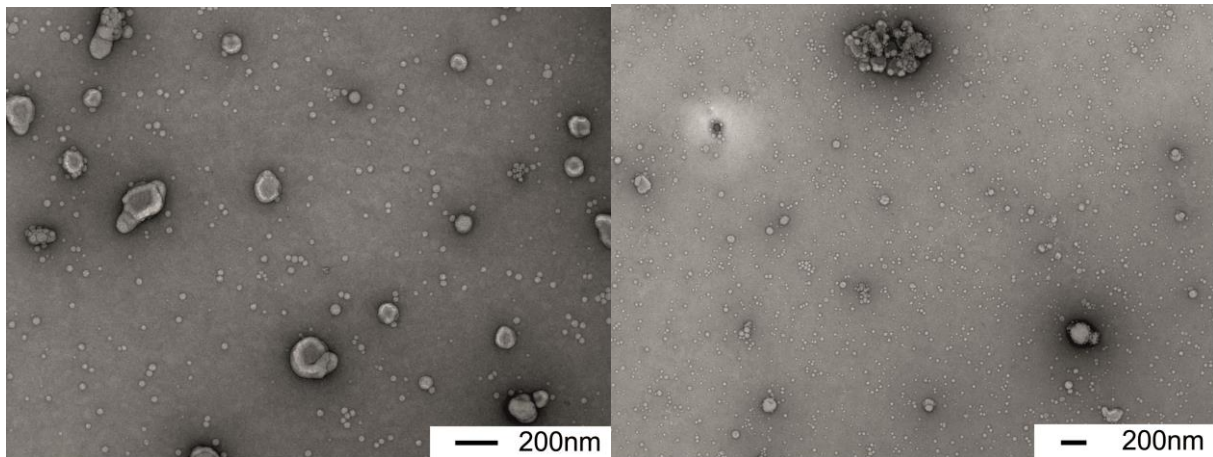
Fig. 36: TEM images of the polymersomes produced via film rehydration from $A_{17}B_{65}A_{17}$ (**7**). Left: 0.25% OG added directly to the ABCP-film; right: the same amount of OG added after film rehydration. In both cases, the detergent was removed again via biobeads.

As can be seen in **Fig. 34** polymersomes of $A_{17}B_{65}A_{17}$ (**7**) should be able to withstand up to 0.25% of OG. Yet, it became clear that the detergent was detrimental to vesicle-formation and the over-all stability and homogeneity of the vesicle-samples. At 0.25% of OG film rehydration did not start under normal conditions. Rehydrating the polymer-film at 4°C resulted in slow film rehydration, as indicated by the solution becoming slightly opaque. Only after addition of biobeads the turbidity increased significantly. The vesicles were half the size as in the absence of detergent. Further experiments imply that less denaturating detergents such as DM are a better choice and even there, the concentration should be 25% below the maximal tolerated concentration.

Adding the OG to preformed vesicles appeared to have no impact on the turbidity, nor on the average vesicle-size, but until the TEM-images were made, the samples had begun to clearly deteriorate. This process apparently continued after the removal of OG via biobeads indicating that even after multiple changes of biobeads, OG remained interacting with the ABCPs. Interestingly, the point of detergent addition determines the stability of the vesicles (see TEM **Fig. 36**). This indicates that OG can interact with ABCP in different ways and probably insert into membranes either homogeneously or in domains; the latter resulting in vesicle degradation.

As noted earlier, liposomes became slightly larger in presence of OmpF. Since OmpF had no chance of displacing the ABCPs inside the membrane, but was added before its formation, it can be assumed that it has no direct influence on the vesicle-size. However, as a porin it has the ability to equilibrate osmotic pressure, which would otherwise compress vesicles and it has been observed especially in case of polymersomes and presence of detergents that OmpF might actually stabilise the membranes. The same was observed for SGLT1, a sodium-galactose symporter, which was used in a side-project:
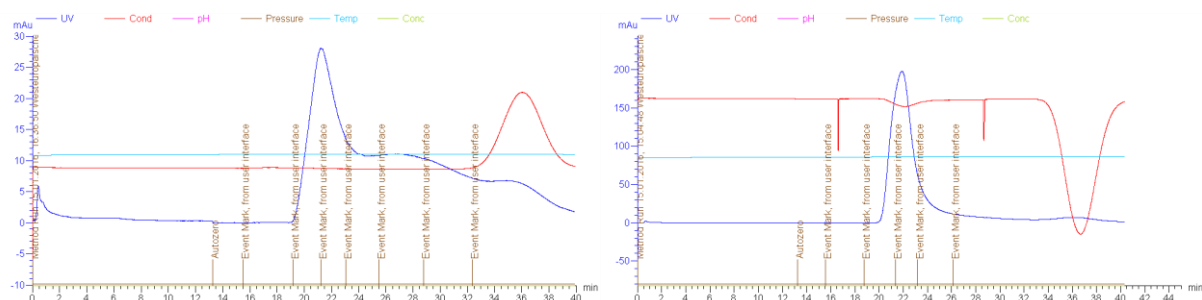
Fig. 37: Size exclusion chromatography of $A_{17}B_{65}A_{17}$ (**7**) polymersomes (encapsulating 100mM NaCl, 0.05mM Galactose) in absence (left) and in presence (right) of SGLT1.

In presence of 0.8% DM the size exclusion chromatography reveals that the vesicle peak measured by UV-absorption, developed a pronounced hunchback and even overlapped with a micelle-peak. Both disappear in presence of SGLT1 and the conductivity-measurement had a peak turning into a valley. The same could be observed for OmpF, but with the opposite sign:
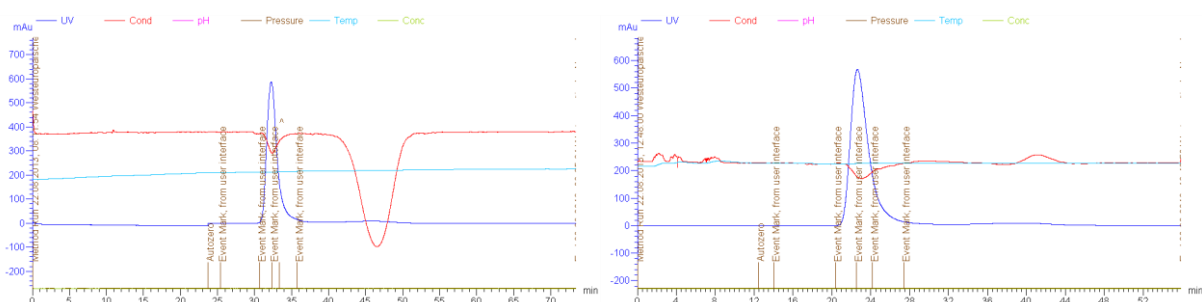
Fig. 38: Size exclusion chromatography of DSPC-mix liposomes encapsulating HRP in absence (left) and in presence (right) of OmpF.

The reason for the change in conductivity remains unclear and was not further investigated but appears to be related to either the presence of micelles and or the amount of unencapsulated cargo.

4 Conclusion

4.1 OmpF-Mutants

D12C, K89C, R270C, D12,K89C, D12,R270C and K89,R270C were successfully produced. Of these, all thiol groups were equally accessible, with the notable exception of D12C containing mutants, which were not even able to react with small compounds such as acrylodan. The rationale behind the

synthesis of the double mutants was to increase the probability that each pore contained at least one stimuli responsive group and ideally increasing the blockage by attaching two short stimuli responsive groups in place of a longer one. However, measurements via mass spectrometry indicate that this was not necessary to ensure labelling of every pore, moreover later kinetic measurements indicate that R270C-Gala3 and K89R270C-Gala3 OmpF-conjugates behave identically.

4.2 Methods for measuring a DOL inside a pore

Due to the low concentrations of the remaining thiol groups, common practice methods such as the Ellmans assay could not be used, moreover assays based on signal amplification cannot be applied to thiols that are partially hidden through pores. Thus, mass spectrometry has to be used to obtain reliable DOLs. However, this method is ill suited for quick reaction control purposes., thus a new assay had to be developed. While Thioglo-1 could be used for a qualitative prove of successful labelling, it was not particularly suited for quantification of DOL, regarding the background fluorescence and difficulty in sample purification. Furthermore, it proved to be highly sensitive to photobleaching even in rather dim ambient light. Acrylodan proved to be cheaper, smaller and more reliable. To the best of my knowledge, it is the first time acrylodan was reported to be used for quantification of thiol groups. Lastly, it should be noted that both methods cannot be compared directly, since they measure different types of DOL: mass spectrometry an individual DOL and acrylodan an overall DOL.

4.3 ATRP based oligomers

Little was published on the topic of short, but well-defined oligomers produced via radical polymerisation. Yet, during this PhD thesis it was shown that well defined oligomers of *tert*. butyl-acrylic acid, in the range of 4-30 repeating units, could be synthesized through ATRP in moderate to good yields with PDIs ranging from 1.10 to 1.35. One procedure yielded a DP of 6-12 with a PDI of 1.3 and another procedure a DP of 6-30 with a PDI of 1.1 (both up to 75% yield). In the prior case, the DP was controlled through the stoichiometry and in the latter case through reaction time. Those oligomers could behave very different from their respective polymers. Oligomers with less than ca. 20 repeating units were oils and could therefore not be precipitated and had an unexpected vapor pressure reducing effect. NIPAAM had no such issues, but the monomer proved to be hard to remove.

Oligo(vinyl-4-pyridine) was promising, but the pyridine-groups interferes with the ATRP and the oligomer is difficult to purify.

The main problem with the oligomers seems to be caused by the initiator itself. Traces of presumably HBr degraded the initiator rapidly, impeded ATRP and slowly turned the oligomer insoluble in water.

Since the bromine group could split off during storage, a nucleophilic substitution might be required, however at that point stimuli responsive peptides were already the point of focus.

4.4 Stimuli responsive peptides

Similar to oligomers, the required size creates several challenges. The stimuli response seen in larger peptide sequences will probably not exist under a certain number of sequence repeats (e.g. allowing stable helices). Moreover short, hydrophilic peptides are known to be difficult to purify and even more so peptides with many repeats of the same functional groups (having 1 or two carboxylic acids makes a far greater difference during purification than having 5 or 6).

Another flaw in the design of stimuli responsive peptides is that they tend to be hydrophobic. The more hydrophobic they are at the conditions Michael additions are performed, the lower the success rate gets.

Nonetheless, peptides were deemed the superior choice due to their tunability, their precise length and the absence of bromine.

4.5 Determination of the DOL

Oligo(acrylic acid) turned out to be particularly difficult to attach to OmpF. Due to its self-deactivation and high tendency to bind water, it was impossible to calculate the required concentrations. Due to the high number of charges, it can be assumed that labelling the same pore twice becomes unlikely. Moreover, it was found that the DOL decreases with increasing length of the *oligo*(acrylic acid). This effect was not observed with peptides which had similar lengths than the longer oligomers of *oligo*(acrylic acid). Furthermore, later kinetic experiments indicated that after reaching a certain length the pore becomes permanently blocked, without showing any stimuli responsiveness. The labelling

with peptides on the other hand worked well, as long as they remained sufficiently soluble (H6 only exception).

4.6 Choice of the building material for Nanoreactors

In principle, there is the choice between well-established liposomes and more stable and customisable polymersomes. However, experiments revealed that attributed characteristics depend on numerous factors and the transition between liposomes and polymersomes is more gradual.

POPC has the highest willingness to form vesicles but is less stable (mechanically and thermally) than the **DSPC**-mix, which in turn is easier to make vesicles and less sensitive to detergents than **ABCPs**. Shorter ABCPs are closer to the DSPC-mix, whereas longer ABCPs represent the ideal polymersomes.

With the length of the ABCP, the water solubility decreases, the mismatch to OmpF and detergents increases making OmpF harder to insert and causing the membranes to behave differently to detergents (and dyes, see chapter **release experiments**). Still, both liposomes and polymersomes tend to get smaller and become eventually micelles, when sufficient detergent concentrations are present.

First **POPC** was used as the simplest solution. Due to the problem of HRP interaction and its removal in general, but also the desire for more stable samples a liposome mix (**DSPC**/POPS/cholesterol mix) was used that was optimised in these aspects. However, the OmpF insertion was too low. Thus, a different method was tried namely detergent removal using the already proven **SM**/POPS/cholesterol mix. The OmpF insertion was greatly improved as was the HRP removal via dialysis. Thus, much better kinetics were obtained. However, the liposomes used there were much less stable than the DSPC/POPS/cholesterol mix and seems to be also more permeable.

Regarding ease of film rehydration, preference towards vesicles, the average vesicle size, the overall robustness and their likelihood of incorporating membrane proteins, the ABCPs can be sorted as follows: $A_4B_{22}A_4 > A_8B_{49}A_8 > A_6B_{44}A_6 > A_{17}B_{65}A_{17}/A_{16}B_{72}A_{16}$ (**1>4>3>7>8**). The rest was not worth further experiments (**2** $A_{14}B_{25}A_{14}$ might have worked previously, but its tendency to form vesicles is too low). It can be thus said that shorter ABCPs are preferable and that the hydrophilic ratio should be between 20 and 30%. Interestingly, neither of these factors appears to determine the average vesicle size. Only few ABCPs allowed the formation of vesicles larger than 100nm in diameter. These included $A_4B_{22}A_4$, $A_{14}B_{25}A_{14}$ and $A_{20}B_{38}A_{20}$ (**1, 2** and **5**). The length of the ABCPs had however some effect on the stability of the vesicles and the ease of their formation. The longer the ABCP the thicker the resulting membrane became, which in turn made the vesicles more stable, but more difficult to form (both slower

dissolution and reorganisation) and less stable towards detergents. Furthermore, thick membranes have to be considered less likely to insert membrane proteins. [18, 30] Interestingly, a higher hydrophilic ratio did not facilitate film-rehydration, but direct dissolution. This would indicate that these ABCPs can produce films that are easily dried too much so that they become poorly soluble (**2** and **5**).

Table 12: list of polymers sorted first according to B then A; N= total monomer number hydrophilic ratio=2A/N

No.	Composition	Hydro philic ratio	B/A	N	Structures	OmpF Insertion	Remarks
1	$A_4B_{22}A_4$	27%	5.5	30	vesicles	yes	
2	$A_{14}B_{25}A_{14}$	53%	1.8	53	worms and micelles	n.d.	direct dissolution better
3	$A_6B_{44}A_6$	21%	7.3	56	vesicles	yes	similar to 4
4	$A_8B_{49}A_8$	25%	8.2	65	vesicles	yes	similar to 3
5	$A_{20}B_{38}A_{20}$	51%	1	78	vesicles; micelles dominating	n.d.	Similar ratio to 2; similar results; less water soluble
6	$A_7B_{67}A_7$	17%	9.6	81	worms and micelles	n.d.	similar in ratio to 3 and 4
7	$A_{17}B_{65}A_{17}$	34%	3.8	99	many vesicles often multilamellar	no	similar to 8
8	$A_{16}B_{72}A_{16}$	31%	4.5	104	small vesicles and micelles	yes	similar to 7

As mentioned in the introduction, the formed structures can be predicted from the hydrophilic ratio. Thus, in **Table 12**, unfavourable ratios are marked red and favourable ratios green. Whenever, a ABCP formed decent vesicles, insertion of OmpF was tested (else it was n.d.: not determined). OmpF appears to insert independent of the length of the ABCP.

Many factors are affecting the vesicle-formation experiments among them are nature of ABCP[23] and its block length ratio,[25a] the temperature during rehydration[22, 25b], the method of rehydration,[22b] the pH[22b] and the presence of additional ions.[22, 25b]

When taking all these parameters into account it is possible to produce vesicles and even inserting MPs fairly reliably (ca. 95% chance for good vesicles and 75% chance of inserting the MP). To further improve the **reliability**, the samples have to be extruded with a membrane having pores close to the smallest naturally occurring vesicles to further homogenise their size. Additionally, bad batches have to be sorted out via light scattering and diluting the samples to the same vesicle concentration (using the samples ability to scatter light as indicator for vesicle density).

4.7 Insertion of OmpF

OmpF is unable to force itself into membranes as the smaller channel proteins (or rather cell toxins) gramicidin, valinomycin etc. are. Like most MPs, OmpF has a significant hydrophobic surface, which makes it inherently unstable in water resulting in aggregation and precipitation. OmpF needs thus to be stabilised with a detergent. Detergents interact not just with the MP, but also with isolated amphiphiles and more importantly with membranes. This has been used to insert MPs in preformed vesicles, or to create proteo-liposomes via detergent removal.

However, these interactions are very complex and sensitive. Two CH_2-groups less, or a different headgroup can determine, whether vesicles or proteins are stable or become denaturated at a certain concentration. Detergents form micelles in solution, stabilise OmpF, isolated amphiphiles and insert into membranes. Thus, the final concentration in solution is hard to tell. To complicate things further, polymersomes are inherently more sensitive to detergents and appear to interact differently due to a larger mismatch between the hydrophobic groups of the ABCP and the detergent. Polymersomes appear to have less self-healing abilities and interact inherently different with detergents. It even makes a difference, if a detergent is added during film rehydration (impeding it), or after (damaging the vesicles and turning them slowly into micelles). Detergents are also practically impossible to remove completely, as they bind to membranes.

On the other hand, MPs are apparently able to stabilise membranes. Their presence also affects the ratio of vesicles to micelles, the vesicle size and the encapsulation efficiency. Fortunately, the complex system can be avoided in case of OmpF, since it is able to refold itself after denaturation. Therefore, its stabilising detergent can be removed and it can be dissolved in organic solvents along with the ABCPs. Upon film rehydration, the ABCPs act as the detergent and stabilise the OmpF.

In case of more sensitive MPs, mild detergents such as DM appear to be far better suited than OG, or TritonX (which have been used before as published by Graff *et al*[18]). Even then, one should stay at least 25% below the maximal tolerated detergent concentration.

5 References

[1] a) R. Koebnik, K. P. Locher and P. Van Gelder, *Mol Microbiol* 2000, 37, 239-253;
b) S. Ihle, O. Onaca, P. Rigler, B. Hauer, F. Rodriguez-Ropero, M. Fioroni and U. Schwaneberg, *Soft Matter* 2011, 7, 532-539.

[2] T. Einfalt, R. Goers, I. A. Dinu, A. Najer, M. Spulber, O. Onaca-Fischer and C. G. Palivan, *Nano Lett* 2015, 15, 7596-7603.

[3] H. Miedema, M. Vrouenraets, J. Wierenga, D. Gillespie, B. Eisenberg, W. Meijberg and W. Nonner, *Biophys J* 2006, 91, 4392-4400.

[4] a) W. Grosse, L.-O. Essen and U. Koert, *ChemBioChem* 2011, 12, 830-839;
b) H. Miedema, A. Meter-Arkema, J. Wierenga, J. Tang, B. Eisenberg, W. Nonner, H. Hektor, D. Gillespie and W. Meijberg, *Biophys J* 2004, 87, 3137-3147.

[5] a) Z. H. Yang and A. B. Attygalle, *J Mass Spectrom* 2007, 42, 233-243;
b) S. Lang, D. E. Spratt, J. G. Guillemette and M. Palmer, *Anal. Biochem.* 2005, 342, 271-279;
c) R. J. Cremlyn, *An Introduction to Organosulfur Chemistry*, John Wiley and Sons, Chichester 1996;
d) P. Nagy, *Antioxidants & Redox Signaling* 2013, 18, 1623-1641.

[6] V. Resch, C. Seidler, B.-S. Chen, I. Degeling and U. Hanefeld, *Eur. J. Org. Chem.* 2013, 2013, 7697-7704.

[7] a) S. Loudwig and H. Bayley, *J Am Chem Soc* 2006, 128, 12404-12405;
b) M. R. Banghart, M. Volgraf and D. Trauner, *Biochemistry-Us* 2006, 45, 15129-15141.

[8] H.-C. Chiu, Y.-W. Lin, Y.-F. Huang, C.-K. Chuang and C.-S. Chern, *Angew. Chem. Int. Ed.* 2008, 47, 1875-1878.

[9] G. Mantovani, F. Lecolley, L. Tao, D. M. Haddleton, J. Clerx, J. J. L. M. Cornelissen and K. Velonia, *J Am Chem Soc* 2005, 127, 2966-2973.

[10] Z. Ge, H. Liu, Y. Zhang and S. Liu, *Macromol Rapid Comm* 2011, 32, 68-73.

[11] B. F. Lin, D. Missirlis, D. V. Krogstad and M. Tirrell, *Biochemistry-Us* 2012, 51, 4658-4668.

[12] *Ellmans Reagent/Invitrogen*, http://products.invitrogen.com/ivgn/product/D8451, accessed: 2016.

[13] *Thiol rective probes/Thioglo-1*, http://www.covalentassociates.com/ThioGlo%20information%20and%20guidelines.pdf, accessed: 2016.

[14] N. M. Griffin and J. E. Schnitzer, *Mol. Cell. Proteomics* 2011, 10, R110.000935.

[15] a) H. Chen, S. S. Ahsan, M. E. B. Santiago-Berrios, H. D. Abruña and W. W. Webb, *J Am Chem Soc* 2010, 132, 7244-7245;
b) M. Möller and A. Denicola, *Biochem. Mol. Biol. Educ.* 2002, 30, 175-178;
c) A. Kawski, P. Bojarski and B. Kuklinski, *Z Naturforsch A* 2002, 57, 94-97.

[16] *DSPC/Avanti Lipids*, https://avantilipids.com/product/850365/, accessed: 2016.

[17] a) L. Redondo-Morata, M. I. Giannotti and F. Sanz, *Langmuir* 2012, 28, 12851-12860;
b) W. W. Sułkowski, D. Pentak, K. Nowak and A. Sułkowska, *J. Mol. Struct.* 2005, 744-747, 737-747.

[18] A. Graff, C. Fraysse-Ailhas, C. G. Palivan, M. Grzelakowski, T. Friedrich, C. Vebert, G. Gescheidt and W. Meier, *Macromol Chem Phys* 2010, 211, 229-238.

[19] P. Tanner, V. Balasubramanian and C. G. Palivan, *Nano Lett* 2013, 13, 2875-2883.

[20] S. Kozo, Y. Tokio and H. Ryohei, *Bull. Chem. Soc. Jpn.* 1961, 34, 237-241.

[21] D. Christina, D. Ina, H. Richard and S. Helmut, *Macromol Rapid Comm* 2011, 32, 1753-1758.

[22] a) K. Kita-Tokarczyk, J. Grumelard, T. Haefele and W. Meier, *Polymer* 2005, 46, 3540-3563;
b) D. Wu, M. Spulber, F. Itel, M. Chami, T. Pfohl, C. G. Palivan and W. Meier, *Macromolecules* 2014, 47, 5060-5069.

[23] L. Zhang and A. Eisenberg, *J Am Chem Soc* 1996, 118, 3168-3181.

[24] J. D. Robertson, G. Yealland, M. Avila-Olias, L. Chierico, O. Bandmann, S. A. Renshaw and G. Battaglia, *ACS Nano* 2014, 8, 4650-4661.

[25]   a) M. Grzelakowski, M. F. Cherenet, Y.-x. Shen and M. Kumar, *J Membrane Sci* 2015, 479, 223-231;^lb) P. L. Soo and A. Eisenberg, *J Polym Sci Pol Phys* 2004, 42, 923-938.

[26]   a) A. M. Seddon, P. Curnow and P. J. Booth, *Biochim. Biophys. Acta, Biomembr.* 2004, 1666, 105-117;
b) J.-L. Rigaud and D. Lévy, *Reconstitution of Membrane Proteins into Liposomes*. In Methods Enzymol., Academic Press: 2003; Vol. Volume 372, 65-86;
c) M. le Maire, P. Champeil and J. V. Moller, *Bba-Biomembranes* 2000, 1508, 86-111.

[27]   V. Visudtiphole, Matthew B. Thomas, David A. Chalton and Jeremy H. Lakey, *Biochem J* 2005, 392, 375-381.

[28]   M. Bieligmeyer, F. Artukovic, S. Nussberger, T. Hirth, T. Schiestel and M. Müller, *Beilstein J. Nanotechnol.* 2016, 7, 881-892.

[29]   a) A. M. Seddon, P. Curnow and P. J. Booth, *Bba-Biomembranes* 2004, 1666, 105-117;
b) J. L. Rigaud and D. Levy, *Method Enzymol* 2003, 372, 65-86.

[30]   a) V. Pata and N. Dan, *Biophys J* 2003, 85, 2111-2118;
b) G. Srinivas, D. E. Discher and M. L. Klein, *Nano Lett* 2005, 5, 2343-2349.

IV Release experiments

IV Release experiments

The most straightforward way of testing the functionality of the OmpF conjugate, would be to insert it into a vesicle membrane and at the same time encapsulate a substance within the vesicles (**Fig. 1**). Then the presence of the substance within the vesicle has to be confirmed and the substance has to be released upon stimuli and detected outside the vesicle. This could be done with a fluorophore, where the diffusion time is observed in fluorescence correlation spectroscopy (FCS), or by measuring the fluorescence directly. The latter requiring encapsulation in self-quenching concentrations. There, the presence within the vesicles can only be tested indirectly, by the destruction of the vesicles.

The difficult part is to prevent the premature release of the cargo; thus, the vesicles have to be formed under conditions where the pores are expected to be in their closed state.
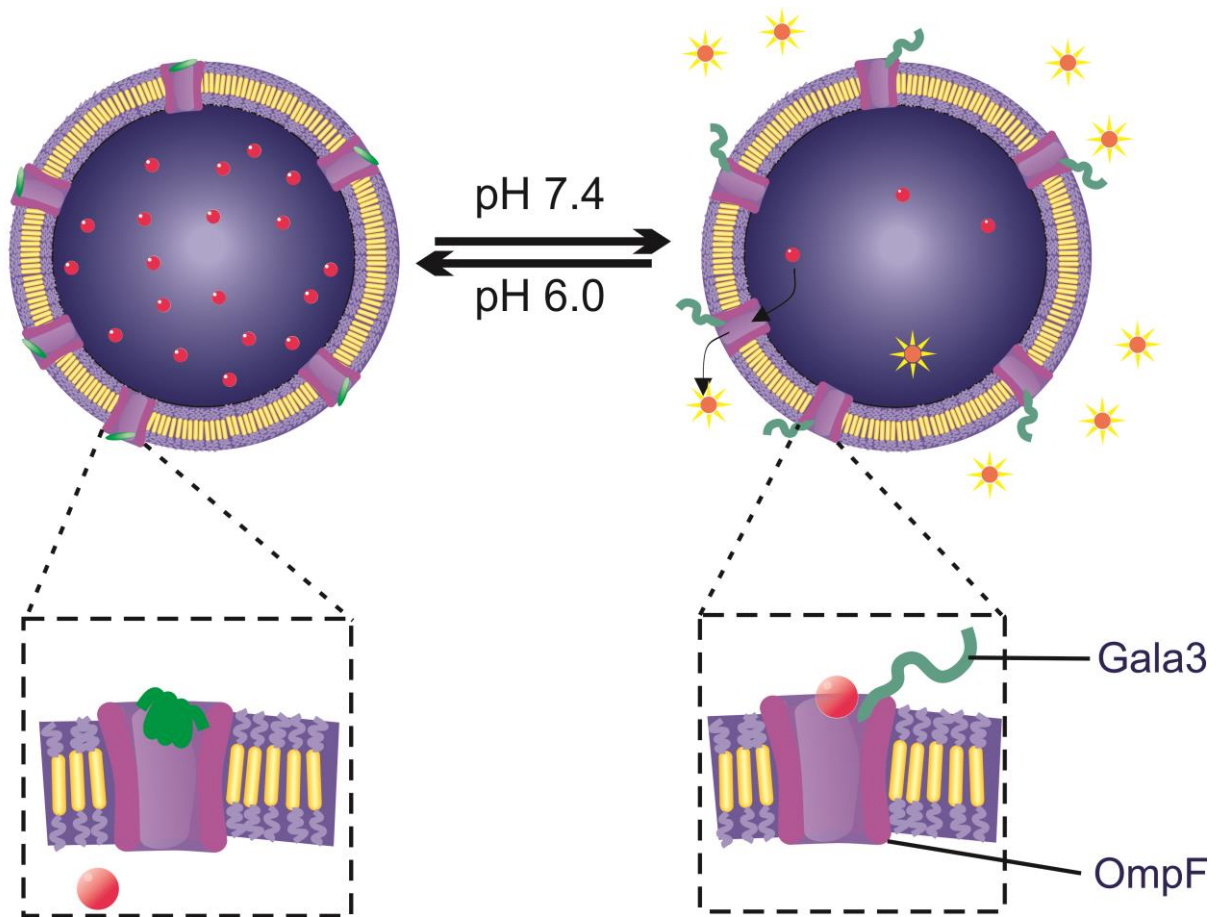
Fig. 1.: Scheme of vesicles containing a fluorescent dye in self-quenching concentrations, being released at pH 7.4 and becoming fluorescent due to dilution effect.

Since vesicles without OmpF can release their cargo too, if the membrane is damaged, or the cargo lipophilic enough to diffuse through the membrane, a control without OmpF is required and since a complete release of cargo is unlikely, a second control with unmodified OmpF is required. These samples will be further labelled S, N and P:

S: sample featuring modified OmpF in the membranes

N: negative control; without any OmpF

P: positive control; a sample with unmodified OmpF inserted

The abbreviation may be followed with the observed pH. These samples may also reveal various parameters affecting size, stability, of the vesicles. This will be discussed later in this and the following chapters.

1 FCS release experiments

FCS would allow to obtain more data from a single measurement than any other method. Asides from recording the diffusion of dye molecules through the membrane, it could give information about how much dye is encapsulated within the vesicles, how big or homogeneous the vesicles are and allows to compare the concentration of various samples. If the OmpF is labelled, it could also tell the number of OmpF pores per vesicle.

1.1 Sulforhodamine B

Sulforhodamine B is a relatively stable dye, whose fluorescence is not dependent on the pH from 3-10.[1] It is one of the smallest and most affordable FCS dyes, but relatively sensitive to bleaching. However, it turned out, that attempting to encapsulate Sulforhodamine B into liposomes was very challenging since Sulforhodamine B strongly interacted with liposomes resulting mostly in micelles and small vesicles with calculated encapsulation efficiencies of up to 180 000%. Of 9 tested Sulforhodamine B concentrations only 2 formed POPC liposomes. There seems to be no correlation with the concentration since the cases where vesicles were found had mid- to high Sulforhodamine B concentrations (5µM and 1mM).

It was thus tested, whether liposomes that feature additional charges and are furthermore PEGylated would perform better. The DSPC mixture, developed for its thermal stability meets these requirements and indeed features encapsulation efficiencies around 100% and being far more stable towards

IV Release experiments

Sulforhodamine B (yet the R_h decreased from 100nm to 55nm). Even in presence of 100μM Sulforhodamine B the vesicles proved to be stable over time, even at a pH of 1. It was thus used for further experiments eventually leading to encapsulating 100μM Sulforhodamine B in vesicles with D12,K89C-Gala3 OmpF,[26] with two controls (one with unmodified OmpF, one without OmpF). The samples were measured in triplicates, then they were acidified and measured again 12h later. In the meantime, a kinetic was measured for the positive control at pH 7.4 and the D12CK89C-Gala3 sample was measured at pH 7.4 and 5.5. At the time, it was assumed that the OmpF pores would unblock, once the Gala3 OmpF transitioned from a random coil to a compact α-Helix, thus releasing the encapsulated dye in acidic conditions.

Table 1.a: FCS data[27]

	No OmpF (N)		unmodified D12,K89C-OmpF (P)		D12,K89C-Gala3 OmpF (S)	
	pH=7.4	pH=5.5	pH=7.4	pH=5.5	pH=7.4	pH=5.5
CR [kHz]	53.4 ±6.6	42.7 ±9.1	15 ±2.9[*]	27.2 ±1.6	33.2 ±0.4	29.3 ±2.3
CPM [kHz]	310.1 ±25.6	304.7 ±116.2	133.5 ±22.1	56.6 ±9.0	120.5 ±7.3	87.5 ±21.0
F$_2$ [%]	99.3 ±1.2	100 ±0	94.4 ±2.9	97.8 ±2.4	96.6 ±0.3	98.3 ±1.7
τ$_2$ [μs]	4419.7 ±14.4	3965.3 ±848.9	4088.4 ±386.6	3616.7 ±88.6	4168.5± 241.7	4032.9 ±326.3
Aggregates []	1.3 ±0.6	1.7 ±0.6	1 ±1	1.3 ±1.2	0 ±0	1 ±1.7
R$_h$ [nm]	60.6 ±2	54.3 ±11.6	56 ±5.3	49.6 ±1.3	57.1 ±3.3	55.3 ±4.5
EE [%]	152 ±20[**]	239 ±177	90 ±30	51 ±4	73 ±13	59 ±21

Table 1.b: relative change upon acidification

	No OmpF (N)	unmodified OmpF (P)	D12,K89C-Gala3 (S)
CR [kHz]	80%	182%	88%
CPM [kHz]	98%	42%	73%
F$_2$ [%]	101%	104%	102%
τ$_2$ [μs]	90%	88%	97%
Aggregates []	125%	133%	-
R$_h$ [nm]	90%	88%	97%
EE [%]	157%	57%	81%

---

[26] Note: this was the first attempt of a double mutant, but the D12C did not prove accessible, thus it was replaced by R270C followed by K89,R270C-OmpF. R270C was originally expressed as a milestone on the way to the double mutant and was kept for comparison.

[27] 10x diluted samples; Neon-laser 543nm, 25% Output; 100nM free SRB gave a CR of 114.7 kHz, a CPM of 3.67 kHz, a TF of 1.1% and a diffusion time of 43.2 μs

Measuring release with FCS (**Table 1**) yields records of many sample properties:

The total count rate **CR**: the total fluorescence of the sample (vesicles and free dye)

The counts per molecule **CPM**: the average fluorescence attributed to a particle of a certain diffusion speed such as free dye, dye in micelle, dye in vesicles (only the CPM of vesicles is listed in the table, as free dye was the only other significant species)

The population of a fluorescent species **F2**: is percentage of the CPM in relation to the CR (fluorescence of enclosed Sulforhodamine B in relation to total fluorescence; F1 would be the fluorescence of free dye in relation to the total fluorescence).

The diffusion speed τ_2: the diffusion speed calculated by the machine from the fluctuations in fluorescence at the confocal volume (diffusion speed of vesicles; τ_1 would be the diffusion speed of free dye).

A typical FCS measurement consists of three sample drops measured in a row, each with 30 individual 20s measurements (except for kinetic measurements; see **materials and Methods** for more details) that become averaged to one value as in the table above. The experimental **error** represents the deviation of the averages of each drop. However, the measurements tend to contain ca. 10% outliers, which are removed from the average by manual selection. These are called **aggregates.** They have diffusion speeds that match neither free dye nor vesicles (micelles, worms, but mostly aggregates of multiple vesicles). They are counted in the table as a secondary error.

Furthermore, the hydrodynamic radius **Rh**: is calculated from the diffusion speed and ambient temperature and the encapsulation efficiency **EE**: is derived from the calculated Rh, the CPM and initial concentration of dye (number of dye molecules found in a vesicle divided by the expected number of dye molecules for the given volume). In table 1 red marks high errors and unusual values, whereas green marks expected changes.

Regarding the **CR**s in **Table 1.a** one can see that the negative control contains far more Sulforhodamine B than the other samples. This extends to the encapsulated Sulforhodamine B, as the **CPM** indicate. CPM of the negative control is almost 3x higher than the other samples at pH 7.4. It also does not decrease unlike **P5.5** and **S5.5**. As can be seen from **Table 1.b**, the positive control loses far more Sulforhodamine B than the actual sample. This could either mean that the sample containing modified OmpF is significantly less permeable, or regarding **Table 1.a**, that it stops releasing Sulforhodamine B after acidification as the CPM is at pH 7.4 significantly lower than the negative control but does not sink much further at pH 5.5. The latter indicates that the pores close at low pH, which implies that the stimuli-responsiveness is the opposite of the anticipated one. In that case, experiment should have

been prepared at low pH and then switched to pH 7.4. Experiments using enzyme kinetics support this theory (chapter **enzyme kinetics, 4.2**).

The fact that the **CR** of the positive control increases (marked [*]), may be explained with significant portions of Sulforhodamine B being released and becoming more fluorescent due to a low concentration regime outside the vesicles resulting in less quenching. This does not apply for the actual sample, probably since far less Sulforhodamine B is released at low pH. Thus, most of the Sulforhodamine B released is removed via size exclusion, whereas **P** kept releasing Sulforhodamine B thereafter.

Regarding the changes in **CPM** (**Table 1b**) it should be assumed that the percentage of Sulforhodamine B within the vesicles (F2) decreases proportionally, but this is unfortunately not the case, as individual Sulforhodamine B molecules are outshined by the vesicles by far and disappear in the background noise. The calculated encapsulation efficiency confirms that **P** releases more than **S**, however, in case of **N**, it increases (marked [**]) which is impossible, unless taking the shrinking of the vesicle into account. Especially not-permeabilised vesicles are exposed to the 50% increase of the Osmotic pressure. A 10% decrease in R_h results in 30% decrease in internal volume. Since the number of encapsulated Sulforhodamine B remained the same, the internal concentration and thus calculated encapsulation efficiency increases. For unknown reasons **P** was apparently shrinking to the same degree, but it lost at the same time Sulforhodamine B, thus overcompensating the shrinkage.
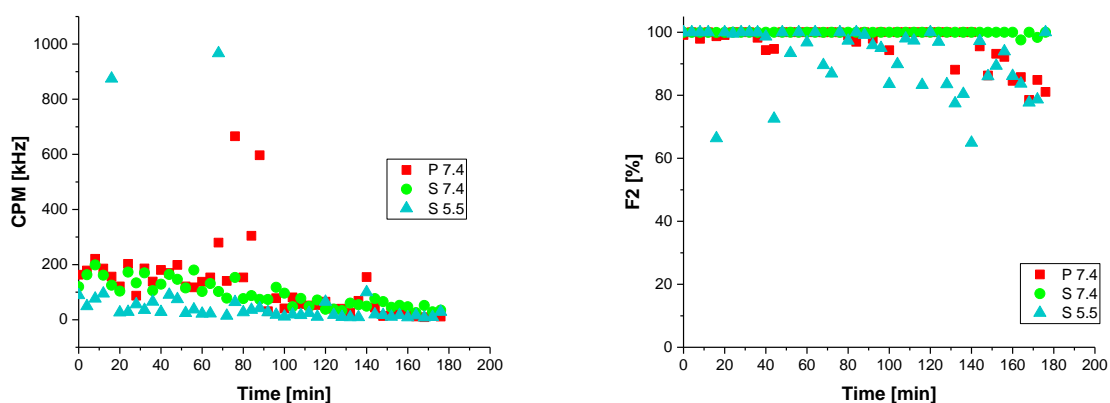
Fig. 2: FCS kinetic on DSPC-mix liposomes[28] **left:** development of the CPM over 3h; **right:** development of the free dye population over 3h.

---

[28] 3mg DSPC, 0.5 eq Cholesterol, 0.5 eq Chol-PEG600 and 0.1 eq POPS were dissolved in 1mL EtOH. The solvent was removed at 40C and 150mBar at 100rpm.The film was rehydrated in 1mL citrate buffer at pH=7.4 containing 1mM SRB.

While it was expected that the stimuli response would manifest itself in a timescale of seconds to minutes, it was absolutely impossible to know for certain without testing it. Thus, not only samples were measured directly (in triplicates taking about 15min), but thereafter a kinetic was measured as well, observing changes of the sample for 3h. During that time, the CPM dropped from ca. 200 kHz to 10kHz. This can be probably better attributed to photobleaching than further dye release, since even in the triplicates a decrease in CR and CPM was observed. Moreover, the sample volume decreased significantly in size due to evaporation due to the heat laser beam.

Regarding the development of the fraction of Sulforhodamine B remaining within the vesicles **F2**, one would be tempted to conclude that **S5.5** loses Sulforhodamine B, similar to **P7.4**, whereas **S7.4** does not. However, as discussed earlier the dye fraction contained in vesicles (**F2**, **Fig. 2**) is a very poor indicator. The short-term development of the CPM actually contradicts the perceived stimuli-responsiveness. However, under these circumstances **N** could reveal a higher Sulforhodamine B-release rate than **P**, since **P** lost most of its Sulforhodamine B content prior size exclusion and lost even more Sulforhodamine B before the measurement finally started. Thus, N has much more Sulforhodamine B to lose at that point which may occur through trans-membrane diffusion, or vesicle disintegration, which are far slower processes than diffusion through OmpF pores.

Initially, it was thought that WT-OmpF would make the vesicle membrane so permeable that Sulforhodamine B would be released before the sample was prepared for FCS. Sulforhodamine B is definitely small enough (559Da) to pass through the OmpF pore. However, due to its non-linear shape (see **Fig. 3**) it could be more difficult for it to pass through than some even heavier, but more linear molecules. In addition, it has four potentially charged groups and is zwitterionic at pH 7. This is a quite common trait of chromophores and in particular water-soluble chromophores. This however, is bound to bias the experiment. For one OmpF is known to be slightly cation-selective[2] and it can bind anionic and zwitterionic antibiotics within the pore, reducing its permeability.[3] This could explain, why OmpF did not release Sulforhodamine B as fast as anticipated and why acidification increased the permeability (giving Sulforhodamine B a positive net charge, or protonating carboxyl groups within the pore that initially interacted with Sulforhodamine B). Lastly, D12,K89C-Gala3 OmpF would constrict the pore and add additional negative charges that are likely to repel Sulforhodamine B.

The kinetic (**Fig. 2**) might seem contradicting the triplicate measurements (**Table 1**) in that it shows that the OmpF conjugate **S** releases far more Sulforhodamine B than the positive control **P**. In fact, it shows that the OmpF conjugate becomes far more permeable at low pH. The positive control lies in between, but was only recorded for pH 7.4, thus it could be that it releases even more at low pH. In this case the conjugate would not be stimuli responsive but only a steric- or ionic hindrance. Thus, the pH dependent diffusion speed of the dye (due to different charge and thus solvation) is responsible for

the observed stimuli response, rather than changes at the OmpF-conjugate). It was not measured for the simple reason that it was impossible to create all three samples at the same time and do six kinetics at once.[29] Measuring the samples consecutively over a day or more creates a potential systematic bias due to the dead time allowing unrecorded leakage. Splitting it in several batches would have had the disadvantage, that the measurements would not be comparable, since the sensitivity of the FCS changed in the course of several days changing the detected CR and CPM, but also the diffusion time (latter due to minor fluctuations of the room temperature).
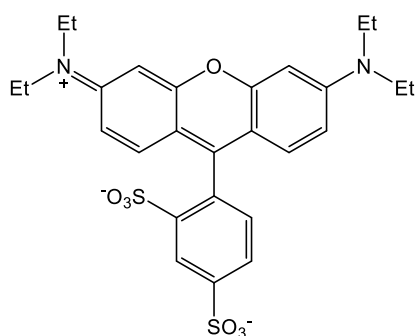
Fig. 3: The structure of Sulforhodamine B at pH 7.

Since the positive control never released more than 70-80% of the Sulforhodamine B even after several days and even less so at pH 7.4, further experiments were conducted: three different types of vesicle samples had 1mM Sulforhodamine B added on the outside. Then after 30min of stirring the external dye was removed through size exclusion again. There are four possible scenarios:

1) If there was **no interaction** between the vesicle and the Sulforhodamine B, then no dye should remain within, or bound to the vesicle.
2) If the membrane is **permeable** to Sulforhodamine B, then some dye should be encapsulated leaking slowly out again.
3) If it enters only through **OmpF**, but **binds** to it, then a low, persistent fluorescence could be anticipated.
4) If the **vesiclemembrane interacts** with Sulforhodamine B however, then it should have a high and persistent fluorescence.

---

[29] It would take over 26h: 18h for the kinetic; 2h for the other FCS experiments and ca. 6h for the SEC/sample preparation

To check these scenarios three samples were prepared:

A: Default DSPC/cholesterol/PEG mix corresponding to the negative control

B: The same type of vesicles as in A but made in the presence of detergent (0.15% OG, corresponding to 50µL 3% OG, as in case of the positive control) to check the influence of the detergent that would be introduced along with OmpF. It was expected to increase the permeability of the membrane.

C: The same as in A, but with OmpF inserted, corresponding to the positive control.

Table 2: Interaction of Sulforhodamine B with empty vesicles (DSPC mix)

	A: no additives	B: 3% OG	C: R270SH
CR [kHz]	213 ±23.4	192 ±28.8	257 ±23.1
CPM [kHz]	728 ±58.2	1050 ±231	929 ±148.6
N_{dye} []	197 ±47.3	284 ±99.4	251 ±57.7
F_2 [%]	97 ±4.9	99 ±3.0	100 ±2.0
τ_2 [µs]	6102 ±244	4508 ±316	5100 ±306
R_h [nm]	86 ±10.3	63 ±5.0	72 ±5.0

A brief look at **Table 2**, tells immediately that scenario **4**) and not **1**) applies. There is still a strong interaction between Sulforhodamine B and the liposomes, despite all the efforts to reduce said interaction. Due to this strong interaction, it can be also assumed that the membrane is permeable (scenario **2**). Theoretically Sulforhodamine B could bind to the surface of the vesicles, but this seems to be unlikely firstly due to the fact that Sulforhodamine B is rather hydrophobic and secondly due to the negative charges from the POPS and the PEGylation. Even if the Sulforhodamine B is capable of permeating though the membrane, it would rather stay in it than going back into the aqueous phase. If it did accumulate in the internal cavity, then it could be assumed that sample **C** should have a lower CPM since it would leak out again due to the pores, which is however not the case. Due to this dye interaction, it cannot be said, whether OmpF binds Sulforhodamine B too (scenario **3**). However, it is more than likely that the detergent softens up the membrane so that more Sulforhodamine B can interact with it, regarding the significantly higher number of dye molecules bound to **B** and **C**. Without repeating the experiment, it cannot be said, whether the difference in the CPM between **B** and **C** is significant. It could be that both also encapsulated some dye. In this case **C** released it again having the OmpF pores whereas B probably became less permeable after removing the external Sulforhodamine B through size exclusion due to partial removal of OG. This could explain why B binds more Sulforhodamine B than **C**, but it is highly speculative. Less speculative is the finding that the diameter of the vesicles decreases with the concentration of OG within the system. This observation was made over and over again with both liposomes and later polymersomes. Originally it was intended that **B**

and **C** have the same amount of OG, but the OmpF solution was more concentrated resulting in 22% less solution being used. Thus, **B** had a slightly higher OG concentration. This shift in diameter is probably a direct, indicator for the loss of stability in the membrane.

While it was possible to create vesicles featuring OmpF that encapsulate Sulforhodamine B and are reasonably stable over time, the Sulforhodamine B still bound to the membrane and OG affected the vesicles size and the properties of the membrane. The experiments strongly indicate that the permeability of vesicles featuring OmpF is pH dependent and that the OmpF conjugate behaves differently. However, it did not prove any stimuli responsiveness of the OmpF conjugate.

1.2 Testing other experimental set-ups for FCS-experiments

Since the experimental set-up should work in polymersomes, which promise a higher long-term stability, it was tested to encapsulate 100µM Sulforhodamine B into polymersomes and it was found that $A_4B_{22}A_4$ and $A_{16}B_{72}A_{16}$ behaved completely different. In the presence of Sulforhodamine B, the shorter ABCP produced mainly micelles and small vesicles (R_h 25-50nm instead of 100nm) and encapsulation efficiency was calculated to 2600% (indicating absorption of dye from solution into the vesicle membrane/into the core of micelles) whereas the longer ABCP did not change its structure due to the presence of Sulforhodamine B and encapsulated only 2-3 dye molecules per vesicle (1% ee). In the latter case, the initial concentration of Sulforhodamine B could be varied from 10nM to 1mM without improving the encapsulation efficiency.

Since many FCS experiments had the problem that the encapsulation efficiency was low and the background fluorescence of free dye relatively high, so that it could overload the detector. Using dialysis instead of size exclusion would take too long. Also, measuring the dye increase on the other side of the dialysis membrane was not feasible, due to the low concentration and diffusion across the dialysis membrane. A more practical approach would be to cause the vesicles to sediment and wash of the free dye. It was thus tested to make liposomes to precipitate by encapsulating 150mM sucrose but unlike giant vesicles no sedimentation could be observed, although the diffusion time increased by 50% (ca. 6000µs). It can be assumed that it works only with giant vesicles, due to emulsion effect.

1.3 Other dyes

Due to the low encapsulation efficiency, apparent interaction with the membrane and due to the rather high photobleaching, other dies were tried. The fluorophore needs to be water-soluble, preferably as hydrophilic as possible in order to avoid membrane interactions. It needs to be pH stable, photostable and excitation must be around 405, 488, 545, or 633nm due to the lasers built into the FCS. Lastly, the dye has to fit through the OmpF pore and should be hence smaller than 550 Da. However, the molecular size is rather large in order to fit in the chromophore (unless it works as a complex, radical, or ion). The requirement for pH-stability also increases the shift towards more hydrophobic structures. Both Carboxyfluorescein and Oregon Green could be used, but are pH sensitive (**Figure 4**):
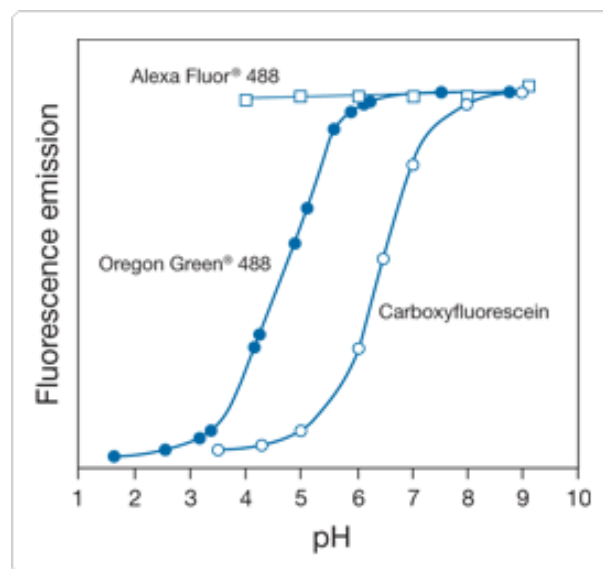
Fig. 4: pH-dependency of the fluorescence according to the supplier[4]

IV Release experiments
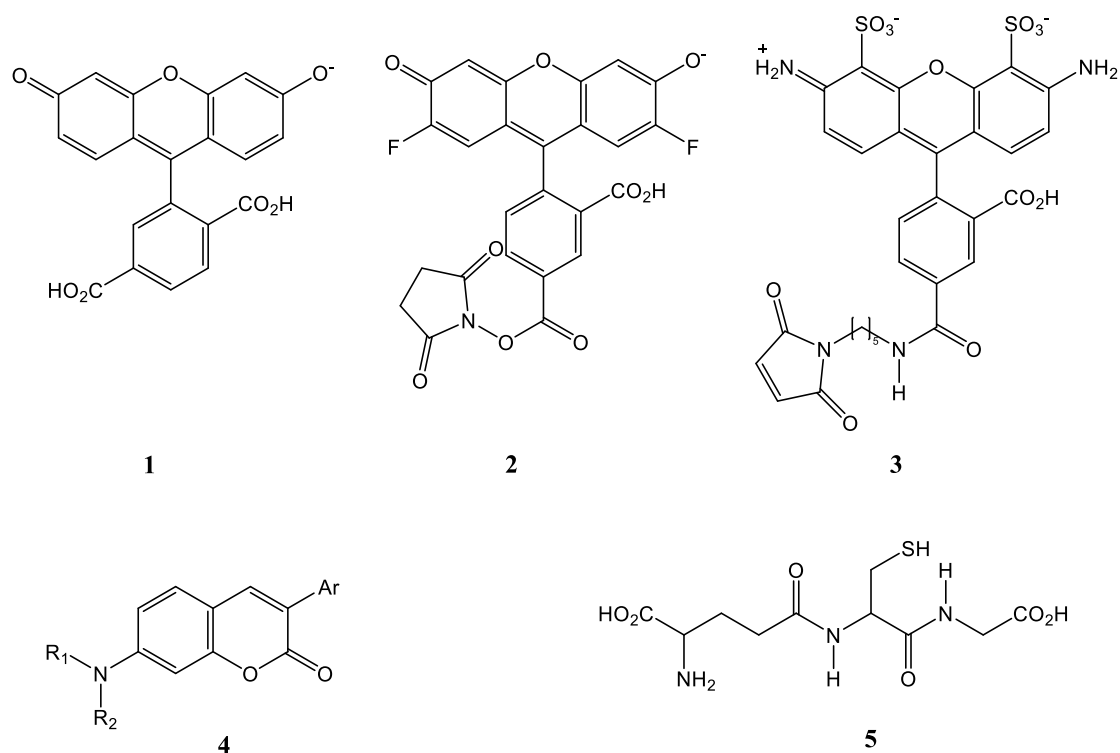
Fig. 5: 1: Carboxyfluorescein (M=376,32 Da; excitation: 492nm); **2**: Oregon green 488 (M=509.38 Da; excitation: 488nm); **3**: Alexa 488 MI (M=720.66 Da; excitation 493nm; assumed structure); **4** Dylight 488 MI (M= ca. 800 Da; excitation: 493nm; structure secret, but presumably as shown with an anchor group at R_2); **5** Glutathion (used to deactivate reactive fluorescent probes and make them more water soluble)

Dylight488 and **Alexa488** are the most popular used fluorophores (**Fig. 5**), as they are known as very photo- and pH stable and for their brightness. In a fluorimeter 2µM of Dylight488 achieved the same fluorescence intensity as 20µM Sulforhodamine B. Alexa488 was 4x as bright as Sulforhodamine B.

It was tried to encapsulate 50- and 300nM of Dylight488 in POPC-liposomes. In both cases micelles appeared to be dominant (only 7-11% vesicles) although the samples had the Tyndall effect and the micelle fraction should have been removed through size exclusion. Since the diffusion times and the vesicle fraction decreased over the course of the FCS measurements, it indicates that vesicles become micelles over time. This explains why size exclusion could not remove the vesicles. While liposomes apparently decomposed at room temperature over the course of 1h, $A_{16}B_{72}A_{16}$ polymersomes were apparently stable, but even they changed during FCS measurements. This indicates that laser-beam heated the samples above room temperature thereby putting additional stress on the vesicle membranes. This is noteworthy, since this kind of polymersomes are temperature stable in absence of this dye.

Assuming that this effect was due to the higher hydrophobicity of Dylight488 and Alexa488 in comparison to Sulforhodamine B, it was tried to make the fluorophore more hydrophobic by attaching

glutathione to the MI-functionalised variant of the dye (**Fig. 5**). The conjugation did not change the properties of Dylight, except the diffusion time, which increased from 33 to 49µs. Interestingly, liposomes filled with the Dylight488-glutathion conjugate did not perform any better; their population was actually even lower (1-2%) and the vesicles smaller (a diffusion time of 1000 instead of 3000µs). It could thus well be that the fluorophore could now act similar to a detergent.

Alexa488 was very similar to Dylight488 in every aspect. Attempting to encapsulate 50nM Alexa488 resulted in only 4-10% vesicles. Rather than observing the shifting diffusion time, a great variety of diffusion times was observed ranging from 700 to 3000µs indicating a very heterogeneous sample from the get go.

Lastly, **Oregon Green488** (**Fig. 5**) was tested for encapsulation within DSPC-mix liposomes and $A_{16}B_{72}A_{16}$. It was a very bright and stable dye like the other two and had less effect on the vesicle stability, but the encapsulation efficiency was very poor (1.4%; ca. 1 molecule per vesicle; even less in case of the ABCPs) and it still changed the vesicle size (50nm instead of 100nm).

Table 3: FCS measurement of DSPC-liposomes[30]

	A	**B**	**C**
CR [kHz]	9.4 ±0.66	5.5 ±2.15	57.8 ±7.61
CPM [kHz]	242.6 ±38.3	260.07 ±112	12.64 ±0.89
F_2 [%]	100 ±0.0	100 ±0.0	9.7 ±8.56
τ_2 [µs]	4034.3 ±845	3136.9 ±2358	3104.7 ±1810
Aggregates []	7.7 ±0.47	14 ±0.82	0 ±0.0
R_h [nm]	51.6 ±10.8	40.1 ±30.2	47.3 ±27.6
Encap. eff. [%]	33.5 ±46.9	82.1 ±816	1.4 ±3.4
Dilution [x]	100	0	100

Sample A and B had 1mM Sulforhodamine B encapsulated. Sample B had Chol-PEG only added once the vesicle formation resulted in visible opaqueness, in the hope of inserting the Cholesterol with the PEG chains only facing outside. C had 1mM Oregon Green488 encapsulated.

The experiment in **Table 3** showed that adding Chol-PEG only after vesicle formation (**B**) resulted in different vesicles, which were far less stable towards Sulforhodamine B. The CPM decreased during the measurement of the triplicate from 412 to 146 kHz and the diffusion time decreased from 6446 to 1127µs (not shown in table) indicating a shift from large vesicles to micelles. Moreover, the vesicle

---

[30] Free dye: 100nM SRB CPM=39 kHz, CR=2.66 kHz, triplet fraction=1.5%, diffusion time=46.3 µs. 10nM OG488 CPM=53.0 kHz, CR=10.78 kHz, triplet fraction=22.2 %, diffusion time=38.9 µs. Both cases: 25% laser output.

concentration had dropped after vesicle-formation and before the purification to such a degree that no sample dilution was required, whereas the other samples would cause a signal overload otherwise. The perceived high encapsulation efficiency is thus rather insertion of the dye into the vesicle membrane. Contrary to it, adding Chol-PEG directly (**A**), resulted in smaller, but far more stable vesicles, with no definite shift during the measurement. The same experiment, but with Oregon Green (**C**) resulted also in stable vesicles, but with a very broad size distribution and very low encapsulation efficiency. Concluding it can be said that only variant **A** was suited for release experiments, although not being ideal either. It demonstrates the impact of dyes on vesicles and Chol-PEG on the stability of vesicles and the repulsion of dyes.

Concluding, it can be said that the encapsulation efficiency decreased from Sulforhodamine B over Alexa488 to Dylight488. Moreover, Alexa488 and even more so Dylight488 weakened the membrane of the liposomes, causing the vesicles to fall apart within 1h at low pH. The attachment of the hydrophilic glutathione did not improve the situation.[31] Oregon Green 488 did not cause such problems, but the encapsulation efficiency was 20-50x lower than Sulforhodamine B at the same initial concentration. Another important aspect is that the size of the fluorophore increases in general from blue fluorescent to red-fluorescent dyes. Thus, only few are expected to be small enough to fit through the OmpF pore. Thus, FCS was considered to be not a valid option.

2 Carboxyfluorescein release experiments

Since, the FCS experiments turned out to be less promising, other methods were envisioned. Working with self-quenched dyes would be the most similar approach and it would be moreover very simple in its execution. While such measurements could suffer of the same problem of dye interacting with the vesicle membrane (especially regarding the high concentrations involved), several variations have been used successfully for similar applications involving liposomes. Ihle *et al* [5] used acridine orange to investigate pH dependent diffusion through OmpF mutants featuring six histidines within the constriction-site of the pore and Lin *et al* [6] used carboxyfluorescein to investigate the pH dependent

---

[31] Fluorescent dyes with maleic imide groups were mixed as stock solutions with 1.5 eq. of glutathion and OG488 which was only available as activated ester was treated with 1.5. eq. of ethanolamine. In either case the solution was shook for 1h and then aliquoted.

diffusion of a membrane based on the Gala-peptide linked to fatty acids. Both dyes could be used in stopped-flow experiments, which would allow a more precise measurement of the diffusion speed, since the dead-time between mixing and measurement is fully under control.

Acridine orange fluorescence is pH-dependent, but also dependent on the interaction with DNA or metal ions. Moreover, it could be that the positive charge of the dye results in it binding to the modified OmpF, thereby blocking it. Carboxyfluorescein (376,32 Da), is also pH dependent, but negatively charged and does not have DNA and ions as additional factors to consider. Furthermore, it can be used in FCS regarding its excitation and emission ranges.

The concentration inside the vesicles was chosen to be so high, that the fluorescence is inhibited through self-quenching. When dye leaves the vesicle, it enters an environment of low concentration, thus enabling fluorescence. In the case, that concentration inside and outside the vesicle equilibrate, the concentration would be still below the self-quenching level.

In order to obtain decent graphs displaying the fluorescence over time, the initial fluorescence I_0 stemming from leakage before the official start of the measurement has to be subtracted. To compare different samples, the fluorescence has to be put into relation with the maximal fluorescence I_{max} obtainable by the sample (**eq. 1**). This is measured by destroying all vesicles through addition of 10% TrtX. TrtX did not influence the fluorescence (which would be the case with e.g. acrylodan, or proteins).

$$R = \frac{I - I_0}{I_{max} - I_0} \, [\%] \qquad \qquad \textbf{eq. 1}$$

However, there is one more factor that should be taken into account, which most papers apparently did not deal with: the pH-dependence of the sample. According to the supplier,[7] the turning point of the fluorescence lies midway between pH 7.4 and 5.5 (the two pH observed in the following experiments, but also in the two publications mentioned above). This means that while it was anticipated that at pH 5.5 the dye would be released manifesting in increased fluorescence, the pH will result in a sharp drop of the fluorescence, cancelling out the other effect.

For the desired pH change from 7.4 to 5.5 the fluorescence drops to 25% (**Table 4**), which is in agreement with published data.[7] However, in several publications[6] it seems that no correction factor has been used. This was actually the reason for even considering carboxyfluorescein, but it turned out that the pH-dependence cannot be ignored.

Table 4: pH dependency of Carboxyfluorescein in citrate buffer measured via FCS:[32]

pH	7.4	6.4	5.5	3.2
CR [kHz]	83.3	53	21.1	3.5
CPM [kHz]	2.57	1.47	0.62	0.08
TF:	9.8	10.3	9.3	84.5
τ_1 [µs]	33.7	33.2	29.9	42

FCS measurements confirmed the results from the fluorimeter. The count-rate drops dramatically with the pH (4x in the desired range and 20x from 7.4 to 3.2). At the same time, the counts per molecule decrease at the same rate. Furthermore, the experiments indicate that the photobleaching is acceptable for kinetics observe via Fluorimeter, but not for FCS.

Another important, but related error source is the precision of the pH-adjustment. Using PBS as in the other publications allows even tiny changes in the acids volume create major changes in the final pH which in turn cause dramatic changes in the fluorescence. To counteract this error source citrate buffer was used instead of PBS, which does not have a sharp turning point in its titration curve as PBS has.
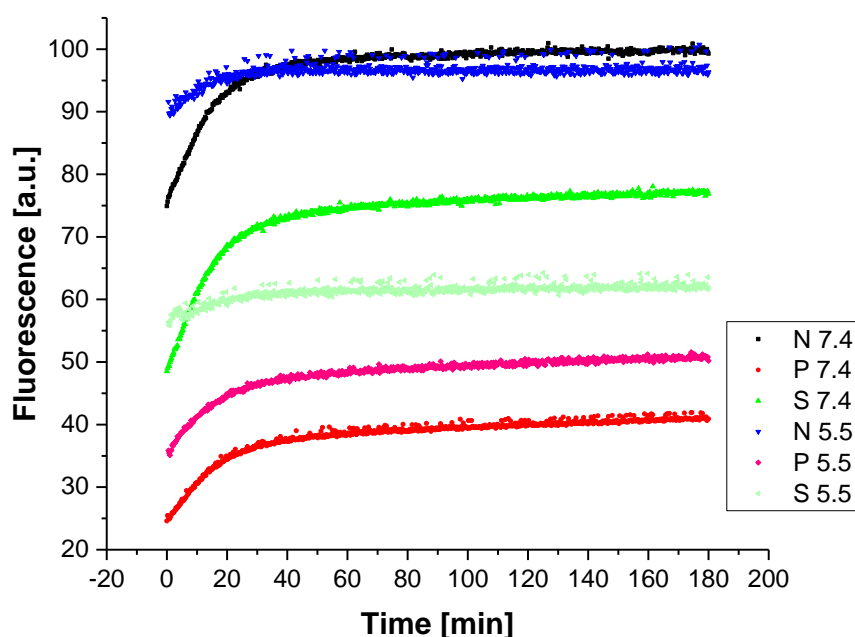
Fig. 5: release kinetic of carboxyfluorescein filled liposomes, sample featuring R270C-Gala3 OmpF.

---

[32] Note: the pH was adjusted from 1mL solutions by adding 0, 2.5, 5, 10µL conc. HCl respectively.

As seen in **Figure 5**, the negative control had the highest fluorescence, followed by the conjugate and by the positive control. With the exception of the positive control the fluorescence of the sample at pH 7.4 was higher. This might indicate that the correction factor of 4.0 was not high enough.

Applying the **equation 1** did not reveal any trend, moreover using the same I_{max} did not work, thus I used both the I_{max} for pH 7.4 and 5.5 (the prior was calculated by multiplying the I_{max}(pH 5.5) with 4, as the measurement resulted in a signal over-load. If the equation is only used for the endpoints[33], then the dye release was clearly pH dependent, but not as expected (**Table 5**):

Table 5: dye release calculated from the endpoints (average of two measurements)

	No OmpF (N)	wt-OmpF (P)	R270C-Gala3 (S)
pH 7.4	24.0% ±0.0	10.5% ±0.5	22.5% ±0.5
pH 5.5	9.5% ±0.5	12.0% ±1.0	5.5% ±0.5

It indicates that the positive control released independently of the pH, whereas the negative control leaked half as much at low pH and the conjugate even only ¼ as much. The fact that the negative control leaked more, could be explained through a combination of the dye weakening the membrane and osmotic pressure, but it appears to be most likely due to fact that the negative control still contained most of the encapsulated dye, whereas the other samples with OmpF lost a significant part during purification. This resulted in **N** releasing far more than **S** and **P** during the measurements.

Instead of looking at the endpoint one can visualize it by rescaling every graph so that the release reaches 100%. This proofs that using the endpoint is dangerous (**Figure 6**):
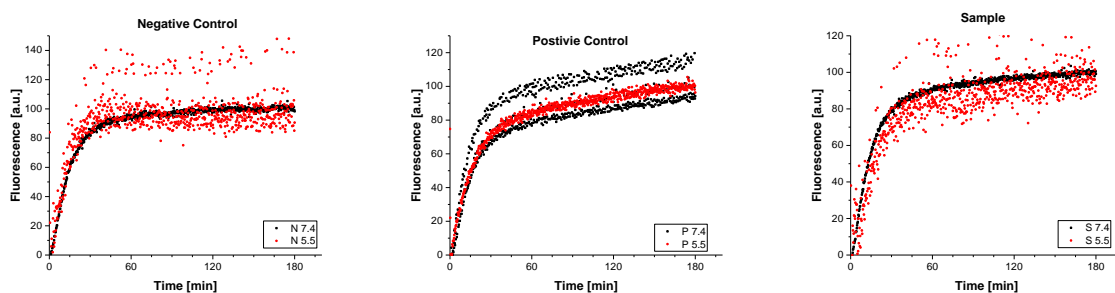
Fig. 6: rescaled graphs from **Fig. 5**, with all endpoints reaching 100 a.u.

The low release of the positive control can be partially explained with the high statistic error of the positive control (which looked, for unknown reasons, as if the device switched for every second

---

[33] The I_0 was calculated from the average of the 4th to 9th data point; I_{max} at pH 5.5 was 1282 a.u. and the I_{max} at pH 7.4 was estimated to be 5131 a.u.

measurement point to the same sample but at a different pH). The reduced leakage in case of the negative control could be due to averaging effects.

From **Fig. 5**. it was evident that the measurement had too much of a dead time and even the negative control leaked much too fast for this experiment. Hence, the experiment was repeated, reducing the dead-time between end of film rehydration and measurement as far as possible, making the purification ca. 3x faster:[34]
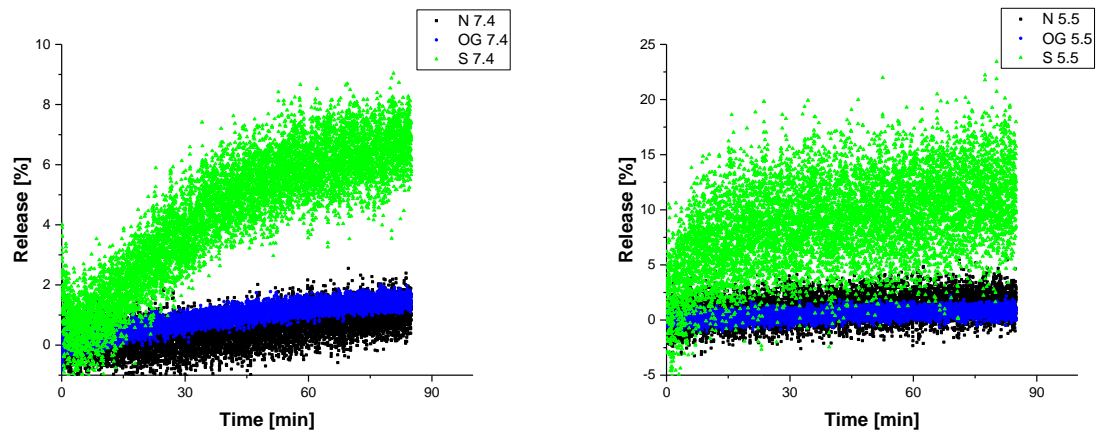
Fig. 9: repetition of the experiment applying the changes discussed above.

Unfortunately, the positive control was lost during purification. This measurement has much more of the initial slope preserved and shows clearly that the sample releases **S7.4** more than the negative control **N7.4** at pH 7.4 and that at pH 5.5 the difference is far smaller (although the starting point of **S5.5** appears to be missing). At low pH, all samples become more permeable towards carboxyfluorescein. This has not been observed anywhere else and seems to be liposome specific. The liposomes themselves are able to withstand the lower pH. Moreover, the presence of 0.15% OG did not make any significant difference towards the permeability of the negative control.

---

[34] The size exclusion column replaced with a minicolumn, which was moreover not relying on gravity, but on a constant pressure from a syringe. Instead of measuring all samples at once using a well plate, each sample was prepared and measured individually using a cuvette. Moreover, the SEC was set up next to the fluorimeter instead of its usual place in the neighbouring lab in order to save time.

It is also worth noting that all samples approach different saturation levels that are apparently independent of the encapsulated dye concentration (similar to later HRP-experiments, in the following chapter). Moreover, the measurement statistical error increased at low pH significantly. Photobleaching was no problem. However, at low pH full release would result in a signal overload.

3 Conclusion

In principle release experiments are the easiest experimental set-up, however, they proved borderline impossible to be used due to several experimental problems:

- Most FCS stable dyes are too big to diffuse through OmpF
- Fluorophores contained in vesicles outshine released fluorophores in FCS experiments
- Most fluorophores had low encapsulation efficiencies, probably due to charge repulsion. Furthermore, increasing the fluorophore-concentration did not help, in most cases, it worsened the problem due to dye interactions with the membrane.
- Most dyes and fluorophores are mostly hydrophobic, with the exception of one or two charged groups. They are thus able to interact with the hydrophobic segments of vesicles. Many dyes appear to prefer to go into the membrane rather than staying dissolved in water, even, if they are far from their theoretical solubility limit. These dye-membrane-interactions reduce also the encapsulation efficiency.
- Dyes were found to act similar to detergents, hindering vesicle formation and destabilising vesicles by inserting themselves into the membrane. Moreover, the latter effect is also delayed, meaning that it can still occur after extrusion and size exclusion. Thus, a sample can consist primarily of micelles according to FCS although the micelle fraction had been removed prior the measurement. Unlike detergents, larger hydrophobic dyes turned out to be worse and polymersomes appear to be more robust towards their presence. This extends to DSPC-mix liposomes being more resilient and long ABCPs being more resilient than shorter ones. Hence, it's the very opposite of how vesicles behave to detergents.
- Experiments with dye added to preformed vesicles, clearly show that even then, after the membrane formation, the dye is able to insert into the membrane and partially diffuse to the other side (but most staying within the membrane).

- The dyes ability to go into the membrane also enables them to diffuse through the membrane. Moreover, weakened membranes have to be assumed to be significantly more permeable and vesicles may also rupture releasing dye directly.

All these problems make it hard to compare samples and the lack of stability decreases the dependability of release experiments. Thus, the experiments have a high statistical error. In addition, due to practical reasons, samples and controls have to be prepared in parallel and measured consecutively. This results in the first measurement being the most accurate and the last having the largest systematic error due to leakage and vesicle-changes during the dead-time until their measurement.

Moreover, FCS measurements were plagued by an instable Argon laser, which needed 30-60min to warm up and run reliably. This could change the CPM of free dye from 2 to 10 and decrease the diffusion speed from 60 to 34 µs. Moreover, these values changed with the room temperature and apparently some other factors so that measurements under the same conditions were not comparable, if they were separated by a month in time or more.

In case of FCS measurements only Sulforhodamine B and Oregon Green488 worked, but the latter suffering of a very low encapsulation efficiency. It appears that **P** releases more than **S** at 5.5, but the experiment would need to be repeated with film rehydration taking place at pH 5.5 in order to prove, that **S** releases more at pH 7.4 than at 5.5. Kinetic measurements made no sense, due to the fast release, unless it is to see the leakage through unmodified membranes or the overall stability of the vesicles. Due to the slow preparation **N** appeared to release most, since the other samples had not much left to release once the measurement started.

Release experiments with carboxyfluorescein were similar. The experiments were extremely time sensitive. Only in very fast preparation it was possible to actually compare the release of N and P/S due to the starting point being easily missed. The experiment was easier comparatively speaking, but still very sensitive and the dye suffered of pH-dependency, diffusion through unmodified membranes and its poor solubility, which required it being encapsulated as a salt, thus reducing the internal pH of the vesicles. Especially **Fig. 6** proves the risk of choosing the wrong value for normalisation. Still, experiments indicate again that **S** blocks at low pH whereas P keeps releasing irrespective of the pH.

4 References

[1]   J. Coppeta and C. Rogers, *Exp. Fluids* 1998, 25, 1-15.

[2]   R. Koebnik, K. P. Locher and P. Van Gelder, *Mol Microbiol* 2000, 37, 239-253.

[3]   Brigitte K. Ziervogel and B. Roux, *Structure* 2013, 21, 76-87.

[4]   *pH dependence of fluorescence of CF, OG488 and AL488*,
        http://www.invitrogen.com/site/us/en/home/References/Molecular-Probes-The-
        Handbook/Fluorophores-and-Their-Amine-Reactive-Derivatives/Fluorescein-Oregon-Green-
        and-Rhodamine-Green-Dyes.html, accessed: 2016.

[5]   S. Ihle, O. Onaca, P. Rigler, B. Hauer, F. Rodriguez-Ropero, M. Fioroni and U. Schwaneberg,
        Soft Matter 2011, 7, 532-539.

[6]   B. F. Lin, D. Missirlis, D. V. Krogstad and M. Tirrell, *Biochemistry-Us* 2012, 51, 4658-4668.

[7]   *pH dependence of the fluorescence of AUR*,
        http://www.invitrogen.com/site/us/en/home/References/Molecular-Probes-The-
        Handbook/Fluorophores-and-Their-Amine-Reactive-Derivatives/Fluorescein-Oregon-Green-
        and-Rhodamine-Green-Dyes.html, accessed: 2015.

V Development of an Enzymatic Assay

As mentioned in the introduction, encapsulating enzymes and measuring enzyme kinetics would offer several advantages over plain release experiments. Theoretically one enzyme per vesicle would suffice; it could be stored and even reused. This makes varying the other experimental parameters significantly easier. However, enzymes introduce numerous new parameters that need to be controlled.

The increase of fluorescence intensity nanoreactors (**NRs**, see **Fig. 1**) represents a direct measure for the transmembrane diffusion of the enzyme substrate. Its detection is as simple as measurement of release experiments using self-quenched fluorophores. It is moreover, not the reverse of a release experiment, since the produced dye is able to leave the vesicles as long as the reaction product remains soluble.

The **ideal enzyme** should be very stable, active and water-soluble. It should be small and ideally not interact with itself, or with the vesicle-membrane. Charge repulsion would reduce the encapsulation efficiency, whereas aggregation of enzyme could disturb the enzyme kinetic and introduce a dependence on the local concentration that would be very hard to predict. Similarly, the enzymes stability and activity should be stable over a broad pH-range and not be influenced by the presence of detergents, lipids, etc.

All these factors are only half of the requirements to meet. The other half depends on the enzyme substrate. Both enzyme and substrate need to be affordable/available and the substrate comes with its own set of requirements: The enzyme substrate, its co-substrate or product need to be quantifiable spectroscopically and stable. Again, the absorption or fluorescence are to be expected to be pH dependent and possibly depending on polarity of the environment etc. All these factors should have minimal impact on the experiment. The **ideal enzyme substrate** should be small, water soluble and stable. While undesirable, it was to be expected that no substrate was water-soluble and free of a net-charge at the same time. Charged substrates, have to be expected to be pH dependent in their solubility and may be repelled by charges at the OmpF-pore, or even bind to the OmpF-conjugate and thereby block the pore. This also implies that even, if the experimental set-up appears to work, it might not be due to pH dependent conformation changes of the group attached to the OmpF pore, but due to substrate specific charge interactions (binding to the pore, being repulsed from the pore or peptide, or becoming more hydrophobic and thus going through the membrane directly), that cannot readily be extrapolated to other substrates.

As with the release experiments described in the previous chapter, control experiments are necessary. For every fully functional NR with encapsulated enzyme and inserted OmpF-conjugate (**NRC**), a sample without OmpF (**NR-**) is required for establishing the baseline (background activity through damaged vesicles, free enzyme, or membrane permeability) and a sample with unmodified OmpF (**NR+**) is required to reveal the maximal possible response of the system. In several cases the influence of

detergent on the stability and permeability of the vesicle membranes was investigated as well. These samples are referred to as **NRD**
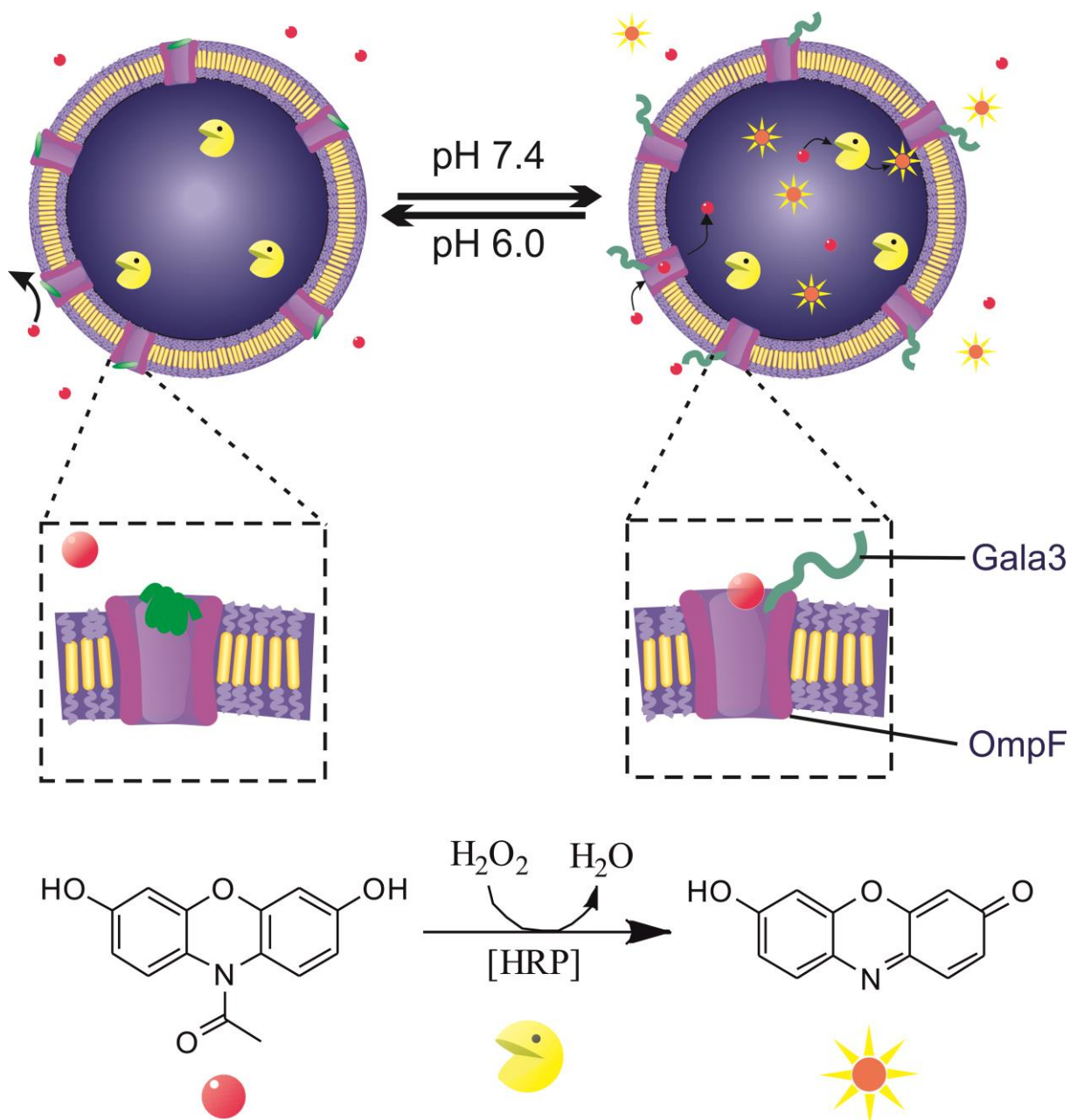
Fig. 1.: Schematic representation of a bio-valve functioning by reversible pore opening and closing inside the membrane of nanocompartments to trigger an *in situ* reaction (left: closed state; right open state). Modified OmpF pore (violet; stimuli responsive group green) is inserted in the polymersome membrane that separates the encapsulated enzyme (HRP) from the environment. The *in situ* reaction is triggered by the bio-valve functionality, which allows the diffusion through the OmpF pores of the substrate Amplex Ultra Red (magenta spheres) and the subsequent release of the fluorescent products (yellow stars).

1 Horseradish peroxidase

Horseradish peroxidase (HRP) is an affordable, comparatively stable enzyme, that is well established in enzymatic assays and functions over a rather broad pH range. It has thus an ample variety of substrates available. It is relatively small with 44kDa and well water soluble as a glycoprotein.[1] A further advantage is that it is not very specific and oxidises a great variety of substrates. It uses hydrogen peroxide as co-substrate. The heme-cofactor gives the enzyme a reddish-brown hue, allowing better measurement of enzyme concentration via absorbance (at 403nm[2]). It is stable from pH 5.0 to pH 9.0, but also known to be more active at pH 6.0 than pH 7.4.[3] Depending on the batch, HRP was 2-3x more active at pH 5.5 than 7.4.

1.1 Potential substrates

1.1.1 Amplex
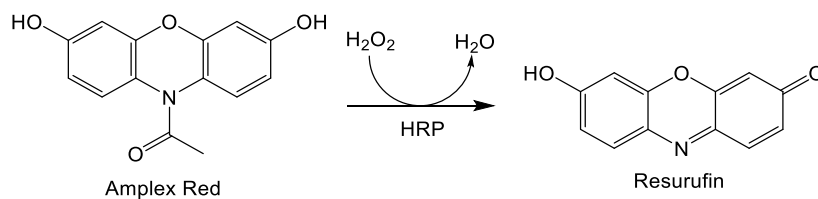
Fig. 2: conversion of amplex into the fluorophore resurufin. Please note that Amplex Ultra Red is an undisclosed derivative of Amplex Red.

Amplex Ultra Red (**Fig. 2**) is one of the smallest available enzyme substrates (ca. 300 Da; 272 Da in its fluorescent form). HRP converts Ultra Amplex Red to a fluorophore (resorufin excitation 570nm, emission 585nm).[4] It is stable between pH 5-10[5] and the activity change is tolerable between pH 7.4 and 5.5. However, when these claims were put to test, a different picture presented itself:
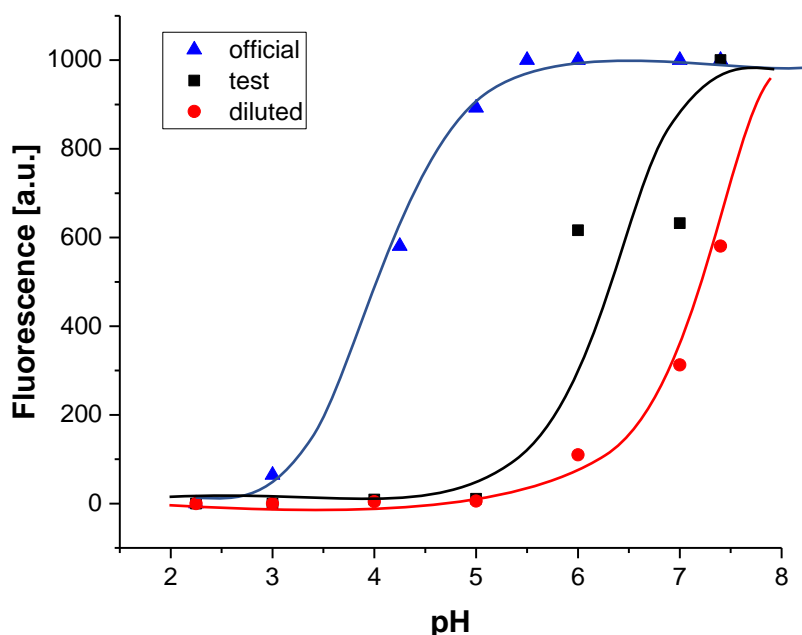
Fig. 3: Dependency of the fluorescence on pH and concentration.

In order to determine the pH dependence of Amplex Ultra Red, 5mg/L HRP, 300µM H_2O_2 and 200nM Amplex Ultra Red were allowed to react. Then the pH was adjusted with a minimal amount of HCl and the fluorescence spectrum was measured at 570nm excitation. Since a part of the samples produced a signal overload, the samples were all diluted 5x and measured again. While according to the producer (**Fig. 3**) the turning point of the pH-dependent fluorescence was supposed to be around pH 4, it appeared to be around pH 6.5. Diluting the sample 5x shifted it further to pH 7.5. Since dilution should shift the pH towards basic conditions (ca. 0.5 pH-units) a higher fluorescence was to be expected. The fact that the opposite occurred indicated that the fluorescence of the undiluted sample was so high that the detector was incapable of quantifying it, thus it appeared only as a plateau, whereas in reality even beyond pH 7 the fluorescence was increasing. Thus, in the worst case, in a pH change from 7 to 6, 80% of the fluorescence would be lost. Regarding the more diluted sample it appears that only 40% would be lost, but the fluorescence would be already well below its maximum. The exact experimental conditions from the producer were not given, but it can be assumed that they used far greater Amplex Ultra Red concentrations than those that are relevant for enzyme kinetics, as required for this thesis.

The system HRP/Amplex produced numerous, unexpected problems, which will be discussed later (**chapters 1.2.1, 1.2.2** and **3**). Yet, after addressing all these issues, it provided one of the best systems available for testing the stimuli-responsiveness of the OmpF-conjugates. Investigation of the stimuli-responsiveness will be addressed at the end of the enzymatic assays.

1.1.2 ABTS
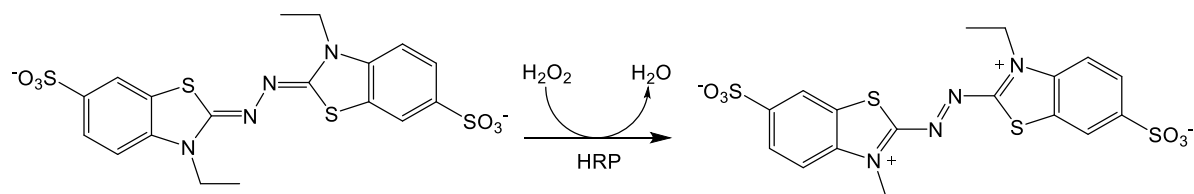
Fig. 4: ABTS oxidation to its diazo-benzothiazole form

Due to the pH dependent fluorescence of Amplex Ultra Red, ABTS (2,2'-azino-bis(3-ethylbenzothiazoline-6-sulphonic acid), **Fig. 4**) was tested as an alternative. The substrate is converted in a dye but not a fluorophore, hence the system is much less sensitive. While pH dependence, bleaching etc. are not a problem here, the substrate has to be added close to its solubility boundary (500µL 10mM ABTS compared to 40µL 5µM Amplex Ultra Red per 1mL cuvette). The reaction is much slower (1h observation time vs 5min) and despite the slow reaction saturation is reached much faster. In other words, to detect significant reaction, a large portion of the substrate has to be converted (**Fig. 5**). Since the substrate is twice as big (514.62 g/mol), it can be expected to pass through OmpF much slower and it might be even more hindered in going through OmpF pores with attached peptides.
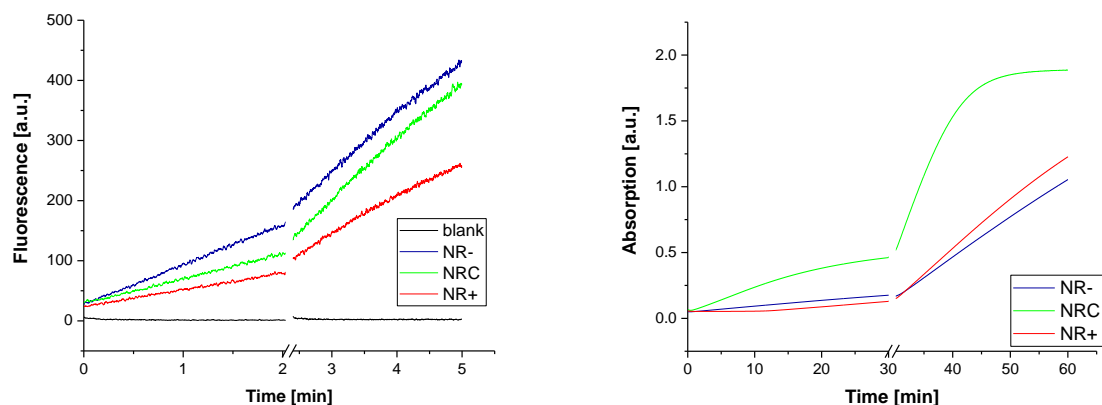

Fig. 5: NRs containing HRP within DSPC-liposomes; left detection with Amplex ultra red; right with ABTS. Blank: buffer without HRP, or NRs; NR- vesicles without OmpF; NRC: D12K89C-Gala3 OmpF; NR+: D12K89C-SH OmpF.

This failed experiment (reasons why NR- had more activity than NR+ will be discussed in **chapter 3**) shows clearly the difference in reactivity and the problem of saturation. Originally, it was anticipated, that only **NR+** would be the only sample reaching saturation, whereas **NRC** and **NR-** would show little conversion, until the samples are acidified, then **NRC** was expected to reach saturation too. However, in course of further experiments, it turned out that even samples produced under ideal conditions and using Amplex Ultra Red, there will be significant background activity (even for NR-). The individual samples activity is best measured in the initial slope and not in the signal-intensity a sample reaches in the end. Hence, the time until the saturation is reached is less relevant, unless multiple pH-changes are to be investigated.

1.1.3 TMB

Even after all apparent problems of the Amplex HRP polymersomes were fixed, NR- had still a visible activity, which could not be further reduced by any means. One plausible explanation hereto would be that the substrate Amplex Ultra red was hydrophobic enough to permeate the membrane causing the background activity. Similarly, the stimuli-responsiveness observed with Amplex and K89CR270C-Gala3 could be attributed to charge repulsion instead of steric hindrance. Thus, a substrate with opposite charge (and different pH-dependence) could provide further insights.

The only potential substrate available meeting the requirements was TMB (3,3',5,5'-tetramethylbenzidine, **Fig. 6**). It works like ABTS but is considerably smaller (240.3Da). Moreover, it was found that it is far more sensitive, reacts faster than ABTS and reaches saturation slower. Hence smaller amounts are required. The product absorbs depending on the protonation state either at 650nm or 450nm (protonated).[6] Compared to Amplex, it requires still significantly more substrate (250µL undiluted TMB solution per 1mL compared to 40µL 5µM) and reaches saturation faster. It is moreover light sensitive, as it turns blue upon exposure to light.

Charge transfer complex
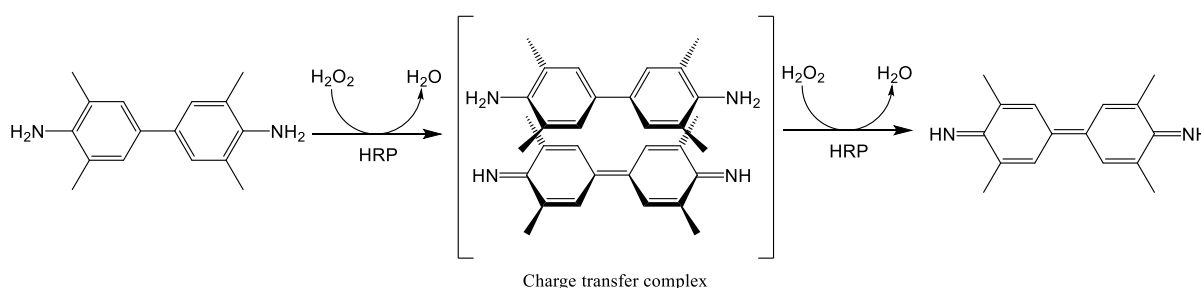
Fig. 6: Oxidation of TMB.
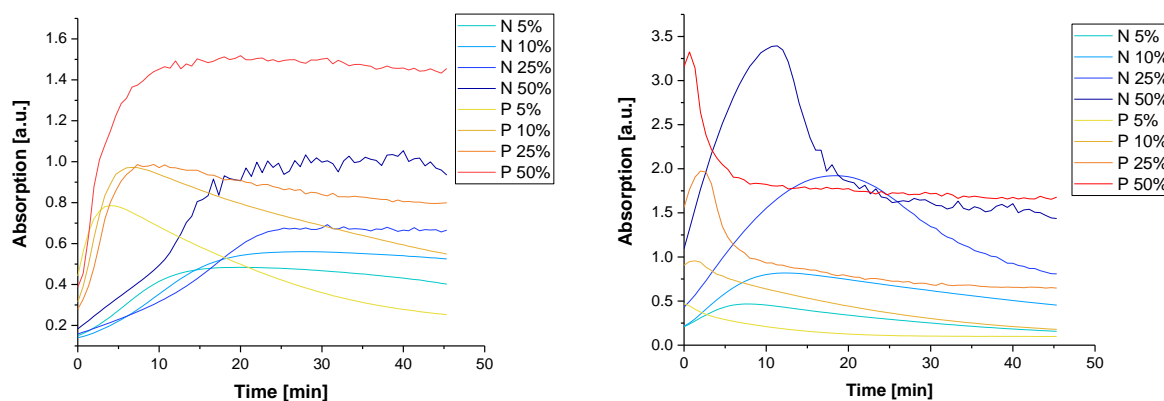
Fig. 7: Variation of the TMB content (96-well plate; 250µL total; 12.5µL DSPC-based nanoreactors; 10µL 10mM H_2O_2); left absorption measured at 450nm; right measured at 650nm; N: NRs without OmpF; P: NRs with WT-OmpF

There is a clear relation between concentration and sensitivity: The higher the TMB content is, the higher are the saturation limit and stability. However, above 25% of the total volume belonging to TMB solution the curves become less smooth (**Fig. 7**).

At 650nm, the sensitivity (apparent saturation level) increases 3x. The reaction appears much faster (**NR-** 2x; **NR+** 10x). Moreover, the curves drop again after saturation has been reached. This indicates that at pH 7.4 the protonated species prevails. However, the other species is produced and its detection is more sensitive.

The working solution was tested on its own, since both the positive- and to a lesser extent the negative control became blue even before the addition of hydrogen peroxide. Fortunately, it does not interfere with the kinetic measurement.
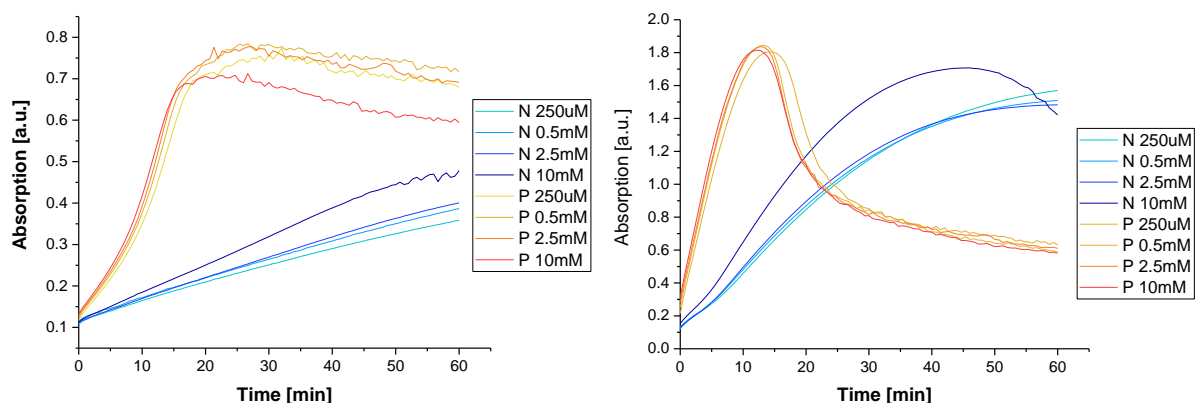
Fig. 8: variation of the H$_2$O$_2$-concentration (96 well-plate; 250µL total; 62.5% TMB, 12.5µL NRs); left absorption measured at 450nm; right measured at 650nm; N: NRs without OmpF; P: NRs with WT-OmpF

The H$_2$O$_2$ concentration is apparently no rate limiting factor in the observed range from 250µM to 10mM. A lower H$_2$O$_2$ concentration seems to make the saturated state more stable and slightly increases the difference between the positive and negative control by lowering the later (**Fig. 8**). Again, the reaction appears 2x as fast at 650nm; moreover, the signal is twice as strong.

Changing form Amplex to TMB does not change the relative activity of samples (**NR-**, **NRD**, **NR+**). The activity of **NR-** was originally explained by Amplex permeating the vesicle membrane, but the fact that TMB gave a similar picture, make this theory dubious, although uncharged TMB might be even more hydrophobic.

1.2.1 HRP separation

The greatest challenge by far when working with HRP based systems turned out to be the suppression of the background activity. Initially, it was tried to remove HRP from vesicles, as fluorophores would be removed. Size exclusion works well for the latter, although dyes are known for their "stickiness". However, it turned out that after the HRP fraction was eluted, even 5 more column volumes of elution buffer were not enough to clean the sepharose column. While the UV/conductivity-detectors did not reveal any contaminations, the eluted buffer had still a significant peroxidase activity (mixing a drop with a drop of TMB sufficed to prove it). Since the size exclusion is capable of separating micelles from

vesicles, the removal of HRP with an even larger discrepancy in size, should have been simple, but apparently HRP interacted both with the vesicles and the sepharose strongly.

Since the HRP within vesicles should be protected from proteases, all undesirable HRP could in theory be deactivated through enzymatic digestion. Of the available proteinases, proteinase K was the most promising, diminishing the HRP activity by a factor of 1000 (regarding the slope measuring kinetics with Amplex). However, this method had some drawbacks: the digestion required 6-12h at 37°C, which restricted the choice of vesicles to those that withstand said conditions (DSPC-liposomes and most polymersomes). Moreover, it did not destroy the heme-cofactor, which precipitated, but was easily carried along due to resuspension. Thus, a second size exclusion was still necessary. For this purpose, a minicolumn sufficed. The first size exclusion was required to reduce the HRP-concentration to a level (<1µg/L), which the proteinase could deal with. Still, multiple additions of proteinase were required, due to cannibalism of the protease.

Dialysis turned out to be the best solution. While it took at least 3 days with 5 buffer changes, it was a very mild method and required little labour. Sensitive liposomes, could be dialysed in the fridge at 4°C in order to minimize degradation and precipitation of vesicles. While even more HRP could be removed with a week of dialysis, increasing the dialysis time or number of buffer changes further did not reduce the background activity any further. This indicates that the model of residual activity due to free HRP is not entirely realistic. It could be thus either, that a part of the HRP can be found on the vesicle surface, or that the vesicles without OmpF are to some degree permeable either through the membrane itself or through defects. Lastly, it could be that some vesicles burst after the purification. Hence, the origin of the background activity was further investigated.

1.2.2 HRP interactions

1.2.2.1 Stability of nanoreactors over time

While the activity of HRP containing samples did not decrease significantly over time, the activity of **NR-** increased indicating that the vesicles deteriorated (**Fig. 9**). This DSPC-mix did not reveal any signs of degradation in TEM or light scattering after treatment for 12h at 40°C or 3 months at RT. This could either imply that the membrane developed cracks without changing its overall structure, or that the vesicles completely disappear upon receiving damage so that only the remaining vesicles are visible. Since the latter would involve the formation of aggregates and precipitation and a significant decrease in vesicle concentration, the former appears more plausible. Moreover, the activity of **NR+** did not

decrease as it would be the case, if vesicles precipitate, nor did the activity increase, as it could be assumed if the HRP was released and thus more accessible.
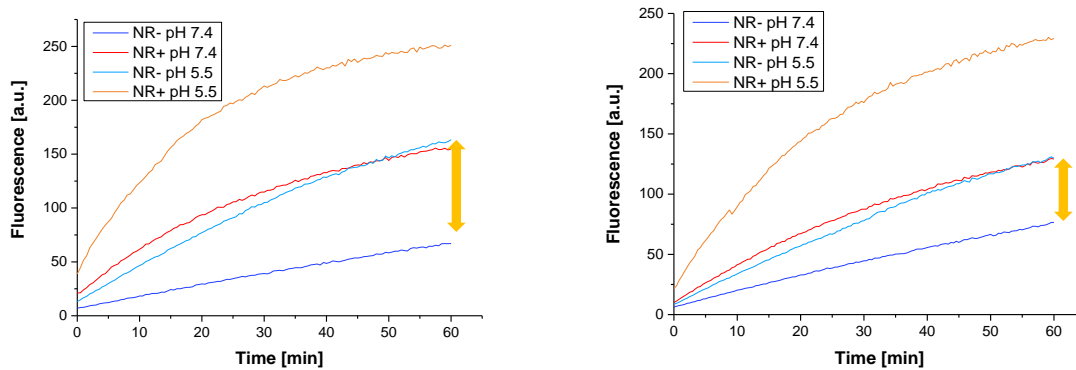
Fig. 9: Change of activity of liposomes after storage for 6 days in the fridge.

Polymersomes (**Fig. 10**) follow the same trend, albeit at a much slower pace:
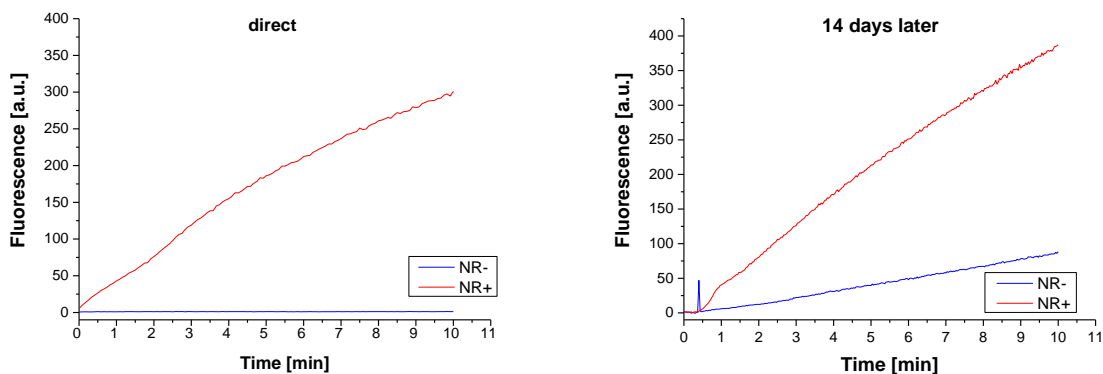
Fig. 10: Amplex Ultra Red conversion kinetics at pH 7.4. Stability of the HRP loaded polymersomes (NR-, blue) and HRP loaded polymersomes equipped with OmpF-M (NR +, red) immediately (left) and after 14 days (right). The left part is taken from the measurement displayed in **Fig. 5 Appendix**.

While the activity of **NR+** remains the same, **NR-** increases its activity due to damaged vesicles allowing access to HRP. This holds true for both lipo- and polymersomes.

1.2.2.2 Binding of HRP to membranes

In order to investigate potential interactions of HRP with liposomes, the following samples were prepared: DSPC-liposomes without HRP, OmpF and detergent (**NR-**) and the same with additional detergent (**NRD**; 0.5% OG, simulating the insertion of OmpF) both had HRP added to the outside in the same concentration as it would have been used for the encapsulation of HRP during film-rehydration. A third sample consisted of HRP in buffer in absence of any vesicles (**HRP**). In each case a part of the sample was treated for 12h at 40°C, as it would have been the case, if HRP was digested with proteinase K. All samples were then dialysed in 100kDa tubes with 5x buffer changes over the course of three days.
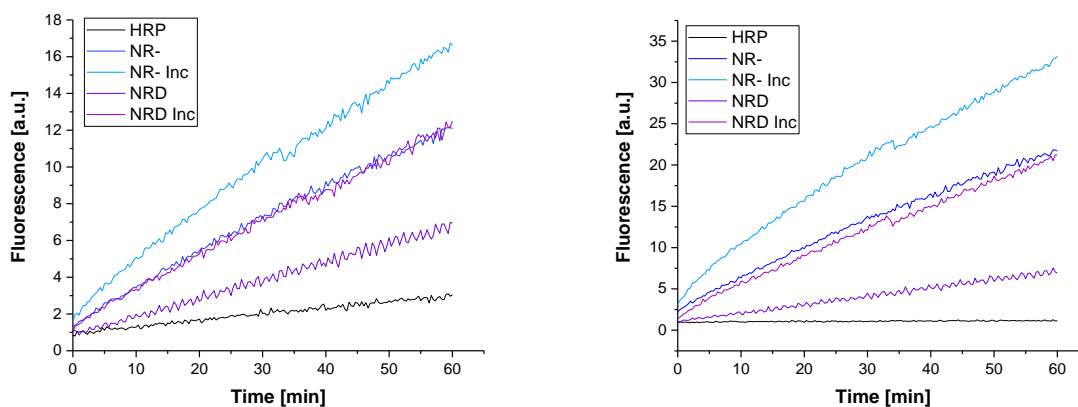
Fig. 11: Left: HRP kinetic using Amplex Ultra Red at room temperature at pH 7.4. Right: HRP kinetic at room temperature at pH 5.5.

In absence of vesicles HRP was removed to the point where no activity could be detected (**Fig. 11**). However, all other samples had residual activity, albeit a low activity. The activity increased from vesicles in presence of OG to those without and increased independent of OG, when the vesicles had been exposed to heat. While it was anticipated that the presence of OG would make the vesicle membrane more fluid and prone to degradation and thus allow the release of HRP, the activity was lower. This could either imply that the vesicles were more stable than expected, or more likely that the vesicles released HRP, which was then removed through dialysis. In the latter case, HRP did probably not interact with the membrane. Heating the samples should have a similar effect in that vesicles release HRP, but then the released HRP should have been removed as well via dialysis, but the activity increased. This indicates that a different mechanism is involved here. Thus, it could be that the vesicle membrane became more permeable due to defects, or that HRP could bind to the membrane while its temperature dependent fluidity was temporarily increased.

According to the Zetasizer, the average diameter of the vesicles was 220nm, unless OG was present, in which case the diameter dropped to 161nm. However, it did not change the size distribution unlike exposure to heat did (polydispersity index going from 0.11 to 0.45; in case of OG only 0.21). All this indicates that the vesicles were less stable than anticipated. However, it seems that the presence of OG affected the vesicles so slowly, that it was not observed before. Most vesicles appeared to have survived the treatment with heat, but some aggregated and precipitated, thus removing themselves from size measurements, unless they resuspended.

The increased activity at pH 5.5 has to be attributed to the pH-dependent activity of HRP itself and was anticipated, as it had been observed before and is well documented. However, the only exception here was the free HRP. Free HRP usually behaves the same but is also more sensitive to a variety of detrimental factors, such as a pH temporarily dropping below 5.5 due to non-instantaneous mixing.

These two experiments indicate that Amplex can to some extent diffuse through vesicle membranes even in absence of OmpF. This applies both for liposomes and polymersomes. It was also tried to encapsulate Amplex into vesicles and add HRP outside, to see whether the substrate diffuses out. However, the experiment failed as not enough fluorescence could be observed even after destroying the vesicles with TritonX. The experiments however, still do not rule out HRP binding to the membrane. Thus, HRP was added to preformed polymersomes and the solution was stirred for 12h and then the samples were dialysed.
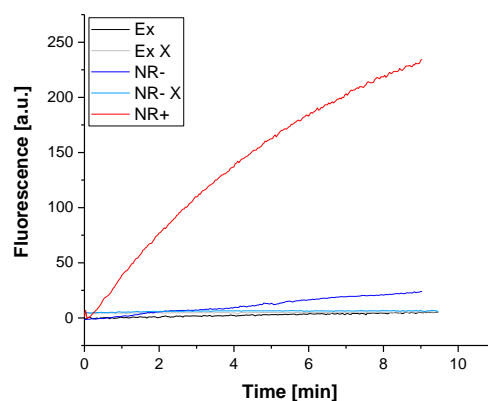
Fig. 12: HRP-Amplex kinetic at pH 7.4 (default conditions), testing permeability and interaction of HRP with polymersome membranes. Ex vesicles that had contact with HRP only externally; X stands for treatment of the vesicles with 0.5% Triton X in order to release the HRP by destroying the vesicles.

As with other successful experiments, the difference between **NR+** and **NR-** in terms of activity was around 11x (compare the initial slope in **Fig. 12**). Vesicles that were in contact with HRP on the outside had 5x lower activity than **NR-**, where HRP was encapsulated. Destroying both samples with 0.5% Triton X evens the difference out to a ratio of 1.3, which could imply that a very small portion of HRP is bound to the membrane, however, the HRP activity drops in presence of the detergent, making this finding less dependable.

The autoxidation of Amplex in absence of HRP but in presence of H_2O_2 is not visible at pH 7.4 but in a similar range at pH 6.0 comparable to the activity of the vesicles that had been only superficially exposed to HRP prior the dialysis step.

Concluding can be said that **NR-** is active either due to small defects or due to a residual permeability towards dyes. Adding HRP to the outside allows nearly all of it to be removed, but a small fraction clings to the membrane.

1.2.2.3 Enzyme kinetics in combination with FCS

Potential membrane interactions could also be detected using the fact that resorufin can be observed in fluorescence correlation spectroscopy (FCS). The experiment was conducted with NRs based on the DSPC-mix.

Following the count-rate over time gives results very similar to normal fluorescence measurements (**Fig. 13**):
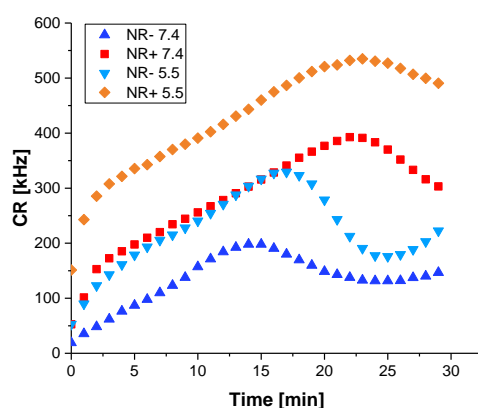
Fig. 13: Kinetic under FCS using the same reaction conditions as for fluorimeter but scaled down in volume.

The high laser intensity causes bleaching and the absence of agitation make FCS less suited than normal fluorescence measurements. However, it allows to measure the vesicle size via its diffusion time and it gives an average number of fluorophores via the CPM (**Fig. 14**):

Fig. 14: The same experiment, but CPM displayed instead of CR.

The CPM does not increase over time, strongly indicating no accumulation in the vesicles or within the membrane. The CPM stays for al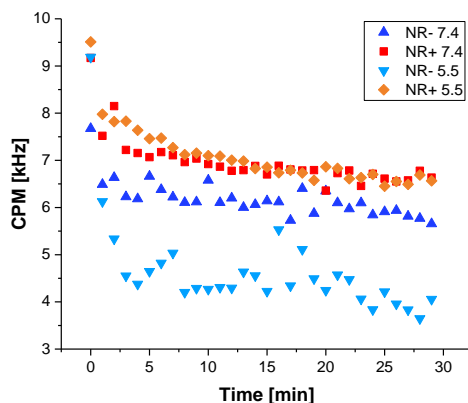l samples between 6 and 8 with the exception of **NR-** at pH 5.5. The CPM of free resorufin was 5.19 kHz indicating that the vesicles had 1.5 molecules of resorufin at any given point in time.

It was anticipated that **NR+** would have a higher CPM since the formation occurs within the vesicles, thus at any given time a few fluorophores should be within the vesicle. The **NR-** should only have a significant CPM, if Amplex manages to diffuse into the membrane or bind to it. The latter is probably pH dependent.

Since it would also be interesting to know the number of HRP enzymes per vesicle and have a better indicator than light scattering for the vesicle concentration, it was attempted to label HRP with AL488, AL633 and OG488. However, even after multiple size exclusion, centrifugal filtration, dialysis, addition of biobead etc. the free dye could not be removed but was clearly visible in FCS. It appeared moreover, that only one dye molecule was attached covalently per HRP. This had to be expected since HRP has only three lysine sidechains on its surface that could serve as an anchor point.[7]

1.3 Enzyme stability
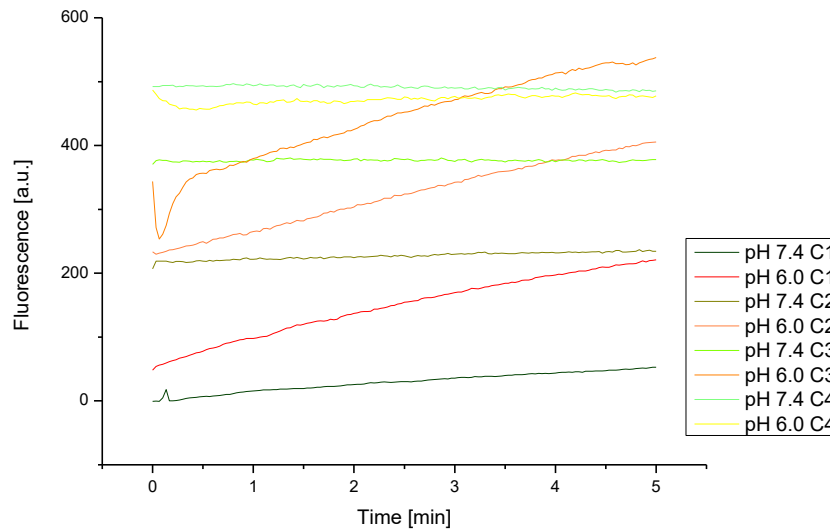
Fig. 15: pH-cycling of free HRP (200ng/mL; detection with Amplex Ultra Red), showing that HRP is more active at pH 6.0 and that the activity decreases with each circle, above all for pH 7.4
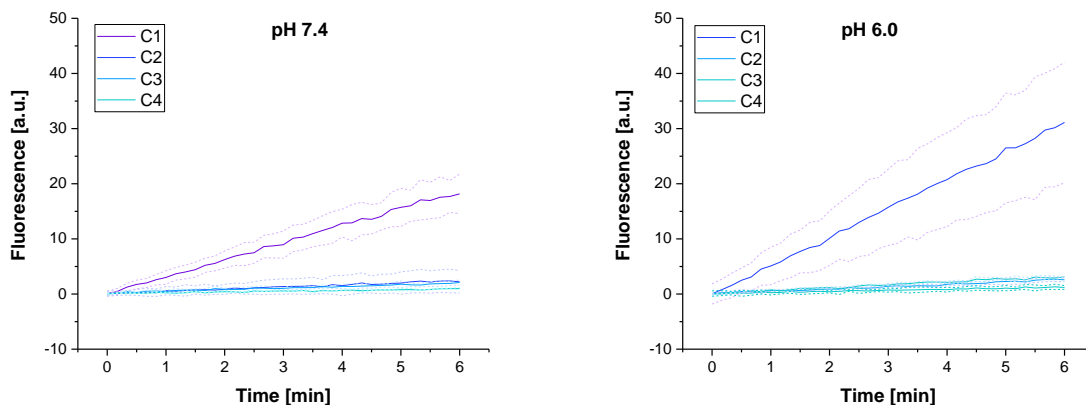
Fig. 16: HRP activity (200ng/mL) over multiple pH changes cycling 4 times (purple to cyan) from pH 7.4 (left) to 6.0 (right) and back, measured with Amplex Ultra Red. The displayed fluorescence increase is the average of triplicates and the dotted lines represent the standard-deviation. Unlike **Fig. 15**, the graphs were all re-zeroed.

Since HRP is more active at pH 6.0 than at 7.4, it is hard to see that acidification could be detrimental. Originally, it was intended to measure the stimuli responsiveness of OmpF-C at pH 7.4 and 5.5. At pH 5.5 the activity is even higher than at pH 6.0, but the experiment reproducibility was poor. As it turned out, HRP becomes irreversibly deactivated below pH 5.0. Changing the pH causes multiple

experimental errors. This can be seen in particular in **Fig. 15**, where each consecutive curve becomes flatter. In **Fig. 16**, it can be seen that the initial drop in activity is the greatest. Primarily, it results in a volume increase. In order to minimise this effect, concentrated acid was used (reducing the volume increase in this example from 10mL to 10.18mL), which in turn creates highly acidic zones before homogenisation. These form temporary and local kill-zones for HRP.

2 Other potential enzymes

2.1 Lactoperoxidase

LPO (77.5kDa) was considered as an alternative to HRP (44kDa) as it is reported to interact less with membranes and was labelled successfully with fluorescent dyes.[8] However, the encapsulation efficiency was too low for a fluorescence assay with Amplex Ultra Red (0.25g/L HRP had a 40x higher activity than 0.5g/L LPO). Moreover, the activity at low pH was too low (6x lower at pH 5.5).

2.2 β-Galactosidase

β-Galactosidase was tried as well, despite its massive size, weighting 465kDa as a tetramer, due to its pH-stability and small substrate. The nanoreactors featuring it, were surprisingly active (samples were 100x diluted compared to HRP-NR and still produced a signal overload; see **Fig. 17**) and there was a distinct, but small difference between **NR+** and **NR-**. The fluorescence decreases 5x when the sample is acidified from pH 7.4 to 5.5. The substrate, o-nitrophenyl β-D-galactopyranoside, had the unfortunate drawback that a significant portion hydrolysed with every thawing, but during the measurement itself, no further hydrolysis was observed in absence of enzyme. After two experiments, the substrate was unusable.
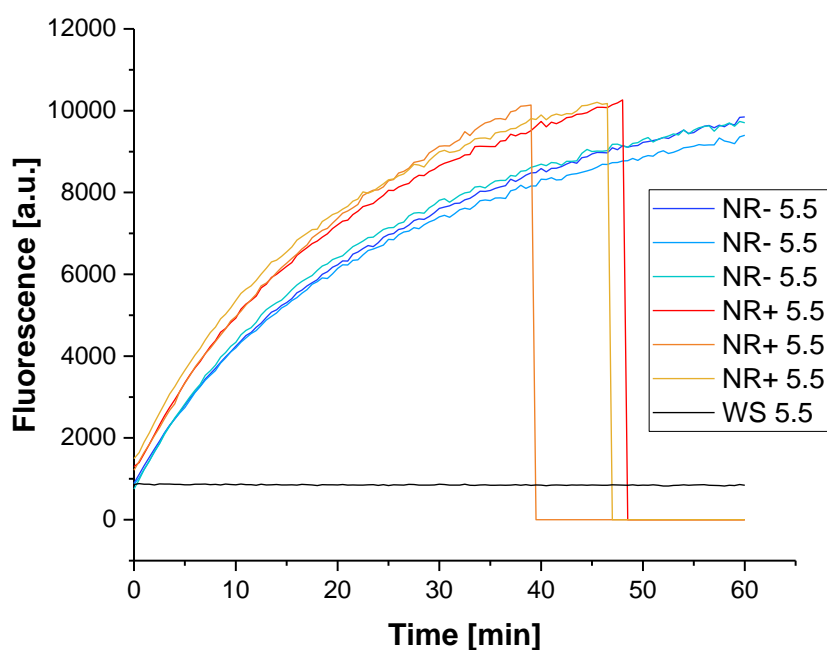
Fig. 17: Kinetic using NRs with 2.5g/L galactosidase encapsulated in DSPC-vesicles and 100x diluted; only pH 5.5 is shown, since pH 7.4 resulted still in a signal overload.

2.3 Uricase

Uricase is another possible alternative. It is weighting only 35kDa and known to be easier to separate via size exclusion from vesicles than HRP. Unlike HRP, Uricase utilises oxygen directly and produces H_2O_2 as byproduct. Its substrate is very small (168 Da) and a weak acid, however, despite all its polar groups, uric acid is only poorly soluble in water (ca. 6mg/L at 20°C). Moreover, there are no specialised enzyme substrates available, that would turn into fluorophores or dyes. However, uric acid absorbs at 293nm whereas its product allantoin does not.[9] As with all absorption based methods, the assay is not very sensitive and hence requires significant concentrations of substrate, but in this case the concentration cannot be increased due to its poor solubility. To complicate matters further, the absorption is overlapping with most sample carriers and uricase has only 10% of the activity at pH 5 compared to pH 7.4.[10] This is unfortunate, since even at pH 7.4 the activity is low. Increasing the temperature from 22°C to 37°C helps in two ways: 1) the enzyme activity increases; 2) the solubility of uric acid increases.
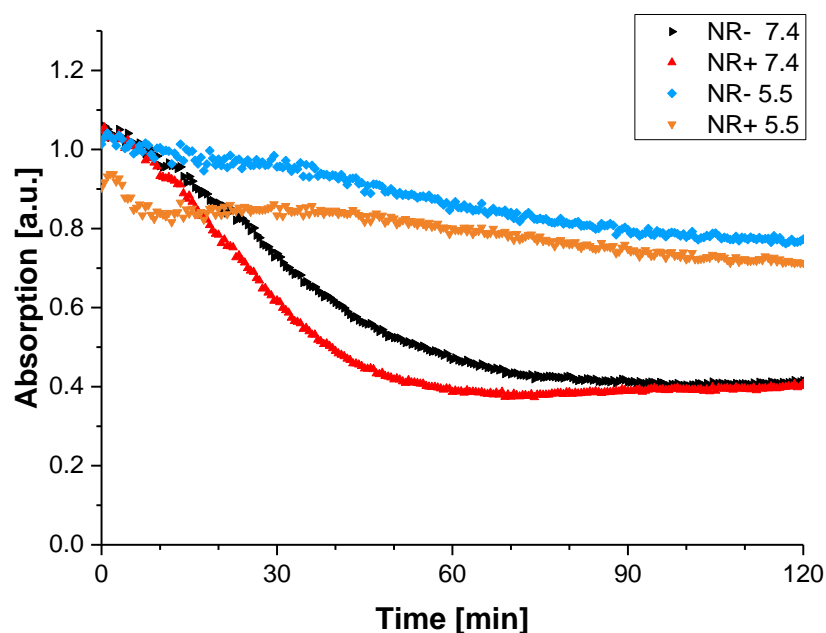
Fig. 18: Kinetic measurement or uric acid consumption using DSPC liposomes (encapsulating 1g/L uricase) at 37°C.

Unlike all other kinetic experiments, the activity is observed as a decrease of absorbance. The experiment shows that uricase is ill suited. At pH 5.5 the activity is at best 1/5th of the activity at pH 7.4 (**Fig. 18**). Moreover, the uricase conversion appears to stop prematurely. This might be caused by the byproduct hydrogen peroxide, which could inactivate the uricase. Thus, after 1h no further activity was observed at pH 7.4. At low pH, this effect is even more pronounced, as an initially sharp decrease in uricase could be observed which soon flattens. Another major problem is the fact that the difference between **NR-** and **NR+** is very small.

2.4 HRP Uricase tandem reaction

Since uricase is not suitable for experiments on its own, a tandem reaction utilising the byproduct H_2O_2 is necessary. This can be achieved with HRP. Since coencapsulation would be an unnecessary complication and uricase was investigated to avoid the problems with HRP in the first place, the only sensible experimental set-up is encapsulating uricase and then adding HRP and Amplex Ultra Red to the outside of the purified vesicles. This approach would solve all conceived problems with two exceptions: the pH-dependence of the enzymes and the possibility that the rate determining reaction step changes with the pH.

As anticipated at both pH uricase remains the limiting factor in terms of activity, which simplifies the evaluation of the experiment. This means also that at pH 5.5 the activity decreases, despite the fact that HRP would be more active at this pH. This has the consequence that at pH 5.5 the activity of the samples is akin to the rate of self-oxidation of Amplex at low pH and elevated temperature, making the assay borderline useless (**Fig. 33, Fig. 34**).

2.5 Glucose dehydrogenase/oxidase

Since most enzymatic substrates are based on dies, they are relatively big and hydrophobic. Moreover, there are no uncharged, water-soluble substrates of this type. Such a substrate could avoid various undesired interactions (charge repulsion; membrane interaction…). Sugars are a prime example for such enzyme substrates. To create a measurable reaction, a tandem reaction similar to Uricase-HRP is required. While this introduces experimental issues as discussed above, none of the enzymes needs to be encapsulated, eliminating a whole set of problems (low encapsulation efficiency, purification, measuring the encapsulation efficiency…). The only disadvantage is that NRs can stay far longer active than cargo releasing systems. Sugars are in general much easier to encapsulate and store than fluorophores or enzymes. The detection can be achieved with glucose oxidase-HRP (**Fig. 19 B**). A more elegant variation would be to use an enzyme which consumes a co-substrate, which can be followed spectrometrically (**Fig. 19 C**). glucose dehydrogenase falls into this category (NAD can be followed at 339nm excitation and 460nm emission). However, glucose dehydrogenase requires basic conditions and elevated temperatures to operate. Moreover, NAD is much harder to detect than Amplex Ultra Red. This leaves still glucose or galactose oxidase in combination with HRP.
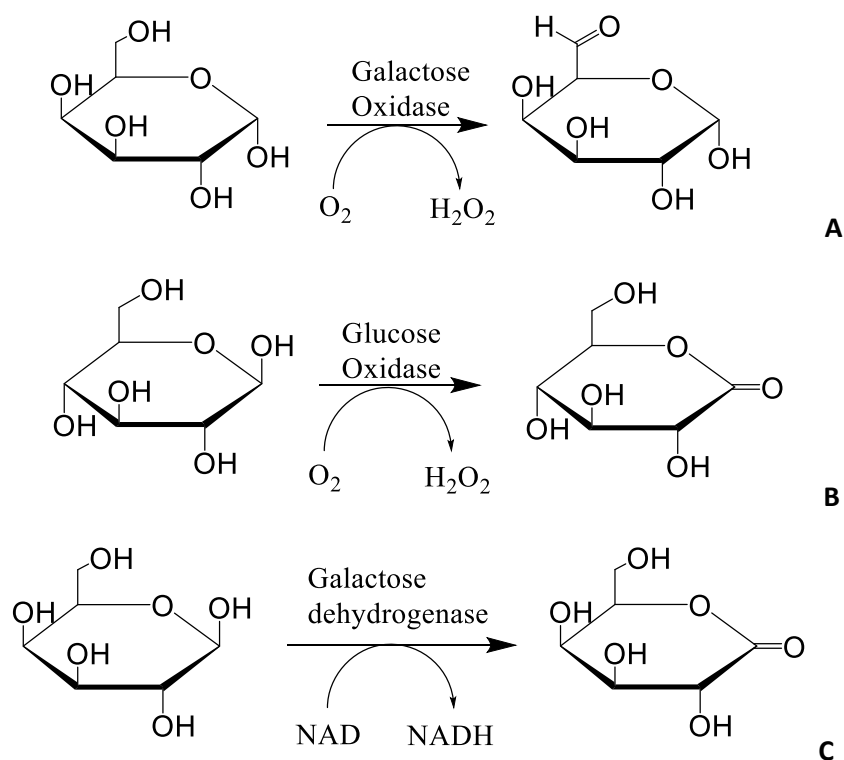
Fig. 19: Possible enzymatic reactions involving sugars. Note that it is always the by-product which allows detection. Furthermore, all enzymes are specific to the shown anomer (which is in equilibrium in solution, as long as the alpha-hydroxy group is not reacted to an ether or ester).

GOX-HRP Galactose detection
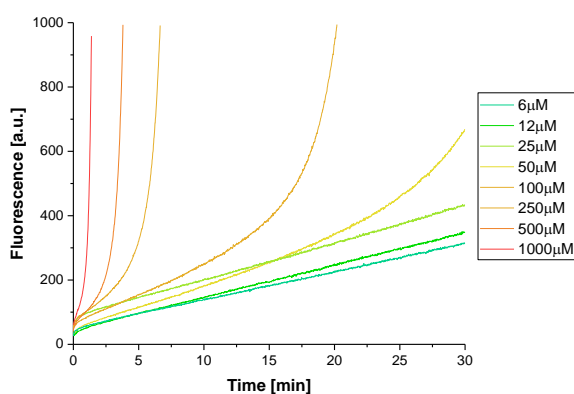
Fig. 20: Testing the detection window of galactose using galactose oxidase-HRP tandem.[35]

---

[35] Reaction conditions: 50µL of working solution containing 2 U/mL GOX, 0.1 U/mL and 50µM of Amplex Ultra Red in PBS pH 7.4 were added to 500µL sample; excitation/emission 530/590nm (at 22°C)

The disadvantage of coupling two reactions for an assay becomes apparent in **Fig. 20**. Depending on the galactose concentration, the rate determining step changes, resulting in a non-linear dependence between sugar concentration and fluorescence per time unit. Fortunately, this was not the case with the related glucose oxidase.
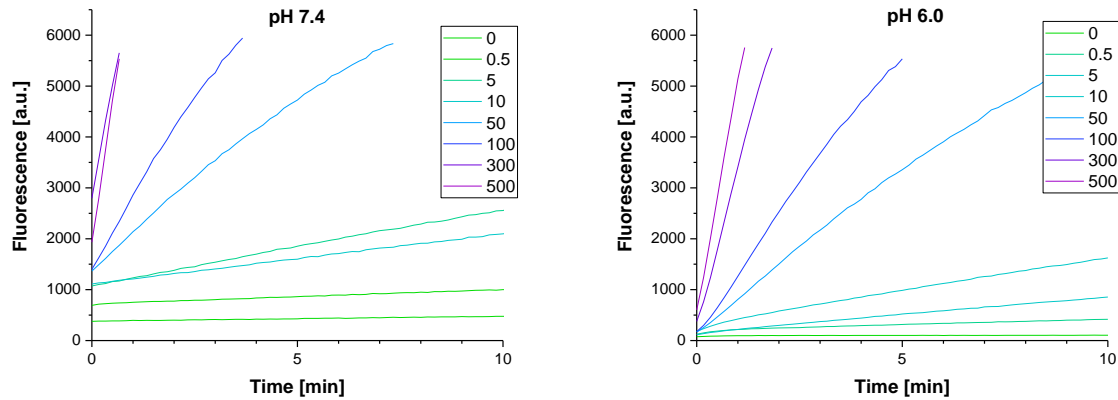
Fig. 21: Amplex oxidation in dependence on pH and glucose concentration in [µL]. Detected with a system of glucose oxidase and HRP.[36]

Glucose oxidase does not suffer from the same limitations (**Fig. 21**). The pH dependence of the reaction is visible, but at both pH the result is still comparable. The reaction is only 30% faster at pH 6.0.
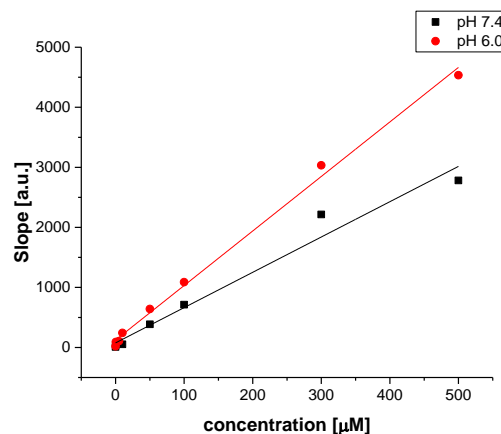
Fig. 22: Dependence on Glucose concentration and on pH.

---

[36] 150µL sample+50µL working solution: 0.2 U/mL HRP (275kU/g→727µg/mL) 2 U/mL GOX (208kU/g→9.62mg/mL) 50µM Amplex Ultra Red; excitation/emission 530/590nm (at 22°C)

Fig. 22: Has the slopes (first 30s) of **Fig. 21** plotted as a function of the concentration of glucose concentration. For practical purposes this assay has an effective detection range of 0.5-50µM. Higher concentrations could be measured, but dead-time during sample preparation would become a major problem. As with HRP kinetics, the reactivity increases at low pH, but in case of this tandem reaction the activity increase is limited to less than 55% implying that the activity of the glucose oxidase decreases at low pH. All in all, this combination of enzymes appears promising for kinetic measurements.

3 Experimental Problems

Enzymatic systems are far more complex systems than experimental set-ups for release experiments. While they do not suffer of low encapsulation efficiency or leaking before the measurement as much as the release experiments, they do have quite a number of experimental error sources:

- **Cofactors** need to be able to diffuse along with the enzyme substrate. For H_2O_2 as with HRP, LPO, or similar this is not an issue (except that it is a fairly aggressive oxidant, which can bleach fluorophores and damage proteins or lipids), but most co-substrates are bigger, like NADH (sugar dehydrogenases etc.). In case of uricase and GOX the problem is that the co-substrate is O_2, which does not dissolve in water,[37] as well as other substrates and the supply is dependent on temperature and agitation of the solution. If most of the O_2 stems from bubbles, then there will be a lack thereof on the inside of the vesicles.

- Enzymes may also stick to membranes or be otherwise hard to remove. Due to their catalytical nature, even traces may cause significant **background activity**. Similarly, a single bursting of vesicles could significantly alter the outcome of a measurement.

- As with release experiments, it can be challenging to adjust the pH, but unlike release experiments, the system is much more **sensitive to deviations of the pH**. Changing the pH requires the addition of acids or bases, which will increase the sample volume and thus dilute the system. The more concentrated they are the higher the difference in local pH will be until the sample is thoroughly mixed (and even then, the pH on the inside of vesicles may take a

---

[37] At atmospheric pressure and 25°C around 6mL oxygen dissolve in 1L of pure water (less in PBS), that results in less than 250µM.

while to adjust). The longer the mixing takes, the longer the dead-time will be and the more damage may occur to the sample.

- Related to the last point, **smaller volumes added have larger titration errors**. Buffers were used to prevent accidental deviations from the pH, but also increase the amount of acid or base required. Moreover, no buffer has a straight titration curve. **PBS** for instance does not buffer at pH 5.5 at all, meaning that at this pH even small additions of acid will drop the pH considerably. Thus, **citrate buffer** was used for many experiments until it was found that it did apparently change the reaction mechanism in unknown ways (see **Fig. 23**). When HRP converted Amplex into a fluorophore, it gave a sudden jolt of fluorescence at the beginning in case of citrate buffer, which did not occur in PBS. It was not noticed for a long time, since the cuvettes were shaken more thoroughly resulting in a dead-time in which both systems equilibrated themselves independently resulting in a similar activity curve thereafter.

- In case of multiple pH changes (pH-cycling experiments), the **error accumulated**. Due to the extended measurement time it also coincides with an accumulation of fluorophores and salts from the titration. The prior reduces the signal noise ratio (see **Table 1**), whereas the latter could potentially quench the fluorescence. In addition, cycling experiments require a very low conversion, or the **saturation level** will be reached within the experiment.

- Also, besides the obvious limitations of all compounds regarding a certain pH range, the fluorescence of the product and the **activity of the enzyme** usually changes with the pH and it can further open new reaction pathways such as further oxidation of the fluorophore. It was observed for Amplex Ultra Red/HRP, that the concentration of H_2O_2 had to be reduced in order to reduce further oxidation of Amplex Ultra Red at low pH. This pH dependency also makes it impossible to compare the activity of an open and close pore NR directly. Thus, controls are stringent.

The system HRP/Amplex Ultra Red proved to be the most reliable. Among the available substrates Amplex Ultra Red was chosen as enzyme substrate due to its size, pH stability and hydrophilicity. In case of kinetic measurements, the safest way of adjusting the pH was to dissolve the sample in buffer of the corresponding pH and adding the working solution (containing the Amplex Ultra Red) of the same pH as the buffer. For changing the pH during a measurement irrespective if only once or over multiple cycles, it was best to use minimal amount of acid or base and shake the sample immediately and thoroughly and then reinsert it into the detector. Changing the pH while caused more HRP deactivation, since the equilibration of the pH was slower.
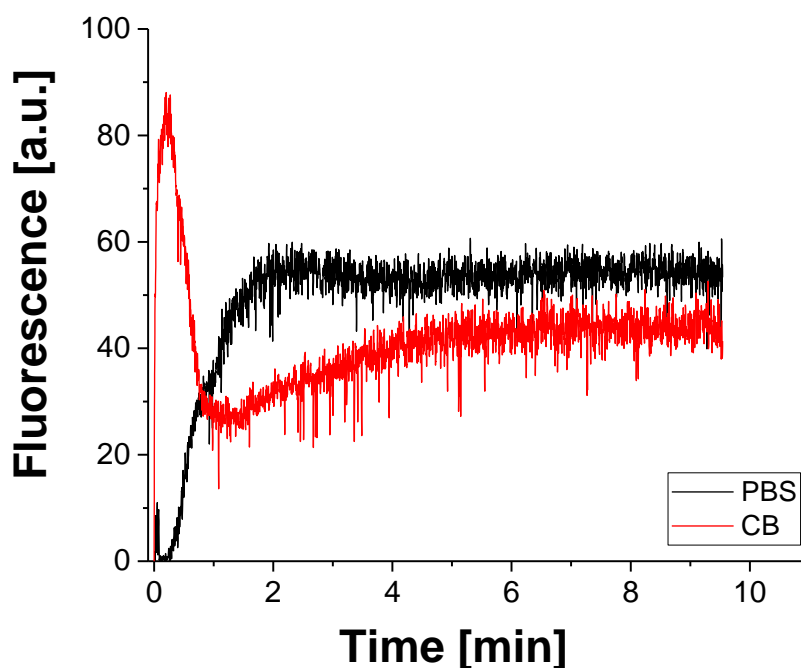
Fig. 23: Liposomes via detergent removal containing HRP and OmpF; one made in citrate buffer (red) and the other in PBS (black).

Table 1.: Example of how the background activity increases over four cycles

cycle	Fluorophore formed [µM]*	Prexisting Fluorophore [µM]*	Ratio []
1	5	0	100%
2	5	5	50%
3	5	10	33%
4	5	15	25%

*= this is just an example and not based on any measurements.

It was intended to measure that the activity of a nanoreactor at one pH, then the pH would be changed and the measurement continued. The slope of the fluorescence increase representing the activity should change with the pH. This principle could be extended to multiple changes proving that the stimuli responsiveness was reversible. However, this was not achieved for a long time for multiple reasons.

Due to the pH-dependence of the fluorescence, the activity of a NR cannot directly be compared at **two different pH**. Still, their activity can be compared to the activity of controls that represent closed pores and open pores. However, the activities of the respective **samples/controls varied too much** to be compared.

Another minor problem is the **saturation effect**. Over the time the reagents become depleted, thus the fluorescence reaches a maximum. Moreover, the detector has only a certain range of fluorescence which it can measure and multiple additions of reagent or adjustments to the pH will produce cumulative errors and at some point, the sample solution will become to concentrated with fluorophore and salts.

At the beginning, all samples, including the controls appeared to **react the same on pH change**. At low pH, the NRs became more active. The samples and controls could however not be compared, since there was too much variation in their activities. Rescaling the kinetics to the same initial activity would not work for several reasons:

1) the NR- should have a lower initial activity;

2) a sample that had initially a low activity, but a higher activity at low pH would invariably result in a different perceived saturation point than a sample with an initially higher activity (see **Fig. 24**).
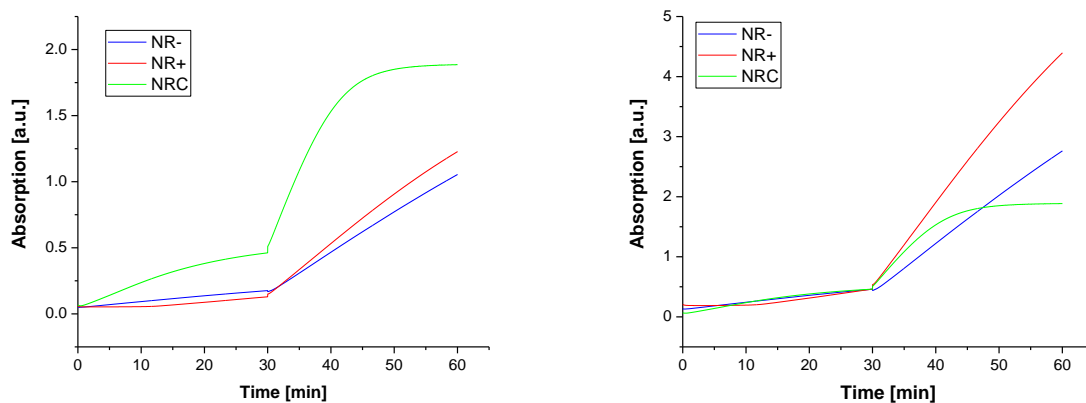
Fig. 24: Oxidation of ABTS using DSPC-vesicles with D12C-K89C -Gala3 attached as NRC; **left** unweighted; **right** weighted such that the endpoint of the measurement at pH 7.4 is in all cases the same.

The situation improved, when the vesicle-formation became more consistent. This was mainly the result of better control over the **detergents** present, in particular ensuring that during the purification and concentration of OmpF, the detergent was not concentrated as well.

With better control over the vesicle size and concentration, but also **HRP encapsulation** (not directly measured, but clearly dependent on vesicle size and concentration) and **OmpF insertion**, the samples became comparable. The remaining variation in the vesicle concentrations could be evened out by **diluting samples** accordingly.

These improvements solved the most troublesome recurring observation that **NR-** was often more active at any given pH than **NRC** and **NR+**. This was apparently the result of a low OmpF-insertion efficiency combined with a low vesicle concentration due to the involved detergents in particular OG. **NR-** had on the other hand the highest vesicle concentration and in case of liposomes, the permeability of the membrane is significantly higher. Both facts together explain a significant HRP-activity.

The only experimental set-up that was not plagued by interfering detergents was vesicle-formation of **liposomes via detergent removal**. This method gave the first results that not only showed a clear difference between **NR-** and **NR+** but a clear stimuli response for **NRC** (R270C-Gala3). This can be explained by the fact that all samples had the same detergent concentration (and thus similar vesicle concentration and stability/permeability) and possibly by a better OmpF insertion compared to the rather crude method used for film-rehydration.

However, when more R270C-Gala3 OmpF was produced the results could no longer be reproduced. The OmpF insertion failed. Apparently, the new batch of chemicals, or the changes in the purification of OmpF extraction made a difference. The latter could change the ternary mixture of bacterial lipids that are bound to OmpF.[11] Similarly, insertion of OmpF into **DSPC-liposomes** during film rehydration worked after reducing the OG concentration but failed with the new batch of R270C-Gala3. That both findings were caused by the batch of OmpF could be proven easily, since the old batch of WT-OmpF was still available and could be still inserted into membranes without a problem.

Interestingly, the new batch of R270C-Gala3 OmpF worked for FRH with polymersomes, when the OG was removed. Still, at times, **NR-** became again the most active sample. It was unlikely that it was again a problem of **free HRP** contaminating the samples. It could have been that the dialysis tubes used for separating HRP, did not work as efficiently as before, but that should affect all samples equally. Even, if the OmpF did not insert again for some reason, all samples should have approximately the same activity. Also, the vesicle **concentration** and their **homogeneity** were much more closely watched.

Thus, it had to be considered that there was a **fundamental difference** between **NR-** and all the other samples. Either in the ability of HRP to bind to the vesicle membrane; the permeability of the vesicle membrane itself or the stability of the liposomes. The **presence of MPs** in a membrane can stabilize it, affect its permeability and ability to bind enzymes. On the other hand, detergents and lipids dragged along with OmpF could affect the membrane.

Hence, the permeability of the membranes towards Amplex Ultra Red was tested. Both liposomes and polymersomes revealed to have a significant residual permeability (ca. 1/10th of the permeability of OmpF-equipped membranes). Detergents such as OG, did not appear to change the permeability of the membranes to a significant extent, but deteriorate the vesicles over time. Interestingly, the

interaction between HRP and the membranes appear to be negligible, despite the fact that HRP was far more difficult than dyes to remove. Hence, it is unlikely, that **HRP binds** stronger to the surface of the vesicles in absence of OG.

Another suspicious finding was that a part of the samples precipitated in the dialysis tubes and the sample volume decreased. This effect was often particularly strong for **NRD**. However, neither TEM nor Zetasizer revealed aggregates. Still, it could be possible, if aggregates precipitate before the sample can be measured, thus making them unavailable to sampling. Speaking against it, is the fact that the samples had both a similar ability to scatter light and similar values in vesicle size and homogeneity. **Precipitation** should decrease the samples concentration, unless larger aggregates falsely indicate higher concentrations. It could still be that different samples had higher rates of releasing HRP, but **no degradation** over time was observed via TEM or Zetasizer (15h 40°C, month on the shelf). If the NRs precipitated the activity should decrease. If the HRP was released, then the activity should increase at first, but then decrease again, because unprotected HRP deactivates faster. Neither of it was observed: NR+ activity remained relatively constant, whereas NR- activity increased over time.

Changes in the volume upon dialysis, could indicate osmotic effects. Vesicles without pores should be far more vulnerable to **osmotic pressure**. However, increasing osmotic pressure by using 5x more concentrated buffers, did not alter the activity or vesicles.

Later, the same problems occurred using **polymersomes**. Thus, it became far more plausible that it was a problem related to the OmpF, or associated detergents and lipids. Supporting this theory, it was observed that **K89,R270C-OmpF** inserted poorly compared to OmpF-WT and R70C-OmpF (**Fig. 25**). It first appeared around the time where I used a **new batch** of POPS and Chol-PEG600, but it turned out to be the same problem with polymersomes. The OmpF could be misfolded. Since OmpF is extraordinarily sturdy, this was deemed unlikely and CD-measurements did not indicate any unfolding. It was however observed that the first batch of K89C-R270C-OmpF had contaminations, either very fine cell-debris, or undigested **DNA**. Due to the sticky, viscous nature of the sample, the latter was assumed and the OmpF protocol improved. Later batches did not have these contaminations, but still inserted poorly. This only changed, when the OmpF samples were dialysed against buffer only, removing all of the OG. This made the OmpF instable in solution but allowed almost all the time successful insertion. This leaves the question why it worked before and without this step. The first OmpF-mutants were extracted with Octyl-POE instead of OG. The latter gave significantly higher yields but is a much harsher detergent. It is known to strip MPs of stabilizing lipids, denature proteins and was found to be much more detrimental to vesicle (see experiments in **Preparation chapter 3.3.3**).[11-12]

Regarding the residual activity of NR-, even in absence of absence of the negative influences such as detergents, the remaining activity has to come either from the permeability of the membrane (either fluidity or defects), or from slow release of enzymes. Since the activity increased faster over time than decomposition was observed, it could be that the aged vesicles are stable in absence of detergents until the moment where they are exposed to shear forces during the pipetting of the sample preparation. This would explain why we see immediately a background activity of **NR-**, but rarely an increase over time unless the sample is remeasured after a week.

To conclude the surprising activity of NR- was due to survivor bias. NR- was very different from all other samples in that the vesicles were never in contact with detergents. In many cases OmpF was apparently poorly inserted and the remaining detergents destroyed over time the vesicles. Thus, even if the permeability of the OmpF-free membrane and the rate of vesicles releasing HRP, due to degradation is low, the sheer number of NR- compared to e.g. NR+ compensated the higher permeability of NR+.

In order to obtain reproducible and comparable results, one must:

- Remove as much detergent as possible, unless detergent removal is used for vesicle-formation. Especially removing the OG below 0.5% tended to be tedious and not fully reproducible, as different batches of dialyses tubes had different efficiencies.
- Depending on the intended method of vesicle-formation, OmpF has to be extracted differently, as it changes its ternary mixture. Milder OPOE is needed for detergent removal, whereas film-rehydration OG can be used, but the detergent needs to be removed thoroughly.
- All controls must have the same residual detergent concentration. This does not imply to add the detergent concentration, the other samples nominally have (0.5% OG directly from storage, or 0% if dialysed against buffer). Instead the detergent concentration has to be measured. Then, e.g. 0.5% OG can be dialysed against buffer along with the OmpF-variants (who had e.g. 0.4-0.6% OG), so that the remaining OG concentration is in the same order of magnitude.
- Adding acid or base to a buffer in order to change the pH, should be avoided, as temporary high local concentrations can damage the sample. Instead the sample should be diluted in buffer of the corresponding pH (unless, pH cycling for testing reversibility is conducted).
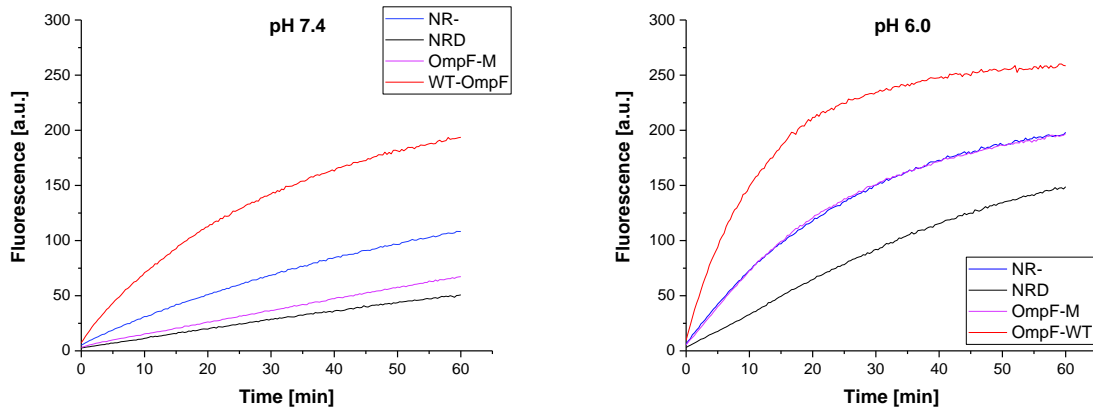
Fig. 25: Amplex-HRP kinetic in order to test the insertion of WT-OmpF (red) and K89R270C-OmpF (purple) into DSPC-vesicles (without OmpF: blue; vesicles exposed to OG: black). Both OmpF variants were stored in 0.5% OG, but WT-OmpF was extracted with 3% OPOE (later dialysed against 0.5% OG) and K89R270C-OmpF was extracted with 3% OG.

4 Testing Stimuli responsiveness

4.1 oligo(acrylic acid)
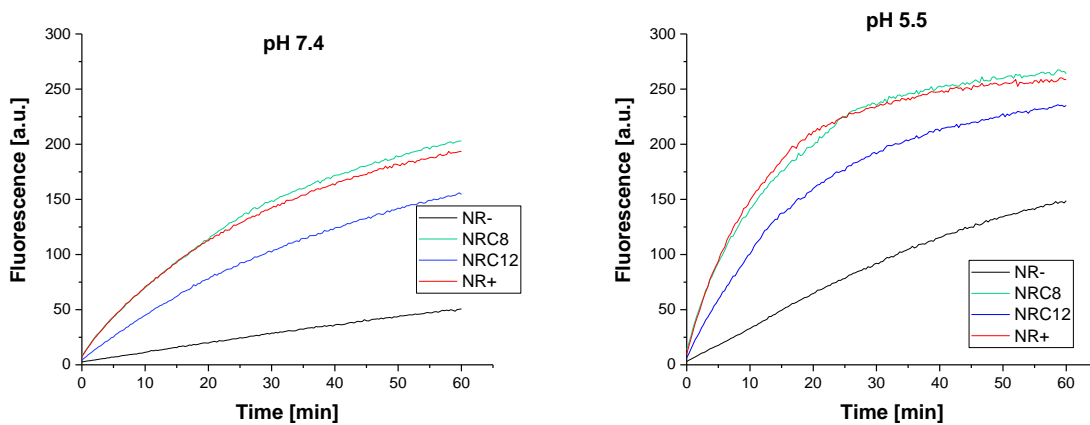
Fig. 26: Amplex-HRP kinetic testing K89R270C-OmpF with *oligo*(acrylic acid attached to it) inserted into DSPC-vesicles. NR- (black), NRC n=8 (green); NRC n=12 (blue), NR+ (WT-OmpF: red)
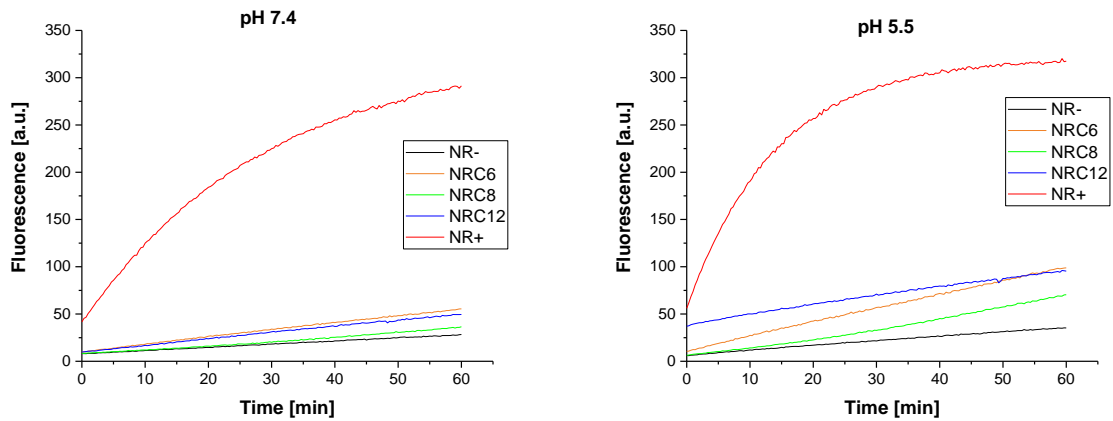
Fig. 27: HRP-Amplex kinetic testing K89R270C-OmpF with *oligo*(acrylic acid attached to it) inserted into $A_8B_{49}A_8$-polymersomes. NR- (black), NRC n=6 (orange); NRC n=8 (green), NRC n=12 (blue), NR+ (K89R270C-OmpF: red)

These experiments suffered of a very poor reproducibility. However, for both lipo- and polymersome NR (**Fig. 26, Fig. 27** respectively) it can be said that no stimuli responsiveness was observed; acidification increased the activity of all samples without changing their relative activity between each other. In case of polymersome NR the activities of **NRC** were significantly lower in comparison to **NR+**, but increased relative to it on acidification, but not enough to speculate on pH responsiveness. Moreover, no clear trend could be seen regarding the length of the *oligo*(acrylic acid) conjugates. It appears to be rather a result of the degree of labelling (DOL). In case of the liposome NR the DOL was around 37% (according to acrylodan assay) and in case of the polymersome NR the DOL was above 50%. Mass spectroscopy indicates a difference in DOL of at least 20%. Thus, the **NRC** were less permeable in the second experiment.

4.2 Gala3

4.2.1 R270C-Gala3 OmpF in POPS/POPC-liposomes
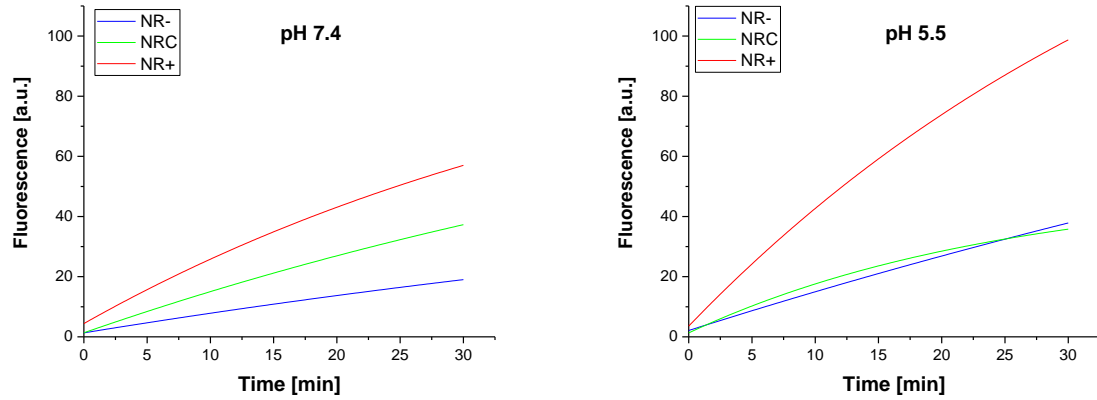
Fig. 28: HRP Amplex Ultra Red kinetic with the NR- (blue), NRC (green; R270C-Gala3) and NR+ (red; OmpF-WT) at pH 7.4 left and pH 5.5 (right) using POPS/POPC liposomes based on detergent removal.
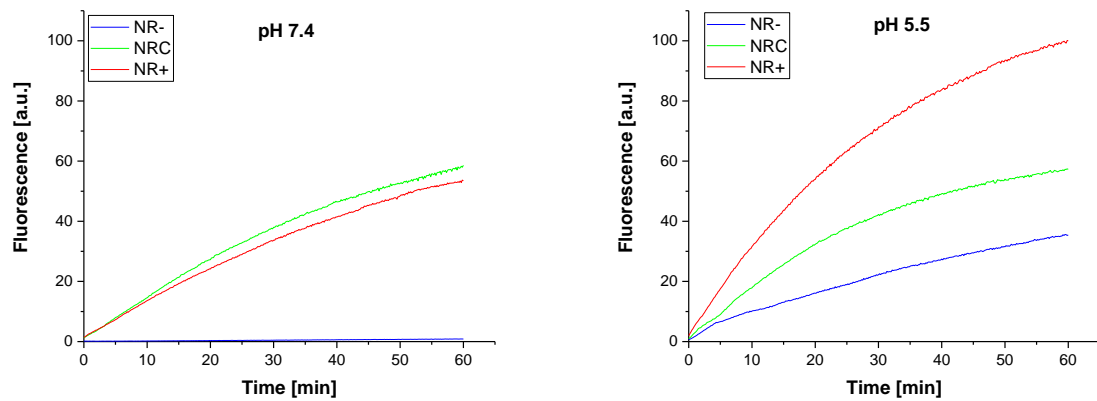
Fig. 29: Repetition of the experiment, with the only difference that the liposomes were dialysed in a fridge.
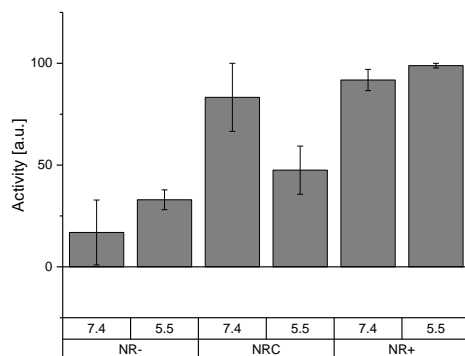
Fig. 30: Activity bars liposomes, combining the activities as seen from the initial slopes from **Fig. 28** and **29**.

Fig. 30: This was the first time (**Fig. 28**) that a clear stimuli responsiveness was observed and it could be reproduced twice in a row. The second time (**Fig. 29**), the vesicles were even in better condition, resulting in a very low activity of NR-. Furthermore, in the repetition NRC had a similar activity to NR+, since both samples had a similar vesicle concentration.

However, the R270C-Gala3 was used up and Gala3-MI could not be resupplied by various companies in the required purity. Then, when the companies finally managed to resupply the Gala3-MI, the experiment could no longer be reproduced with a new batch of OmpF. With the new batch **NR-** had by far the highest activity indicating that no OmpF could be inserted and that most vesicles were damaged.

4.2.2 K89R270-Gala3 in DSPC-liposomes

4.2.2.1 Amplex
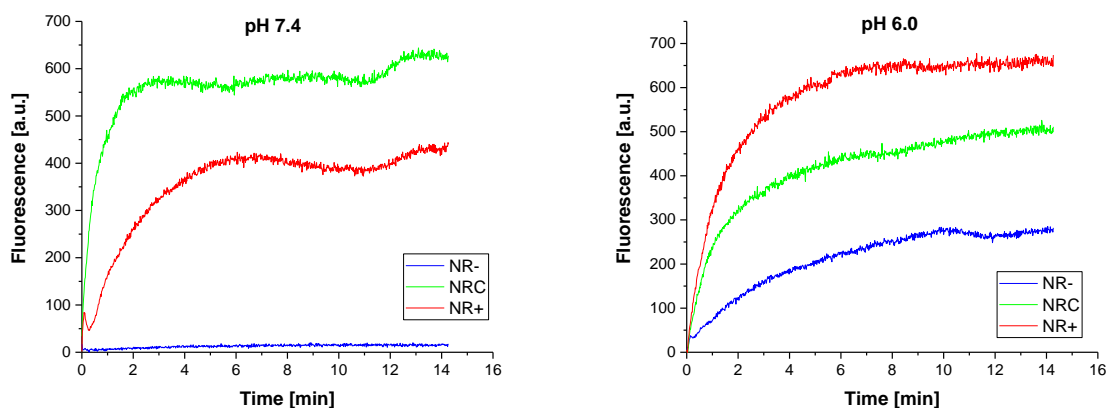
Fig. 31: HRP Amplex Ultra Red kinetic with the NR- (blue), NRC (green; K89R270C-Gala3) and NR+ (red; K89R270C-OmpF) at pH 7.4 left and pH 6.0 (right) using DSPC-liposomes produced via film-rehydration.

Since the new batch of OmpF could no longer be inserted via detergent removal (probably due to changes in the ternary lipid mixture surrounding OmpF stemming from its purification;[11] see **chapter 5.2**) and since the more stable DSPC-vesicles can only be produced via film-rehydration (or demixing will occur), film rehydration was used. It turned out that DSPC-liposomes are not just more stable than other liposomes but behave more like polymersomes in that they are more sensitive to detergents and other disrupting factors and that insertion of OmpF is particularly difficult.

Once polymersomes with OmpF could be obtained with reasonable reproducibility, the experiments with DSPC were stopped. Hence no repeats of this experiment (**Fig. 31**) were performed. This experiment shows however even more clearly the stimuli responsiveness of K89R270C-Gala3. The difference in activity between **NR-** and **NR+** is greater and so is the drop in activity of **NRC** with lowering the pH, which overrides the pH-dependent activity of HRP itself. The slope of the first 30s of NR+ (and free HRP) increases 3x from pH 7.4 to 6.0, whereas NRC is going from 4.5x the activity of NR+ to 0.74x the activity of NR+

4.2.2.2 TMB
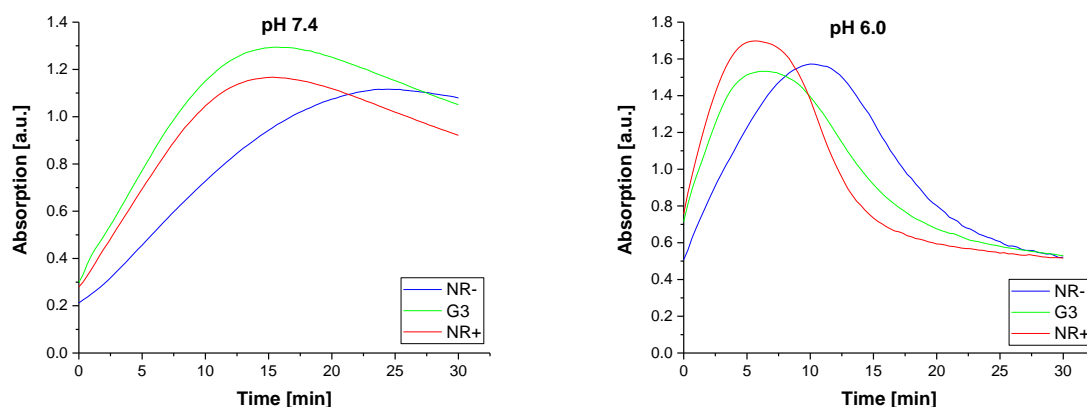
Fig. 32: HRP TMB kinetic measured at 370nm with the NR- (blue), NRC (green; K89R270C-Gala3) and NR+ (red; K89R270C-OmpF) at pH 7.4 left and pH 6.0 (right) using DSPC-liposomes produced via film-rehydration.

Measuring the same NRs with Amplex Ultra Red (**Fig. 31**) and TMB (**Fig. 32**) gives the same results (activity of **NRC/NR+** goes from 1.2 to 0.56), although it is harder to see with TMB, due to the higher perceived reaction rate and due to the further reaction of the product. Moreover, **NR-** is considerably

more active. Still, it confirms the significant decrease in activity of **NRC** at pH 6.0 and confirms that **NRC** was more active (20%; the difference between the activities of the different samples is much less pronounced with this assay) at pH 7.4 than **NR+**. The latter could be due to inconsistencies of the NR formation, such as variations in vesicle size, concentration, HRP encapsulation, or OmpF insertion. **NR+** scattered light 10% more than **NRC** and the Rh was 143nm compared to 122nm (**NRC**) and 137nm (**NR-**) according to the Zetasizer. Both observed deviations are significant, but would rather increase the activity of **NR+**, hence it is more likely related to OmpF insertion or HRP encapsulation.

It is noteworthy that while TMB changes in absence of HRP, in particular in presence of light, it does not cause the high activity of **NR-**. Thus, TMB is probably better at bypassing the liposome membrane due to its lower polarity.

While the kinetic with TMB is not as appealing as the Amplex Ultra Red kinetic, it does reveal an important aspect: the blocking of the pore is most likely independent of the charge of the enzyme substrate.

4.2.2.3 Uricase
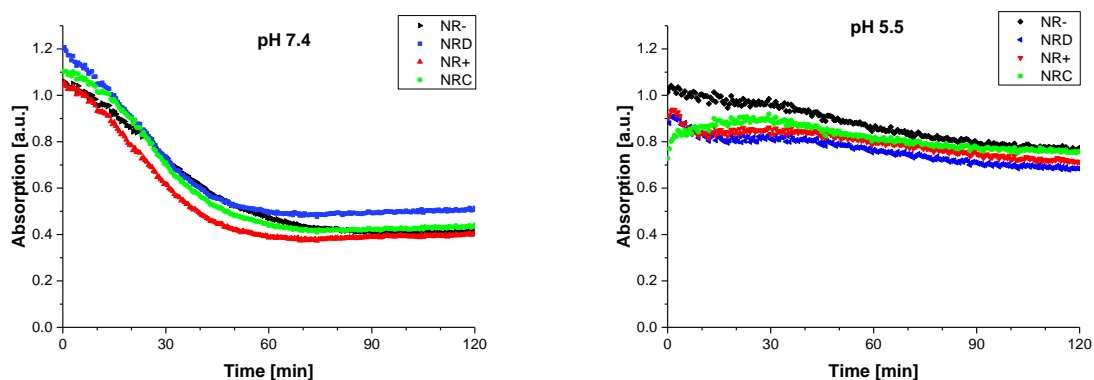
Fig. 33: Kinetics using uricase containing liposomes. NRC featured R270C-Gala3 and NR+ R270C-SH. NRD is NR- formed in presence of the same amount of OG as NR+ during its formation.

The kinetic of uricase consumption (**Fig. 33**) was not conclusive since the difference between **NR-** and **NR+** was not very pronounced and **NRC** remained in between. It is however interesting to note that **NR-** is visibly more active in presence of OG (**NRD**) at pH 7.4 and becomes far more active at pH 5.5.
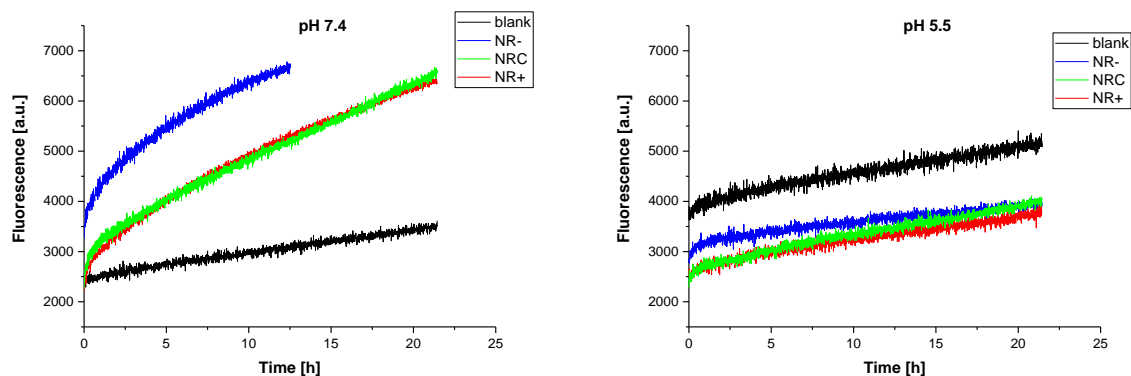
Fig. 34: Kinetics using uricase containing liposomes in presence of HRP and Amplex Ultra Red. NRC featured R270C-Gala3 and NR+ R270C-SH. Blank refers to the buffer with the working solution (uric acid, HRP and Amplex Ultra Red) added.

The first experiment (**Fig. 33**) did not reveal any stimuli responsiveness. Again, **NR-** had a higher activity than **NR+** and **NRC**, although the experiment was performed with the intention to prevent enzyme sticking to the outside of the membranes (since uricase is known to be easy to remove). This indicates that something else must be responsible for the comparatively high activity of the negative control. Later experiments exploring the interactions between HRP and membranes confirmed this suspicion. It rather seems to be that the presence of detergents inactivated the NRs without decreasing the vesicle concentration or significant changes in their size distribution. This would further imply that **NR-** released uricase, or that the vesicles are permeable to uric acid. In addition, it was tested how OG affects the activity of **NR-**, when added in concentrations as found for the insertion of OmpF, though these experiments remained inconclusive (not shown; some more active, some less). The reason, why the blank (**Fig. 34**) had the highest activity at pH 5.5 of all samples remains unknown. Under normal circumstances no oxidation of Amplex Ultra Red was observed in absence of H_2O_2 at pH 7.4 and little to none at pH 5.5. This experiment, however is at a different time-scale (hours instead of minutes, as with regular Amplex oxidation kinetics).

Another odd observation was that **NR-** had only a higher activity at pH 7.4 and this effect was not observed, if uricase was measured directly, without relying on Amplex Ultra Red/HRP. This is probably linked to the fact that the activity of uricase decreases dramatically at low pH whereas the activity of HRP doubles under the same conditions.
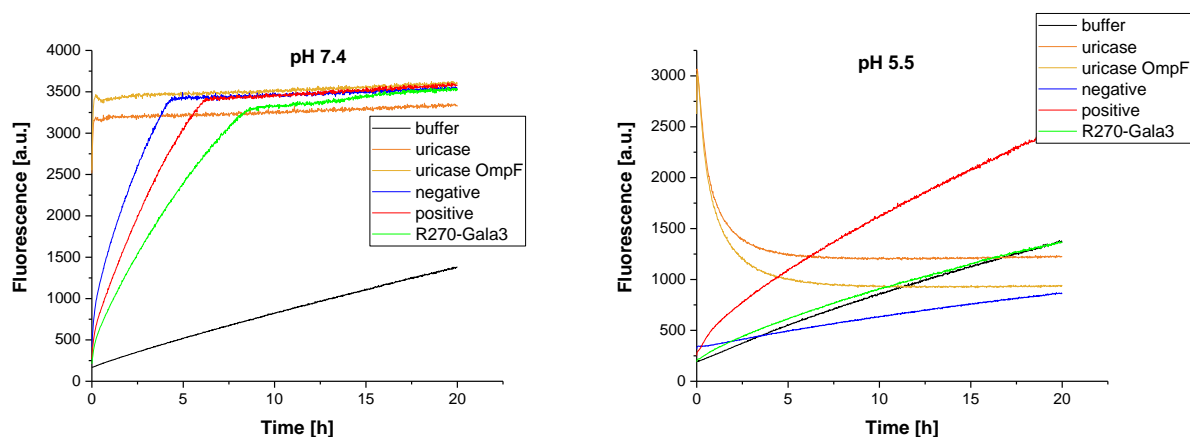
Fig. 35: Repetition of the experiment with the same samples with 10x lower HRP- and Amplex concentration and at 37°C instead of 22°C. Two additional samples were measured: a working solution with uricase added and one with uricase and OmpF solution.

Surprisingly, minor changes of the experimental system changed the picture completely (**Fig. 35**). The intention was to increase the activity of the uricase by doubling the temperature. Since, HRP was far more active than uricase, the HRP concentration was reduced. The same is true for the Amplex Ultra Red concentration, since high concentrations thereof appear to be prone to auto-oxidation and are definitely prone to further oxidation (in particular at low pH and elevated temperatures). Implementing these changes, decreased the measured fluorescence by half, but significantly increased the observed activity of the NRs. This time **NRC** reveals a stimuli responsiveness, unfortunately, **NR-** does too and has still the problem of a too high activity at pH 7.4. Thus, the experiment is not conclusive.

Unencapsulated uricase is highly active under the measured conditions. Full conversion is reached in less than 5 minutes. At low pH, further oxidation of Amplex Ultra Red can be seen and since no new Amplex Ultra Red is formed and since elevated temperatures are used, its further oxidation is drastic. In presence of OmpF and OG the same trends could be seen, but the reaction speed was somewhat higher.

4.2.3 K89R270-Gala3 in polymersomes

4.2.3.1 Amplex

In an attempt to design an experiment with immediate visual feedback for direct comparison and as a self-explanatory image for the publication, a pre-experiment was performed, **NRC** and its controls **NR-**, **NR+**, but also buffer only and free HRP were added into a 96-well plate and the reaction was run by adding the working solution comprised of Amplex Ultra Red and H_2O_2. After the reaction produced visible coloration, a photo was taken. The idea was to allow a different perspective on the different activities of the samples. Unlike later kinetic measurements the concentration of both reagents and the reaction time had to be reduced in order to avoid a signal-overload.
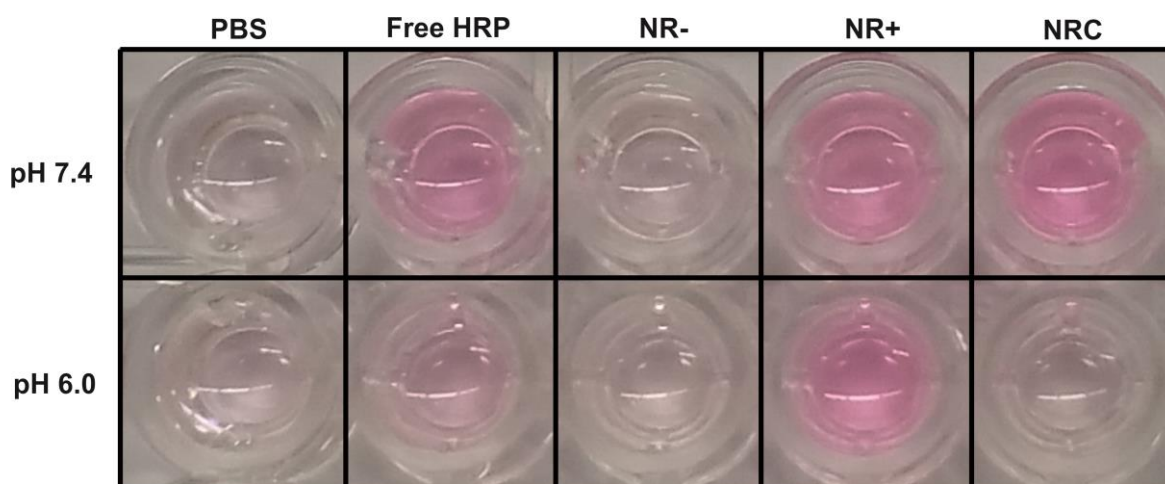
Fig. 36: Oxidation of Amplex Ultra Red in presence of H_2O_2 under different conditions. The pink colour indicates a high concentration of the resorufin derivative being formed. The first sample contains nothing but PBS, Amplex and H_2O_2 and serves as negative control. The second sample contains additional free HRP as positive control. The other three samples contain NRs: NR- without OmpF (revealing low background activity); NR+ with OmpF (revealing the maximal activity) and NRC with stimuli responsive OmpF-C.

As expected, the qualitative evaluation of the colour change (**Fig. 36**) associated with the production of resorufin indicates negligible auto-oxidation of Amplex Red in **PBS** both at pH 7.4 and 6.0, similarly to **NR-** in which the compartment membrane had no OmpF. **Free HRP** had the highest activity of all

samples, with the sample at pH 6.0 being far more active than at pH 7.4. The reason why it is less deeply coloured being that it became red first and started to bleach through further oxidation of resorufin. On the other hand, **NR+** at both pH and **NRC** at pH 7.4 were stained as free HRP at pH 7.4.

The experimental conditions are unavoidably different, due to our less sensitive eye-sight. It still tells a few things: Stimuli responsiveness is visible and it has a low background reaction even in concentrated solutions.
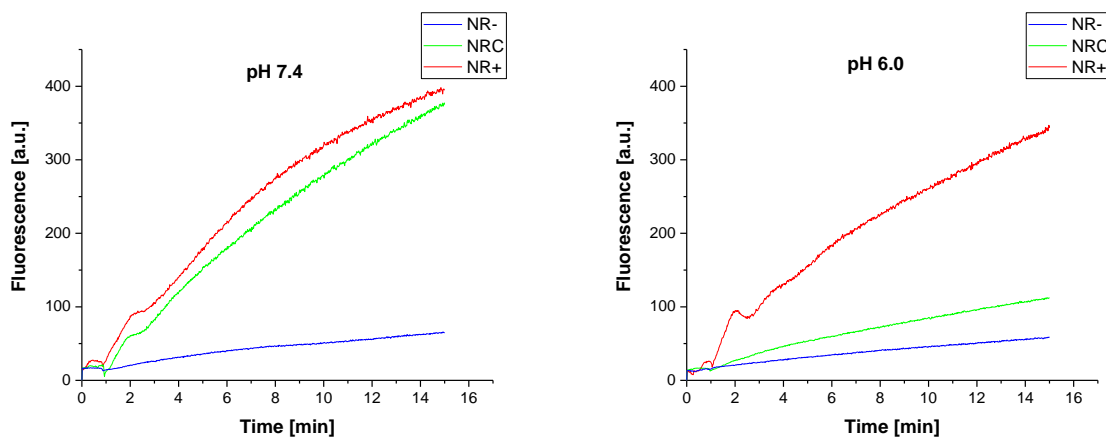
Fig. 37: Amplex Ultra Red conversion kinetics of HRP loaded polymersomes (NR-, blue), HRP loaded polymersomes equipped with K89R270C-Gala3 (NRC, green) and HRP loaded polymersomes equipped with K89R270C-OmpF (NR+, red) at pH 7.4 (left) and pH 6.0 (right).

This experiment (**Fig. 37**) was repeated thrice and the initial activities of **NRC** are represented in **Table 4 (Appendix)**. The initial HRP activities of the NRs (NRC, NR-, NR+) were normalised for a simpler comparison, such that the highest activity of NR+ was set to 100%. (**Fig. 38**). HRP activity values represent the mean value of three independent measurements. The initial slopes taken from each experiment; normalised and volume corrected. Volume correction increased the fluorescence, or more precisely the slope by factor v_t/v_0.
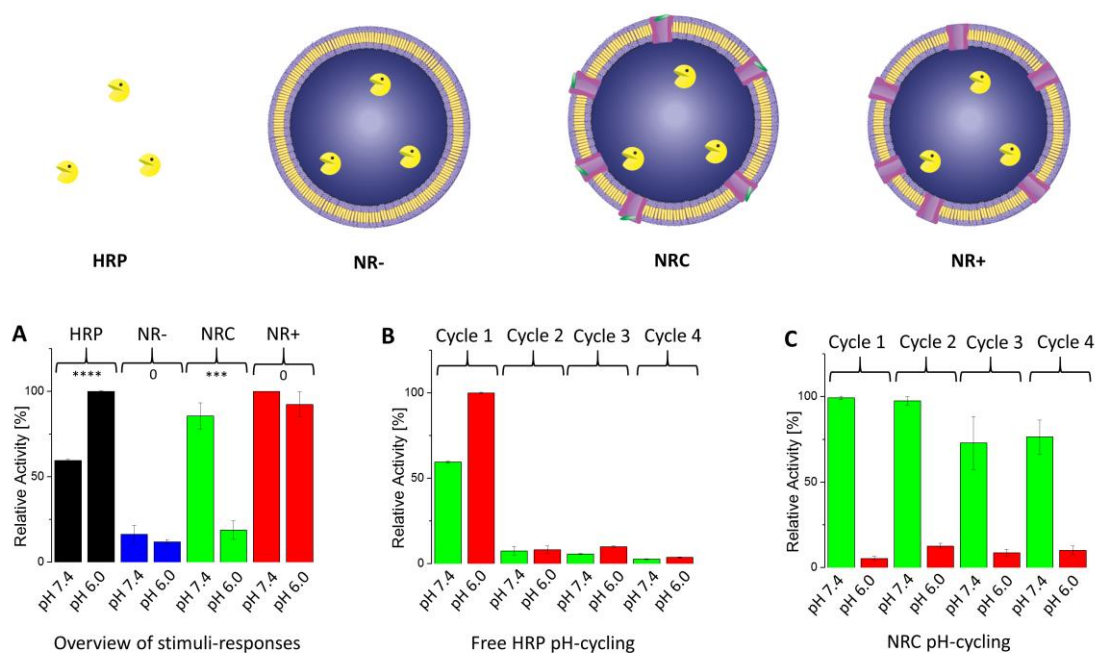
Fig. 38: A) Activity of HRP based on the increase in fluorescence intensity of HRP product, measured at pH 7.4 and pH 6: free HRP (black), NR- (blue), NRC (green), and NR+ (red). The stars indicate the statistical significance (P value; **Table 5 Appendix**). B) Free HRP activity by changing the pH from 7.4 to 6.0 and adding Amplex Ultra Red and H_2O_2 in each cycle. Green: pH 7.4 and red: pH 6.0. C) Bio-valve functionality of OmpF-C when inserted into the membrane of HRP loaded polymersomes (NRC) by changing the pH from 7.4 to 6.0 and adding Amplex Ultra Red and H_2O_2 in each cycle. Green: pH 7.4 and red: pH 6.0. The activities were corrected by taking the volume increase into account.

4.2.3.2 Glucose

The effective detection range of glucose was determined to be 0.5-50µM. Therefore, 100mM glucose were used for encapsulation taking into account that only a fraction might be released within the measuring time. The non-encapsulated glucose was removed via size exclusion. The pH was adjusted by diluting the samples 20x the volume in buffer of the according pH. The experiment started at pH 6.0 and the pH was only then changed to pH 7.4, since experiments with Amplex Ultra Red implied that OmpF-C blocks at pH 6.0. Otherwise, the vesicles would leak already during purification.
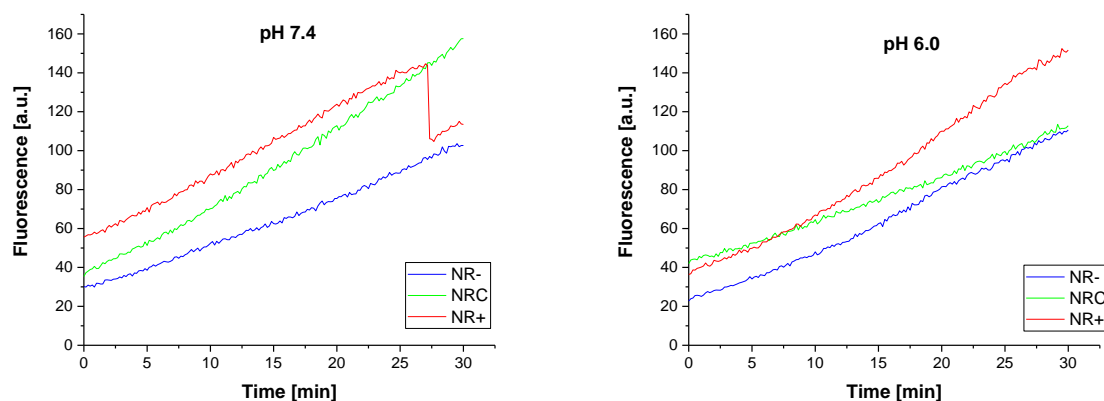
Fig. 39 Glucose release experiments using polymersomes and K89R270C-Gala3 OmpF

The experiment (**Fig. 39**) revealed that vesicles without OmpF (**NR-**) released the least amount of glucose and vesicles with unmodified OmpF (**NR+**) released the most. This comes to no surprise (NRs follow the same pattern of activity), however, it has to be expected that **NR+** releases glucose before the measurement. It could thus release less glucose than **NR-** in case most of the glucose diffused out of the vesicles, before the size exclusion took place, or **NR+** could start with a high initial glucose concentration, which shows only minimal increase in case the diffusion out of the vesicles was slow enough so that most glucose remained encapsulated up to the size exclusion, but the diffusion was fast enough to release most of the glucose before the measurement. Thus, this result gives an indication about the diffusion speed. Due to the expected release, the **NR+** sample was prepared last. The size exclusion took ca. 40min, of which the vesicles eluted during 7-12min and glucose came at 24-30min. Since, the measurement was prepared a soon as the sample eluted, the sample had ca. 15min in which glucose could leak before the leakage was recorded. This corresponds very well to the offset seen in the measurement. However, the detector had apparently, a malfunction at pH 7.4 in case of **NR+** at 28min resulting in a sudden drop of fluorescence. Lastly, since neither glucose nor water were supposed to diffuse through the polymersome membrane at all, thus, regarding **NR-** it has to be assumed that the membranes are by no means perfect.

The vesicles featuring K89R270C-Gala3 (**NRC**) start at the same height as **NR-** and approach the height of **NR+** at pH 7.4 and do the opposite at pH 6.0. The prior indicates that the pores open at pH 7.4. In the blocked-pore state **NRC** was expected to behave more like **NR-** than **NR+**. Since some leakage is still anticipated, a higher offset was to be expected and a somewhat higher slope than in case of **NR-**, thus resulting in **NRC** diverging from **NR-** further with time. Instead the **NRC** converges with **NR-**. This indicates that the rate of leakage was higher before the measurement (for unknown reasons). To complicate things further, **NR-** at pH 7.4 was remeasured resulting in an overlapping curve indicating that **NR-** stored at pH 6.0 did not release any significant amount of glucose during the 30min between

the measurements (the first measurement featured a jump too). These effects might be attributed to the fact that the fluorescence increase might not represent the increase of the glucose concentration at the time, but the conversion of glucose through the GOX.

In order to prove that all three samples (NR-, NR+ and NRC) had the same amount of glucose (same concentration inside and same vesicle concentration) a third row was measured in which all samples had 0.5% TritonX added at pH 7.4. This measurement (**Fig. 40**) proved that all samples including **NR+** had glucose encapsulated in fact, **NR+** and **NR-** had approximately the same glucose concentration, but **NRC** had ca. 2x as much. Since the vesicles scattered light to the same degree, it has to be a higher encapsulation efficiency.
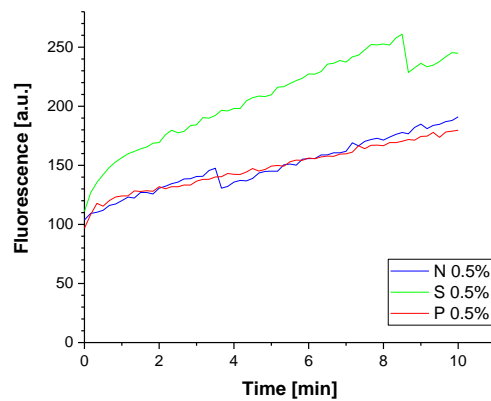
Fig. 40.: The three samples with the vesicles destroyed and the glucose concentration measured thereafter.

4.3 HLG4

4.3.1 HLG4 in DSPC-liposomes

4.3.1.1 Amplex
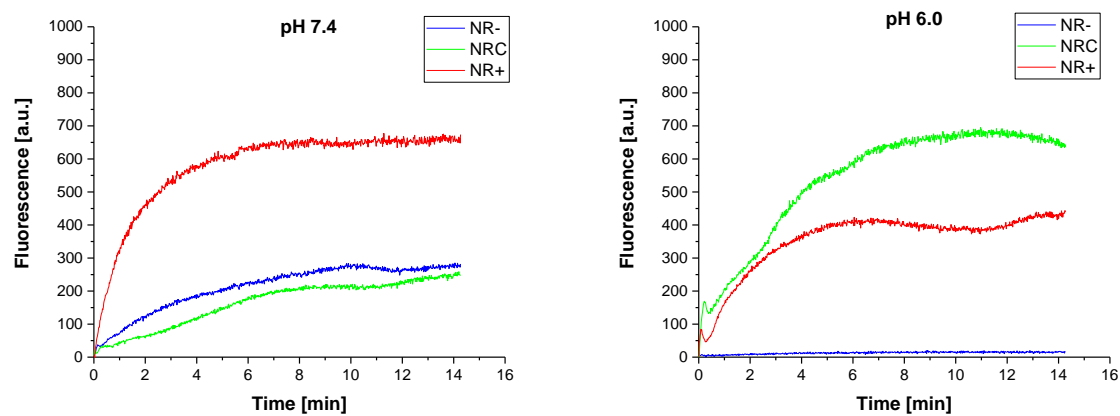
Fig. 41: Amplex Ultra Red kinetic using NRs featuring K89R270C-HLG4 OmpF in DSPC liposomes.

The experiment (**Fig. 41**) reveals a clear stimuli responsiveness of **NRC**. Moreover, the HLG4-peptide has exactly the opposite effect as the Gala3-peptide. The curves are not particularly smooth since the stirrer of the cuvette failed.
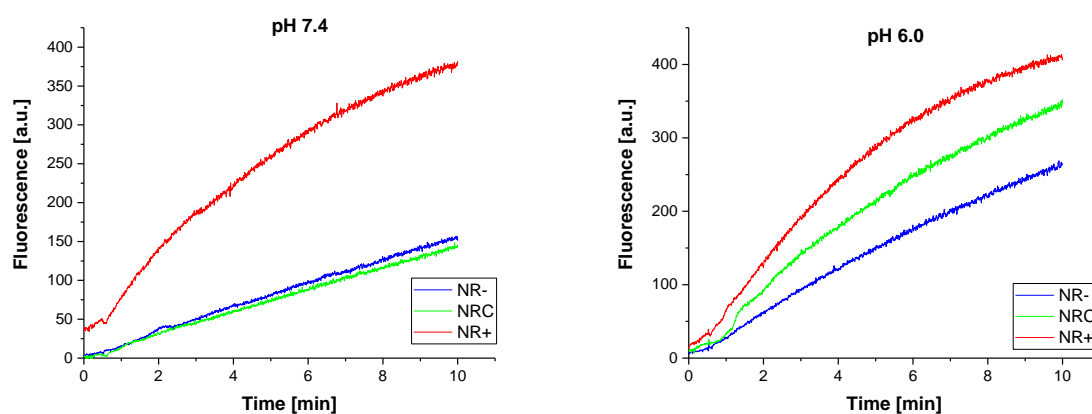
Fig. 42: Amplex Ultra Red kinetic of a new batch of HLG4-featuring NRs.

The repetition (**Fig. 42**) confirmed the result although the magnitude of the stimuli response varied significantly compared to the prior measurement.

4.3.1.2 TMB
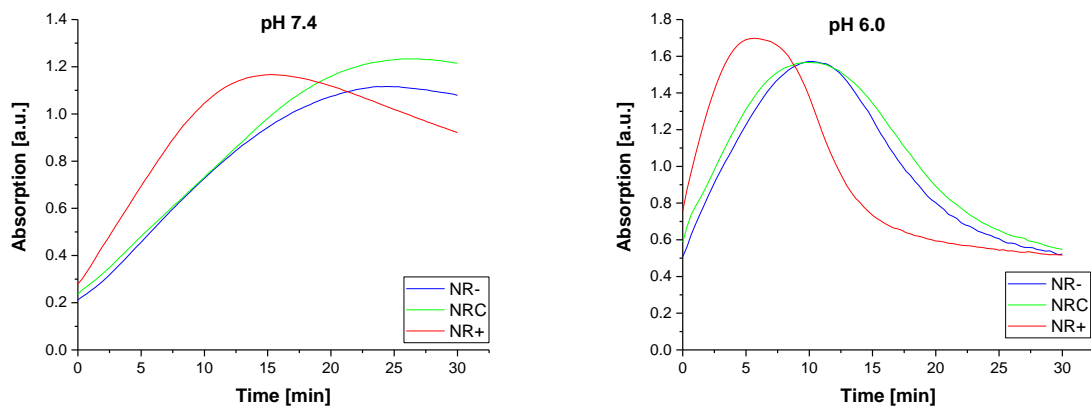
Fig. 43: TMB kinetic using the same samples as in **Fig. 42**.

Unlike the Amplex Ultra Red kinetic no stimuli responsiveness could be observed (**Fig. 43**). At both pH the NRs remained inactive. This is in sharp contrast to the Gala3-variant, which was tested in the same measurement (see **Fig. 31** and **Fig. 32**).

Since the same sample was measured in the Amplex Ultra Red kinetic, it cannot be explained by poor insertion of OmpF. It could be though that TMB interacts with HLG4 by charge repulsion, whereas Gala3 blocked Amplex Ultra Red and TMB predominantly due to steric hindrance.

4.3.2 HLG4 in polymersomes
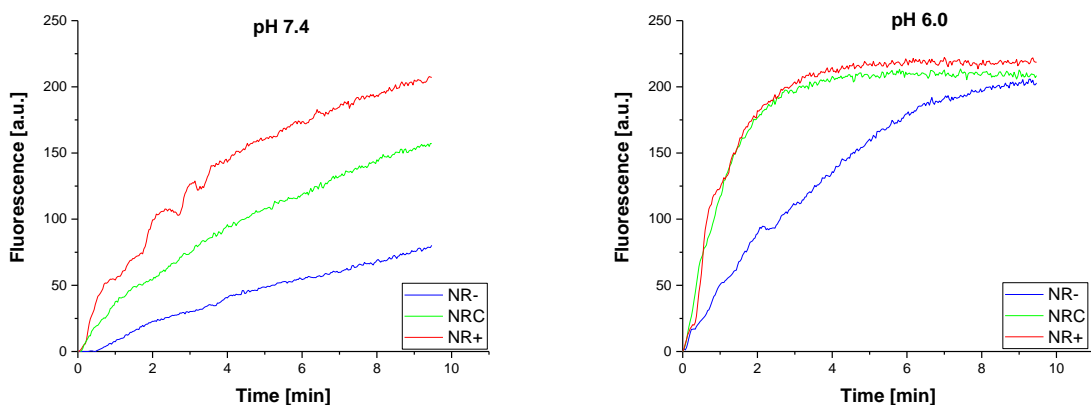
Fig. 44: Amplex Ultra Red kinetic featuring polymersome NRs with K89R270C-HLG4.

While **NRC** clearly does not display a closed state at pH 7.4 it certainly opens its pores at pH 6.0, as the activities of **NRC** and **NR+** overlap (**Fig. 44**). Unfortunately, something went wrong with **NR-** at pH 6.0. It appears as the vesicles were disintegrating at the beginning of the measurement. Before the measurement all samples had vesicles in the range of 120nm and none stood out in terms of size-distribution (0.25). However, for some reason **NR-** had a 4x lower ability to scatter light than the other samples, which would hint an unusually low vesicle concentration. Adding 4x more **NR-** would result in the same activity as **NRC** at pH 7.4.

5 Conclusion

5.1 Choice of the Assay

All the dye-release systems were not working, with the exception of carboxyfluorescein. However, it still interacted with the vesicle membrane and leaked fast making it impossible to measure the begin of the release. The only other release-based system worth mentioning, is Glucose in combination with enzymes for detection. Whilst being more complex, it appeared to be a far more stable system.

The enzyme-based systems were much more reliable experimental platforms, but also much fickler in their nature, in particular towards pH-changes. There are far more parameters to consider than in case of dye-release systems, but, if all requirements are met, then the systems proved to be very stable providing significant experimental results. Of all the considered enzymes HRP proved to be the best choice, despite the difficulty in removing free enzyme. In particular, due to its stability and available enzyme substrates, it proved superior to other candidates. The only other enzymes worth mentioning, had still to be used in conjunction with HRP: uricase and glucose oxidase. Both allow a NR- that has a very low background activity but complicate the experimental set-up. In case of GOX, it offers the additional advantage that the diffusion is not influenced by charge (and by being much faster and less pH-dependent than uricase). As enzyme substrates for HRP, Amplex Ultra Red stood out, due to its size, stability and its ability to be detected via FCS. TMB was the second-best choice (due to its light and pH-sensitivity) and offered a substrate with the opposite charge. This is particularly interesting, since it could shed light on a general problem, that is not a technical problem but a shortcoming of the experimental design, which was not discussed yet: the observed stimuli response, could be the result of different mechanisms. The OmpF pore could be blocked for the substrates either by steric hindrance (as hoped for) or by charge repulsion. The latter would probably only block a specific charge, unless the opposite charge interacts strongly enough to block the pore. However, there are few comparable

enzyme substrates available with opposite charges to verify this mechanism (such as Amplex and TMB). There are no pre-fluorescent enzyme substrates that remain uncharged and water-soluble. This is where sugars become relevant substrates.

5.2 Experimental results

The HRP-Amplex Ultra Red system gave over all the best results, however for some reason it often occurred that NR- was the most active sample despite being the negative control (mainly Amplex Ultra Red experiments, but also uricase and uricase&Amplex). Obviously, results of such experiments could not be used. Contributing to the confusion was the finding that **NRD** produced in the same batch as **NR-** had the lowest activity, despite the fact that **NRD** were introduced to see, whether the presence of OG, as in the other samples **NRC** and **NR+** increases the permeability or damages the vesicles, both would be expected to increase the activity.

As mentioned in a prior chapter, detergents do negatively affect vesicle formation, the homogeneity and stability of vesicles. Still, in low concentrations detergents are tolerated, especially after removing as much as possible by dialysis.

NRD was later relabelled **NR-**, since all relevant samples had contact with detergents. At the beginning of the experiments relying on film rehydration, 0.025% OG was added to the DSPC mix directly, whereas in the later experiments using polymersomes 0.5% OG (as used for stabilising OmpF) was dialysed off and then added to the polymer film, resulting in a much lower final OG concentration and better representing the actual OG interference with the membrane, since the OmpF samples were also dialysed against buffer, whereas in the earlier experiments the OmpF samples were used directly, containing 0.5% OG or more (since OG micelles can be concentrated, when OmpF is concentrated).

While this alteration of the negative control formally solves the problem, it would be still interesting to know what exactly causes this behaviour, which occurred both with liposomes and polymersomes. Especially in case of liposomes low pH and the use of TMB increased the activity of **NR-** considerably. Also, the activity of **NR-** increased over time. In case of liposomes produced via detergent removal within several hours (at room temperature), in case of liposomes formed from the DSPC-mix via film rehydration within 6 days (at 4°C) and in case of polymersomes within 14 days (at 4°C). This is quite noteworthy, since the latter two appeared stable for at least 3 months at room temperature, or 12h at 40°C, according to light scattering and TEM.

It was thus tested, if HRP binds to the membrane, by adding it to preformed vesicles and then dialysing the mixture. Irrespective of whether liposomes or polymersomes were used, little residual activity remained. In case of DSPC-liposomes, it was observed that heating the sample and (paradoxically[38]) the absence of detergents increased the residual activity. In case of polymersomes, the difference between **NR+** and **NR-** in terms of activity was around 11x. Vesicles that were in contact with HRP on the outside had 5x lower activity than NR-, where HRP was encapsulated.

Concluding it can be said that the residual activity of NR- stems from the permeability of the membrane itself, or from cracks or other defects within it. While the less polar TMB had a higher residual activity than Amplex Ultra Red, even very polar substances like glucose were leaking from vesicles without OmpF.

The autoxidation of Amplex in absence of HRP but in presence of H_2O_2 is not visible at pH 7.4 but in a similar range at pH 6.0 comparable to the activity of the vesicles that had been only superficially exposed to HRP prior the dialysis step.

Another noteworthy observation was that the purification of OmpF determined whether or not OmpF could be inserted into vesicle membranes. The OmpF extracted with Octyl-POE could be used with POPC/POPS and detergent removal, whereas OmpF extracted with the more efficient OG could not, but allowed insertion in DSPC-mix and polymersomes, when the OG content was kept at a minimum. This speaks for the importance of coextracted bacterial lipids in the ternary mixture. It also showed again that the DSPC mixture liposomes are closer in their behaviour to polymersomes, which is probably explained by the fact that they become almost rigid at room temperature.

The activity of free HRP increased from pH 7.4 to pH 6.0 about 2x and was even higher at pH 5.5 (2.5-3x), but the experiments reproducibility was poor. As it turned out, HRP became irreversibly deactivated below pH 5.0. Cycling pH changes between 7.4 and 6.0 revealed that the free enzyme lost its activity very fast. Already after the first full cycle of pH change, a drop in activity of the free HRP up to 12.5% of its initial value was observed, and it further decreased after the second complete pH change cycle. The decrease in enzymatic activity of the free HRP was mainly due to the adjustment of pH with small amount of concentrated HCl in order to avoid dilution (diluting a sample of 10mL to only 10.18mL). A temporary, local pH decrease below the final pH probably deactivated the enzyme before the pH could equilibrate through homogenisation of the solution.[3] Remarkably, this jump in activity did not carry over to NRs with unmodified OmpF. In some early (less reliable) experiments it was still

---

[38] Detergents were expected to make the membrane more fluid, like heating the system, allowing HRP to better interact with the membrane or even become encapsulated, but instead detergents caused predominantly a decrease in vesicle concentration and hence less chance of HRP being dragged along with vesicles.

observed, but to a lesser degree (<50% increases) in liposomes. It is less surprising that the vesicles gave some protection against the pH changes, but it was anticipated that it would come at the cost of activity, due to a lower number of HRP and diffusion limitations, but HRP was apparently operating at its fullest potential irrespective of the pH.

Oligo(acrylic acid)-conjugates were investigated using both lipo- and polymersomes and using Amplex Ultra Red-HRP, but the results were not conclusive. It seems that *oligo*(acrylic acid) of any length could block the pore independent of the pH and that the degree depended mostly on the degree of labelling and not on the length.

Gala3-conjugates worked perfectly well as proven in POPC/POPS-liposomes, DSPC-mix liposomes and polymersomes. The experiments with liposomes had a higher statistic error and **NRC** did not close as much as in polymersomes thus **NRC** never overlapped with **NR-**. In polymersomes, **NRC** changed from a perfectly open state as **NR+** to a perfectly closed state as **NR-** and the pH dependent change was reversible for multiple cycles. TMB gave the same result as Amplex Ultra Red although it has the opposite charge indicating that the pore is blocked rather by conformational changes than changes in its charge. Tests releasing glucose and detecting it via Glucose oxidase and HRP revealed the same trend offering additional proof, since glucose is uncharged and polar. The pH-responsiveness was also confirmed using Uricase in combination with HRP, but the experimental error was high and the trend rather weak.

HLG4-conjugates provided the opposite stimuli response according to HRP-Amplex Ultra Red experiments, but not according to TMB, which indicates that the oppositely charged TMB apparently interacted with the peptide.

6 References

[1]   W. Straus, *Histochemistry* 1981, 73, 39-47.
[2]   M. T. Neves-Petersen, S. Klitgaard, A. S. L. Carvalho, S. B. Petersen, M. R. Aires de Barros and E. P. e Melo, *Biophys J* 2007, 92, 2016-2027.
[3]   a) K. Bamdad, B. Ranjbar, H. Naderi-Manesh and M. Sadeghi, *EXCLI Journal* 2014, 13, 611-622;
b) K. Chattopadhyay and S. Mazumdar, *Biochemistry-Us* 2000, 39, 263-270.
[4]   *Amplex® Red Enzyme Assays*, https://www.invitrogen.com/site/us/en/home/brands/Molecular-Probes/Key-Molecular-Probes-Products/Amplex-Red-Enzyme-Assays/amplex-red-technology-overview.html, accessed: 2016.
[5]   *Peroxidase Enzymes*, https://www.sigmaaldrich.com/life-science/metabolomics/enzyme-explorer/analytical-enzymes/peroxidase-enzymes.html, accessed: 2016.
[6]   *TMB Substrate Solution*, https://www.thermofisher.com/order/catalog/product/N301, accessed: 2017.
[7]   L. Navapour, N. Mogharrab and M. Amininasab, *Plos One* 2014, 9, e109062.
[8]   a) P. Tanner, O. Onaca, V. Balasubramanian, W. Meier and C. G. Palivan, *Chemistry – A European Journal* 2011, 17, 4552-4560;
b) P. Tanner, V. Balasubramanian and C. G. Palivan, *Nano Lett* 2013, 13, 2875-2883.
[9]   F. C. Smith, *Biochem J* 1928, 22, 1499-1503.
[10]   A. Anderson and S. Vijayakumar, *Purification and Optimization of Uricase Enzyme Produced by Pseudomonas aeruginosa*, 2011.
[11]   M. le Maire, P. Champeil and J. V. Moller, *Bba-Biomembranes* 2000, 1508, 86-111.
[12]   a) A. M. Seddon, P. Curnow and P. J. Booth, *Biochim. Biophys. Acta, Biomembr.* 2004, 1666, 105-117;
b) J.-L. Rigaud and D. Lévy, *Reconstitution of Membrane Proteins into Liposomes*. In Methods Enzymol., Academic Press: 2003; Vol. Volume 372, 65-86.

VI Theoretical calculations

VI Theoretical calculations

There were many things that would have been interesting to know in context of this thesis, but either impossible to measure, or not possible to measure within the constraints of this thesis. These questions can be categorised within two groups: composition and properties.

Regarding composition, it would have been nice to know how many vesicles are present within 1mL of sample and how the nanoreactors actually look like, in particular how many enzymes and OmpF are found per vesicle. This would allow comparing NRs with free enzyme and discuss diffusion limitations, due to pore-size and total percentage of the vesicles-surface that is actually hollow.

Regarding the properties, the questions revolve around three aspects:

1) The behaviour of the enzyme: Why does it become more active at pH 6.0? Why do NRs stay active at pH 7.4? What exactly deactivates the enzyme in free solution and why does it not apply to NRs? Do enzymes aggregate at certain pH, or do they interact with the membranes and how?

2) What explains the residual activity of the membrane? Does the substrate diffuse through it, or only through cracks? How much of the residual activity is caused by release of enzymes from vesicles? Why do liposomes and polymersomes behave differently to detergents? What mechanism weakens the membrane? How do detergents interact/distribute themselves in the system?

3) How does the stimuli response actually work? Is it due to changes in charge (repulsion), or conformation (steric hindrance)? Do the stimuli responsive groups interact with the OmpF-pore or the substrate?

These questions are definitely worth discussing even without hard data. Some of these questions can be answered with educated guesses and by excluding the impossible. However, more value can be added to the discussion by estimating some of the properties that could not be measured during this PhD.

1 Estimating the composition of the NRs:

1.1 Version A: Estimate based on surface

If all the PMOXA$_6$-b-PDMS$_{44}$- b-PMOXA$_6$ formed 125nm diameter polymersomes and all the OmpF was integrated in it, we obtain following ratio of OmpF to polymer:

Polymer: $\frac{100\mu L*50g/L}{4488.43g/mol} = 111nmol$ (1a)

OmpF: $\frac{20\mu L*0.8g/L}{39333g/mol} = 407pmol$ (1b)

Thus, (dividing **1a**, through **1b**) for every OmpF, there are 2738 polymers surrounding it. Assuming that polymers require a circular area of 2Å in diameter and OmpF a circle of 20Å in diameter, within the surface of the vesicle, we can calculate how much of the surface belongs to OmpF:

Surface OmpF: $407pmol * N_A * 31.4\text{Å}^2 = 7.7cm^2$ (2a)

Surface polymer: $111nmol * N_A * 3.14\text{Å}^2 = 210.6cm^2$ (2b)

Percentage: $\frac{7.7cm^2}{7.7cm^2+210.6cm^2} = 3.7\%$ (2c)

With the surface of a 125nm diameter vesicle being 49062.5 nm^2, one can estimate the number of vesicles in solution per 1mL:

Number of vesicles: $\frac{218.3cm^2}{49062.5\text{nm}^2} = 445 * 10^9$ (3a)

Thus, the maximal number of OmpF per vesicle is: $\frac{407pmol*N_A}{445*10^9} = 550.5$ (3b)

In our group, fluorescently labelled OmpF has been used to determine how many OmpF molecules are inserted in reality.[1] In this publication, the same polymer and OmpF insertion procedure were used, with the small difference that 80μg OmpF instead of 16μg were used. They found that on average 55 OmpF per 100nm diameter vesicle were inserted. In relation to the 1760 OmpF molecules theoretically present in a 100nm vesicle, the insertion efficiency is:

$\frac{55}{1760} = 3.1\%$ (4)

Thus, for a 125nm diameter vesicle, with theoretically 550.5 OmpF, one can assume 17.2 OmpF to be inserted.

1.2 Version B: Estimate based on density

Assuming that the vesicle-membrane has the same density as dry ABCP, which is slightly heavier than water (ρ = 1.1 g/L), the number of polymers per vesicle can be calculated. The membrane volume is defined as:

$$V_{ves} = V_{(out)} - V_{(in)} \tag{5}$$

The radius of the sphere is 125/2 nm and for the internal radius the membrane thickness of 10nm has to be subtracted.

$$V_{ves} = \frac{4}{3}\pi \left(\left(\frac{125}{2}\right)^3 - \left(\frac{125}{2} - 10\right)^3 \right) \tag{6}$$

Now, the number or ABCPs per vesicle can be calculated using the molecular weight of the ABCP of M_{pol}= 4488.43 g/mol:

$$N_{pol/_{ves}} = \rho \frac{V_{ves}}{M_{pol}} N_A \tag{7}$$

The number of polymer chains/vesicle is according to (7): 6.707×10^4 pol/ves. The number of vesicles in solution by considering that all polymer chains are involved in vesicles formation is obtained as 1.4353×10^{12} vesicles.

The maximum number of OmpF/vesicle, $N_{OmpF/_{ves}}$ is obtained by dividing the amount of OmpF (407 pmol) by the number of vesicles.

$$N_{OmpF/_{ves}} = 245 \text{ OmpF/ves}$$

As the insertion procedure and conditions are similar to that used by Einfalt *et al* when OmpF has been fluorescently labelled and determined by FCS,[1] we calculated the number of OmpF/ves taking into account that the initial amount of OmpF has been significantly lower (16µg OmpF instead of 80µg OmpF[1]). We obtain 11 OmpF/ves, which is indicating that in the present conditions there is a lower number of porin/polymersome.

1.3 Comparing both variants:

Table 2: comparison of the results

Estimate:	A	B
Vesicles in solution	$4.45 \cdot 10^{11}$	$1.44 \cdot 10^{12}$
Theoretical no. OmpF/Vesicle:	555	245
Assuming 3.1% inserted:	17.2	11
Surface belonging to OmpF	0.13%	0.06%

Both estimates yield surprisingly similar results with all values in the same order of magnitude and the maximum deviation at the theoretical number of vesicles (3.2x) and the smallest at the number of OmpF per vesicle (1.6x).

1.4 Estimating the encapsulation efficiency of HRP from its activity:

Once the HRP/Amplex Ultra Red was optimised with free HRP, it was tested with **NR+**. Since in most encapsulation experiments only 1-10% are encapsulated and most of the solution never becomes enclosed in vesicles, 100 0000x the concentration needed for optimal results with free HRP was used. Experiments with free HRP had an activity of 10a.u./min at pH 7.4 and 32a.u./min at pH 6.0 (1000x less HRP than used for encapsulation). Experiments with **NR+** (polymersomes) had ca. 30a.u./min for both pH. Ignoring diffusion limitations or other effects of encapsulation on the enzymes activity, one has to assume that 0.1% of the enzyme has been encapsulated.

Taking diffusion limitations into account one could assume a far higher encapsulation efficiency, but the fact that the activity was independent of the pH indicates that other effects have to be taken into account too which result in the enzyme operating at its fullest potential even at pH 7.4. Thus, the initially assumed 1-10% encapsulation efficiency are perfectly plausible.

As a side-note: both the **liposomes** formed through detergent removal and from film-rehydration had similar activities (max 400 a.u./10 min), despite the fact that the liposomes had probably 10x more vesicles per sample. Why they did not have a higher activity cannot be said with certainty but will be discussed in the following chapter.

1.5 Estimating the number of HRP per vesicle from the initial concentration:

The HRP concentration was 0.2 g/L, or 4.55µM (44kDa). Assuming the same concentration of HRP inside vesicles as outside, the number of HRP per vesicle can be calculated:

$$N = V_{Ves} \cdot c_{HRP} \cdot N_A \qquad (8)$$

As calculated above (6), V_{ves} for a 125nm diameter vesicle would be $5.887 \cdot 10^{-19}$ L. Thus, the number of HRP per vesicle would be 1.613 and only assuming 100% encapsulation efficiency.

1.6 Encapsulation efficiency: conclusion

It was intended to actually measure the HRP concentration, via FCS, but it turned out to very challenging, for mainly two reasons:

1) Of the few Lysines on the surface only 1 or two appeared to bind reactive dye.
2) The excess of dye on the other side could only partially be removed (independent of SEC, dialysis, biobeads etc.)

Thus, it was hard to tell how many dyes are encapsulated. Moreover, it would still be required to label the vesicles themselves in order to know the number of vesicles, in case some do not contain HRP. The only alternative would have been to destroy vesicles and then measure the HRP activity again, which would require that all enzymes are released and no HRP enzyme becomes deactivated, by the harsh treatment.

Later, the labelling was done successfully by a colleague (using dozens of consecutive centrifugal filtrations in order to remove the non-covalently bound dye) with the result of 3-4 HRP molecules per 100nm diameter vesicle.[1]

The estimate based on the activity indicated that the HRP concentration decreased 1000x, indicating a very low encapsulation efficiency (0.1%).

Contrary to it, the concentration-based estimate limits the number of HRP per vesicle to 1.6, which would require an encapsulation efficiency of 100% to even get close to the number of HRP found in FCS.[2]

The latter estimate heavily implies that a significant number of vesicles are actually empty. FCS cannot detect empty vesicles, unless the vesicles themselves are labelled with a different FCS-active dye. Thus, the latter estimate is plausible.

Regarding the first estimate, it has to be said, that a loss of 99.9% of the HRP is still plausible. In order to understand this, it has to be considered what encapsulation efficiency actually means. If it is defined as the ratio of the concentration of enzyme found within the vesicle divided by the concentration of enzyme used during vesicle-formation, then it does not say anything about the total concentration of HRP in solution.

As discussed above (equations **3a**, **6, 7 and 8**), we can assume that we have around $1 \cdot 10^{12}$ Vesicles per 1mL and that each vesicle has an internal volume of $5.887 \cdot 10^{-19}$ L. This would imply that less than 0.06% of the sample solution is inside the vesicles. Thus, the majority of HRP is lost after purification of the vesicles. The 0.06% is actually surprisingly close to the estimated encapsulation efficiency of 0.1% based on the comparison of the enzyme activities.

2 Theoretical calculations of Gala3-peptide protonation

Neglecting the polarity of the environment and the interaction with other acid or base groups of the protein (which can have a significant effect on the acidity[3]), the degree of protonation can be estimated with a variation of the Henderson-Hasselbalch equation:

$$pH = pK_A + lg\left(\frac{[A^-]}{[HA]}\right) = K_A + lg\left(\frac{1-\theta}{\theta}\right) \ (9)$$

It usually describes the pH as a function of the dissociation constant of the acid and the present concentration of the acid and corresponding base. The relation of those two concentrations can be described by the degree of protonation θ. Solving the equation for this parameter gives:

$$\theta = \frac{1}{1+10^{pH-pK_A}} \ (10)$$

The pKa value can be estimated. For carboxylic acid groups the pKa is typically between 4 and 5. According to computations using Marvinsketch, it is at the lower end:
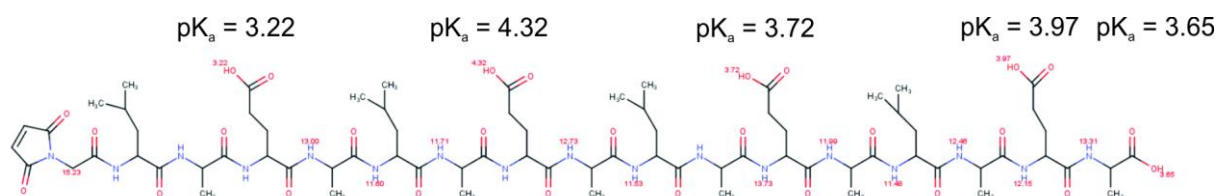
Fig. 2: pKa values of individual amino acid residues of Gala3 peptide calculated with Marvinsketch 15.10.19; the pI was calculated to be 0.16.

Taking an average pKa for the carboxylic side-chain of Glu of 4.25 and 9.0 for the aromatic alcohol groups of Amplex and 6.4 for the oxidised product (both estimated with MarvinSketch version 15.10.19) the following protonation can be expected:

Table 4: estimation of the protonation degree of an individual acidic group (θ) depending on the pH and pKa (Calculated by Marvinsketch 15.10.19) Substrate: Amplex Ultra Red, Product: Resorufin

	pKa	Protonation (%)		pH required for % of protonation	
		pH 6.0	pH 7.4	10%	90%
Glu	4.25	1.75	0.07	5.2	3.3
Substrate	8.9	99.87	96.93	9.9	7.9
Product	6.35	69.12	8.18	7.3	5.4

Regarding the substrate, Amplex (**Table 4**), one can assume that the fluorophore precursor is **protonated until** it is **oxidised** (>96% protonation at both pH). It then becomes **predominantly negatively** charged (91% at pH 7.4) unless the pH is changed to 6.0 at which point only 21% are charged.
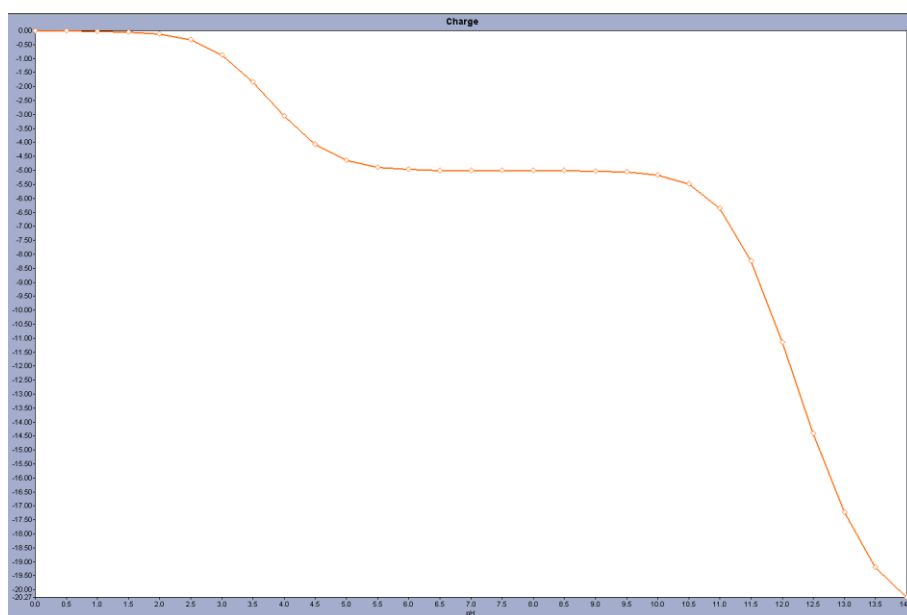
Fig. 3: Protonation-degree of Gala3 peptide as a function of the pH calculated with Marvinsketch 15.10.19

From **Table 4** and **Fig 3**, it can be assumed that the peptide will never be completely uncharged, especially at the investigated pH-range the peptide will vastly remain negatively charged. According to **Table 4**, even at pH 5.2 90% of the carboxylic groups will be deprotonated and it would take pH 3.3, to reduce it to 10% (inverse numbers of the table, since it depicts protonation).

The number of peptides, with complete change of protonation state is exponentially lower, regarding the number of acid groups:

Chance that no acid group is protonated: $= (1-p)^N$ (11a)

Chance that n acid groups are protonated: $= \binom{N}{n} p^n \cdot (1-p)^{N-n}$ (12b)

N: number of acid groups in peptide; n: the number protonated acid groups; p: the probability that the individual group is protonated.

3 Discussion

3.1 Composition of nano-reactors

Regarding the composition of the nano-reactors, pretty detailed calculations can be made giving interesting estimates, with implications that will be discussed later in this chapter. The main take-away is that the NRs appear to have only few HRP encapsulated and few OmpF molecules inserted, both of which should significantly slow down the substrate conversions, yet this was not observed experimentally.

Both estimates regarding the OmpF-ABCP-ratio ignore that some of the ABCP-film remains undissolved (depending on the length of the ABCP probably between 5-40%) and that nearly all vesicle samples feature micelles or even aggregates as side product. These two facts probably explain why only a small fraction of the OmpF is actually inserted in vesicles. In case the MP is added to the solution, as other MPs would be, then the percentage has to be assumed even lower due to precipitation and denaturation. OmpF however, does not denature that easily and is already surrounded within a matrix of ABCP, which increase the likelihood of the OmpF being dragged along with the ABCP rather than precipitating out of solution.

For these reasons, the question arises, why not use more OmpF and HRP, or use more concentrated solutions. In order to improve the number of HRP per vesicle, one could increase the concentration of the enzyme, but above 1g/L its solubility becomes a problem and experimentally it did not make sense, since the activity was more than sufficient. Alternatively, the ABCP-concentration could be increased or the sample volume decreased. All of these changes result however in thick solutions, which behave differently in vesicle-formation, resulting in more aggregates and micelles and increasing the need for higher OmpF-concentrations and thus amounts.

It was never tested how thick an OmpF solution could be made. Extracted OmpF came often in a concentration range between 0.2-0.8 g/L and for practical purposes the solution was concentrated to 0.5-1.2g/L. The concentrating process is however far less trivial than one may assume, as detergent micelles, the remaining DNA (after digestion), cell debris and in particular lipids and detergents dragged along with OmpF accumulate as well. This increases the viscosity of some samples considerably and makes the removal of detergents much harder. Lastly, OmpF-peptide conjugates were mostly produced in 1mL batches due to the price of the synthesised peptides. Smaller volumes would have been impossible to handle regarding dialysis tubes, thus further concentrating samples was often impossible. This explains why the most important batch K89,R270C-Gala3 OmpF was inserted in 4x lower concentrations as the same mutant in my colleagues experiments.[2] The

unmodified K89,R270C-SH OmpF was not the limiting factor, but having only 0.8mL of 0.5g/L K89,R270C-Gala3 OmpF, when the batch of the Gala-peptide was used up and it took 5 attempts to order the peptide as the purification of this peptide is challenging.

3.2 Activity of the nano-reactors

It has been observed previously that confining enzymes does not only protect them, but enhances their activity.[4] We can assume that our 125 nm diameter polymersome have about **10-20 OmpF molecules**/vesicle corresponding to 0.06-0.13% of the vesicles surface and 1.6 molecules of HRP inside. In addition to these restrictions to the reaction, we have to take into account that the OmpF pore is in fact even 50% smaller and allows only molecules with less than 600 Da to pass through. If it was about a filter, then the pores of the membrane should be at least 2x the molecular weight cutoff of the substrate that should pass through and this does not take into account any charge interactions, or the orientation of an oblong molecules relative to the pore. Amplex Ultra Red is about 300 Da, but the Gala-peptide attached to the pore is itself already 1322.4 Da. This 12-amino acid long peptide would be 48Å long when fully stretched. That is 4x the actual pore size. For these three reasons, it has to be expected that OmpF does slow down diffusion significantly.

Considering the few and small holes on the vesicle surface, it has to be assumed that it takes thousands of collisions until one substrate molecule diffuses in and then on the inside it must hit the enzyme and it has to collide with its active centre at the right orientation. The enzyme kinetic was investigated in FCS indicating that at any given point in time only 1.5 molecules of the fluorescent product are within the vesicle.

All that being said, one should anticipate a lower activity due to the diffusion limitation, but the diffusion limitation is a blessing in disguise for three reasons:

1) Upon pH change droplets of acids or base are dispersed in the buffer solution. During the time needed for homogenisation, a significant part of free enzyme would come into contact with these local zones of extreme pH which in turn will deactivate the enzymes permanently. In case of NRs, it takes some time for the inside and outside of the vesicle to equilibrate, thus giving the solution the time required for homogenisation, thus the encapsulated enzymes are not exposed to the extreme pH and last over much more cycles.

2) Once an enzyme substrate manages to diffuse into a vesicle, it can collide countless times with the vesicle wall and the enzyme encapsulated before having a chance of diffusing out again. This increases the duration of the substrate in proximity of the enzyme significantly. Since the vesicles are rather small the frequency of collisions with the substrate and enzyme are high. This in turn increases the frequency of substrates colliding with the active site in the required orientation allowing the substrate to be converted.

3) In case only few enzymes are encapsulated, the odds of the enzyme aggregating are small eliminating a reason of low activity. This could potentially explain why NRs do not suffer a decreased activity at pH 7.4.

It should be mentioned that this model is flawed since, the collisions are inelastic collisions[5] and long-range interactions have to be taken into account. Enzymes have moreover been reported to guide substrates on their surface towards their active centre.[6] Lastly, it cannot be completely excluded that both enzyme and substrate slide along the surface of the vesicle membrane rather than bouncing and moving through the entire space of the vesicle interior.

3.3 Membrane permeability

Little can be predicted on the permeability of the membrane and its interactions with detergents. However, it was noticed repeatedly that hydrophobic molecules, in particular FCS dyes interact with the membrane and are able to diffuse in and out and are thus able to go through the membrane as well.

Regarding AUR, it can be assumed that the uncharged version is hydrophobic enough (and also small and flat) to permeate through membranes. It was thus calculated how much of the substrate and product will be uncharged at pH 7.4 and 6.0. At both pH above 97% of the substrate should be uncharged and thus more likely to diffuse through the membrane. Since liposomes have thinner and more fluid membranes than polymersomes, this effect should be more pronounced there, explaining the higher activity of the negative control in case of liposomes. However, unlike polymersomes, liposomes are often charged in their hydrophilic surface. This could be more repelling for hydrophobic molecules than PEG or PMOXA groups of polymersomes. An alternative explanation would be the fact that liposomes are generally less stable and could thus release more enzymes. Either way it emphasises the relevance of a matching negative control (with similar contaminations etc. that might affect the membrane). As no significant pH-dependency was found the latter appears more plausible. Moreover,

the dominance of the protonated form speaks against charge repulsion between enzyme substrate and the stimuli responsive peptide.

As experiments discussed in the prior chapter indicate, HRP has only limited capabilities of attaching itself to membranes. The activity of NR- thus must either stem from the membrane permeability itself (including defects) or from HRP release from breaking vesicles. Experiments never showed a sudden jump in the activity of NR-, but only a gradual increase over storage time. Thus, the membrane permeability becomes the more likely culprit. In addition, even experiments with glucose indicate that highly polar substances can escape vesicles, at least when detergents are involved (in concentrations that should not destroy the vesicles).

3.4 On stimuli responsiveness

Regarding the expected pKa of the asparagine groups of Gala3 being close to acetic acid (4.76), it can be further assumed that by decreasing the pH from 7.4 to 6.0 only few carboxylic groups become protonated. In fact, a significant change of the protonation state would be only expected for pH-values below 5. The iso-electric point can also be expected at around pH 3. However, as mentioned earlier, both GALA and *oligo*(acrylic acid) are known to present a stimuli responsiveness between pH 7.4 and 5.0.

In order to understand the behaviour of the GALA-peptide better calculations and Zeta potential measurements were undertaken. The peptide (1322.42g/mol) was dissolved in PBS yielding a 45.4µM solution. The pH was adjusted by taking 10µL of the peptide solution a diluting it 100x with buffer of the corresponding pH.

Tab 5.a: Zeta potential of Gala3 at pH 7.4 to 4.5 (single measurement)

Sample Name	Zeta Potential (mV)	Mobility (µcm/Vs)	Conductivity (mS/cm)
GALA3 pH 7.4	-20	-1.5	16.5
GALA3 pH 6.5	-14.8	-1.1	16.3
GALA3 pH 5.5	-5	-0.4	16.3
GALA3 pH 4.5	-1.7	-0.1	16.6

Tab 5.b: Zeta potential of the buffer alone

Sample Name	Zeta Potential (mV)	Mobility (µcm/Vs)	Conductivity (mS/cm)
PBS pH 7.4	-21.9	-1.7	16.6
PBS pH 6.5	-8.4	-0.6	16.7
PBS pH 5.5	-6.4	-0.5	16.7
PBS pH 4.5	-4.6	-0.4	16.8

Tab 5.c: Subtraction of the background (x.b)

Sample Name	Zeta Potential (mV)	Mobility (µcm/Vs)	Conductivity (mS/cm)
pH 7.4	1.9	0.2	-0.1
pH 6.5	-6.4	-0.5	-0.4
pH 5.5	1.4	0.1	-0.4
pH 4.5	2.9	0.3	-0.2

No aggregation could be observed due to the low concentration, but the Zeta-potential changed considerably with the pH (**Table 5.a**). However, the changes of the buffer alone had to be taken into account (**Table 5.b**). The change in Zeta potential had to be expected since the pH decreases the effect of cations and vice versa.[7] Unfortunately, the change in Zeta potential was very small compared to the background caused by the ions of the buffer. Still, around pH 6.5 something appears to happen, as it was the only measured Zeta-potential with a negative voltage, which coincides with the anticipated turning point (middle between 7.5 and 5.5, **Table 5.c**).

Regarding possible interactions of the peptide with the environment, it has to be said that OmpF-WT has 8 lysines inside the pore region and 10 outside; 9 arginines (2 outside); 9 glutamines (4 outside) and 11 asparagines (8 outside). Thus, it is nearly impossible to predict interactions of the peptide with the pore. The carboxylic groups of the Gala3-peptide could interact with lysine and arginine groups inside the OmpF pore, binding the peptide to the pore surface at pH 7.4. For example, negatively charged carbenicilin is known to bind in proximity to the K89C mutation.[8] On the opposite side of the pore, in mid distance between K89C and R270C, amino acids with carboxylic groups dominate that would probably interact in a competing fashion. On the part of the pore exposed to the membrane, tyrosines dominate. Binding interactions between the peptide and the inside of the pore would reduce the ability to sterically block the pore and to repel anionic substrates by charge repulsion. Another situation that would unblock the pore is if the peptide preferentially stood out and away from the pore. This could be caused by interactions with the rim of the OmpF or by structural changes. All these interactions appear less plausible than a change in conformation, since in the case of the double mutant it would have to apply for both peptide anchoring points.

Since R270C-Gala3 OmpF proved already a significant pH response, the experiment was once repeated in more stable polymersomes with results comparable to the measurements with K89CR270C-Gala3 OmpF. This indicates that already one peptide attached to the OmpF can be enough to control the diffusion through the pore. According to the DOL measurements both mutation sites are equally accessible and hence labelled to the same extent. They could be therefore expected to work similarly, however the mutation at R270C allows the peptide to protrude more dominantly into the pore than from the K89C-site, which is placed above an internal loop of OmpF which effectively reduces the molecular cutoff. Thus, it would be more depending on the length of the peptide and its conformation.

4 Conclusion

We can assume that our 125 nm diameter polymersome have about 10-20 OmpF molecules/vesicle corresponding to 0.06-0.13% of the vesicles surface and 1.6 molecules of HRP inside. In addition, FCS experiments indicate that at any given time no more than 1-2 molecules of oxidised AUR are within the NRs. Regarding the fact that probably no more than 0.06% of the HRP enzymes were encapsulated an activity comparable to 0.1% of the concentration used for encapsulation, the activity is still very impressive. Since the vesicles provide considerable protection against temporary zones of extreme pH, diffusion limitations in this system are apparent. It is possible that multiple AUR molecules become trapped within the NRs in the sense that they bounce from wall to wall until they either collide with the enzyme or the OmpF pore and leave. Regarding collisions with the enzymes, it is likely that the substrate is guided to the active site, as it has been reported for other enzymes.[6]

Regarding the stimuli responsiveness of Gala3-peptides, it can be said that charge repulsion can be excluded for two reasons: it worked against differently charged substrates and regarding the observed pH-range it is highly unlikely that major changes in protonation occur. It would take pH 3.3 to have over 90% of the glutamic acid groups protonated. While the OmpF pore would offer numerous ways of interacting with the peptide, the experiments with single and double mutants indicate that such effects do not have any crucial effect.

Regarding the activity of NR- little further inside can be obtained from theoretical calculations. It appears that at both pH AUR is predominantly uncharged and thus rather hydrophobic. It thus is likely to diffuse though membranes directly, but it seems to be slow compared to diffusing though the few OmpF pores available. Repeating experiments with older samples indicate that HRP is released over time. However, this should not be a major issue with fresh samples, as long as detergent

concentrations are kept in check, as experiments with HRP/membrane interaction and HRP removal indicate.

4 References

[1]   T. Einfalt, R. Goers, I. A. Dinu, A. Najer, M. Spulber, O. Onaca-Fischer and C. G. Palivan, *Nano Lett* 2015, 15, 7596-7603.
[2]   T. Einfalt, D. Witzigmann, C. Edlinger, S. Sieber, R. Goers, A. Najer, M. Spulber, O. Onaca-Fischer, J. Huwyler and C. G. Palivan, *Nature Communications* 2018, 9, 1127.
[3]   a) D. Bashford, *Frontiers in bioscience : a journal and virtual library* 2004, 9, 1082-99;
        b) M. R. Gunner, J. Mao, Y. Song and J. Kim, *Biochim. Biophys. Acta, Bioenerg.* 2006, 1757, 942-968;
        c) G. M. Ullmann, E. Kloppmann, T. Essigke, E.-M. Krammer, A. R. Klingen, T. Becker and E. Bombarda, *Photosynth. Res.* 2008, 97, 33-53;^ld) J. M. Antosiewicz and D. Shugar, *Mol. BioSyst.* 2011, 7, 2923-2949.
[4]   a) P. Baumann, M. Spulber, O. Fischer, A. Car and W. Meier, *Small* 2017, 13, 1603943;
        b) A. Kuchler, M. Yoshimoto, S. Luginbuhl, F. Mavelli and P. Walde, *Nat Nanotechnol* 2016, 11, 409-420.
[5]   J. Z. Hearon and R. Katzman, *The bulletin of mathematical biophysics* 1954, 16, 259-277.
[6]   a) A. Shafferman, A. Ordentlich, D. Barak, C. Kronman, N. Ariel and B. Velan, *Contribution of the Active Center Functional Architecture to AChE Reactivity Toward Substrates and Inhibitors*. In Structure and Function of Cholinesterases and Related Proteins, Springer US: Boston, MA, 1998; Vol., 10.1007/978-1-4899-1540-5_54203-209;
        b) D. Cockburn and B. Svensson, *Surface binding sites in carbohydrate active enzymes: an emerging picture of structural and functional diversity*. In Carbohydrate Chemistry: Volume 39, The Royal Society of Chemistry: 2013; Vol. 39, 204-221.
[7]   S. Salgın, U. Salgın and S. Bahadır, *Int. J. Electrochem. Sci.*, 2012 712404-12414.
[8]   Brigitte K. Ziervogel and B. Roux, *Structure* 2013, 21, 76-87.

VII Discussion

1 Achievements

The greatest challenge was that neither an established system nor analytical method existed and that one cannot confirm the well-defined nature of a system in absence of a reliable assay and *vice versa*. Thus, the task had too many variables for a straightforward optimisation process. Still, this complex system consists of many parts which can be individually analysed and optimised regarding yield and reproducibility.

Various types of **vesicles** were produced under several different conditions and the influence of the insertion attempts, in particular the presence of detergents could be investigated. The results will be discussed later in this chapter. Concluding it can be said that several methods were found that could be used to insert OmpF and resulted in vesicles stable enough for the planned experiments. The vesicles were investigated via light-scattering, FCS, TEM and *cryo*TEM. All these methods gave information about vesicle concentration, hydrodynamic radius and size-distribution and had a different bias each. Combining all these methods, the errors cancel out and a conclusion can be reached confirming vesicles in case of Liposomes with 200nm diameter and in case of polymersomes with 100nm. In both cases the samples had been extruded through a membrane with pore size in the same range

Similarly, various **OmpF mutants** could be produced. The mutations were confirmed via sequencing and after the expression by testing the accessibility of the thiol groups using acrylodan as a fluorescent label. The OmpF expression itself was confirmed using SDS-gel chromatography and indicated good purity, due to the lack of additional bands in the Coomassie stained gel. The occasionally observed splitting of the OmpF band (D12K89C, R270C, D12R270C) is attributed to the presence of residual signalling peptide (2000 Da as seen from the difference between the bands at 38 and 40 kDa, whereas the anticipated band was 39kDa), which was not cut in time in the E.coli cells due to the rapid overexpression.[1] A concentration of 0.75 ± 0.25 mg/mL (extract without further concentration steps) was determined by BCA total protein assay. D12C, K89C, R270C, D12CK89C, D12CR270C and K89CR270C were successfully produced. All thiol groups were equally accessible, with the notable exception of D12C containing mutants, which were not even able to react with small compounds such as acrylodan.

Later, the degree of labelling (**DOL**) of the OmpF mutants was tested with the acrylodan assay. As an orthogonal assay, the protein was digested and analysed via mass spectrometry. As it turned out the acrylodan assay was more of a qualitative test, whereas mass spectrometry confirmed a high degree of labelling for most attached peptides.

Of all the **tested groups** only Gala3 and HLG4 stood out and both enzyme kinetics and release experiments indicated a stimuli responsiveness (details in the following subchapters).

Besides achieving the set goals, other discoveries were made on the way:

- Since the commercial thiol assays do not work on thiols located on the inside of the OmpF pore, a new assay had to be developed. This acrylodan assay utilises a fluorophore which apparently was not used before for this purpose despite its availability and aptitude. While mass spectrometry was used for obtaining dependable results, it was nowhere near fast and available enough as a quick screening, very unlike the new acrylodan assay.
- While the originally intended *oligo*(acrylic acid) groups failed as a stimuli responsive group, the synthesis of the oligomer is the first to be described in literature, proving that ATRP can be used for such short oligomers (n = 4-30). Furthermore, my synthesis allowed unusually narrow molecular mass distribution (DPI = 1.1-1.3) oligomers through radical polymerisation.
- While liposomes were used as a preexperiment, they proved inadequate regarding their stability. Thus, a liposome mix of unusual stability was created.
- This new liposome mixture behaved in between other liposomes and polymersomes, thus giving further insights in vesicle stability and self-assembly.

2 Discussions stimuli responsiveness

2.1 Sulforhodamine B and carboxyfluorescein release experiments

FCS turned out to be too slow for measuring the release so that it could only indicate that N lost less dye than P regarding the CPM of the vesicles (but not the percentage of free dye due to the vesicles outshining free dye) and that S was in between, with some indication that it stopped releasing at low pH.

In case of carboxyfluorescein release experiments, using self-quenching concentrations worked far better, but were still not reliable enough. The experiments still suffered from a missing recording of the initial release making it impossible to quantify the release. They also suffered from a high statistical error regarding sample preparation and measurement. The negative control appeared to release the most, which has to be attributed to the other samples releasing most of the dye before the actual measurement. Still, it gave more information than the FCS in that it gave a clear indication that the sample had blocked pores at pH 5.5.

2.2 Liposomes vs polymersomes in HRP/Amplex Ultra Red kinetics

Liposome based nanoreactors (Chapter **enzyme kinetics 4.2**) revealed a clear stimuli response of R270C-Gala3-OmpF in that the activity of **NRC** decreased on acidification to 46% (see **Fig. 27 in chapter enzyme kinetics**), thereby overruling the pH dependent activity of the free enzyme. The experiment was repeated with the same result; except that the **NR-** control had initially a lower activity until it became acidified indicating some release of HRP over time, otherwise the controls did not change their activity upon acidification (See **Fig**. **28 in chapter enzyme kinetics**). Both findings regarding NR- can be attributed to the inadequate thermal stability of the vesicles.

The experiments were repeated with the more stable DSPC-mix liposomes. In that case, K89R270C-Gala3 OmpF was used instead of R270C-Gala3 OmpF, since the DOL of the OmpF conjugates appeared to be only moderate according to the acrylodan assay, a double mutant was developed, which achieved higher DOL. Also, the pH was only reduced to 6.0 instead of 5.5, since it was found that this makes the pH adjustment and thus the entire experiment more reliable. Here, the activity of **NRC** went down to 74%. Since the DSPC-mix was harder to work with and more challenging to insert OmpF, but also because the experimental graph (see **Fig. 31 in chapter enzyme kinetics**) had more noise, it can be assumed that the prior experiment is more trustworthy regarding the magnitude of the decrease in activity.

While liposomes insert membrane proteins far more readily than most polymersomes (due to the thicker and more rigid membrane of polymersomes),[2] the reproducibility of the results was significantly higher once OmpF was successfully inserted in polymersomes (compare **Fig. 30** and **38 in chapter enzyme kinetics**). Whenever the hydrodynamic diameter and the polydispersity were similar according to the Zetasizer, the vesicle concentration could be estimated by the samples ability to scatter light. Thus, after concentration adjustments the reproducibility increased significantly. The remaining fluctuations between repeats may arise from different encapsulation efficiencies of HRP or different OmpF densities in the membrane. Polymersomes increased the stability of the enzyme kinetics considerably. The liposomes needed to be measured on the same day since the negative control was slowly releasing enzyme, whereas the polymersomes showed identical behaviour remeasuring samples after one week.

In case of polymersomes, the activity of the **NRC** dropped to 16% of its activity at pH 7.4 (see **Fig. 38 in chapter enzyme kinetics**), thereby changing from an activity close to **NR+** (90%) to an activity close to

NR- (90%). Thus, the pore of the OmpF conjugate underwent a change from an almost completely open state to a perfectly closed state (deviation in the realm of experimental error).

Stimuli-response due to different permeability of the membrane, in particular phospholipids, can be excluded due to the **NR-** controls. Moreover, polymersomes had similar behaviour whilst lacking protonisable groups in the membrane.

The residual activity of the **NR-** controls and the **NRC** at low pH (OmpF with blocked pores) was significantly higher in case of liposomes compared to polymersomes (the activity at pH 5.5 of **NR-** was twice as high as those found in the experiments with polymersomes). This could be either explained by a higher permeability of liposome membranes or a higher rate of breaking vesicles. The latter is more probable, as liposomes had to be measured on the same day, while polymersome samples could be measured one week later without significant increase of background activity (**Fig. 9 and 10 in chapter enzyme kinetics**). All these factors make polymersomes the superior choice as membrane.

2.3 Amplex, TMB, glucose assays

Originally, alternatives to Amplex Ultra Red/HRP were searched, due to the recurring problem that **NR-** had a higher activity than **NR+** and due to the fact that the fluorescence of the product is strongly pH-dependent. As it turned out, the problem with the controls lay elsewhere (as discussed above). However, it is still interesting since the substrates have different sizes, charges and should have different permeability regarding vesicle membranes. More importantly, it can give insight into the mechanism of the stimuli responsiveness.

For instance, the stimuli responsiveness could be explained by mere charge repulsion, as it was in case of the previously published 6xHis OmpF mutant.[3] The Gala3 peptide has 5 carboxylic acid groups, which are negatively charged in solution except for very low pH and the oxidised Amplex Ultra Red is negatively charged as well for most pH. Thus, using a substrate with positive charge would be interesting to see, whether the pore is blocked as well and if so under the same experimental conditions. TMB is the only suitable substrate of this kind. The ideal substrate is however uncharged, but water soluble for all pH values. This is however technically impossible, since all fluorophores are hydrophobic, unless enough charged or polar groups are added. As it was seen from experiments of attaching glutathione to FCS-fluorophores, it may increase the solubility, but it ads mainly to the size and it does not prevent the hydrophobic part of going into membranes and disrupting them. The only feasible option to avoid this dilemma is implementing a tandem reaction which converts a hydrophilic

compound and the side product can be used for producing a fluorophore. Glucose oxidase/HRP is such a system.

As mentioned before Amplex Ultra Red/HRP kinetics indicate that K89R270C-Gala3 OmpF goes from a fully open to a completely closed state from pH 7.4 to 6.0. Experiments with TMB revealed (see **Fig. 32 in chapter enzyme kinetics**) the same trend, although the kinetic with TMB is not as appealing as the Amplex Ultra Red kinetic. It does reveal an important aspect: the blocking of the pore is most likely independent of the charge of the enzyme substrate. The Gluc/GOX/HRP system suffered of **NR-** being more active than **NR+**, but here it was evident beyond doubt, that most of the glucose was released from the **NR+** before the actual experiment started. Tests releasing glucose from **NRC** and detecting it via glucose oxidase and HRP revealed the same trend offering additional proof to the aforementioned results.

2.4 *Oligo*(acrylic acid), Gala3 and HLG4

In the original concept, a short pH responsive oligomer was envisioned as a stimuli responsive plug. It was supposed to be a random coil with negative charges from carboxylic groups around pH 7. At low pH it was supposed to be protonated and uncharged making it hydrophobic. It should thus change from a random coil dangling around the pore effectively blocking it, to a compact dehydrated state, precipitated on the pore wall, thus opening the pore at low pH.

*Oligo***(acrylic acid)**-conjugates were investigated using both lipo- and polymersomes and using Amplex Ultra Red-HRP, but the results were not conclusive (**Fig. 26 and 27 in chapter enzyme kinetics**). It seems that *oligo*(acrylic acid) of any length could block the pore independent of the pH and that the degree depended mostly on the DOL and not on the length.

Gala3-conjugates worked perfectly well as proven in POPC/POPS-liposomes, DSPC-mix liposomes and polymersomes **(chapter 4.2 in enzyme kinetics)**. However, despite being functional analogues of the originally intended *oligo*(acrylic acid)-conjugates, they proved to have the very opposite stimuli response than anticipated. The experiments with liposomes had a higher statistical error and **NRC** did not close as much as in polymersomes thus **NRC** never overlapped with **NR-**. In polymersomes, **NRC** changed from a perfectly open state as **NR+** to a perfectly closed state as **NR-** and the pH dependent change was reversible for multiple cycles. TMB gave the same result as Amplex Ultra Red although it has the opposite charge indicating that the pore is blocked rather by conformational changes than changes in its charge. Tests releasing glucose and detecting it via glucose oxidase and HRP revealed

the same trend offering additional proof, since glucose is uncharged and polar. The pH-responsiveness was also confirmed using uricase in combination with HRP, but the experimental error was high and the trend rather weak.

HLG4-conjugates provided the opposite stimuli response according to HRP-Amplex Ultra Red experiments, as planned, but not according to TMB, which indicates that the oppositely charged TMB apparently interacted with the peptide (**chapter 4.3 in enzyme kinetics**). However, not enough experiments were performed to come to a final conclusion. Most importantly, the TMB experiment was not repeated, since TMB was not particularly interesting to prove the stimuli responsiveness of Gala3 (the other assays worked better). It could be thus that it was not due to the charge, but to a faulty assay.

HLG4 seems to have the opposite behaviour, which contributes to the concept of a modular system, though the observed stimuli response was weaker. This could be for multiple reasons. For instance, the pKa of histamine is at 7 (chosen for a stronger change in the state of protonation) while the one of glutamine is at 4.3, thus the peptide is not a direct opposite of the acidic Gala3. The opposite behaviour is remarkable as it cannot be expected that it transforms from a random coil to a helix in the opposite direction complementing conveniently Gala3. If it did work the in the same way but had just a pKa around 7 instead of 4, then one could expect the turning point to be around pH 9 and not 6. In that case, it would be expected that at a transition from pH 7.4 to 6.0 the pore would switch from a half-open to a completely open state, but it turned out to be the other way around: from a closed to a half-open state.

2.5 Anchor sites

The mutation sites D12C (asparagine, the 12th amino acid of the OmpF amino acid sequence replaced by cysteine) K89C (lysine) and R270C (arginine) located inside the pore in the eyelet-region were replaced by cysteines (**Fig. 1 in chapter preparation**). These locations allow the attachment of molecular groups that can block the molecular flow at the beginning of the pore or point outwards without obstructing the pore, in different conditions. (**Fig. 3 in chapter preparation**).[4] The mutation-sites are roughly equally distanced so that multiple anchor points could be used at once. Since the acrylodan assay indicated a low DOL, primarily the double mutant K89R270C-OmpF was used in order to increase the chance that a pore has one or more stimuli-responsive groups.

K89C and R270C work equally well as anchor point, but D12C was never labelled successfully by any *oligo*(acrylic acid). D12K89C and D12R270C-OmpF behaved like a single mutant, indicating that D12C is buried or shielded. This might be due by E2 and K46 which flank D12C, or possibly tyrosine Y14 shields it.

2.6 Single vs double mutants

Since D12K89C- and D12R270C-OmpF failed as double mutants, only K89R270C-OmpF remained. In earlier experiments it was indicated that K89C and R270C OmpF behave identically, thus both anchor sites were expected to behave identically within K89R270C-OmpF. While the acrylodan assay did not indicate that the DOL of K89R270C-OmpF being the sum of the DOLs of K89C and R270C OmpF. However, the experiments using in-gel digestion and mass spectrometry leave little doubt that both groups are equally accessible (94 and 92% respectively).

Before the high DOL was confirmed via mass spectrometry, the experimental set up was changed from R270C-OmpF to K89R270C-OmpF as a basis. Thus, experiments using Amplex Ultra Red/HRP and liposomes were conducted with the single mutant and those conducted in polymersomes were using the double mutant. From the results it appears that the single mutant OmpF-C did not block as well as the double mutant OmpF-C, however, when the experiment was repeated using R270C-Gala3 OmpF in polymersomes, no difference could be seen from K89R270C-OmpF. This indicates, that the lower stimuli response stems from the more permeable and fragile nature of liposomes and not from the blocking or DOL of the OmpF-C.

3 Lessons learned

3.1 OmpF insertion

Due to OmpF's exceptional stability and ability to properly refold (as long as the thiol groups cannot form a disulphide bridge), it can be inserted into vesicle membranes in ways otherwise impossible. It could thus be inserted in presence of high amounts of detergents using a detergent removal method for liposome-formation or it could be dried along with ABCP to a film for polymersome-formation (and DSPC-liposomes). However, the fact that some batches lend themselves only to one of these two

methods strongly indicates that other, easily overlooked factors play a role. It appears that OmpF extracted with Octyl-POE allowed the prior method, and OmpF extracted with OG could only be used for the latter method. This speaks for the importance of co-extracted bacterial lipids in the ternary mixture.[5] It also showed again that the DSPC mixture liposomes are closer in their behaviour to polymersomes, which is probably explained by the fact that they become almost rigid at room temperature.

3.2 Vesicle stability

It has been noticed that NPC and DSPC liposomes behaved very differently and the same could be said for short and long ABCPs. In many ways the DSPC-mix was far closer to polymersomes than the other liposomes. This trend obviously comes from the length of the hydrophobic parts and the density of the packing. In general, it can be said, the longer the hydrophobic section of the ABCP, the:

- lower the solubility and rate of film-rehydration
- slower the film-rehydration becomes (NPC 1-3h; DSPC 16-20h; ABA 16-24h)
- higher the sensitivity towards oxygen during vesicle-formation (although unsaturated lipids are also sensitive, but due to photo-reactions and not due to perturbation of the self-assembly)
- the higher the sensitivity towards detergents becomes during self-assembly.
- less likely to co-assembly with lipids and additives such as cholesterol TDOC, etc.
- harder insertion of OmpF becomes (mismatch in thickness, lacking mobility of the membrane and sensitivity towards stabilising detergents)
- higher the stability of the vesicle-membranes regarding time and temperature.
- lower the membrane permeability (thicker, less fluid membrane).
- lower the sensitivity of membranes towards detergents becomes (but not as stable as liposomes in that regard). Similarly, the stability towards FCS-dyes increases (in this case outclassing liposomes).
- less likely the vesicles are able to recover from damage (disruptive detergents, sonication, centrifugation … presumably because ABCPs are less likely to go from a micelle into solution and are less likely to insert themselves into a damaged membrane)

Asides from the ternary mixture surrounding OmpF, there is another factor greatly reducing **reproducibility** of experiments: Amphiphiles can age and in case of ABCPs, even nominally identical batches can differ in their PDI, the amount of AB in ABA, or the content of unreacted PDMS. Similarly, aging could break up ABA in AB+A, or separate the blocks completely or alter them through oxidation. PDMS is moreover known for hydrolysis catalysed either through acids or bases,[6] however, it is slow around pH 7.

Why the vesicle-formation in case of liposomes withstood higher detergent concentrations might be explained through the short hydrophilic block. Liposomes are also less sensitive to **detergents** probably since the mismatch in length and physical-chemical nature of the detergent is less pronounced as in polymersomes. These effects most probably the way detergent interact with ABCP micelles and vesicles, stabilising one and destabilising the other. For instance, it could be that the detergent inserts in liposomes, evenly whereas it produces detergent domains in vesicles which weaken the membrane. Furthermore, it could be that detergents stabilise isolated ABCPs and thus alter the equilibrium or interact with AB-ABCPs within ABAs causing phase separation.

Detergents are problematic for another reason as well: Detergents are also from a practical perspective impossible to removed completely, as they bind to membranes. Size exclusion chromatography, dialysis, the addition of biobeads etc. fails in that respect. The harmful effect is only observed to the full extent with delay. This explains that a detergent titration curve, vesicle analytics etc all imply that the polymersomes withstand e.g. 0.25% OG, but then perform very different to expectations in that the vesicle-formation is hindered and that over time the vesicles deteriorate. While detergents and dyes have the tendency to break vesicles up into micelles, it seems also that even remaining vesicles have a different behaviour than those vesicles that did not have contact to detergents.

Interestingly, the **time of the detergent addition** has an equally great impact on vesicle stability as the detergent concentration does. It is possible to use a higher detergent concentration during film-rehydration than, after completion of the process. In addition, while the film-rehydration is hindered, it is possible to apply dialysis or biobeads during vesicle-formation, which gradually remove the detergent, so that vesicle-formation starts and all the excess of detergent, which does not bind to the membrane is removed. While the presence of detergents increases the micelle-fraction considerably and reduces the average vesicle-size, it has been found to be better for MP-insertion than trying to destabilise polymersomes with detergents afterwards.

In this context it was observed that MPs such as SGLT and presumably OmpF (regarding **NR-** with and without detergent) are able to **stabilise polymersomes** against the negative influence of detergents. This effect would be probably far more noticeable, if higher MP-concentrations would be used. This

would also imply that controls without OmpF, will never correctly represent the vesicle-membranes with blocked OmpF.

Dyes were found to act similar to detergents, hindering vesicle-formation and destabilising vesicles by inserting themselves into the membrane (various interactions of dyes with lipid membranes was reported before, both above and below the phase transition temperature of the lipids).[7] Moreover, the latter effect is also delayed, meaning that it can still occur after extrusion and size exclusion chromatography. Thus, a sample can consist primarily of micelles according to FCS although the micelle fraction had been removed prior to the measurement. Unlike detergents, larger hydrophobic dyes turned out to be worse and polymersomes appear to be more robust towards their presence. This extends to DSPC-mix liposomes being more resilient and long ABCPs being more resilient than shorter ones. Hence, it's the very opposite of how vesicles behave to detergents.

4 Conclusion and outlook

A new modular stimulus triggered system was successfully developed allowing to establishing control over the transport via membrane of self-assembled nanoreactors. In addition, a reliable assay for testing the functionality of the new biovalve was developed and further used. The developing of this new stimulus triggered biovalve opens new ways of using this artificial self-sustained nanoreactors for nanosensors and successful replacements of failed organelles in living cells. As a colleague proved, polymersomes of this type (same ABCP, same OmpF-mutant, same vesicle size), can be uptaken into cells and show low cell-toxicity,[8] while maintain the activity of the encapsulated enzyme. The modular system allows various stimuli responses based on conformational changes opening and closing the pore.

The best results were obtained for Gala3 modified OmpF that showed a reliable transition from the opened to closed state triggered by a pH change of only 1.4 units from the physiological pH. The stimuli triggered response was so fast that the transition between the states could not be observed directly with the employed methods. Moreover, this transition is reversible so the nanoreactors containing Gala3 modified OmpF show practical infinite self-supporting activity of the entrapped enzyme.

The discussed system is a significant advancement in the field of nanoreactors since the other stimuli responsive systems are either not reversible, lack control (reversible disassembly), do not regulate the flow of molecules except metal-ions, or require complex genetic engineering (multiple mutations that could affect structure or functionality). Our modification method with the selected peptides is reliable

and robust and can be used for any membrane porin with a single mutation for pores of the size of OmpF. The modification can be can be easily adapted to other stimuli responses peptides (changing Glu for His, Lys or Arg, or possibly even creating temperature responsive ELP-peptides). For enabling larger substrates to pass through, a larger pore would need to be used and multiple anchor sites introduced in order to maintain control. Our designed biovalve offers options of tailor made solutions for all possible problems. That is why our system opens the door for a new way of successful usage of nanoreactors as efficient, personalized, non-invasive alternative for cell metabolic diseases.

5 References

[1]   M. E. Jackson, J. M. Pratt, N. G. Stoker and I. B. Holland, *The EMBO Journal* 1985, 4, 2377-2383.

[2]   a) W. Meier, C. Nardin and M. Winterhalter, *Angewandte Chemie-International Edition* 2000, 39, 4599-4602;
b) F. Itel, M. Chami, A. Najer, S. Lörcher, D. Wu, I. A. Dinu and W. Meier, *Macromolecules* 2014, 47, 7588-7596.

[3]   S. Ihle, O. Onaca, P. Rigler, B. Hauer, F. Rodriguez-Ropero, M. Fioroni and U. Schwaneberg, *Soft Matter* 2011, 7, 532-539.

[4]   a) R. Koebnik, K. P. Locher and P. Van Gelder, *Mol Microbiol* 2000, 37, 239-253;
b) W. Grosse, L.-O. Essen and U. Koert, *ChemBioChem* 2011, 12, 830-839;
c) H. Miedema, M. Vrouenraets, J. Wierenga, D. Gillespie, B. Eisenberg, W. Meijberg and W. Nonner, *Biophys J* 2006, 91, 4392-4400;
d) H. Miedema, A. Meter-Arkema, J. Wierenga, J. Tang, B. Eisenberg, W. Nonner, H. Hektor, D. Gillespie and W. Meijberg, *Biophys J* 2004, 87, 3137-3147.

[5]   M. le Maire, P. Champeil and J. V. Moller, *Bba-Biomembranes* 2000, 1508, 86-111.

[6]   R. M. Hill, M. He, Z. Lin, H. T. Davis and L. E. Scriven, *Langmuir* 1993, 9, 2789-2798.

[7]   I. R. Calori, D. S. Pellosi, D. Vanzin, G. B. Cesar, P. C. S. Pereira, M. J. Politi, N. Hioka and W. Caetano, *J Brazil Chem Soc* 2016, 27, 1938-1948.

[8]   T. Einfalt, D. Witzigmann, C. Edlinger, S. Sieber, R. Goers, A. Najer, M. Spulber, O. Onaca-Fischer, J. Huwyler and C. G. Palivan, *Nature Communications* 2018, 9, 1127.

VIII Materials Methods

1 Chemicals and Consumables

Reagents and materials were of the highest commercially available grade and used without further purification, unless indicated.

1.1 OmpF-related

The **K89C-OmpF** plasmid was produced previously in our group. The **plasmid** pXβG-ev1 was originally constructed by Gregory M. Preston. **Omp8** *E.coli*/BL21-(DE3)omp8 was prepared by Prilipov *et al* 1998.[1] Chemically competent **XL1-Blue** *E.coli* **ultracompetent** cells were obtained from Invitrogen. Subcloning Efficiency™ **DH5α**™ competent cells was obtained from **Invitrogen**. **PfuTurbo DNA polymerase (No. 600254-52) was obtained from Agilent. Primers** for the mutations came from Microsynth (quality: desalted), who also did the sequencing of the plasmids. **DpnI** was obtained from New England Biolabs**. RNAse** and **DNAse** were purchased from Roche**. Trypton**, **Yeast**-extract, LB-**Agar** and **Terrific Broth** were obtained from BD. **Glycerol**, **SDS**, **ampicillin**, **IPTG**, **DTT** were from Applichem. Pierce **BCA** Protein Assay Kit; **X-Gal** and **HRP** (No. 31491) were obtained from Fischer Thermoscientific. QIAprep Spin **Miniprep** Kit; QIAquick **Gel Extraction Kit** were purchased from Qiagen. **Amplex** Ultra Red was obtained from Invitrogen and stored as a stock solution of 1g/L in DMSO at -20°C. **Octylglucopyranoside** was obtained from Affymetrix**. OPOE** came from Enzo. **Na_2HPO_4, KH_2PO_4, $CaCl_2$** (anhydrous granular), **Trizima** base, 30% **H_2O_2** and the following solvents in HPLC-quality: **Ethanol**, **DMSO**, **Chloroform**, **Methanol** were obtained from Sigma Aldrich. **NaCl** was purchased from Merck. **$MgCl_2$** hexahydrate, **$MgSO_4$** heptahydrate, **KCl** were obtained from Fluka**.** Pure **water** was obtained from a Milli-Q Divect 8 from Milipore. **Spectra/por** Dialysis tubes: 3.5-5; 8-10; 100 and 300kDa MWCO CE 16mm were obtained from Spectrumlabs. 6-8kDa 850μL **Gebaflex** were purchased from Molecular Dimensions. **Biobeads**/SM-2 Adsorbents were obtained from Biorad.

1.2 Oligomer related

The technical grade solvents **DCM, ethyl acetate, ethanol 96%, hexane** and **THF** came from Brenntag Schweizerhall AG. Ethyl acetate, hexane and THF were distilled before use. ***Tert*. butanol** was

purchased from Fluka, **MTBE** from Alfa Aesar. **anisole** 99.7%, **toluene, DMF, acetonitrile** and **DMSO** were supplied by Sigma-Aldrich. **Maleic anhydride** 98% was supplied by Alfa Aesar, **furan** and **bromoisobutyrylbromide** 98% by Aldrich, **ethanol amine** 98% and **triethylamine** 99% by Sigma-Aldrich. **Copper (I) bromide** and **copper (II) bromide** 99% were supplied by Aldrich. **PMDETA** and **Me$_6$Tren** supplied by Alfa Aesar. *Tert.* **butyl acrylate** 98% and **NIPAAM** 97% were purchased by Aldrich. **TFA** 99% came from Alfa Aesar, **TIPS** 99% from Aldrich, **NaHCO$_3$** technical from Sigma-Aldrich. **Silica gel** P60 300 mesh came from Fluka, **ALOX** activated basic Brockmann from Sigma-Aldrich and the **TLC** plates from Merck (silica 60 F254 and ALOX neutral F254). The **peptides** modified at the N-terminus with 3-maleimidopropionic acid (CAS No: 7423-55-4) were supplied by Genscript. The peptide LAEALAEALAEA came in 97% purity and had later to be resynthesised by CPC scientific in 87%. The other Genscript peptides had a purity of 95% or more.

1.3 Vesicle related

The following solvents in HPLC-quality were obtained from Sigma Aldrich: **ethanol**, **chloroform**, **methanol**. Pierce **HRP** (no. 31491) was obtained from Fischer Thermoscientific. **Spectra/por** Dialysis tubes: 8-10 and 100 MWCO CE 16mm diameter tubes were obtained from Spectrumlabs. **Biobeads/SM-2** adsorbents were obtained from Biorad.

The ABA triblockcopolymers were previously synthesised in our group:[2]

Amplex Ultra Red was obtained from Invitrogen and stored as a stock solution of 1g/L in DMSO at -20°C. 30% **H$_2$O$_2$** was obtained from Sigma Aldrich. **ABTS** was purchased from Sigma-Aldrich

Natural **phosphatidylcholine** (P3556-25MG type XVI >99% TLC from egg yolk), **SM** (sphingomyelin from bovine brain TLC>97%), **cholesterol** (>99%) and **cholesterol-PEG600** (**polyoxyethyl-cholesteryl sebacate;** C1145-1G) were obtained from Sigma Aldrich. **POPS** (1-palmitoyl-2-oleoyl-*sn*-glycero-3-phospho-L-serine (sodium salt); 840034P) and **DSPC** (1,2-distearoyl-*sn*-glycero-3-phosphocholine; 850365P) were obtained from Avanti Lipids.

1.4 Other Chemicals and Consumables

Thioglo 1 and 3 came from Covalent Associates Inc. **Acrylodan** was purchased from Invitrogen. **Bodypy FL** and **DyLight488** were obtained from Thermo Fisher Scientific. **OregonGreen 488** and **Alexa488** were obtained from Invitrogen. **Sulforhodamine B** was purchased from Sigma Aldrich. **Phenol** and **H_2SO_4** ACS grade were purchased from Sigma-Aldrich. **FloatALyzer** (200-400Da Cutoff) was obtained from Spectrumlabs. 6-8kDa 850µL **Gebaflex** were purchased from Molecular Dimensions and 10k-**Amicons** from Milipore.

10x PBS pH 7.4: 80g NaCl (1.37M), 2g KCl (26.8mM), 14.4g Na_2HPO_4 (101mM) and 2.4g KH_2PO_4 (17.6mM) were dissolved in 900mL of distilled water and filled up to 1L. No pH adjustment was required.

10x Citrate Buffer pH 7.4: 56.8g Na_2HPO_4 (400mM), 57.6g citric Acid (300mM) were dissolved in 900mL of distilled water and the pH was adjusted with KOH (ca. 51.6g, or 100mL of 10M KOH). The solution was diluted with water, if required in order to reach 1L.

Note: 10x buffers, are buffers that need to be diluted 10x prior use (10x in volume), but without further adjustment of the pH.

2 Devices

2.1 Vesicle analytics

Zetasizer: For quality-control, vesicles samples were measured with a Malvern Zetasizer nano ZSP. The samples were diluted 10-100x (to the point where they were no longer visibly opaque in order to avoid multiple scattering). The DLS-measurements were carried out using the parameter recommended by the producer.

Light scattering experiments were performed using an ALV goniometer (ALV GmbH, Germany) equipped with an ALV He -Ne laser (JDS Uniphase, wavelength λ = 632.8 nm). The vesicle solution (1.25, 0.625, 0.313 and 0.156 g/L) was measured in a 10 mm cylindrical quartz cell at angles ranging from 30° to 150° at 293 K. ALV/Static & Dynamic FIT and PLOT program version 4.31 10/10 was used in the process. Static light scattering data were processed according to the Guinier-model.

Transmission electron microscopy: 5 μL polymer vesicle solution were negatively stained with 2% uranyl acetate solution and deposited on a carbon-coated copper grid. The samples were examined with a transmission electron microscope (Philips CM-100) operated at 80 kV.

Vesicle concentration: After confirming the purity and homogeneity using Zetasizer, the vesicle concentration of different samples could be compared by observing their ability to scatter light using the Spectramax M5 in fluorescence mode (point-measurement at 650/650nm excitation/emission) in semi-micro fluorescence polystyrene cuvettes (VWR).

2.2 Kinetic measurements

For absorption and **fluorescence** semi-micro fluorescence polystyrene cuvettes from VWR were used. The fluorimeter LS 55 came from PerkinElmer and the **Spectramax** M5e, used in particular for absorbance measurements, from Molecular Devices (settings described in the methods section). It replaced also the previously used **UV-Vis** Specord 210 Plus from Analytik Jena.

Note: the Spectramax was more convenient and faster to operate, allowed the use of well plates and had a larger measuring range, but was less sensitive than the specialised machines. **NanoDrop** 2000c from Witec AG was used for checking purity and concentration of plasmids and OmpF.

2.3 Other devices

Pure **water** for bioapplications was obtained from a Milli-Q Divect 8 from Milipore.

The **PCR** machine was a Mastercycler gradient from Eppendorf.

The **cell culture flasks** were 2.5L ultra high yield flasks with AirOtop seal from HTS-labs. The vortexer was a MS2 minishaker from IKA.

For the **sonication** of small sample volumes an ultrasonic processor GE 130 from Cole-Parmer was used and for greater volumes a sonication bath type Bandelin from Sonorex.

The tabletop centrifuge was a **Minispin** from Vaudaux Eppendorf, the default **centrifuge** was a 3-18K (using either a 19776 rotor or a 11180-13190 swing bucket rotor) from Sigma. The **ultracentrifuge** was

an Optima XE-90 ultracentrifuge with a 70.1Ti rotor from Beckman Coulter (using 38.5mL PC thick wall with thread tubes from Herolab).

The **French Press** EmulsiFlex C3 came from Avestin.

For vesicle **extrusion** an extrusion apparatus from Avanti Lipid was used with 1 ml Hamilton syringes (passed 10-20x through a 100 or 200nm membrane). For special cases a custom made, gas-powered barrel extruder was used. It consisted of three parts that could be screwed together similar to a vice. The lower part collected the flow-throw and pressed the membrane against the middle part which held the liquid and the headspace for applying pressure. The top had an inlet for the sample and for the pressurised air. The operating pressure was between 2-15mBar. The sample was passed 6x through 400nm and 6x through a 100nm and then 6x through a 200nm membrane. The membranes were Nuclepore track-etch membrane from Whatman.

Mass spectroscopy: LC-MS column *ReproSil-Pur C18–AQ, 1.9 μm resin* Dr. Maisch GmbH, Ammerbuch-Entringen, Germany combined with a dual pressure *LTQ-Orbitrap Elite* mass spectrometer connected to an electrospray ion source (both Thermo Fisher Scientific)

For **MALDI-TOF** a Microflex from Bruker with either *MSP 96 target ground steel microScout Target* or *MSP Big Anchor Chip 96* from Bruker Daitonik GmbH were used. For analysing the oligomers 1mg of the sample was dissolved in 250μL 50% aqueous acetonitrile with 0.1% TFA. The sample was mixed 1:1 with sinapinic acid (20mg in 1mL of the same solvent). The 10μL drop was allowed to dry for 30-60min and the sample was measured at 20% offset; 40% laser output and 90% laser intensity using the *RN:peptide* method (detecting negative charged ions and using a reflector).

NMR Experiments 400 MHz: All NMR experiments were performed on a Bruker Avance III NMR spectrometer operating at 400 MHz proton frequency. The instrument was equipped with a direct observe 5-mm BBFO smart probe. The experiments were performed at 295 K and the temperature was calibrated using a methanol standard showing accuracy within +/- 0.2 K.

LSM-FCS: measurements were performed on a confocal laser scanning microscope (Zeiss LSM 510-META/Confocor2, Carl Zeiss, Jena, Germany). For 488 dyes an argon-2 laser with λ = 488 nm (15 mW output) and for sulforhodamine B a He-Ne laser (λ = 543 nm) and for confocal adjustments a He-Ne laser with λ = 633 nm (15 mW output) was used.

For the **488 nm** laser, a main dichromatic beam splitter (HFT 488/543/633), a secondary dichroic beam splitter (NFT 545) and a low pass filter (LP 505) were used. The laser intensity was typically tuned down to 40% using 10% transmission; 1% *probleach*. For the **543 nm** laser, a dichroic beam splitter (DBS HFT 543), a secondary dichroic beam splitter (NFT 545) and a band pass BP 560 - 615 nm filter were used. The laser intensity was typically tuned down to 60% (a second down-tuning step). The laser intensity

was typically tuned down to 20%. For **633 nm** laser, a main dichromatic beam splitter (HFT 488/543/633), a secondary dichroic beam splitter (NFT 545) and a low pass filter (LP 650) were used. The light was focused on the sample using a *C-Apochromat 40x water immersion objective* (NA=1.2). The default settings were: 20x10s measuring time for free dye and 30x20s for vesicles (30 points in 30min for kinetics). For calibration 100nM SRB was used, applying a 1 component model else two component model was applied with a triplett relaxation time of 3 and a structural parameter of 5 and a 1e-6 cuttoff. The sample of at least 6µL was placed on a glass plate or in a 2x4 *nunc glassbox* with lid. The latter was used in particular for longer measurements using larger samples in order to reduce evaporation.

GPC-measurements were conducted on a TDA305 from Viscotek using two 5um Mixed-C columns from Agilent and a Malvern detector equipped with UV-Vis, IR, 90° LS and viscometer. The samples were dissolved in THF, which was also used as eluent at 1 mL/min at 40°C. The system was calibrated with polystyrene-standards.

3 Methods

## 3.1 Oligomer Synthesis

3.1.1 Synthesis of the ATRP-initiator

3.1.1.1 Protected maleic anhydride

The maleic anhydride was dissolved in toluene as a 2M solution (for 50mL a 100mL 3-neck round bottom flask equipped with stirring bar, condenser, thermometer and argon inlet were used). Oxygen was removed through brief bubbling with argon. The solution was then heated to 80°C. Under stirring 1.2eq of furan was added and allowed to react for 3h. Then another 1.2eq. were added. After cooling down over 1h, the crystalline product was filtered off and washed with cold hexane. Ten grams of maleic imide yield about 16g of product (92%).

Notes: the reaction does not require true Schlenk conditions, but too much would oxidise in presence of air. The reaction can be followed *via* TLC using 1:1 ethyl acetate/hexane and $KMnO_4$-staining solution. The maleic anhydride has a RF of 0.67, the furan (poorly visible) 0.27 and the product 0.44.

It appeared that the furan vapours were able to diffuse away thus another equivalent had to be added. This increased the yield dramatically (original literature had 42%[3]). During the reaction, the argon was supplied from the condenser to avoid vapours getting into the Schlenk-line.

The filtrate contains some product, but it is not the worth the time to purify it. The crystalline product was used without further purification.
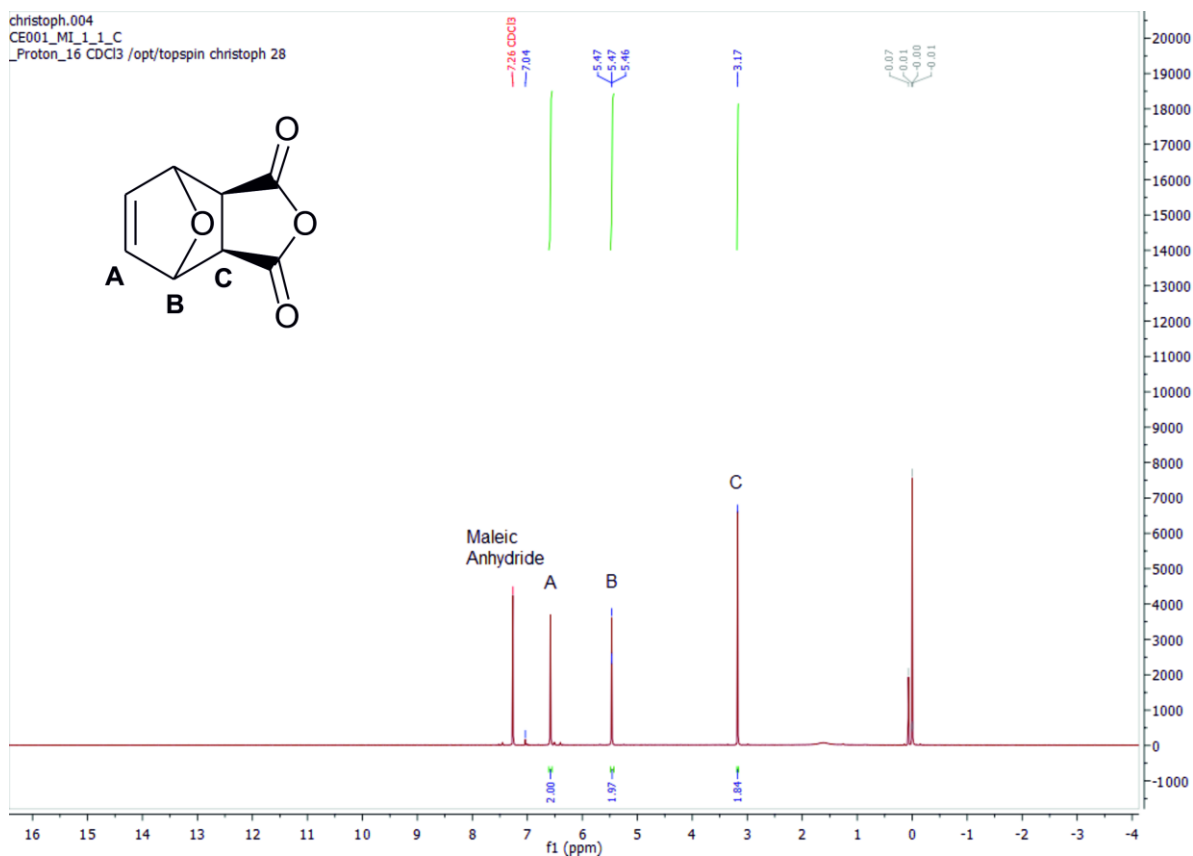

Fig. 1: 1H-NMR of Maleic anhydride; δ=6.58ppm (2H, m, CH=); 5.46 (2H, m, CH-O); 3.18 (2H, s, CH-CO); Note: 7.04ppm is the starting material maleic anhydride

3.1.1.2 Protected maleic imide

The starting material was dissolved in ethanol (2M solution; for 8g a 100mL round bottom flask equipped with a stirrer was used) and cooled with ice. Then 1.05eq of ethanol amine (10M solution) was added dropwise. After 30min the solution was allowed to warm up to room temperature (ca. 30min). Then a condenser was attached and the solution refluxed for 6h at 85°C. After cooling down to 4°C, the product was filtered off. 8g of the starting material resulted in 7.1g product (75%).

Notes: In order to obtain the yield described in the original publication[3] the reaction time, had to be extended and impure product had to be purified a second time as every purification resulted in high- and low-purity product. Washing the product with cold hexane reduces the yield somewhat. In the rare case that the product did not become pure enough, it was dissolved in DCM and washed with

water. Then, flash column chromatography using silica and ethyl acetate (TLC 100% ethyl acetate: RF=0.26) could be performed.
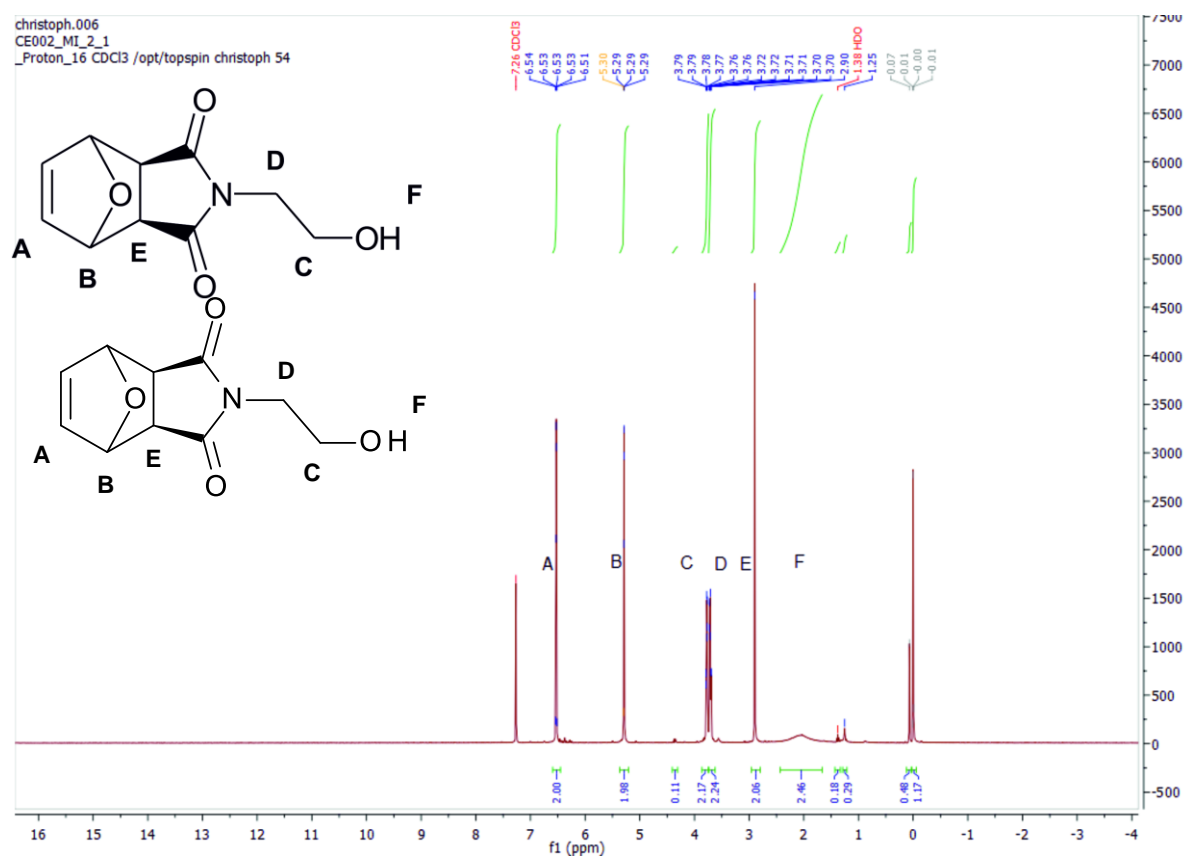

Fig. 2: 1H-NMR of the maleic imide δ=6.53ppm (2H, m, CH=); 5.29 (2H, m, CH-O); 3.79-3.76 (2H, m, CH$_2$-O); 3.72-3.70 (2H, m, N-CH$_2$); 2.90 (2H, m, CH-CO); 2.1 br (1H, s, OH); Note: No traces of ethanol nor amino ethanol found

3.1.1.3 Protected Initiator

The starting material was dissolved in THF as a 0.1M solution (500mL round-bottom flask equipped with a stirrer for 1.6g of starting material). 1.1 eq. of triethylamine were added and the solution cooled to 0°C. 1.1eq. of bromoisobutyrylbromide as a 0.25M solution in THF was added in the course of 30min. The solution was stirred for further 3h at 0°C and 12h at room temperature. The resulting NEt$_3$HBr was filtered off and the solution was concentrated and redissolved in ethyl acetate, which was then washed with NaHCO$_3$ solution and brine. The organic phase was then concentrated again and dried together with silica, so that a thin layer of powder can be put on top of a silica column. The product was then eluted with a 1:1 mixture of ethyl acetate in hexane. 1.6g starting material gave 2g yield (71%).

Notes: if the triethylamine is coloured, it needs to be distilled. It seems to be more efficient to add less of the bromoisobutyrylbromid, even if the conversion gets reduced, because an excess it difficult to separate from the product. Moreover, remaining reagent seems to make the product unstable. The washing step was introduced to eliminate HBr that hinders ATRP. The bromoisobutyrylbromid-solution is added best *via* syringe as it tends to degrease the joints in dropping funnels. The conversion can be checked *via* TLC using 100% ethyl acetate and KMnO$_4$ stain. The crude product is best dried with silica, as it is a sticky gel that can solidify within pipettes. Large quantities are better purified *via* two flash columns rather than using one big column and a long gradient. If the initiator blackens, it can be purified by dissolving it in 40mL THF and passing it through 5mL of celite and 25mL of basic ALOX (using a 50mL syringe as a makeshift column). It can be combined with a 45µm PTFE filter.
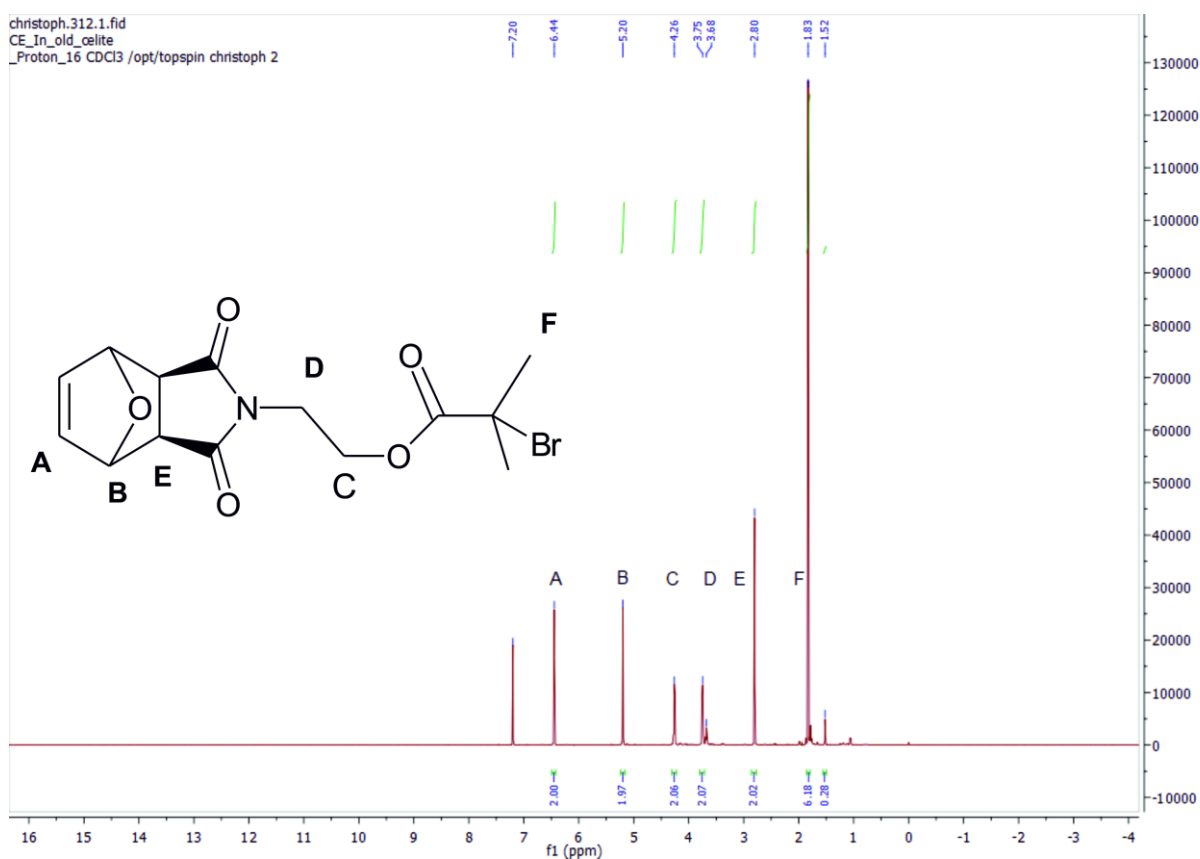
Fig. 3: 1H-NMR of the initiator: δ=6.44 ppm (m, 2H, CH=), 5.20 (m, 2H, CH-O), 4.26 (m, 2H, CH$_2$-O), 3.75 (m, 2H, CH$_2$-N), 2.80 (m, 2H, CH-CO), 1.83 (s, 6H, CH$_3$); note: the acylation of the alcohol splits the multiplettes of the neighbouring groups.

3.1.2 ATRP

3.1.2.0 General Remarks

The ATRP were carried out under Schlenk conditions since oxygen stops the reaction. Water was not an issue, moreover the reaction seems to be robust enough that traces of oxygen are tolerated (decreasing somewhat the yield). For instance, it was possible to mix all components together and add the copper salt directly in a light counter argon flow thus starting the reaction without degassing the salt.

Also, radical scavengers and substance such as HBr had to be avoided. Thus, pure solvents (dry or distilled) and distilled ligands were used. Distilled substances were stored under argon at -20°C. The monomer contains radical scavengers. It was initially distilled at 30°C and 30 Torr and stored in the freezer. Later the monomer was passed through basic ALOX (utilizing a syringe filled ALOX up to 2/3 of the volume over a thin layer of glass wool) twice thus avoiding the chance that a drop bypasses the minicolumn. The latter method lost probably even more monomer but was much faster to apply thereby allowing fresh monomer whenever needed. Similarly, yellowed ligands could be diluted in 16mL DCM and passed through 2mL celite and 10mL basic ALOX using a 20mL syringe as a makeshift column. It can be further combined with a 45µm PTFE filter.

Schlenk tubes were stored at 80°C and were assembled whilst being hot. They were evacuated and refilled with argon. Afterwards the cycle was repeated twice reheating the tubes with a heatgun. Copper salts and pulverized initiator were filled as powder in the Schlenk tubes. They were carefully evacuated and set under argon. This procedure was repeated twice taking about 15min unless the initiator appeared to be containing moisture or solvents.

The initiator-monomer mixture and the copper-salts-ligand mixture were homogenised through sonication. The solutions were originally bubbled through with argon for 15min, as it is difficult to degas the monomer or ligand without losing much material. However, this resulted still in a volume loss (e.g. using MTBE) or in freezing of the solvent (tBuOH). Thus, the procedure was changed into the freeze thaw process (freezing the solution; evacuating and closing valve; thawing solution; quickly evacuating without making the solution boil; and allowing argon in; repeat once or twice until bubble formation was greatly reduced).

Note: Freeze drying changes the colour of the copper-complex temporarily to violet, deep blue and green. During the ATRP it becomes an opaque malachite-green (in case of tBuOH as solvent). If the solution becomes reddish Cu_2O is formed. This is probably caused through a bad initiator.

The wrong ALOX or glass-fritte can result in low yields, as the product can become stuck. The THF used for washing the ALOX should be distilled since technical THF contains methyl-di-*tert*.-butyl-phenol as stabilizer (often not mentioned on the label). This compound accumulates during the work up and overlaps with the 1H-NMR.

The deprotected oligo acrylic acid is sensitive to moisture and heat. It has to be stored in the freezer.

3.1.2.1 Oligo(acrylic acid)

3.1.2.1 Method A (DP=12-30; PDI=1.1)

The typical batch size was 100mg of initiator. For it, two 25mL Schlenk tubes were prepared. One was filled with the initiator (1eq., finely ground) and the other with 400mg CuBr (10eq) and 62mg $CuBr_2$ (1eq). The initiator was dissolved in 5.6mL dry anisole (producing a 0.05M solution) and 4.1mL *tert.*-butyl acrylate (3xDP eq.) were added. The solution was further homogenised through sonication. In the other tube, 5.6mL anisole and 600μL PMDETA were added suspending the copper. Both solutions were stirred for 30min at 75°C, then 10vol% of the copper complex solution was added to the other tube. After 16h at 75°C the reaction was stopped by bubbling oxygen through the solution and passing the solution through a column of basic ALOX (filled up to 2-3x the column diameter). The solvent was removed and the oligomer was redissolved in a minimal amount of THF. The product was then obtained through precipitation in cold 80vol% methanol.

The oligomer can be further purified with column chromatography (3x12cm SiO_2, 200mL 2:1 hexane/ethyl acetate; 300mL 1:1 hexane/ethyl acetate; 300mL ethyl acetate; 20mL-Fractions; TLC: 1:1 hexane/ethyl acetate; stained with $KMnO_4$).

Note: using 100eq of monomer resulted in a DP of 31. With only 20eq. of monomer a DP of 6 is reached. It can be assumed that 3xDP corresponds to the required number of equivalents. However, the DP is dependent on the reaction time (unlike method B, where the reaction can be left longer). The shorter the oligomer the less likely precipitation works (below 12?). The product can appear as foam (higher PD makes this more likely).
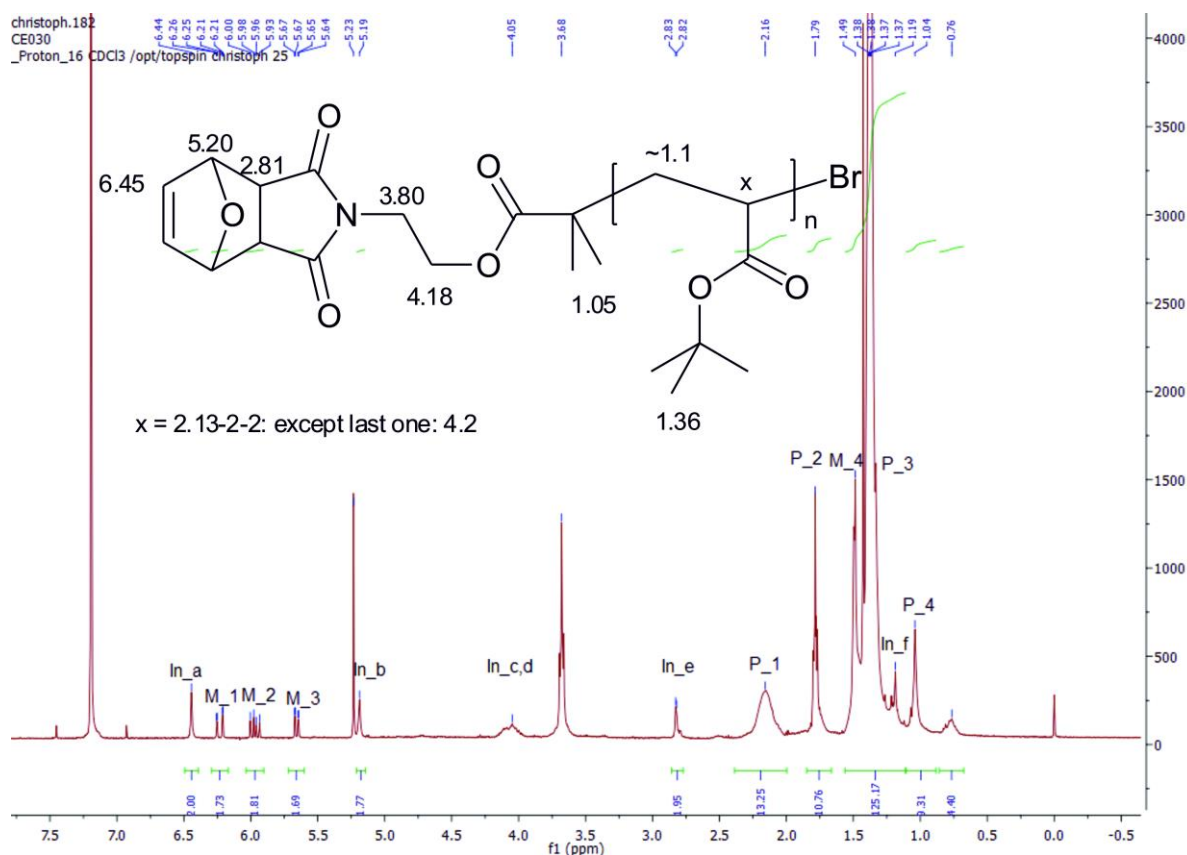
Fig. 4: An example of a NMR spectrum of *oligo*(*tert*. butylacrylate) PD=15 with protected maleic imid group and unreacted monomer. In_a to In_f represents the signals from the initiator (which have not changed except for the resolution of the multiplette caused by the slower tumbling of the CH_2-CH_2-group); P represents signals of the polymerised monomer, with P1 (m, 1H, CH-CO_2; except CHBr-CO_2), P2 (m, 1, C**H**,H-$CHCO_2$), P3 (s, 9H, COO-*t*Bu) and P4 (m, 1H, CH,**H**-$CHCO_2$) and M_1 –M_4 represents the signals of the residual monomer.

3.1.2.1 Method B (DP=6-12; PDI=1.3)

For a batch of 100mg initiator, two 25mL Schlenk tubes were prepared. In one the initiator is placed (2eq., finely ground) and in the other 20mg of CuBr (1eq). Both tubes were evacuated carefully for 5min and then slowly filled with argon. The freshly prepared monomer (2*DP equivalents) was then added to the initiator and the Me_6tren (1eq.) to the CuBr. To both tubes 3mL of distilled *t*BuOH were added and homogenised through sonication. Traces of oxygen were removed by 2-3 freeze-thaw cycles from both tubes and the solutions were warmed to 30°C. Then a syringe was used to transfer the more homogeneous solution to the other and the mixture was stirred for 3h. The reaction was stopped by passing the solution through a column of basic ALOX (filled up to 2-3x the column diameter). The

solvent was removed and the oligomer was redissolved in a minimal amount of THF. The product was obtained through precipitation in cold 80vol% methanol.

The oligomer can be further purified with column chromatography (3x12cm SiO_2, 200mL 2:1 hexane/ethyl acetate; 300mL 1:1 hexane/ethyl acetate; 300mL ethyl acetate; 20mL-Fractions; TLC: 1:1 hexane/ethyl acetate; stained with $KMnO_4$)

Notes: Polymerisation seems to change the 1H-NMR signal of the $N-CH_2CH_2-O$ group from two peaks to one. Adding 10eq. of ascorbic acid cause complete conversion. At a certain chain-length precipitation does not work any longer as the oligomers become oils (ca. DP<20).
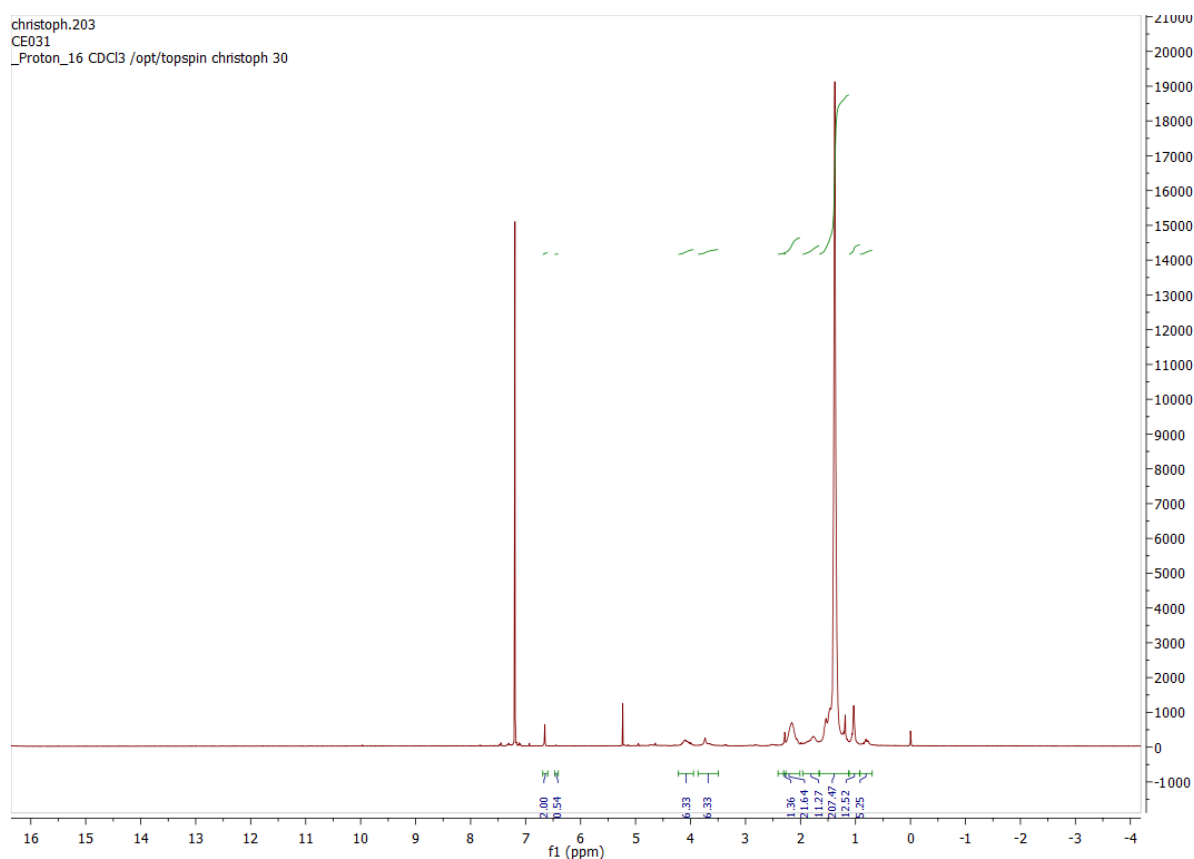
3.1.2.2 Retro-Diels-Alder reaction

The maleic imide was deprotected by refluxing the oligomer in toluene as a 0.05M solution, under argon for 20h. The solvent was removed at 75°C and $2*10^{-2}$mBar. The yield was 95-100%.

Notes: The evolving furan vapours will attack argon balloons, if not cooled sufficiently. Solvents like toluene, anisole and DMF experience a remarkable reduction in vapour pressure effectively denying the possibility of using a rotavapor. Instead a Kugelrohr can be used. Therefor for greater amounts it is recommended to use the bottom flask of a Kugelrohr device since rotating the flask is more efficient than stirring the thickening solution. For smaller quantities it is recommended to use a pear-shaped flask as the can be more readily redissolved in a minimal amount of THF.

DMF leads to decomposition of the polymer and is furthermore even harder to remove.

Isooctane seems to work and can be removed easily, but the conversion seems to be somewhat lower. The main problem was the poor solubility of the polymer and the high contamination with stabilizers (cresol produced the highest peaks in the 1H-NMR).

christoph.203
CE031
_Proton_16 CDCl3 /opt/topspin christoph 30

Fig. 5: An example of NMR (see method A for comparison) after deprotection of the maleic imide through a Retro Diels Alder reaction. The alkene signal is shifted from 6.5 to 6.7 and slightly decreases the integral through a side reaction. Furthermore, the peak at 5.2 disappears when the resulting furane is removed

3.1.2.3 Deprotection of the carboxylic acids

The carboxylic acid groups were deprotected by dissolving the oligomer in DCM (making a 0.1M solution), cooling it to 0°C and adding 2eq. TIPS, water and 20eq. of TFA per COO*t*Bu group. The solution was stirred for 1h at 0°C and 5h at room temperature. The product was recovered through precipitation in cold hexane. For further purification it was redissolved in methanol which was then added dropwise to an excess of cold water precipitating contaminations. The product was finally lyophylised and stored at -20°C. The yield ranged between 40%-95%.

Notes: the purification procedure removes TFA under mild conditions but separates also partially protected oligomers and monomers. The deprotection seems to fail on oligomers with a DP of less than 6, resulting in an ill-defined product. TFA vapours attack septums, thus Teflon stopper should be

used instead. The TFA has to be removed before the solution becomes concentrated as it would attack the other ester bond and possibly even other functional groups (thus the precipitation in hexane). The aqueous phase can be dried directly, risking however the crosslinking of the oligomer under these harsh conditions. Traces of acid (HBr from the initiator or TFA from this reaction step) render the product unstable causing it to crosslink (no visible changes, but insoluble) and turning slowly from a white solid over yellow and brown to a black oil. Attempts of dialysis failed, as the product seemed to polymerise.
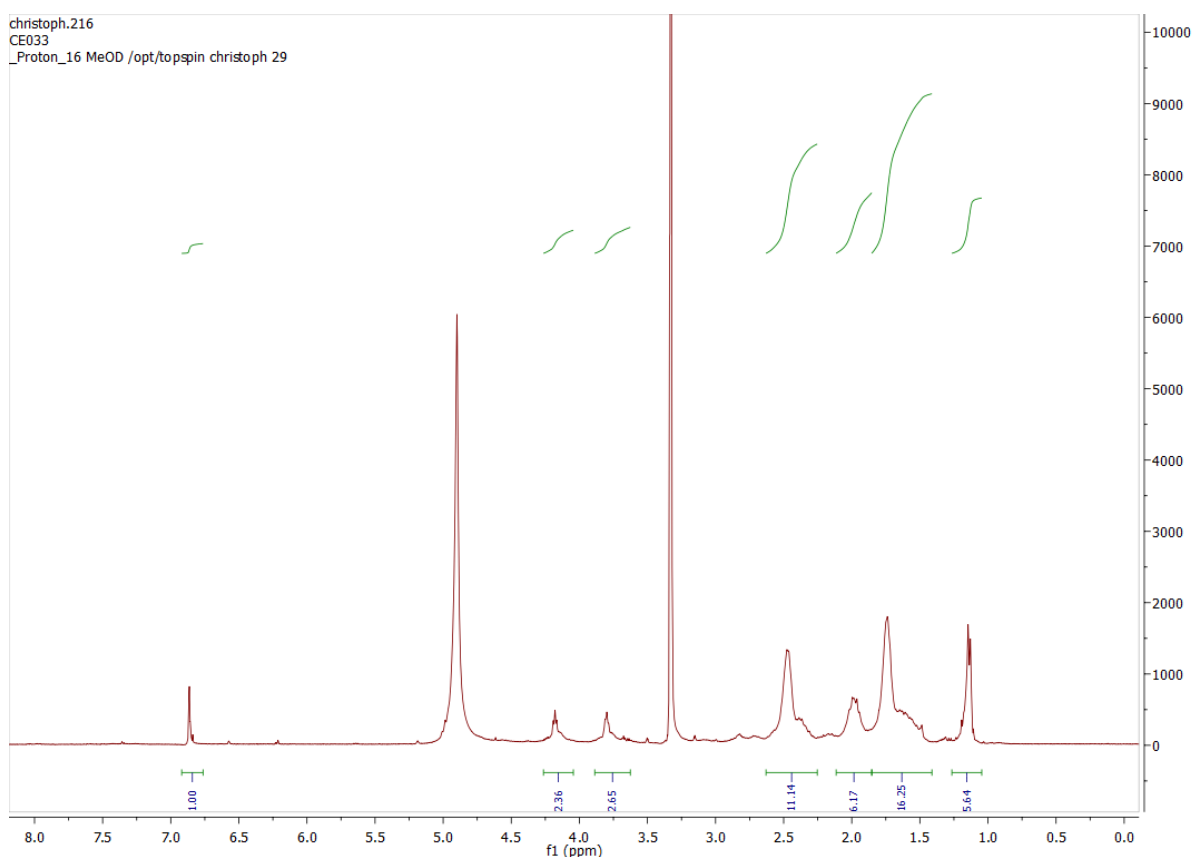
Fig. 6: An example of NMR (compare with method A and the first step of the deprotection) after the *tert*. Butyl of the carboxylic acids is removed with TFA.

3.1.2.4 Oligo(NIPAAM)

For a batch of 100mg initiator (finely ground), a 25mL Schlenk tube was prepared. The finely ground initiator was placed therein and was carefully evacuated for 5min and put under argon atmosphere. The NIPAAM (2*DP equivalents; purified *via* sublimation) and the Me$_6$tren (1eq.) were then added to

the initiator. The tubes content was then dissolved in 5.6mL of dry *t*BuOH (0.1N) and homogenised *via* sonication. The solution was warmed to 30°C and briefly degassed through bubbling argon into the solution. The reaction was started by addition of 20mg of CuBr (1eq) in mild argon counter flow. The solution was stirred for 3h at 30°C. The reaction was stopped by passing the solution through a column of basic ALOX (filled up to 2-3x the column diameter). The solvent was removed and the oligomer was redissolved in a minimal amount of THF. The product was obtained through precipitation in 20mL of a cold mixture of 2:1 hexane and diethyl ether. The product was redissolved in n-propanol and dialysed with a 10mL FloatALyzer (200-400Da Cutoff) using 500mL of n-propanol. The solvent was exchanged every day for three days. The yield was ca. 40%.

Note: Since even oligomers are able to crystalize, precipitation remains an option independent of the chain-length. However, the product is poorly soluble in *t*BuOH, causing precipitation already during the reaction. Moreover, the monomer cannot be removed in vacuum. Nor can the product be purified through column chromatography since the product remains stuck on silica. The product has therefore to be dialysed. N-propanol was the only organic solvent that did not damage the dialysis membranes.

3.2 OmpF mutants

3.2.1 Media and general remarks

The growth media and related material were prepared before usage under sterile conditions:

LB miller (10g of tryptone, 5g of yeast extract and 10g of NaCl per litre)

2YT (20g of tryptone, 10g of yeast extract and 10g of NaCl per litre)

LB-plates (LB medium with 15g/L Agar; optional: 300µM of ampicillin and 122µM of X-Gal)

SOC: 2wt% tryptone, 0.5wt% yeast extract, 10mM NaCl, 2.5mM KCl, 10mM $MgCl_2$, 10mM $MgSO_4$ and 20mM glucose

1000x **ampicillin**: 300mM in 50% aqueous ethanol

1000x **IPTG** 0.4M in water

The **OmpF mutants** were kept as a library of DH5α *E.coli* (in LB-medium with 10% Glycerol stored at -80°C) which is optimised for plasmid amplification. For expression of the protein, the plasmid was transfected into Omp8 *E.coli*, a custom strain suited for protein over expression (using IPTG) lacking several membrane proteins that would interfere with the Omp8 purification. In every case ampicillin resistance was used for selection. X-Gal was used to make colonies more visible for picking, but more

importantly to make sure that Omp8 for transfection was without plasmid, as these *E.coli* did not have an ampicillin resistance and had to be freshly grown for electroporation.

Bacteria were generally thawed on ice and kept there (especially as long as the bacteria were needed to be alive). Thawed bacteria were not pipetted or vortexed as they are particularly sensitive (unlike freshly grown E.coli). E.coli samples were never frozen without 10% glycerol or 5% DMSO (or in pellet form) in order to avoid freezing induced cell damage.

The expressed OmpF is extracted in the final step with 3% detergent. For many vesicle-formation methods this can decrease the performance. However, the concentration can be lowered to about 0.5g/L via dialysis (for instance with 7.5kDa cutoff Gebaflex) without causing precipitation, although it is below the cmc.

The expressed OmpF featured at times two bands in **SDS-gels** (in particular D12K89C, R270C and D12R270C) approximately at 38- and 40kDa, whereas the expected weight was 39kDa. Excluding cysteine bridges (could only apply for double mutants) and OmpA (37kDa, but not present in Omp8) it might stem from the overexpression resulting OmpF with partially remaining signalling peptide (2000 Da).

3.2.2 PCR and introduction of single mutations

The following describes the mutation of K89C-OmpF to R270CK89C-OmpF. R270C-OmpF was produced in analogous fashion from wt-OmpF bearing *E.coli*. The plasmid was obtained by growing **Omp8** *E.coli* containing the plasmid with K89C-OmpF in LB-Amp (10μL stock solution in 10mL LB-Amp in a 50mL Falcon tube shaken overnight at 37°C at 200rpm). After centrifugation for 5min at 6654 rcf (8000rpm) a **MiniPrep** kit was used. The plasmid was amplified by transfecting it into **DH5a** using the **heatshock** procedure (as recommended by the supplier)[39] and repeating the procedure for obtaining the **plasmid**.

The mutations were introduced *via* site-directed mutation using a two-step PCR protocol based on Wang W, Y.[4]: Two PCR reactions were run; one for the forward and one for the reverse primer. To 25.5μL of nuclease free water 5μL 10X Pfu-Buffer, 2.5μL 10mM dNTPs, 1μL plasmid (K89C-OmpF, 50ng/μL), 6μL 2.5μM primer (R270C), 2.5μL DMSO (facilitating unbinding) and 1.5μL Pfu polymerase

---

[39] Thaw an aliquot of DH5α on ice and take 30μL from the aliquot. Add 50-100ng DNA. Keep it for 30min at 0°C, then heat it for 45s to 42°C and cool it again to 0°C for 2min. Add 200μL of LB-Medium and incubate it for 1h at 37°C and smear 30μL across a LB-Amp plate the rest of the solution using glass-beads on a second plate (in case the cellular uptake is low).

were added and gently mixed. The following temperature program was used for the PCR: 5min 95°C hotstart; cycle 10x(1min 95°C melting; 1min 63°C annealing, 10min 68°C elongation). The content of both tubes was then mixed and split again for a second round using the same temperature program but for 25 cycles and a 30min 68°C final elongation. Thereafter 1µL each of DPNI was added and the sample was incubated for 1h at 37°C.

The product was purified *via* electrophoresis using a 1% agarose gel (TAE-buffer, see **Fig.7**), cutting the relevant band and applying the **gel-extraction kit**. Since the plasmid is no longer coiled a much more efficient *E.coli* was required for transfection. The uptake into **XL1-Blue ultra-competent cells** was done as follows: A LB-Amp-plate was preincubated for 30min at 37°C and an aliquot of the ultra-competent cells was thawed on ice. 8µL 0.2M DTT and 10µL of plasmid were added and the mixture was incubated for 15min on ice. The entire volume was smeared on the preincuabted plates and incubated for another 12h. Colonies were picked with Eppendorf tips and regrown in 10mL LB-Amp in a 50mL falcon tube (cap screwed on loosely) overnight at 37°C and 200rpm.The samples were centrifuged and the **plasmid** was obtained as described before. Note: 50% of the sample were saved as stock solution by adding 10% glycerol and storing them at -80°C. The correct sequence of the plasmid was verified.

List of primers for the mutations (altered tricodon made bold):

K89C

     A 5'-CGC-GGG-TCT-T**TG-C**TA-CGC-TGA-CGT-TGG-3'

     B 5'-CCA-ACG-TCA-GCG-TAG-CAA-AGA-CCC-GCG-3'

R270C
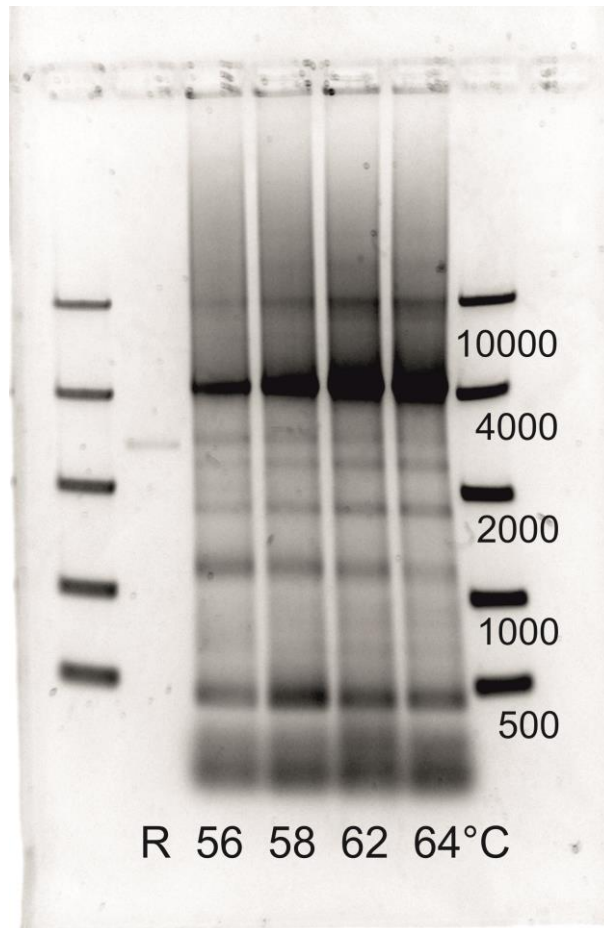
     A 5'-GTG-TAA-GCG-ATG-GAC-GGG-CAC-AGA-CCG-AAA-TCG-3'

     B 5' CGA-TTT-CGG-TCT-G**TG-C**CC-GTC-CAT-CGC-TTA-CAC-3'

D12C

     A-5'-GAT-GGC-AAC-AAA-GTA-**TGC**-CTG-TAC-GGT-AAA-GCT-GTT-GG-3'

     B-5'-CCA-ACA-GCT-TTA-CCG-TAC-AGG-CAT-ACT-TTG-TTG-CCA-TC-3'

Fig. 7: 1% Agarose gel displaying the PCR-product of K89R 270C OmpF mutant produced at 4 different annealing temperatures. The product was not purified nor digested with Dpn1 at this point, the template R is thus still visible. The shift in the run-time of the plasmid stems from the supercoiled nature of the template.

Table 1: Sequenced part of the DNA of the final product after amplifying it in XL1 ultra competent cells translated to the corresponding amino acids. The underlined cysteine residues are the K89R270 mutation sites.

> … L A F A G L **C** Y A D V G S F D Y G R N Y G V V Y D A L G Y T D M L P E F G G D
> T A Y S D D F F V G R V G G V A T Y R N S N F F G L V D G L N F A V Q Y L G K N E
> R D T A R R S N G D G V G G S I S Y E Y E G F G I V G A Y G A A D R T N L Q E A Q
> P L G N G K K A E Q W A T G L K Y D A N N I Y L A A N Y G E T R N A T P I T N K F
> T N T S G F A N K T Q D V L L V A Q Y Q F D F G L **C** P S I A Y T K S K A K D V E G I
> G D V D L V N Y F E V G A T Y Y F N K N M S T Y V D Y I I N Q I D S D N K L G V G
> S D D T V A V G I V Y Q F **Stop**

3.2.3 Insertion in Omp8

The plasmid was inserted into **Omp8** *E.coli* using the following procedure: 20-50µL of the Omp8 *E.coli* were plated on LB-plates without ampicillin (with blue-white-staining) using glassbeads. The plate was incubated overnight at 37°C. The colonies were carefully scratched off and suspended in 1mL of Elga water. Then the suspension was centrifuged at max-speed for 30s using a tabletop centrifuge. The pellet was resuspended in 10% glycerol and the centrifugation was repeated. The pellet was resuspended in 100µL of 10% glycerol. The solution was put for 10min on ice (along with the electroporation cuvette and the thawed SOC-medium) and 2µL (ca. 200ng/µL) of the plasmid were added. The solution was mixed briefly with a vortexer and 40µL of the solution were placed in the cuvette. The outside of the cuvette was wiped clean and placed in the device. The solution was pulsed 2x at 2500V. Immediately thereafter 1mL of SOC medium was added and mixed through pipetting up and down. The culture was incubated for 1h at 37°C in a water bath. The culture was centrifuged and 4/5 of the supernatant was removed so that the pellet was resuspended in ca. 200µL. 30µL were smeared across an LB-Amp plate. The rest of the solution was applied on another plate using glass-beads on a second plate (in case the cellular uptake is low). Colonies were picked and *E.coli* stock was prepared as described above. This time however IPTG was added and half was pelleted and sonicated in minimal amount of PBS with 10% SDS to produce a sample for running a SDS-gel.

3.2.4 OmpF expression and purification

The procedure is based on Grzelakowski 2009.[5] Grow *E.coli* Omp8 on LB-Amp plate overnight at 37°C (can be skipped for fresh and pure aliquots, by adding 10µL of the aliquot directly to the preculture). Select a colony using a 200µL plastic pipette tip. Add it to 50 ml of LB-Amp in a 250 ml Erlenmeyer flask with lid. Incubate the culture with vigorous shaking (250 rpm) overnight at 37°C. Incubate 1000 ml of 2YT-Amp in 2.5-litre cell culture flask with 12-15 ml of overnight culture to yield OD600=0.1. Incubate with vigorous shaking (250 rpm) at 37 °C until the culture has reached the mid-log phase of growth (OD600=0.5-0.8, ca. 2.5-3h). Induce the OmpF overexpression by addition of IPTG (final concentration 0.4mM). A (for K89C-OmpF): pellet it at 4250 RCF for 10min at 4°C after 6h (OD600=2-3); B (for K89R270C-OmpF) let it cool to room temperature and add mercaptoethanol (final concentration 1mM) and shake it for 20h at 300rpm at 25°C. Continue as above. Both procedures yield about 20-25g pellet which has to be stored at -20°C.

Lysis of the cell: Resuspend the cell pellet in 10 ml Lysis buffer (200mM TrisCl pH=8; 25mM MgCl$_2$; 1mM CaCl$_2$) per g cell pellet. Put the solution on ice and treat it with the sonicator A (3x2min pulses of

2s period 50 Hz and 2min wait). Press it 3x though the French Press using 1000bar. Add a spatula tip of DNAse and RNAse and shake it 30min at 25°C. Add 1ml 20 % SDS per 10 ml cell suspension and incubate it for 1 h at 60 °C with gentle stirring in a water bath. Ultracentrifuge it at 22'000 rpm at 4°C for 60 min and keep the pellet.

Pre extraction: Rinse the pellet with 20 mM phosphate buffer pH 7.4 to remove residual SDS. Add 5 ml/g cell pellet 0.125wt% OG in phosphate buffer. Homogenize the pellet by using a Potter-Elvehjem homogenizer and shake it for 1 h at 37 °C. Ultracentrifuge it at 4 °C for 40 min and keep the pellet.

Extraction: Add 3 ml/g cell pellet 3wt% OG in phosphate buffer and homogenize the pellet by using a Potter-Elvehjem homogenizer. Shake it for 1 h at 37 °C and ultracentrifuge it at 40'000 rpm at 20 °C for 40 min and keep the solution.

The purity was verified with 12% SDS-Gels and the concentration was measured both with Nanodrop 2000c (Witec Ag; with the settings E=5.21; M=39.33) and a BCA-Kit (measured with a Spectramax M5 from Molecular Devices).

Notes: 15g of E.coli pellet can yield 30mL 1g/L OmpF. In case that it is more dilute it is advisable to use Vivapore 7.5kDa over 10kDa Amicons (who would also concentrate the detergent). The concentration was determined *via* Nanodrop and BCA-Assay. In case of further concentration steps the detergent concentration should be determined through a colorimetric assay.[6]
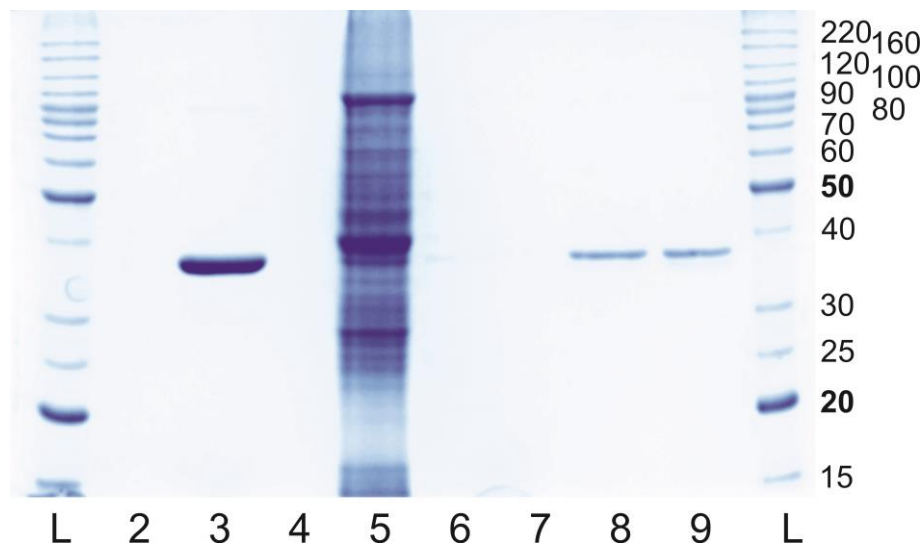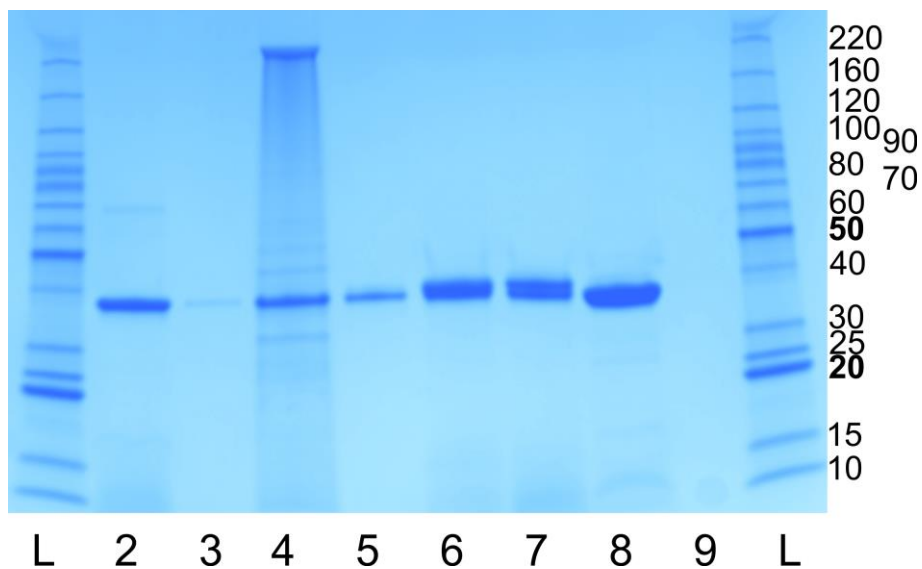

Fig. 8: 12 % SDS gel (200V 50min stained with Coomassie blue), showing the purification steps of the OmpF double cysteine mutant OmpF K89R270C (OmpF-M): L Benchmark ladder; 3 R270C-OmpF as reference; 5 supernatant of the first ultracentrifugation; 6 supernatant of the second ultracentrifugation; 8 product; 9 product (different 1L-cell culture flasks with similar OD_{600})

The occasionally observed splitting of the OmpF band is attributed to the presence of residual signalling peptide (2000 Da).[7]
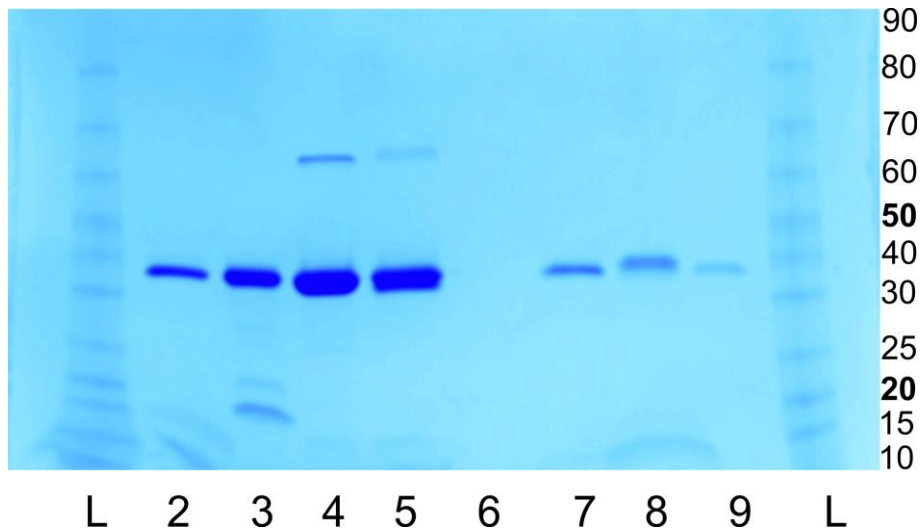
Fig. 9: 4-12% gradient SDS Gel (run at 200V for 35min stained with simple blue; 10µL Ladder; mutants ca. 4-6µg) comparing the unmodified and labelled OmpF-2M with OmpF-WT and single mutations: L Benchmark ladder; 2 OmpF-WT, 3 K89C-OmpF, 4 R270C-OmpF, 5 K89R270C-OmpF/OmpF-M, 6 Gap, 7 R270C-Gala3-OmpF, 8 K89R270C-Gala3-OmpF/OmpF-C, 9 K89R270C-HLG4-OmpF Note: this gel was made one year after the synthesis of the samples, thus some signs of degradation can be seen

Fig. 10: 12 % SDS gel (200V 50min stained with Coomassie blue), showing various OmpF-conjugates: 1) Benchmark Ladder, 2) K89R270C-SH OmpF as reference, 3) R270C-(acrylic acid)$_6$ OmpF, 4) R270C-

(acrylic acid)$_{12}$ OmpF, 5) R270C-Gala3 OmpF, 6) K89R270C-HL3 OmpF, 7) K89R270C-GHLL3 OmpF, 8) R270C-SH OmpF as reference, 9) gap, 10) ladder

3.2.5 Reactivating old OmpF samples

After keeping the OmpF at 0% OG in the fridge for one month only little difference in activity could be seen compared to the negative control. Since there was no other R270C-Gala3 left an attempt was made to reactivate the sample:

OG was dissolved within the sample until it reached 3wt%. Then it was sonicated for 5min at room temperature and shaken for 1h at 37°C. The sample was then dialysed against buffer again in order to remove the OG.

As it turned out the samples prepared thereafter had almost the same concentration and the same activity as those prepared with the fresh sample.

3.2.6 Molish assay

50μL of buffer containing OG was mixed with 250μL 5wt% phenol. Then 600μL concentrated sulphuric acid was added. The solution was stored in a dark container and was allowed to cool down for 15min. Then the absorption was measured at 489nm.

Notes: The Molish assay was used for determining the remaining OG concentration after dialysis or concentration steps (as OG inhibits vesicle-formation). It is based on the works of Urbani et al..[6] To obtain optimal results the OG concentration has to lie between 0.05-0.6wt%. At least 6 known concentrations and 3 sample dilutions should be done. The accuracy increases if the sample is vortexed (in a closed 2.5mL glass vial) after each step including immediately before measurement. Since the sulphuric acid releases gas, most pipetting systems fail. However, a 1mL plastic syringe (without needle) worked well.

Attention: this reaction is quite exothermic, spilling or splashing of hazardous chemicals may occur

3.2.7 Michael addition of Peptide to OmpF

In a GC-vial 50μL peptide (16mM in DMSO; 3x20eq.) were added dropwise to 1mL 0.5g/L OmpF-mutant (30μM). The solution was stirred at room temperature for 12 h. The sample was dialysed twice against 1L of buffer containing 0.5% OG using Midi GEBAflex-tube 50-800μL; 6-8kDa MWCO. The solution was concentrated 2x using 10kDa Amicons (8000rpm).

The reaction was carried out at a pH between 6.5-8 and the DOL was estimated with the acrylodan assay and measured *via* in gel-digestion and LC-MS.

Notes: For basic peptides a pH of 6.5 improved the DOL significantly (due to better solubility).

3.2.8 Acrylodan Assay for determining the DOL

Typically, 5μL of a 0.5g/L mutant OmpF sample were diluted to 30μL using phosphate buffer containing 3%OG. 10eq per thiol group of 1mM acrylodan in DMSO were added and the solution was shaken for 2h at room temperature. Then the solution was diluted to 500μL using 1% OG in citrate buffer and the solution was stirred overnight at 4°C. The fluorescence was detected at 380nm excitation in the range of 450-550nm (maximum around 492nm) using 15nm slit size and 50nm/s scanning speed (triple measurement).

Subtracting the background fluorescence (WT-OmpF), the ratio between the intensity of the sample and the OmpF control (featuring the same mutations) gave the DOL:

$$DOL = 1 - \frac{I_{conjugate} - I_0}{I_{mutant} - I_0} \ (1)$$

Rather than using triplicates several dilutions were measured in the range of 2-5 mg/L. This reduces the risk of artefacts caused by sample concentrations outside the optimal range.

Remarks: 0mg/L is below the best fit line, since acrylodan changes its fluorescence upon reaction with thiol groups and should therefore not be included. The calibration curve changes its slope at 2mg/L and below. At this point the concentration is too low for the measurement.
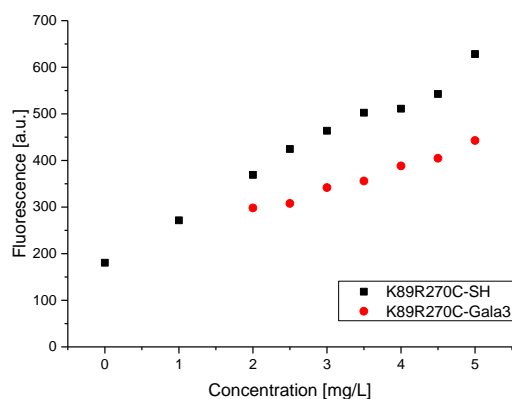
Fig. 11: Acrylodan-assay of K89R270C-Gala3 OmpF (squares) using K89R270C-OmpF for calibration (excluding concentrations below 2.5mg/L the DOL was calculated to be 68%)

3.2.9 Mass spectroscopy

Mass spectroscopy was used to measure the degree of labelling of the OmpF-peptide conjugates. The spectrometer consisted of a LC-MS column (liquid chromatography-mass spectrometry) *ReproSil-Pur C18–AQ, 1.9 µm resin* Dr. Maisch GmbH, Ammerbuch-Entringen, Germany combined with a dual pressure LTQ-Orbitrap Elite mass spectrometer connected to an electrospray ion source (both Thermo Fisher Scientific). The in gel digestion is based on Glatter 2012.[8] Briefly, the band of interest was cut out of the SDS-gel and the sample was cut to tiny cubes. The Coomassie was washed out and the protein was alkylated with iodoacetamide and digested using trypsin. The peptides were then washed out and desalted with C18 reversed phase spin columns Microspin, Harvard Apparatus. After drying, the samples were redissolved and subjected to LC–MS analysis using a linear gradient from 95% solvent A (0.15% formic acid, 2% acetonitrile) and 5% solvent B (98% acetonitrile, 0.15% formic acid) to 28% solvent B over 40 min at a flow rate of 0.2 µl/min. The 20 most intense ions were released from the linear ion trap and subjected to a MS-MS analysis. The intensity of the mutation carrying fragment was put into relation with another fragment of the same sample to eliminate the dependence on the concentration and the ratio was then compared to the same ratio of OmpF with free thiol groups. Note: the peptide fragment bearing the conjugate introduced by Michael addition itself could not be seen probably due to its hydrophobic nature.

$$DOL = \left(\frac{I_{SH-fragment}}{I_{other-fragment}}\right)_{conjugate} \Big/ \left(\frac{I_{SH-fragment}}{I_{other-fragment}}\right)_{mutant} \quad (2)$$

3.3 Creation and testing of the Nanoreactors

3.3.1 Liposomes *via* film rehydration

In a 20mL glass vial 3mg of DSPC; 0.5eq cholesterol-PEG600 (50g/L in chloroform), 0.5eq. cholesterol (50g/L in Ethanol) 0.1eq. POPS (10g/L in chloroform) were added. It was then filled up to 1mL with ethanol and the solution was homogenised through sonication. Then the OmpF (50-100µg e.g. 50µL 1g/L in 0.5% OG containing PBS) and another 1mL ethanol were added and the solution was vortexed. The solvents were then removed in a rotary evaporator at 40°C and 150mBar. The resulting film was slowly rehydrated by adding 1mL of buffer (containing fluorophore or enzymes) and putting it in the incubator at 37°C shaking it at 180rpm for 20h. The vesicles were extruded whilst being warm by pressing it 20x through a 400nm and 200nm membrane. The sample was then dialysed 8x against 1000x the volume of buffer using 100kDa cut-off tubes.

Remarks: Since DSPC does not feature unsaturated carbons it has a transition temperature of 55°C, which is lowered by the other additives, however film-rehydration does still require more than room temperature. At 37°C it takes about 17-20h for rehydration, whereas unsaturated lipids may form vesicles at room temperature in less than one hour. On the other hand, extended periods at elevated temperatures cause a reduction on opaqueness indicating the decline of the vesicle population. Even warm the vesicles are hard to extrude. Thus, the use of a gas operated barrel extruder is advisable.

The mixtures film rehydration is sensitive to detergents (not as much as polymersomes, but notably more than other lipids tried). Using OmpF in 3% OG rather than 0.5% results thus in less and more heterogeneous vesicles. 0.5% is around the cmc of the detergent and the lowest concentration OmpF is stable in. Attempting detergent removal (which works to a limited extend also with polymersomes) fails due to demixing of the components.

3.3.2 Liposomes *via* detergent removal

In a 20mL vial 4mg of sphingomyelin (0.8eq. 10g/L in 66vol% chloroform and 34vol% methanol), 0.2eq. of POPS (10g/L in chloroform) and 0.5eq. of cholesterol (25g/L in chloroform) were added and the solvent was removed using a rotary evaporator at 40°C and 450mBar. The film was redissolved in 2mL buffer containing 3% OG and 100µg/mL OmpF (lipid:protein ratio 1000:1) and 0.25 g/L HRP, shaking it 30min at 37°C. The solution was dialysed over night against buffer containing 200mg Biobeads using

3-5kDa-dialysis tube. The solution was rediluted to 2mL. The vesicle solution was pressed twice through a 1000nm filter, thrice through a 400nm filter and 6x through a 200nm filter using a barrel extruder. The sample was then dialysed over three days using a 100kDa tube exchanging the buffer 7 times.

3.3.3 Polymersomes

To 100µL 50g/L polymer in ethanol and 15µg OmpF (15-75µL) were added in a 5mL pear shaped flask. The film was dried 1h at 150mBar and 40°C and 175rpm and 30min at 0mBar at the Rotavap. 1mL of 0.2g/L HRP in PBS pH 7.4 (freshly dialysed against pure PBS to remove OG) was added and the film along with a small stirring bar. The film was allowed to rehydrate within 12h stirred at 100rpm. The vesicles were then passed 21x through a 100nm membrane using a syringe driven extruder. The sample was then dialysed against 1000x the volume in PBS with 2x buffer changes per day for 3.5 days.

Important: the vesicle-formation is impeded by traces of detergents. The OmpF had thus to be freshly prepared through dialysing the protein 1x against 0.5% OG (1000x the volume; over-night) and 2x pure PBS (2h each).

3.3.4 HRP Kinetics

All samples were diluted to the same final vesicle concentration in case that the scattering varied among the samples. The kinetic were measured at 530/590nm excitation/emission using 7.5nm slits for 600s (300 datapoints). The reaction was started by mixing 500µL PBS; 40µL 0.2µM H_2O_2, 30µL 10µM Amplex Ultra Red and 30µL vesicle-sample (ca. 3 g/L) in a disposable 1mL PS cuvette equipped with a 3mm stirring bar. The measurements were carried out in PBS at pH 7.4 and 6.0 (working solution was also adjusted to the pH).

3.3.5 Carboxyfluorescein encapsulation

Carboxyfluorecein was neutralised with NaOH and diluted in citrate buffer until it had a concentration of 100mM. The solution was then used to rehydrate a film of the DSPC-mix and the 20mL vials were

covered in aluminium to exclude light. The samples were processed as described earlier and the external carboxyfluorescein was removed via minicolumns.

From all samples 10μL were added to 1mL buffer with the corresponding pH. The kinetic was measured at RT for 3h at pH 7.4 and 5.5 (4.62μL concentrated HCl added). Default settings: excitation: 480nm; emission 520nm; slit 5nm; 60nm/min

Note: just as with HRP, carboxyfluorescein contaminates the column to such an extent that it should not be used for anything else.

4 References

[1]   A. Prilipov, P. S. Phale, P. Van Gelder, J. P. Rosenbusch and R. Koebnik, *Fems Microbiol Lett* 1998, 163, 65-72.
[2]   F. Itel, M. Chami, A. Najer, S. Lörcher, D. Wu, I. A. Dinu and W. Meier, *Macromolecules* 2014, 47, 7588-7596.
[3]   G. Mantovani, F. Lecolley, L. Tao, D. M. Haddleton, J. Clerx, J. J. L. M. Cornelissen and K. Velonia, *J Am Chem Soc* 2005, 127, 2966-2973.
[4]   W. Y. Wang and B. A. Malcolm, *Biotechniques* 1999, 26, 680-682.
[5]   M. Grzelakowski, O. Onaca, P. Rigler, M. Kumar and W. Meier, *Small* 2009, 5, 2545-2548.
[6]   A. Urbani and T. Warne, *Anal. Biochem.* 2005, 336, 117-124.
[7]   M. E. Jackson, J. M. Pratt, N. G. Stoker and I. B. Holland, *The EMBO Journal* 1985, 4, 2377-2383.
[8]   T. Glatter, C. Ludwig, E. Ahrné, R. Aebersold, A. J. R. Heck and A. Schmidt, *J. Proteome Res.* 2012, 11, 5145-5156.

IX Appendix

Chapter II

1 Characterisation of SM-mix NRs; see Fig. 17

**Table 1:** Characterisation of SM-mix NRs by DLS using a Zetasizer

Sample	Scattering intensity at 650nm [a.u.]	Concentration/ scattering ratio []	diameter [nm]	Intensity/fraction of population [%]	Polydispersity []
NR-	56581	1.4	190	100	0.08
NR+	52633	1.3	221	100	0.11
NRC	40203	1	208	100	0.11

The samples in **table 1** refer to kinetic experiments (see chapter **kinetics; Fig. 29**). All three samples encapsulated 0.2g/L HRP. In addition, NR+ had R270C-OmpF inserted and NRC had R270C-Gala3 OmpF inserted. The scattering refers to measuring the sample in a fluorimeter at 650nm "excitation" and 650nm "emission" (in truth only scattering occurred and no fluorescence). It allows a comparison of the vesicle concentration. Of these three samples TEM images were also made:
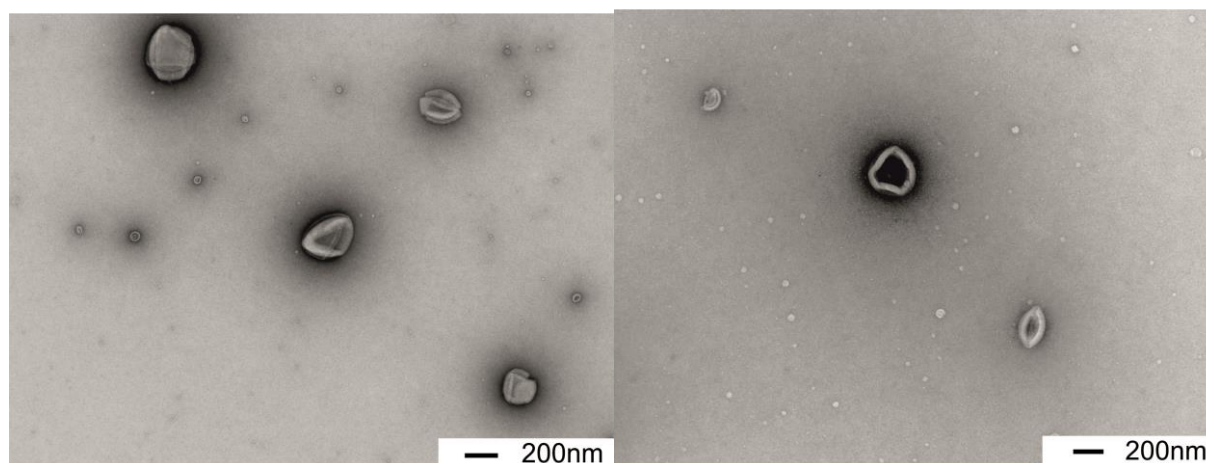
Fig. 1a: NR- at pH 7.4 (left) and 6.0 (right)
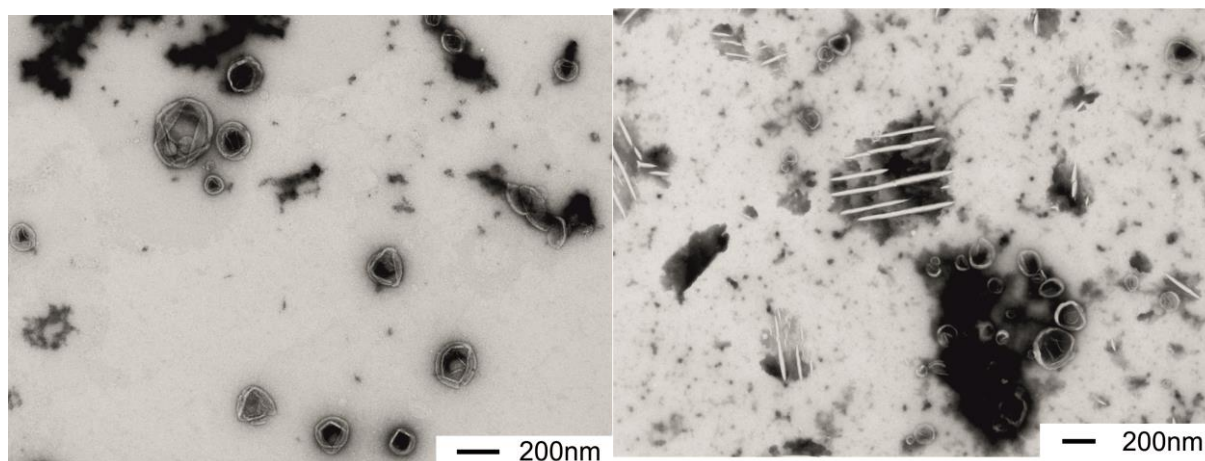
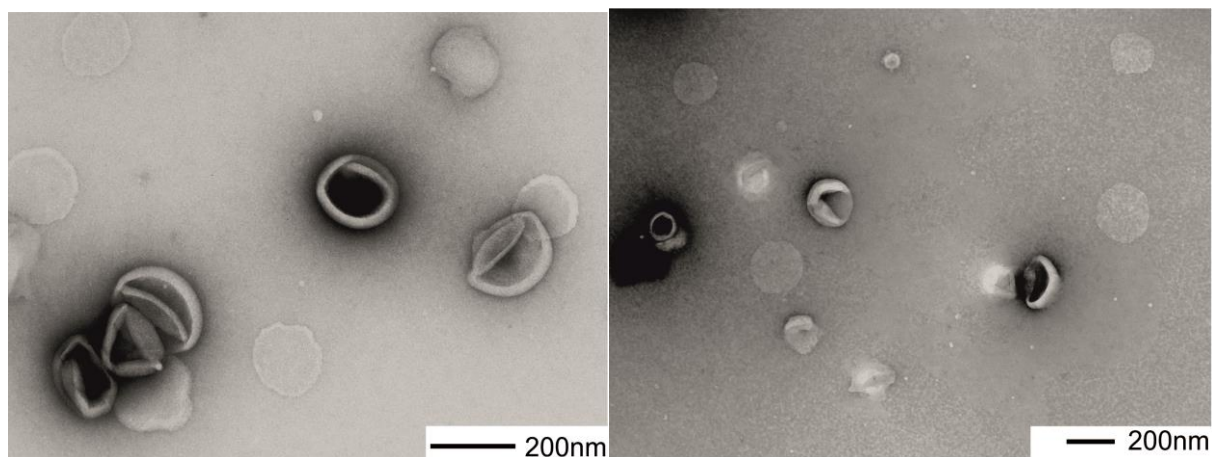**Fig. 1b:** NRC at pH 7.4 (left) and 6.0 (right) featuring R270C-Gala3 OmpF
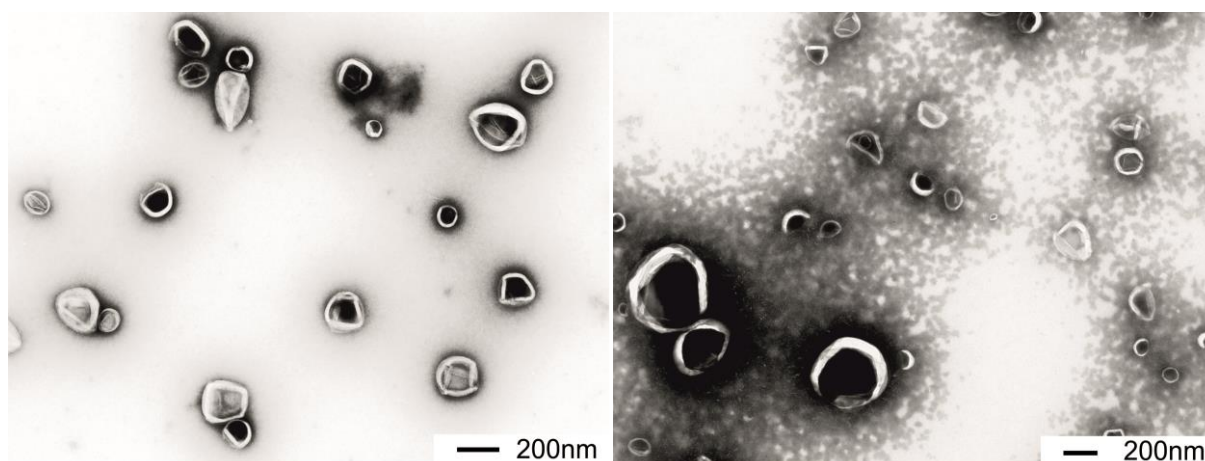
**Fig. 1c:** NR+ pH at 7.4 (left) and 6.0 (right)

It is worth noting, that most TEM made in this thesis were of poorer quality and contained more artefacts, when the samples were acidified. It seems to increase the tendency of vesicles to aggregate and increases the salt concentration. This and possibly the pH, in turn seem to affect the sample preparation/fixation for TEM, where other salts are added.

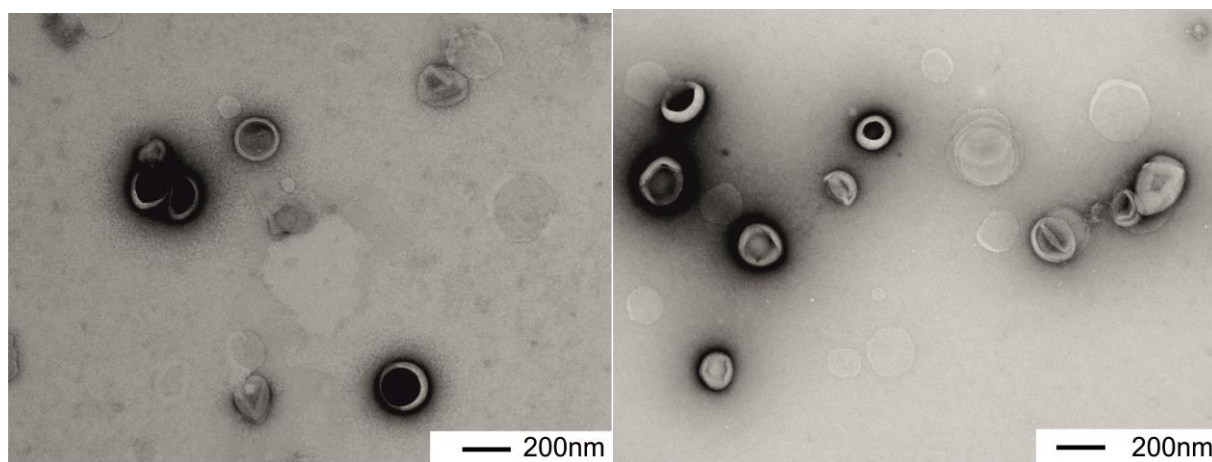## 2 Characterisation of DSPC-Mix NRs see Fig. 19

For the enzyme kinetic (eponymous chapter; **Fig. 31** and **Fig. 41**), SLS-DLS and TEM of the samples were measured:
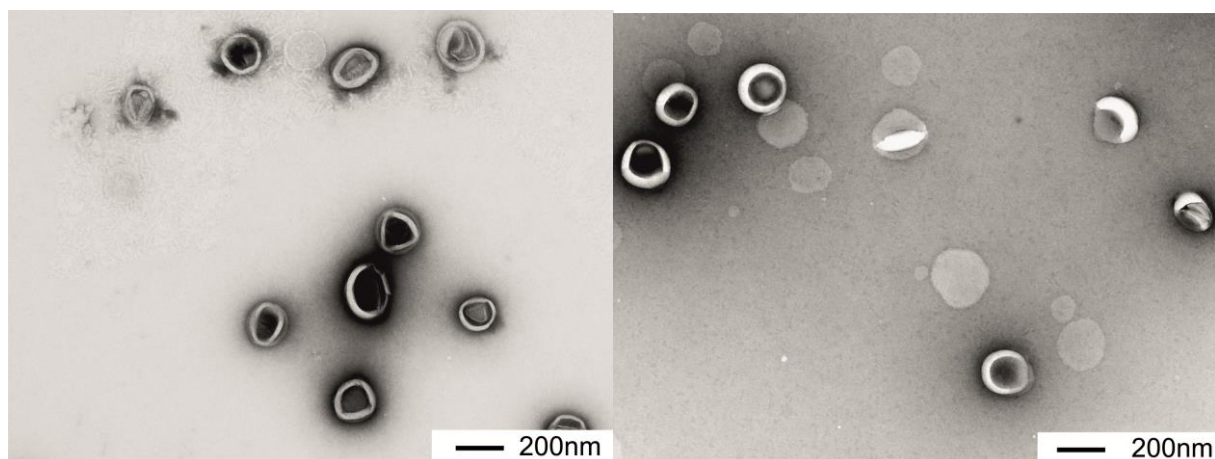
Fig. 2a: NR- at pH 7.4 (left) and 6.0 (right)
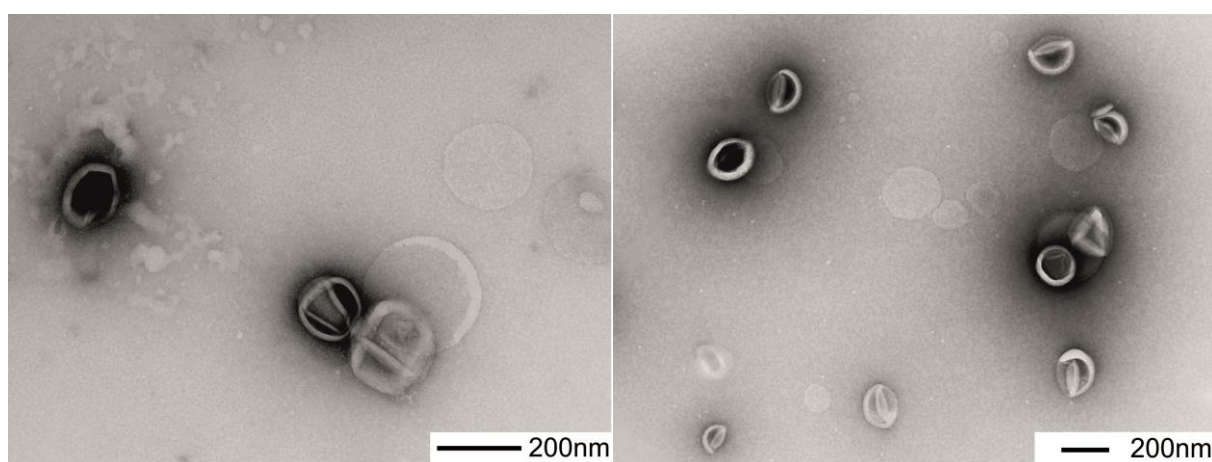
Fig. 2b: NRC1 featuring R270C-Gala3 OmpF at pH 7.4 (left) and 6.0 (right)

Fig. 2c: NRC2 featuring R270C-HLG4 OmpF at pH 7.4 (left) and 6.0 (right)

Fig. 2d: NR+ featuring R270C-OmpF at pH 7.4 (left) and 6.0 (right)

At pH 7.4 it seems that the vesicles are slightly larger and numerous than at pH 6.0 (with the exception of the positive control). It should be noted that TEM images were made after the SLS-DLS-measurements and thus the vesicle samples were approximately 1 day at room temperature and 3 resp. 6 days in the fridge.

Table 2: Light Scattering analysis of the DSPC-mix vesicles; pH 7.4 left; pH 6.0 right; A: negative control; B R270C-Gala3 OmpF; C: R270C-HLG4 OmpF; D: R270C-SH OmpF

|	pH 7.4				pH 6.0			
	A	**B**	**C**	**D**	**A**	**B**	**C**	**D**
R_h [nm]	131	125	105	112	132	133	125	127
R_g [nm]	95.7	90	85	88	96	93	87	92
ρ	0.73	0.72	0.81	0.78	0.73	0.7	0.7	0.72

Although all samples were extruded through 100nm filters, their average diameter appears to be 180-260nm (regarding R_g or R_h). According to TEM, the liposomes appear to be smaller than 200nm rather 100-150nm. Moreover, the large aggregates that were indicated in the light scattering could not be seen in the TEM images.

3 Characterisation of polymersome NRs see Fig 26

The vesicle samples from chapter enzyme kinetics (**Fig. 37**) and the cryoTEM in the chapter preparation (**Fig. 26**) were characterised via SLS-DLS and TEM:
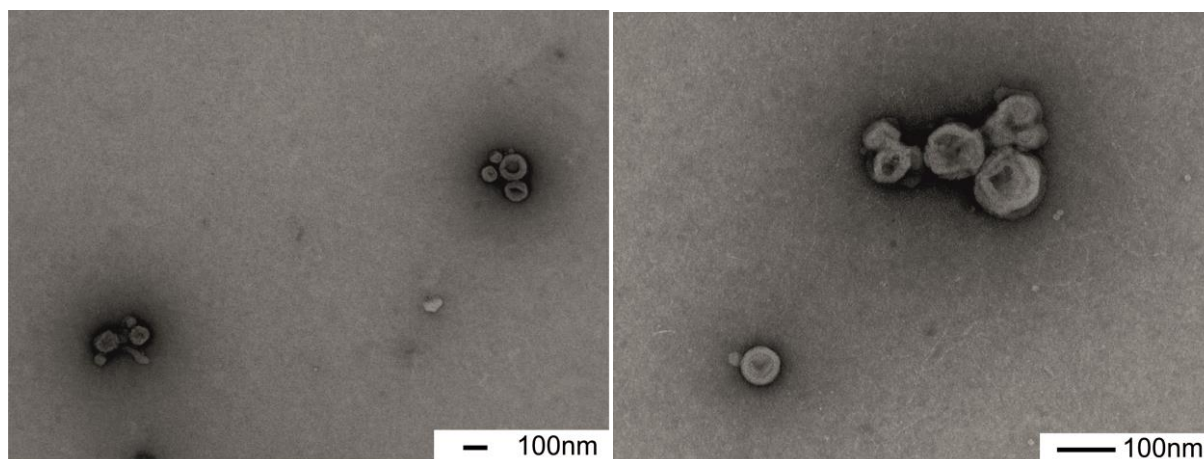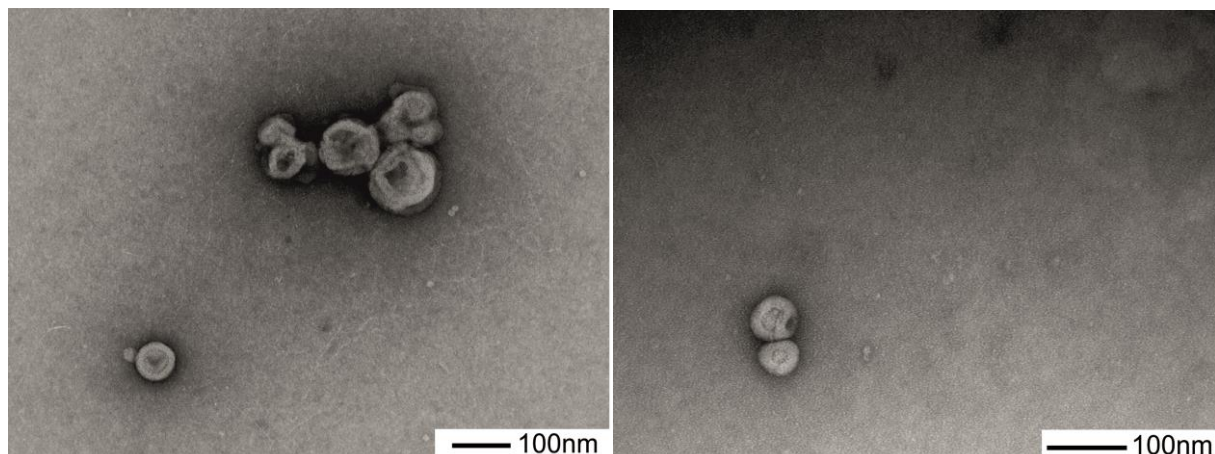
Fig. 3.a: TEM micrographs of HRP[40] loaded polymersomes, NR-, at pH 7.4 (A) and 6.0 (B). Scale bar 100nm.
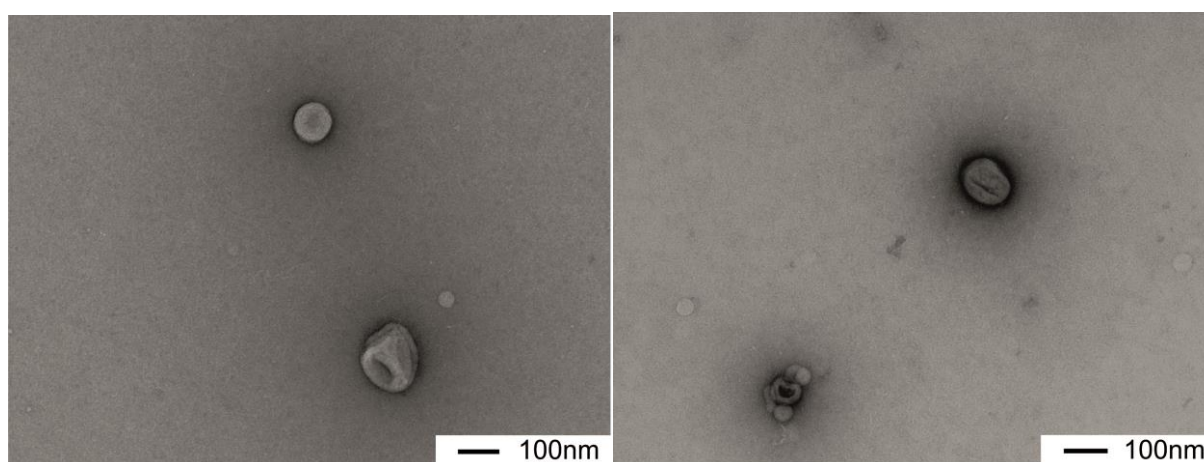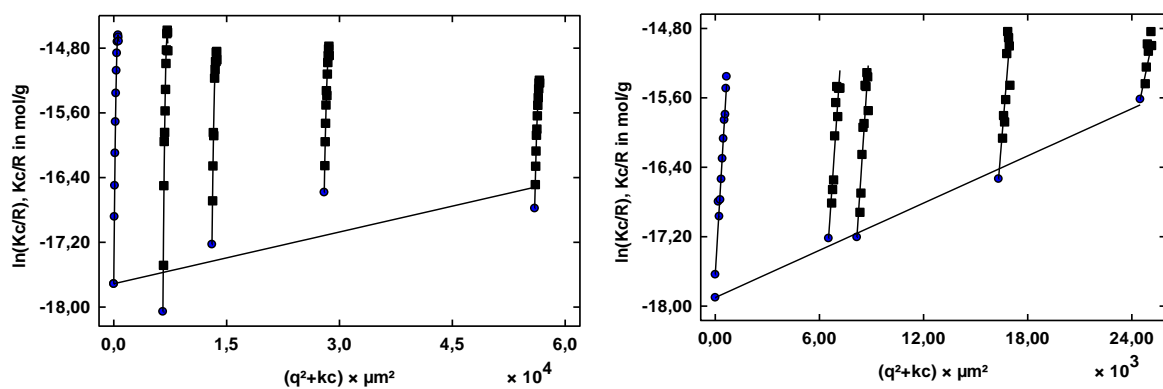

Fig. 3.b: TEM micrographs of HRP loaded polymersomes equipped with OmpF-M, NRC at pH 7.4 (A) and 6.0 (B). Scale bar 200nm.
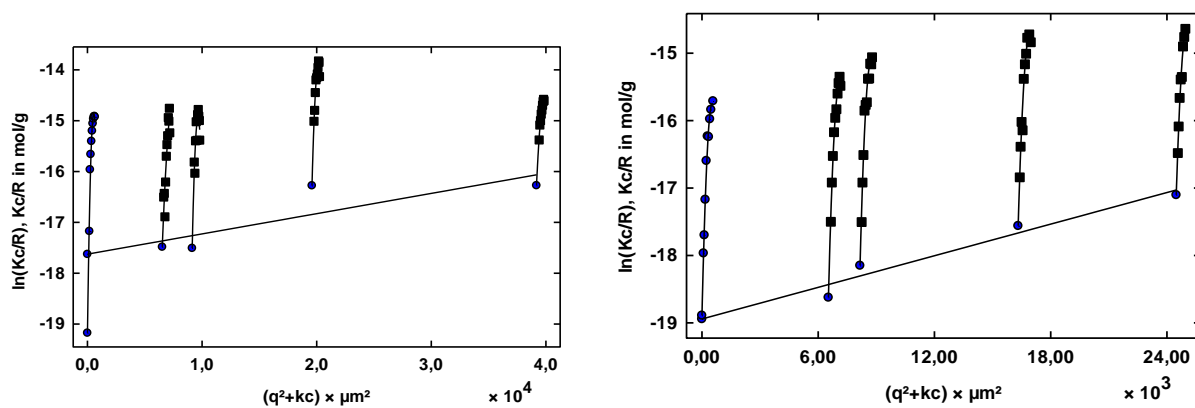

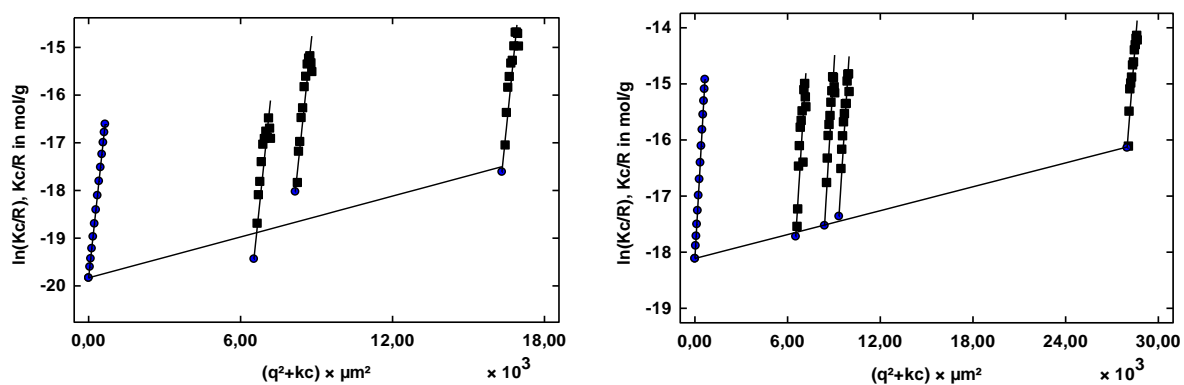[40] See chapter enzyme kinetics

Fig. 3.c: TEM micrographs of HRP loaded polymersomes equipped with OmpF-WT, NR+, at pH 7.4 (A) and 6.0 (B).

Fig. 4.a: Guinier plot representation of SLS data for. HRP loaded polymersomes at pH 7.4 (left) and 6.0 (right)

Fig. 4.b: Guinier plot representation of SLS data for HRP loaded polymersomes equipped with OmpF-M at pH 7.4 (left) and 6.0 (right).

Fig. 4.c: Guinier plot representation of SLS data for HRP loaded polymersomes equipped with OmpF-WT at pH 7.4 (left) and 6.0 (right).

Table 3: Light scattering parameters of: HRP loaded polymersomes (NR-), HRP loaded polymersomes with inserted OmpF-C (NRC), and HRP loaded polymersomes with inserted OmpF-M (NR+).

	pH 7.4			pH 6.0		
	NR-	**NRC**	**NR+**	**NR-**	**NRC**	**NR+**
R_g [nm]	61±8	58±4	61±3	61±1	62±2	63±2
R_h [nm]	64±8	61±4	64±3	66±2	65±2	67±2
ρ []	0.96	0.94	0.95	0.93	0.95	0.93

Chapter III

1 Additional kinetics used for Fig. 38
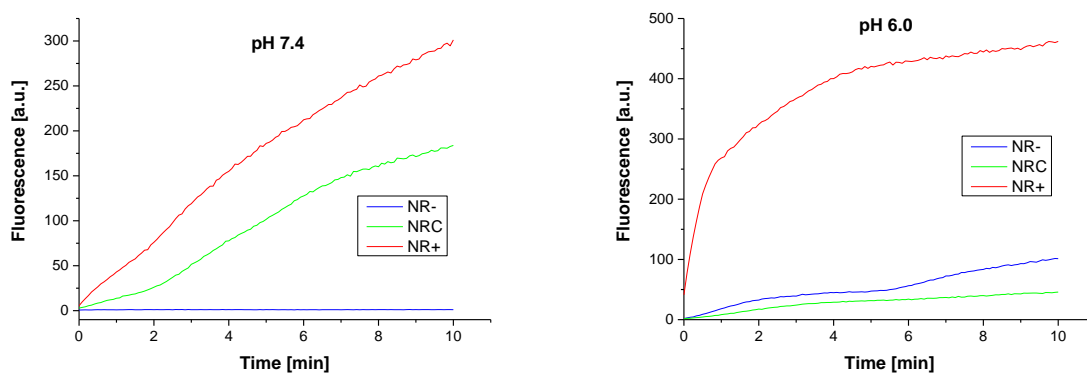
Fig. 5 Amplex Ultra Red conversion kinetics (of the second batch freshly prepared vesicles) of HRP loaded polymersomes (NR-, blue), HRP loaded polymersomes equipped with K89R270C-Gala3 (NRC, green) and HRP loaded polymersomes equipped with K89R270C-OmpF (NR+, red) at pH 7.4 and pH 6.0.
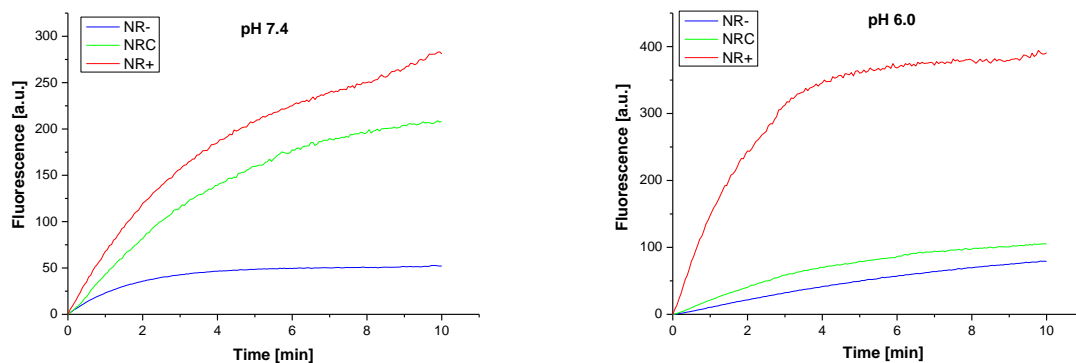
Fig. 6: Amplex Ultra Red conversion kinetics (third batch) of HRP loaded polymersomes (NR-, blue), HRP loaded polymersomes equipped with K89R270C-Gala3 (NRC, green) and HRP loaded polymersomes equipped with K89R270C-OmpF (NR+, red) at pH 7.4 and pH 6.0.
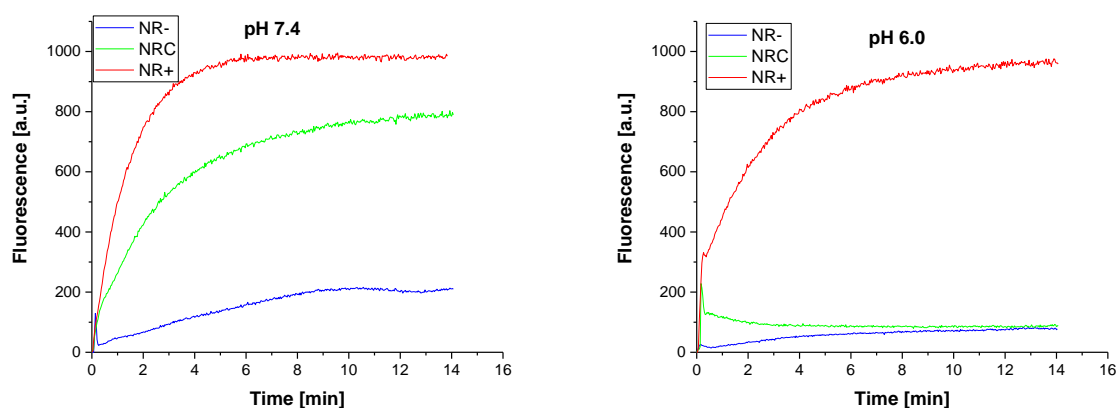
Fig. 7: Amplex ultra red conversion kinetics (fourth batch) of HRP loaded polymersomes (NR-, blue), HRP loaded polymersomes equipped with K89R270C-Gala3 (NRC, green) and HRP loaded polymersomes equipped with K89R270C-OmpF (NR+, red) at pH 7.4 and pH 6.0.

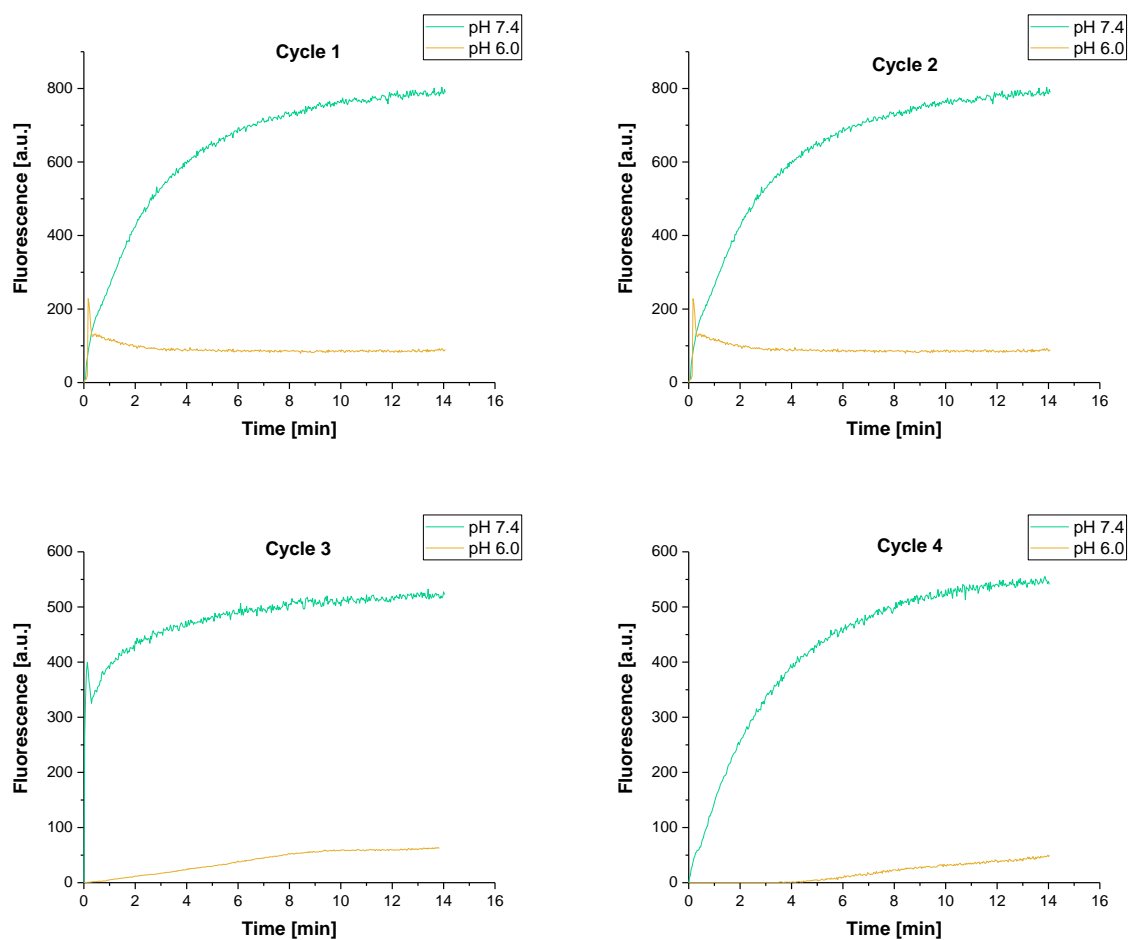**Fig. 8:** Amplex red conversion kinetics of HRP loaded polymersomes equipped with K89R270C-Gala3 in relation to pH cycling (using batch 4, see Fig. 39, enzyme kinetics). green: pH 7.4, ochre: pH 6.0 After every cycle new Amplex and H_2O_2 was added to the same sample.

Table 4: Activity change (slopes) of the pH cycling experiment

Cycle	Initial slopes: Batch 0	Batch 1	Batch 2	Batch 3	Slopes corrected by taking dilution into account: V_{total} [μL]	Batch 0	Batch 1	Batch 2	Batch 3
C1 pH 7.4	100	100	100	100	1000	100	97.9	100	100
C1 pH 6.0	0	6.9	4.8	3.8	1046.4	4.36	7	5	4
C2 pH 7.4	74.2	93.2	90	85.9	1095.2	87.32	100	98.6	94.1
C2 pH 6.0	8.3	9.4	12.6	11.2	1141.6	13.97	10.5	14.4	12.8
C3 pH 7.4	40.7	69.6	42.9	72.5	1190.4	57.12	81.2	51.1	86.3
C3 pH 6.0	5.3	4.9	7.9	8.3	1236.8	10.15	5.9	9.8	10.3
C4 pH 7.4	46.5	60.9	68.7	49.8	1285.6	73.92	76.7	88.4	64
C4 pH 6.0	0.4	6.6	10.2	5.9	1332	4.89	8.5	13.6	7.8

This experiment (chapter enzyme kinetics, **Fig. 37**) was repeated thrice and the initial activities of **NRC** are represented in **Table 4**. The initial HRP activities of the NRs (NRC, NR-, NR+) were normalised for a simpler comparison, such that the highest activity of NR+ was set to 100%. (**Fig. 38**). HRP activity values represent the mean value of three independent measurements. The initial slopes taken from each experiment; normalised (left) and volume corrected (right). Volume correction increased the fluorescence, or more precisely the slope by factor v_t/v_0. C# refers to the cycle no. #. Batch 0 provided **Fig. 37**, the three repeats were used for **Fig. 38**.

In addition, ANOVA was performed regarding pH (**Fig. 38**), respectively. It has been demonstrated (**Table 5**) that the influence of the pH factor is significant (statistically the averages are not the same) F critical < F experimental in the case of **NRC** (**catalytic nanocompartments** with reconstituted pH triggered gate protein-conjugate). In addition, two factor analysis (**Table 5**) confirmed again significance of pH influence on NRC system and revealed insignificant of experimental cycles.

Table 5: Single factor analysis

pH variation HRP	SS	df	MS	F	P-value	F crit
Treatment	2400	1	2400	626.087	1.51E-05	7.708647
Residuals	15.33333	4	3.833333			
Total	2415.333	5				

pH variation NR-	SS	df	MS	F	P-value	F crit
Treatment	4.167	1	4.167	0.14109	0.726269	7.708647
Residuals	118.127	4	29.532			
Total	122.2933	5				

pH variation NRC	SS	df	MS	F	P-value	F crit
Treatment	6680.007	1	6680.007	101.6486	0.000544	7.708647
Residuals	262.867	4	65.7167			
Total	6942.874	5				

pH variation NR+	SS	df	MS	F	P-value	F crit
Treatment	213.6067	1	213.6067	7.067998	0.056474	7.708647
Residuals	120.8867	4	30.22167			
Total	334.4934	5				

In **table 5**, SS stands for the sum of squares (name derived from the equation of the variance of the measurement): Df for the degrees of freedom (number of independent pieces of information that went into the estimate); MS for mean squares; P-value for the probability for a given statistical model that the null hypothesis is true (two observed parameters independent) and the F-value: is based on the F-test (F-distribution under the null-hypothesis) and is used as a secondary test to see whether the results are significant. For that F must be smaller than F-crit. On the final graph, the P-value becomes illustrated with stars, which are referred to as the significance, as defined in **table 6**:

Table 6: P-value and significance

Significance	P-value
0	$P > 0.05$
*	$P \leq 0.05$
**	$P \leq 0.01$
***	$P \leq 0.001$
****	$P \leq 0.0001$

X Curriculum Vitae

Name: Christoph Edlinger

Address: Grienstrasse 32,
4055 Basel, Switzerland

Nationality: Austrian

Birthday: 21.07.1986
(In Vienna)

E-Mail: christoph.edlinger.ce@gmail.com

Mobile:0799608744

Higher Education

09.2011-today: PhD in the lab of Prof. Wolfgang Meier at the University of Basel (Topic: controlling diffusion across artificial, polymeric membranes utilising membrane proteins)

11.2010-04.2011: Scientific co-worker in Prof. Reto Dorta's group at the University of Zürich (Synthesis of Sulfoxide ligands for catalytic hydroaminations and Michael additions). The position terminated, when Prof. Dorta's contract was not extended

10.2009-04.2010: Postgraduate studies in informatics at the TU Munich

06.-09.2009: Diploma thesis in molecular catalysis in the group of Prof. Fritz Kühn at TU Munich (Topic: Synthesis of modified cycloalkyl-ansa-molybdenum-compounds for catalytic epoxidations with TBHP; research in molecular catalysis) Final Grade: 1.7

10.2004-09.2009: 10 semester chemistry at the TUM (Technical University Munich); major subject: chemistry of macromolecules; minor subjects with emphasis on organic chemistry and catalysis

School (European School Munich)

09.1997-07.2004: Secondary school

09.1992-07.1997: Primary school

optional subjects: Mathematics: 5h; Chemistry and Physics: 4h

Language skills

German: Native
English: Fluent (12 years of studies in school with native speakers, regular use since 2009)
French: As second foreign language (certified B2)

Technical Knowledge

Macromolecular Chemistry: Polymer synthesis and analytics; molecular self-assembly

Organic Chemistry: Synthesis und analytics; retrosynthesis; chemistry of radicals

Catalysis: Asymmetric catalysis; molecular catalysis; refining (silica based catalysts); complex chemistry

Basic knowledge   Biochemistry, Drug Delivery, natural product synthesis and analytical methods in general (NMR, HPLC, GC, SEC, MS, enzymatic assays, UV-Vis…)

Computer skills

General purpose: MS-Office; basic knowledge in Linux and Mac operating system; Webpage maintenance and the use of origin

Chemistry: ChemDraw; Chemsketch; EJournal (electronic lab journal); Reaxis; Scifinder; Chimera (protein viewer)

Miscellaneous: Corel Draw, Java-programming; Dreamweaver (all basic knowledge)

Publications

1) *The Engineering protein channels as pH-reversible bio-valves to trigger functionality of catalytic compartments at the nanoscale* C. Edlinger, T. Einfalt, M. Spulber, A. Car, W. Meier, C. G. Palivan *ACS Nano-Letters* **2017** (publication submitted)
2) *Biomimetic artificial organelles with in vitro and in vivo activity triggered by reduction microenvironment* T. Einfalt, C. Edlinger, W. Meier, C. G. Palivan *Nature Communications* **2017** (publication submitted)
3) *Polymer Nanoreactors* C. Edlinger, X. Zhang, O. Fischer-Onaca, C. G. Palivan *Encyclopedia of Polymer Science and Technology* **2013**, DOI: 10.1002/0471440264.pst581.
4) *Polymer Vesicles* A. I. Dinu, C. Edlinger, E. Konicheva, C. G. Palivan *Encyclopedia of Polymeric Nanomaterials* **2014**, ISBN 978-3642296475